



# THE UNIVERSITY *of* EDINBURGH

This thesis has been submitted in fulfilment of the requirements for a postgraduate degree (e.g. PhD, MPhil, DClinPsychol) at the University of Edinburgh. Please note the following terms and conditions of use:

This work is protected by copyright and other intellectual property rights, which are retained by the thesis author, unless otherwise stated.

A copy can be downloaded for personal non-commercial research or study, without prior permission or charge.

This thesis cannot be reproduced or quoted extensively from without first obtaining permission in writing from the author.

The content must not be changed in any way or sold commercially in any format or medium without the formal permission of the author.

When referring to this work, full bibliographic details including the author, title, awarding institution and date of the thesis must be given.

# **Modulation of OPC migration: improving remyelination potential in multiple sclerosis**

Elitsa Peeva

Doctor of Philosophy  
The University of Edinburgh  
2018

# Declaration

I declare that this thesis was composed by myself, that the work contained herein is my own except where explicitly stated otherwise in the text, and that this work has not been submitted for any other degree or professional qualification except as specified.

Elitsa Peeva, February 2018

## Acknowledgments

First, I would like to thank my supervisor Anna Williams for the constant support, understanding and guidance and for providing the perfect environment for me to grow as a scientist and a person. I would also like to thank my second supervisor, Scott Webster, who believed in me when no one did and helped me find my way more than once. I would also like to thank the medical research council for supporting this work. I would like to thank past and present members of the Williams and French-Constant labs who have taught me many techniques and given me a lot of useful advice throughout the years. I am also very grateful for the help of the imaging staff at Centre for regenerative medicine, Bertrand and Eoghan.



Secondly, I would also like to thank all the visiting students who have been involved in this work under my supervision: Ana Rondelli, Gregor Skeldon, Issy Teriyapirom and Catherine Boldurat (from left to right with me in the middle). Ana Rondelli did her 3 month PhD mini project and was involved in the cryostat cutting, staining, imaging and analysis of the NP1(Sema3A-) mice. Ana Rondelli produced a short report at the end of her project. Gregor Skeldon was in the lab during his MSc project and was involved in the in vitro studies performing the motility assay and the majority of the maturation, survival and proliferation assays. He isolated the rat OPCs, performed the assays, imaged and analysed them. He produced a MSc dissertation at the end of this project. Issy Teriyapirom spent 5 months of her summer holidays during her BSc degree in the lab and isolated rat OPCs, performed the migration assays and analysed them. In addition to this, she performed IHC on the NP1(Sema3A), PDGFR $\alpha$  x flx-NP1-flx and their WT counterparts and imaged them. Finally, Catherine Boldurat is a final year high school student who performed an in vitro binding assay which did not find its way into this

## *Acknowledgments*

thesis. She presented her work in a report and a poster. I hope they have learnt as much as I have from them.



Finally, I would like to thank my family and friends who have been invaluable moral support through the ups and downs of PhD life. Particularly, thank you to Stoyan for the relentless support and encouragement. I would also like to thank Thea for being the best possible reason for studies interruption. Thank you so much, I could not have done it without you.

# Abstract

In the brain, axons are wrapped by myelin sheaths which ensure fast saltatory conduction of impulses and provide metabolic support. In multiple sclerosis (MS), the myelin sheaths are lost which leaves the axon denuded. This not only results in slower conduction of action potentials, but if prolonged, can also lead to axon death due to the loss of metabolic support. This neurodegeneration is the main cause of permanent disability in multiple sclerosis patients.

The axon death and disability which stem from it could be prevented by restoring the myelin wrap before axon damage has occurred. This remyelination process is carried out by oligodendrocyte precursor cells which are present throughout life. To remyelinate, OPCs migrate to the area of damage and differentiate into myelinating oligodendrocytes which ensheath axons with new myelin. In multiple sclerosis, this process occurs but is insufficient to overcome the damage.

Therefore, central to the therapeutic efforts in multiple sclerosis is the aim to improve endogenous remyelination. Enhancing recruitment of oligodendrocyte precursor cells (OPCs) to the areas of damage is a clinically unexplored target. To investigate the therapeutic potential of OPC recruitment modulators, I have looked at 2 different targets involved in migration NDST1/HS and Sema3A/NP1.

The first target, heparan sulfate (HS) is a proteoglycan which is important to OPC migration, investigated by Pascale Durbec's group in France. In a demyelinating mouse model, its key synthesising enzyme, NDST1, is upregulated by oligodendroglia in a belt around the lesion to aid OPC recruitment. Loss of NDST1 in oligodendrocytes was found to impair remyelination and reduce OPC migration in mice. In collaboration with them, I investigated the relevance of this molecule in post-mortem MS human tissue.

I found that in human as well as mouse, NDST1 was primarily expressed by oligodendroglia. The protein level and the proportion of oligodendroglia expressing NDST1 was increased in MS compared to control indicating NDST1 upregulation as a disease response in human. We also found that low numbers of NDST1+ oligodendroglia correlate with bigger sizes of lesions and chronic lesion types that fail to repair, highlighting its importance in repair. Moreover, high numbers of NDST1+ cells in a patient correlated with increased remyelination potential. This indicates that in human, intra-patient variation in NDST1 level may explain differences in potential for endogenous repair.

Secondly, I looked at Sema3A, a chemorepulsive molecule which is upregulated in demyelinated injury rodent models as well as multiple sclerosis lesions, particularly in OPC-depopulated chronic active lesions. Research has consistently found that the level of Sema3A negatively correlates to remyelination because Sema3A hinders OPC migration. This has highlighted Sema3A

as a potential target to improve OPC recruitment in MS however the size and shape of the molecule make it hard to design therapeutics against it.

Therefore, I looked at its druggable receptor, Neuropilin 1 (NP1), to see whether inhibition of NP1 had the same positive effect on OPC recruitment and remyelination as lowering the level of Sema3A. NP1 is a tyrosine kinase receptor for both Sema3A and vascular endothelial growth factor (VEGF) and is found in many cell types.

To check if NP1 inhibition is beneficial, I assessed remyelination in a mouse where the Sema3A binding site of NP1 has been mutated to prevent Sema3A binding and exerting its effect. This is a proxy for a (currently unavailable) ideal NP1 inhibitor of the Sema3A site only. Contrary to my expectations, OPC recruitment and remyelination in the mutant mice were not improved. However, the NP1 mutation resulted in an altered immune response.

To exclude the possibility that no improvement in the OPC recruitment and remyelination of those mice was seen because it was negated by the altered immune response, I explored a cell specific mutant mouse in which NP1 was deleted in oligodendroglia only. In this mutant as well, I did not see improvement of OPC recruitment and remyelination. I therefore propose that Neuropilin 1 is not imperative for Sema3As action in remyelination and is not suitable as a therapeutic target in multiple sclerosis.

Loss of the whole NP1, but not loss of the Sema3A site also resulted in bigger myelinated and unmyelinated axons as well as a different myelin thickness post remyelination. This showed that VEGF and the VEGF site on NP1 in oligodendroglia have a previously unknown but important role in determining axon size and myelin thickness which should be further investigated.

To further elucidate those results in a simple system, I looked at how Sema3A, NP1-Sema3A inhibitors, VEGF and NP1-VEGF inhibitor affect OPC behaviour. I confirmed Sema3As chemorepulsive effect but also showed that at different concentrations it can improve proliferation and survival of OPCs. Inhibiting the Sema3A site and the VEGF site of NP1 by specific blocking antibodies also affects OPC proliferation and maturation. This suggested that NP1s ligands are involved in more than just OPC migration.

In summary, this work supports the relevance of the mouse findings that NDST1 is upregulated in demyelination and important for repair for human illustrating that it might be a suitable therapeutic target to investigate. However, despite the importance of Sema3A in MS models, its only reported receptor, NP1, is not essential for Sema3As action. Therefore, it is an unsuitable therapeutic target. The fact that NP1 is an inappropriate drug target for MS is further demonstrated by the involvement of its ligands in multiple OPC behaviours both in positive and negative aspects.

ahaha

## Lay abstract

Multiple sclerosis results from our own immune system damaging the protective myelin sheet of neurons. Since neurons are the cells responsible for transmitting all signals in the brain and removing the protective sheet is akin to stripping the insulation of a cable, this results in the neurons malfunction and eventually death. Currently, there are drugs which dampen the immune system and aid in the very early stage of the disease. Despite their usefulness, those drugs cannot do anything after the protective sheet has been lost. Our body has capacity to repair by placing new myelin sheets on the neurons which have lost them, restoring normal function. This is done by oligodendrocyte precursor cells, a small migratory cell type capable of producing myelin sheaths. This repair process occurs in multiple sclerosis however it is insufficient to overcome the damage. Therefore, a lot of effort is currently placed at aiding our body to replace the myelin sheets on the neurons by recruiting more cells that do the repairs.

The oligodendrocyte precursor cell recruitment is a complex process with many factors and cells involved in it. In my PhD, I have investigated 2 targets with therapeutic potential. The first one, NDST1, has been proven to be important for repair in a mouse model of multiple sclerosis. I have found that the same is true for human multiple sclerosis. Secondly, I investigated Semaphorin3A, a free floating molecule which increases in areas of damage and repels oligodendrocyte precursor cells. Research has repeatedly and consistently shown that because it prevents recruitment of the cells which repair the damage, it is bad in multiple sclerosis. However, targeting Semaphorin3A with a drug would be extremely challenging because it is like a football which has no sides or edges for the drug to bind.

Luckily, semaphorin3A exerts its action by binding to Neuropilin 1 which is found on oligodendrocyte precursor cells. Neuropilin 1 has a pocket in which Semaphorin3A binds. This pocket can be occupied by a drug which would prevent Semaphorin3A to take up its place. My research is focused on determining if blocking the pocket of Neuropilin 1 would have the same beneficial effects as reducing the level of Sema3A. To test this, I used genetically modified mice which have the pocket of Neuropilin 1 altered so it no longer fits Semaphorin3A and mice which do not have Neuropilin 1 in oligodendrocytes. When I assessed how well they repair after multiple sclerosis-like lesion, I expected that they would repair better because the harmful effect of Sema3A is removed. However, they did not repair any better. This means that Neuropilin 1 is not essential for Sema3A's negative action in multiple sclerosis and it is therefore not a suitable therapeutic target for multiple sclerosis.

# Abbreviations

A active

ANOVA Analysis of variance

APP amyloid precursor protein accumulation

ALS amyotrophic lateral sclerosis

ATP Adenosine triphosphate

BBB blood brain barrier

BSA bovine serum albumin

CA chronic active

cAMP Cyclic adenosine monophosphate

C control

CC Corpus callosum

CC1 Anti-APC

CD68 Cluster of Differentiation 68

CI chronic inactive

CNS central nervous system

CTL control DNA Deoxyribonucleic acid

EAE Experimental autoimmune encephalomyelitis

ECM extracellular matrix

EM electron microscopy

FGF-2 fibroblast growth factor-2

flx floxed

GAG glycosaminoglycan

GAP GTP-ase activating protein

GnRH gonadotropin-releasing hormone

HS heparan sulfate

HRP Horseradish peroxidase

IBA1 ionized calcium-binding adapter molecule 1

IHC immunohistochemistry

iNOS inducible nitric oxide synthase

KD knock down

KO knock out

LFB luxol fast blue

LINGO1 leucine rich repeat and Ig domain containing 1

LPC Lysophosphatidylcholine

## Abbreviations

MAG Myelin-associated glycoprotein  
MEM minimum essential media  
MBP myelin basic protein  
MHC major histocompatibility complex  
miRNA micro ribonucleic acid  
MOG myelin oligodendrocyte glycoprotein  
MMPs matrix metalloproteases  
MRI magnetic resonance imaging  
mRNA messenger ribonucleic acid  
MS multiple sclerosis  
NAWM normal appearing white matter  
NDST1 N-deacetylase N-sulfotransferase1  
NG2 Neural/glial antigen 2  
NP1 Neuropilin 1  
NP2 Neuropilin 2  
OPC oligodendrocyte precursor cell  
OLIG2 Oligodendrocyte transcription factor 2  
PBS phosphate-buffered saline  
PDGF platelet-derived growth factor  
PDGFR $\alpha$  platelet-derived growth factor receptor  
PDL Poly-D-lysine  
PET Positron Emission Tomography  
PFA paraformaldehyde  
PhD Doctor of Philosophy  
PLL poly-L-Lysine PLP proteolipid protein  
PSI plexin-semaphorin-integrin  
RM remyelinated  
ROI region of interest  
RPM rounds per minute  
S3A/Sema3A Semaphorin3A  
Shh Sonic hedgehog  
shRNA short hairpin RNA  
SICHI semaphorin-induced chemorepulsion inhibitor  
SVZ subventricular zone  
TdT terminal deoxynucleotidyl transferase  
TEM transmission electron microscope  
TG transgenic  
TNF $\alpha$  Tumor necrosis factor alpha  
TNFR2 Tumor necrosis factor receptor 2  
TUNEL Terminal deoxynucleotidyl transferase dUTP nick end labeling  
Ulip/CRMP Unc-33-like phosphoprotein/collapsin response mediator protein

## *Abbreviations*

VEGF vascular endothelial growth factor

WM white matter

WT wild type

# Contents

<b>Declaration</b>	<b>i</b>
<b>Acknowledgments</b>	<b>ii</b>
<b>Abstract</b>	<b>iv</b>
<b>Lay abstract</b>	<b>vi</b>
<b>Abbreviations</b>	<b>vii</b>
<b>1 Introduction</b>	<b>1</b>
1.1 Multiple Sclerosis-introduction . . . . .	1
1.1.1 MS in numbers . . . . .	2
1.1.2 Symptoms and diagnosis of MS . . . . .	2
1.2 Pathology of MS . . . . .	2
1.2.1 Cause . . . . .	3
1.2.2 Demyelination:Oligodendrocyte and myelin damage . . . . .	6
1.2.3 Axonal damage . . . . .	7
1.3 Current MS therapies . . . . .	9
1.3.1 Relapse treatment and treatment of symptoms . . . . .	9
1.3.2 Disease-modifying therapies . . . . .	9
1.4 Remyelination . . . . .	10
1.4.1 Remyelination leads to functional recovery . . . . .	11
1.4.2 The dual role of inflammation in MS . . . . .	12
1.4.3 Remyelination occurs in multiple sclerosis . . . . .	13
1.5 OPCs . . . . .	14
1.5.1 OPC recruitment and maturation are required for remyelination . . . . .	14
1.5.2 OPCs: discovery, detection and heterogeneity . . . . .	15
1.5.3 Oligodendroglial roles . . . . .	16
1.6 Why does remyelination fail in MS? . . . . .	18
1.6.1 OPC recruitment failure . . . . .	18
1.6.2 OPC maturation block . . . . .	18
1.6.3 Novel therapeutic targets for MS . . . . .	19
1.6.4 Recruitment and proliferation of OPCs . . . . .	20
1.7 ECM and NDST1/HS . . . . .	21
1.7.1 Role of ECM . . . . .	21

1.7.2	ECM changes in MS	22
1.7.3	Heparan sulfate	22
1.7.4	NDST1	23
1.8	Neuropilin 1 and Semaphorin3A	24
1.8.1	Semaphorin3A	24
1.8.2	NP1	25
1.8.3	Coreceptors	28
1.9	Sema3A and Np1 role	31
1.9.1	Sema3A and NP1 in injury, repair and MS models	31
1.9.2	Sema3A and NP1 on oligodendroglia	33
1.9.3	Sema3A and NP1 effects on immune response	34
1.9.4	Other Sema3A and NP1 effects	35
1.10	Sema3A and NP1 in human	37
1.10.1	Sema3A and NP1 in MS	37
1.11	Inhibitors	39
1.11.1	SICHI	39
1.11.2	Xanthofulvin	40
1.11.3	L1	40
1.11.4	anti-NP1 antibodies	40
1.12	The connection between NDST1, heparan sulfate, and Sema3A and NP1	41
1.13	Rationale for study	42
<b>2</b>	<b>Materials and Methods</b>	<b>44</b>
2.1	In vivo methods	44
2.1.1	Animal genotype	44
2.1.2	Animal surgery	45
2.1.3	Animal termination and tissue preparation	47
2.2	In vitro methods	47
2.2.1	OPC cultures	48
2.2.2	OPC proliferation assay	49
2.2.3	OPC survival assay	49
2.2.4	OPC motility assay	49
2.2.5	OPC maturation assay	50
2.2.6	OPC migration assay	50
2.2.7	Purity of culture assay	50
2.3	Immunohistochemistry	51
2.3.1	Fluorescent IHC on fixed frozen mouse brain	51
2.3.2	Colorimetric IHC on fixed frozen <i>post-mortem</i> human tissue	51
2.4	Imaging, analysis and statistics	52
2.4.1	Imaging	52
2.4.2	Image analysis	52

2.4.3	Statistics	58
2.5	Materials	59
2.5.1	Human tissue	59
2.5.2	Antibodies list	61
<b>3</b>	<b>NDST1 is upregulated in MS and correlates with remyelination</b>	<b>62</b>
3.1	Introduction	62
3.2	Results of tissue staining	63
3.2.1	NDST1 is upregulated in multiple sclerosis tissue	63
3.2.2	NDST1 is primarily expressed in oligodendroglial cells	64
3.2.3	The majority of OLIG2+ cells in MS (but not control) are NDST1+	67
3.2.4	OLIG2+ NDST1+ cell numbers are reduced in CI lesions and negatively correlate with lesion size	68
3.2.5	NDST1+ cells correlate with remyelination potential	70
3.3	Discussion	72
3.3.1	Upregulation of NDST1 in MS	73
3.3.2	NDST1 is expressed in oligodendroglia in human	73
3.3.3	High NDST1 cell number is linked to smaller and less chronic lesions	74
3.3.4	NDST1 and remyelination	74
3.3.5	Summary	75
3.3.6	Model	75
<b>4</b>	<b>Assessing remyelination in the NP1(Sema3A-) mice</b>	<b>78</b>
4.1	Introduction	78
4.1.1	Does NP1 inhibition aid remyelination?	78
4.1.2	Animal models	79
4.1.3	Method	79
4.2	EM Results	80
4.2.1	NP1(Sema3A-) mice do not remyelinate better than WT mice	80
4.2.2	No difference between genotypes in myelin thickness and axon diameter	85
4.3	IHC	89
4.3.1	Finding lesions	89
4.3.2	The innate immune response is different	91
4.3.3	OPC recruitment is similar in WT and TG mice	94
4.3.4	Discussion	97
4.3.5	Remyelination	97
4.3.6	OPC migration	98
4.3.7	Immune response	99
4.3.8	Summary	102
<b>5</b>	<b>Assessing remyelination in the PDGFR<math>\alpha</math>-Cre x flx-NP1-flx mice</b>	<b>103</b>
5.1	Introduction	103

5.2	EM Results . . . . .	103
5.2.1	PDGFR $\alpha$ -Cre x flx-NP1-flx mice do not remyelinate better than WT . . . . .	103
5.2.2	Myelin thickness and axon diameter . . . . .	109
5.3	Cryo IHC . . . . .	116
5.3.1	Finding lesions . . . . .	116
5.3.2	Innate immune response is the same . . . . .	118
5.3.3	Do not have more OPCs in lesions . . . . .	121
5.4	Discussion . . . . .	124
5.5	Immune response . . . . .	125
5.6	OPC recruitment . . . . .	125
5.7	Remyelination . . . . .	126
5.7.1	Is NP1 the only receptor for Sema3A? . . . . .	126
5.7.2	Unexpected changes in PDGFR $\alpha$ -Cre x flx-NP1-flx mice . . . . .	127
5.7.3	Summary . . . . .	129
5.7.4	Model . . . . .	129
<b>6</b>	<b>In vitro work</b>	<b>131</b>
6.1	Introduction . . . . .	131
6.2	Migration assay . . . . .	133
6.2.1	Transwell assay can be used to detect chemorepulsion . . . . .	133
6.2.2	Sema3A is a chemorepellent but anti-NP1(Sema3A) antibody and xanthofulvin does not rescue OPC migration decisively . . . . .	134
6.2.3	VEGF increases OPC migration and anti-NP1(VEGF) blocking antibody reverses this . . . . .	139
6.2.4	Migration assay discussion . . . . .	141
6.3	Motility . . . . .	143
6.3.1	Motility discussion . . . . .	143
6.3.2	Motility and migration discussion . . . . .	144
6.4	Proliferation assay . . . . .	145
6.4.1	Sema3A . . . . .	145
6.4.2	Sema3A-NP1 inhibitors . . . . .	147
6.4.3	Proliferation assay discussion . . . . .	149
6.5	Survival assay . . . . .	150
6.5.1	Sema3A . . . . .	150
6.5.2	NP1-Sema3A inhibitors . . . . .	152
6.5.3	Survival discussion . . . . .	152
6.6	Maturation assay . . . . .	153
6.6.1	Sema3A . . . . .	153
6.6.2	NP1-Sema3A Inhibitors . . . . .	153
6.6.3	VEGF . . . . .	160
6.6.4	Maturation discussion . . . . .	161

*Contents*

6.6.5	In vitro summary . . . . .	163
6.7	Appendix . . . . .	164
6.7.1	Motility . . . . .	165
6.7.2	Proliferation . . . . .	168
6.7.3	Survival . . . . .	174
6.7.4	Maturation . . . . .	184
<b>7</b>	<b>Discussion</b>	<b>192</b>
7.1	Remyelination failure . . . . .	192
7.2	NDST1 . . . . .	193
7.3	Sema3A and NP1 . . . . .	193
7.4	Future prospects . . . . .	195

# List of Figures

1.1	Electron microscopy image of OPC surrounded by unmyelinated axons in an optic nerve (postnatal day 1)	15
1.2	Heparan sulfate is a polymer of alternating D-glucuronic acid and N-acetylglucosamine	22
1.3	NDST1 enzyme catalyses the N-deacetylation and N-sulfation of heparan sulfate	23
1.4	NDST1 sulfotransferase domain is spherical with an open cleft	23
1.5	Structure of Sema3A, NP1, and Plexin in a complex	29
2.1	NP1(Sema3A-) genotype	45
2.2	NDST1 staining is specific	52
2.3	Analysis method for human <i>post-mortem</i> tissue analysis	53
2.4	Analysis pipelines for proliferation and survival (TUNEL) assays were identical	55
2.5	Analysis pipeline for motility assay	56
2.6	Analysis pipeline for maturation analysis	57
2.7	Analysis pipeline for purity assay	58
2.8	Schematic representation of different MS lesion pathological types and their hypothesised relationship to each other	60
3.1	NDST1 is upregulated in MS	64
3.2	NDST1 is expressed by oligodendroglia, astocytes, microglia/macrophages and neurones.	65
3.3	NDST1 is primarily expressed in oligodendroglia	66
3.4	NDST1 is expressed in isolated rat oligodendroglia in vitro	67
3.5	NDST1 is expressed in around 2 times more oligodendroglia in MS than in control.	68
3.6	There are less absolute NDST1+ oligodendroglia numbers in CI lesions compared to NAWM	69
3.7	The number of oligodendroglia expressing NDST1 is inversely correlated to lesion size	70
3.8	The number of NDST1+ cells is no different between lesion types, NAWM and control brain	71
3.9	NDST1+ cell numbers positively correlate with the remyelination potential score	72
3.10	Comparison of mouse and human results	76
4.1	Summary of the in vivo methods used to assess remyelination	80

*List of Figures*

4.2	Representative EM images of unlesioned corpus callosum and areas of the lesion . . . . .	81
4.3	There is no significant difference in the proportion of unmyelinated axons between TG and WT mice either before or after a demyelinated lesion. . . . .	82
4.4	Absolute numbers of myelinated and unmyelinated axons. . . . .	84
4.5	There is no difference in the myelin thickness between TG and WT mice . . . . .	86
4.6	Frequency distribution (histogram) of axon diameter of myelinated axons. . . . .	87
4.7	The relationship between myelin thickness and axon diameter . . . . .	88
4.8	Representative images of initial staining with antibodies against MBP and IBA1 used to find lesions . . . . .	90
4.9	Lesions are a similar size between WT and TG mice and they have similar amount of IBA1+ cells. . . . .	91
4.10	Representative images of staining using CD68, Arginase-1 and iNOS antibodies on WT tissue . . . . .	92
4.11	Representative images of staining using CD68, Arginase-1 and iNOS antibodies on TG tissue . . . . .	93
4.12	NP1(Sema3A-) mice have a different innate immune response. . . . .	94
4.13	Representative images of IHC with antibodies against NG2 and CC1 on WT and TG tissue . . . . .	95
4.14	Representative images of IHC using antibodies against PDGFR $\alpha$ and NogoA on WT and TG tissue . . . . .	96
4.15	NP1(Sema3A-) mice do not have more OPCs in lesions. . . . .	97
4.16	OPC migration in NP1(Sema3A-) mice has been shown to be increased in a previous publication . . . . .	98
4.17	Addition of Sema3A decreases the number of activated macrophages/microglia in lesions . . . . .	100
4.18	Sema3A affects the in vitro migration of pro-inflammatory (M1) and pro-repair (M2) differently. . . . .	101
5.1	Representative EM images . . . . .	104
5.2	There is no difference in proportion of unmyelinated axons between TG and WT mice. . . . .	106
5.3	Absolute numbers of myelinated and unmyelinated axons per field of view are reduced in TG animals . . . . .	108
5.4	There is no difference in the myelin thickness between TG and WT mice . . . . .	109
5.5	Myelin and unmyelinated axon diameter . . . . .	111
5.6	Frequency distribution (histogram) of axon diameter . . . . .	113
5.7	The relationship between myelin thickness and axon diameter . . . . .	115
5.8	Representative images of initial staining with antibodies against MBP and IBA1 used to find lesions . . . . .	117

*List of Figures*

5.9	Lesions are similar size between WT and TG mice and have similar amount of IBA1+ cells. . . . .	118
5.10	Representative images of staining using CD68, Arginase-1 and iNOS antibodies on WT tissue . . . . .	119
5.11	Representative images of staining using CD68, Arginase-1 and iNOS antibodies on PDGFR $\alpha$ -Cre x flx-NP1-flx tissue . . . . .	120
5.12	PDGFR $\alpha$ -Cre x flx-NP1-flx mice have a normal immune response. . . . .	121
5.13	Representative images of IHC with antibodies against NG2 and CC1 on WT and TG tissue . . . . .	122
5.14	Representative images of IHC using antibodies against PDGFR $\alpha$ and NogoA on WT and TG tissue . . . . .	123
5.15	PDGFR $\alpha$ -Cre x flx-NP1-flx mice do not have more OPCs or mature oligodendrocytes in lesions. . . . .	124
5.16	Model of roles of NP1 and its ligands . . . . .	130
6.1	Summary of different OPC behaviours tested in the assays . . . . .	131
6.2	In vitro method summary . . . . .	132
6.3	Summary of tools used in in vitro studies . . . . .	132
6.4	Transwell assays can be used to detect chemorepulsion. . . . .	134
6.5	Sema3A is chemorepellent for OPCs but addition of anti-NP1(Sema3A) antibody does not rescue OPC migration. . . . .	136
6.6	Xanthofulvin does not rescue OPC migration in response to Sema3A. . . . .	138
6.7	VEGF increases migration and anti-NP1(Sema3A) antibody reverses it. . . . .	140
6.8	A representative example of a cell in the motility assay. . . . .	143
6.9	High concentration of Sema3A increases proliferation of rat OPCs in vitro. . . . .	146
6.10	anti-NP1(Sema3A) blocking antibody increases proliferation at some concentrations. . . . .	148
6.11	Low concentration of Sema3A in solution improves survival. . . . .	151
6.12	anti-NP1(Sema3A) blocking antibody has no effect on maturation. . . . .	154
6.13	anti-NP1(Sema3A) blocking antibody significantly increases the area of MBP+ cells. . . . .	155
6.14	Example images of the effect of Sema3A and inhibitors on maturation. . . . .	157
6.15	Combinations of Sema3A and NP1-Sema3A inhibitors influence maturation. . . . .	159
6.16	Example images of the effect of VEGF and anti-NP1(VEGF) on maturation. . . . .	160
6.17	Anti-NP1(VEGF) blocking antibody influenced maturation while VEGF did not. . . . .	161
6.18	Coated Sema3A did not influence motility. . . . .	165
6.19	Sema3A and anti-NP1(Sema3A) do not influence motility significantly. . . . .	166
6.20	Xanthofulvin did not influence motility. . . . .	167
6.21	VEGF and anti-NP1(VEGF) blocking antibody do not influence motility. . . . .	168
6.22	Semaphorin3A coated on the surface does not influence proliferation. . . . .	169

*List of Figures*

6.23	Xanthofulvin did not influence proliferation. . . . .	171
6.24	SICHI did not influence proliferation. . . . .	172
6.25	VEGF and anti-NP1(VEGF) blocking ab did not influence proliferation. . . . .	173
6.26	Coated Sema3A slightly decreases survival. . . . .	175
6.27	anti-NP1(Sema3A) blocking antibody does not influence survival. . . . .	177
6.28	SICHI does not influence survival. . . . .	179
6.29	Xanthofulvin does not influence survival significantly. . . . .	180
6.30	Sema3A together with NP1-Sema3A inhibitors do not significantly influence survival. . . . .	182
6.31	VEGF and anti-NP1(VEGF) blocking antibody do not influence survival. . . . .	183
6.32	Sema3A in solution did not influence maturation of rat OPCs. . . . .	184
6.33	Quantification of concentrations of Sema3A in solution and control showed that they did not influence maturation of rat OPCs. . . . .	185
6.34	Coated Sema3A appears to decrease maturation. . . . .	186
6.35	Quantification of the effect of coated Sema3A on maturation revealed no statistically significant effect. . . . .	187
6.36	Example images of the effect of Xanthofulvin on maturation. . . . .	188
6.37	Xanthofulvin does not influence maturation. . . . .	189
6.38	Example images of the effect of SICHI on maturation. . . . .	190
6.39	SICHI did not influence maturation. . . . .	191

# List of Tables

1.1	Affinity of anti-NP1(Sema3A) and anti-NP1(VEGF) blocking antibodies . . . . .	41
2.1	Classification and characteristics of human <i>post-mortem</i> samples . . . . .	60
2.2	List of primary and secondary antibodies used . . . . .	61

# 1 Introduction

## 1.1 Multiple Sclerosis-introduction

In the brain, oligodendrocytes wrap axons to create protective myelin sheaths. Each oligodendrocyte wraps many axons and each axon has multiple myelin segments (internodes) separated by nodes of Ranvier where sodium channels cluster. This clustering of sodium channels because of the myelin sheath ensures fast saltatory conduction of impulses from node to node [126]. In addition to this, the oligodendrocyte provides metabolic support to the axon [170] [100].

In multiple sclerosis (MS), there are focal areas of inflammation-driven destruction of myelin and oligodendrocytes which leave the axon denuded. This results in conduction block or slower conduction of action potentials, longer refraction period and thus impairment in high frequency signal transmission [193]. If the loss of myelin is prolonged, the loss of metabolic support together with the increased energy demand and vulnerability of the denuded axon can result in axon death. This neurodegeneration is the main cause of permanent disability in multiple sclerosis patients [69].

Multiple sclerosis is a chronic disease with a heterogeneous clinical presentation and complex pathology. Around 80% of the patients exhibit relapsing-remitting MS which is initially characterised by appearance of neurological deficit (relapse) and complete recovery (remission), then partial recovery following relapses, and finally secondary progressive stage with irreversible accumulation of disability in spite of relapses [23]. The functional deficit (relapse) is due to episodic autoimmune-driven inflammation and demyelination in different areas of the central nervous system (CNS) while the functional recovery (remission) results from resolution of inflammation, remyelination as well as brain compensation [129]. The other 20% present with primary progressive MS which is characterised by only the progressive stage with accumulation of disability without relapses caused again by inflammation, demyelination and axon degeneration [56] [23].

The disease is both inflammatory and neurodegenerative. The relapsing-remitting stage of the disease shows the hallmarks of inflammatory disease and demyelination while the the progressive stage of the disease with gradual accumulation of disability is reminiscent of degenerative diseases [31]. Those different disease processes which occur separately as well as simultaneously make it particularly hard to treat. Even though life expectancy from disease onset is only slightly shortened [56], the disease can be highly debilitating and considerably reduce quality of life.

### 1.1.1 MS in numbers

Multiple sclerosis is the most common cause of nontraumatic neurological disability in young adults [56] and affects 0.1% of the world population [50]. Multiple sclerosis affects twice as many women as men and has a life time risk of 1 in 400 or 0.25% [56].

The prevalence of MS increases with increasing distance from the equator [295]. For example, the prevalence rate in Spain is 54 per 100000 [254] increasing to 63 per 100000 in south England, 203 per 100000 in the Lothians (Edinburgh area) [266] and peaking at Orkney with 258 per 100000 [295]. Overall, the highest prevalence in the world is in Scotland [254].

Due to the chronic character of the disease and the fact that it affects adults in their prime often making them unable to work, MS has a considerable economic impact. It has been estimated to affect 380000 individuals in the 28 European countries and the total annual cost was estimated at 12.5 billion euro [283]. This comes at 27 euro per European inhabitant per year and around 400000 euro per MS patient a year.

### 1.1.2 Symptoms and diagnosis of MS

The symptomatic presentation of MS is variable between patients as symptoms depend on the areas of the brain affected. Sensory disturbances, fatigue, recurring episodes of neurological dysfunction, motor and coordination deficit, and cognitive impairment are observed with varying severity in the disease [212] [226].

MS was diagnosed clinically by having evidence of at least 2 time separated CNS neurological symptoms and at least one neurological dysfunction demonstrated by neurological examination [248]. The repeated exacerbations of symptoms (relapsing-remitting MS) or their progressive worsening (primary progressive MS) is essential to allow any one-off reasons for a CNS neurological deficit to be separated from chronic multiple sclerosis. Magnetic resonance imaging can now be used to define a second CNS neurological event, monitor lesion load in the brain and lesion progression which aids diagnosis [203]. However, the heterogeneous presentation and severity of the disease can still pose a challenge for clinical diagnosis.

## 1.2 Pathology of MS

Even though it can be hard to diagnose MS in patients, MS has very clear characteristics on *post-mortem* examination of the central nervous system (CNS) from MS patients. The demyelination and immune infiltration can be clearly observed using histological stains and be used to describe and classify the different types of MS lesions based on how much immune response and repair is present.

### Lesion types

The classic classification of MS lesions places them into 4 distinct types: active, chronic active, chronic inactive and remyelinated. Active lesions can either remyelinate or turn into chronic ac-

tive and then chronic inactive lesions (shown in figure 2.8). In pathology, active lesions are described as having indistinct borders between normal myelinated tissue and the demyelinated lesion using myelin staining and macrophages/microglia throughout the lesion. Chronic active lesions also lack myelin staining (they are demyelinated) but have a ring of macrophages/microglia around the lesion with a core devoid of immune cells. Chronic inactive lesions have a distinct borders between normal myelinated tissue and the demyelinated lesion using myelin staining and very few immune cells. Finally, remyelinated lesions or shadow plaques have less intense myelin staining throughout.

Remyelinated lesions (shadow plaques) have reduced myelin stain because of the reduced myelin thickness, shortened internodes and widened nodes of Ranvier [242] and also some reduction in axon density ([155]). There has been much debate about whether those lesions are truly remyelinated or just not completely demyelinated. Actively demyelinating lesions which have not completed demyelination do show a similar reduction in myelin stain however those are infiltrated with phagocytic macrophages with myelin containing lysosomes and the myelin sheaths in the lesion are the same thickness as NAWM [242]. Alternatively, reduction of myelin staining could be observed because of loss of axons with the remaining axons having the same thickness of myelin as the NAWM [242]. Both of those alternative reasons for reduction of myelin staining are easily distinguished by immunohistochemistry from remyelinated lesions

There are also grey matter demyelinated lesions which tend to have less immune cell infiltration possibly because there is less myelin to be stripped of axons and cleared by phagocytes [56] leading to an attenuated immune response. Clearly, such a classification is an oversimplification of an enormously complex disease process and in light of recent changes to MS lesion classifications, it does not account for whether demyelination has just started, is still ongoing or has been completed [164]. However, in order to study study a disease so complex and heterogeneous, simplification can be helpful. Most of these classifications are also based on pathological examination of *post-mortem* tissue, therefore are not able to examine the same MS lesion over time. We can only postulate their pathological course.

The clear cut pathological description of MS lesions is in clear contrast to the overall unclear cause of MS. An enormous number of studies has been done on the subject to disappointingly conclude that an unclear combination of genetic and environmental factors are responsible.

### 1.2.1 Cause

The classical view is that MS is an autoimmune disease in which environmental factors trigger the auto-reactive immune system (possibly via epigenetic changes) in genetically-susceptible people [254]. Those result in focal areas of demyelination in the CNS characterised by inflammation, oligodendrocyte and axonal damage, and subsequent death. An alternative hypothesis is that neurodegeneration is the primary cause of the disease with the immune response being secondary [310]. However, what exactly causes the autoimmune response or the neurodegeneration is unknown.

### Genetic

There is a genetic susceptibility to multiple sclerosis. Although the general population lifetime chance to get multiple sclerosis is 0.25% [56], it is more than 10 times higher if a sibling has MS (2.9%) and 100 times higher if a twin has MS (25.3%) [329]. On the other hand, the chance for a spouse of MS patient is same as the general population [79] implying that the higher lifetime risk is due to genetic and not environmental factors. However, MS has a complex genetic predisposition with many genetic risk alleles making a small contribution to the overall risk [346]. Major histocompatibility complex (MHC) has the strongest genetic association with many of the risk genes in the complex being involved in regulation of the immune system [346]. However, another 110 risk alleles not associated with MHC have also been found [346] making the genetic pool of susceptibility heterogeneous and diverse. One of the genes involved in MS risk is a heparan sulfate proteoglycan called GPC5 [15]. GPC5 which is found on the outer plasma membrane and is possibly involved in sequestering pro-inflammatory chemokines [15]. Moreover, it has been associated with different patient responses to interferon $\beta$  [33]. Although genetics obviously play a role in MS, they are not the sole determinant.

### Environmental and lifestyle

In addition to genetics, many environmental and lifestyle factors have been associated with MS; however, each of them is probably only responsible for a small contribution. Factors associated with increased risk of MS include high latitude, smoking, low vitamin D, Epstein-Barr Virus infection, and adolescent obesity [231]. Some of those (e.g. obesity and smoking) can directly upregulate or downregulate MS risk genes and therefore contribute to the genetic predisposition by modulating adaptive immunity [231]. This indicates the complex interplay between the extraneous and genetic factors in the pathology of MS; however, it does not bring us any closer to finding a preventable cause.

Although the causes of MS are still elusive and likely to be multiple and combinatorial, there are two hypotheses about the sequence of events leading to demyelination: placing inflammation or neurodegeneration as the primary event.

### Inflammation-caused demyelination

As discussed above, it is well known that the action of the immune system destroys the myelin and oligodendrocytes; however, it is overall unknown what causes the immune system to be tricked into seeing those as 'foreign' [310]. One of the possible reasons is molecular mimicry. This is when a molecule (e.g. Epstein-Barr virus mentioned in section 1.2.1) is presented to MHC II (MHC variants increase genetic risk [98] as discussed in section 1.2.1) is sufficiently similar to myelin or oligodendroglial proteins to cause auto-reactive T cells [56] [50]. To support this hypothesis, microglia have been shown to be able to present oligodendroglial proteins in combination with MHC class II and activate T cells in vitro [39].

Even though this hypothesis could explain MS development in a simple way — there does not seem to be a single or even a few antigens involved and the contribution of this mechanism to the disease is unknown. Regardless of the cause, it is the autoimmune T cells that are believed to be the primary pathogenic cell type in MS and they have been found in much higher numbers in active than in chronic human MS lesions [313]. Lymphocytes from MS patients' blood samples have shown reactivity towards MOG, MBP, PLP (myelin components), or combination of those [67]. Reactivity towards at least one of those tested myelin components was detected in the majority of patients (15/25)[67]. This supports the idea that MS lesions are caused by autoimmune reactivity to myelin. It is possible that many causes converge on this triggering of the autoimmune response. Similarly, cerebrospinal fluid of relapsing-remitting MS patients was found to contain antibodies against OPC surface proteins in two independent studies [11] [224]. This means that autoimmunity against OPCs could contribute to the pathology of MS as well. Of course, other cells of the immune system are involved in MS pathogenicity with B cells being involved in regulation of self-antigens [5] and macrophages being involved in maintaining ongoing demyelination [313].

Activated immune cells can enhance BBB permeability by secretion of numerous cytokines, soluble factors as well as reactive oxygen species and enter the CNS [168]. Upon meeting with myelin components, the autoimmune T cells would be further activated to produce additional pro-inflammatory cytokines (e.g.  $\text{TNF}\alpha$ ), soluble factors as well as reactive oxygen and nitric oxide species. This results in an inflammatory loop which leads to further BBB permeability and recruitment of further immune cells [56] which ultimately results in demyelination, oligodendrocyte death [17], block in axonal conduction, and axon death.

In the initial relapsing-remitting part of the disease, the inflammation subsides, remyelination occurs, and the brain compensates for the lost axons which results in clinical recovery [310]. However, with time and in the primary progressive disease, instead of resolving, inflammation turns chronic, which limits remyelination and ultimately results in accumulation of axonal damage for which the brain is unable to compensate, correlating with the irreversible accumulation of disability in the patients [310]. Therefore, it is reasonable to speculate that the disease transitions from relapsing-remitting to secondary progressive when the brain can no longer compensate for the axonal loss [310]. Even though the brain is not very good at repair, it is amazing at compensating for damage. In the EAE model of demyelination, up to 30% of the axons can be lost before impairment and as many as between 45% and 84% of the axons are lost in paralysed MS patients [25].

The alternative hypothesis about the events leading to MS is that the autoimmune reaction follows primary neurodegeneration.

### **Neurodegeneration-driven inflammation**

Since axonal loss is much better correlated to disease progression than the extent of demyelination and grey matter lesions have limited immune infiltration, it has been suggested that axonal pathology is primary and inflammation and demyelination secondary [310]. This is further

supported by the widespread axonal loss found in regions which are not in a lesion [155] [304]. However, these can be explained by loss of axons in a network having a secondary effect on a different area of the network which is distant from the initial damage.

Regardless of whether inflammation or neurodegeneration are primary, the disease results in demyelination and oligodendrocyte and axonal death by numerous possible mechanisms briefly discussed below.

### 1.2.2 Demyelination:Oligodendrocyte and myelin damage

#### Inflammation-driven oligodendrocyte death

In a study of 51 biopsies and 32 autopsies containing active lesions with short disease duration, 4 distinct patterns of demyelination were found [180]. The first 2 types, I and II, were characterised by macrophage and T lymphocyte infiltration, close proximity to a blood vessel and were differed only in the Type II's deposition of antibodies and complement antigens [180]. Therefore, both those active lesion types were reminiscent of an autoimmune disease with the damage in type I probably caused by immune cells products and the damage in type II caused by antibody and complement dependent mechanisms [180].

To support type I oligodendrocyte cell death and demyelination, multiple immune cell products were found to induce oligodendrocyte-specific cell death. For example, fas ligand is up-regulated in immune cells, fas receptor is upregulated in oligodendrocytes in MS and fas ligand can induce oligodendrocyte death in vitro [77]. Similarly, TNF, a pro-inflammatory cytokine, was found to kill oligodendrocytes on in vitro spinal cord explants [272]. On the other hand, secreted factors from immune cells might not be enough to cause demyelination and oligodendrocyte death. Injection of supernatant from activated immune cells was not enough to cause demyelination when injected into a myelinated tract; however, injection of CNS-directed antibodies together with activated immune cells caused demyelination [30] similarly to the type 2 demyelination described above.

#### Oligodendrocyte dystrophy

Conversely, the other two types of demyelination, type III and IV, were reminiscent of oligodendrocyte dystrophy. They were not centred around a blood vessel and did not show any deposition of antibodies and complement [180]. Instead, type III lesions were characterised by loss of the myelin protein MAG and oligodendrocyte apoptosis and are believed to be caused by a virus or toxin which impairs the oligodendrocytes functionally [180]. Similar lesions were observed in rare but very severe cases of relapsing-remitting MS which resulted in the patient's death during or shortly after a relapse [17]. Finally, type IV active lesions were characterised by loss of all myelin proteins and extensive non-apoptotic oligodendrocyte death with unknown mechanism for the oligodendrocyte damage [180]. This oligodendrocyte damage and death could be caused by metabolic strain due to hypoxia [169].

Overall, the demyelination type was thought to be different between patients but the same within different lesions of the same patient [180]. Although this system of classification of MS lesions on the basis of their possible mechanistic cause is somewhat controversial, it was an important step in trying to understand the heterogeneous nature of MS lesions and the mechanisms causing them. There is extensive heterogeneity and interplay between immunity and degeneration in MS which is not only true in the progression of the disease [31] but also between different patients [180]. This complexity begs the question about the usefulness of animal models which we use to study MS as they can only approximately represent a single one of those numerous stages and demyelination types. Moreover, the heterogeneity in the mechanism of demyelination and oligodendrocyte death indicates that the MS causes could be highly diverse between patients and require different treatment.

How demyelination and oligodendrocyte death correlates with disease presentation and course is controversial in the literature. One study found that lesion locations observed in MRI are related to symptomatic presentation in a cohort of 452 MS patients with some lesion locations being much more likely to induce disability than others and some being 'silent' [49]. This indicates the significant consequences of demyelination and the subsequent conduction impairment. However, this study has the inevitable caveat that the lesions observed in MRI could be just demyelinated or the demyelination could have led to axonal damage and death which is the reason for the symptoms [56].

### 1.2.3 Axonal damage

#### Inflammation

It is widely accepted that demyelinated axons can get new myelin sheaths and oligodendrocytes can be replenished; however, axonal death is irreversible and is the factor that correlates best with disease progression [32] [69]. There are multiple possible mechanisms for the axon damage which could cause or contribute in combination with axon death as discussed below.

It is easy to speculate that the rogue immune system which is responsible for myelin and oligodendrocyte damage is also responsible for axon damage. Indeed, it was found that acute axonal damage (measured by accumulation of amyloid precursor protein accumulation (APP) whose axonal transport is ceased by transection or damage to the axon) directly correlates to inflammatory infiltration of the lesion [163] [88]. Similarly, axonal transection measured by terminal axonal ovoids was found to correlate with the degree of inflammation of the lesion [311]. All of those studies indicate that inflammation is likely to be the reason for the axonal damage however it is unclear whether this is direct or secondary to a toxic environment or a loss of myelin.

There are some indications that immune cells could be directly responsible for the axonal damage. Namely, T cells have been found in close proximity to axons in multiple sclerosis [222] and have been shown to attack and transect neuronal neurites in vitro [194]. Alternatively, signalling molecules from activated immune cells could be responsible. For example, nitric oxide from macrophages could contribute to the degeneration of electrically active axons [282]. It has

been found that nitric oxide reversibly blocks action potentials in CNS neurones by blocking ATP production and that demyelinated axons are more susceptible to this block than myelinated axons [256]. Reactive oxygen and nitrogen species can also cause mitochondrial damage and oxidative damage has been found in oligodendrocytes and neurones in active MS lesions [119] giving another possible explanation for the observed axonal and oligodendroglial damage and death.

In addition to the immune-mediated mechanisms, it is possible that the chronic demyelination of the axons is due to loss of metabolic support from the oligodendrocyte.

### **Metabolic strain**

The direct effect of the immune infiltrate cannot be the only mechanism of axonal damage since axonal damage is also evident (but to a lesser extent) in normal appearing white matter (NAWM) and chronic lesions both of which lack immune infiltration [155]. Demyelination leads to loss of metabolic support from the oligodendrocyte to the axon (discussed in section 1.5.3) and also leads to higher energy demand on action potential conductance in the denuded axon. Normally clustered at the node of Ranvier, upon demyelination, sodium channels redistribute along the axon [82] which allows impaired impulse propagation at high energy cost [325]. This leaves the axon with less metabolic support and increased metabolic need in a state that is referred to as virtual hypoxia [312]. In vitro, demyelinated axons were shown to respond to this increased energy demand by increasing the size of mitochondria as well as their transport [151]. Similarly, in chronic multiple sclerosis lesions, mitochondrial mass is increased in demyelinated axons compared to myelinated axons [35] in an effort to compensate for the energy mismatch. However, when energy deficit is prolonged, compensation fails and a cascade of pathological events similar to the ones described in the next section ( 1.2.3) [312] lead to axonal death.

### **Convergence on axonal damage**

Numerous factors from immune cells, increased energy need in the demyelinated axon, mitochondrial dysfunction, hypoxia, free radicals, and loss of trophic support [92] all converge on insufficient energy production (ATP) [292]. This in turn impairs the action of the sodium/potassium ATPase which normally exchanges 3 sodium ions from the cell for 2 potassium ions extracellularly [282] [122]. This results in very high intracellular sodium which is further amplified by upregulation of sodium conductance due to sodium channel reorganisation in the demyelinated axons [91]. This can lead to reversal of the sodium/calcium exchanger which normally takes calcium ions out and sodium ions in [291] [281]. Finally, this would lead to high intracellular calcium concentration which could kill the axon [282]. Therefore, myelin could be a protective coat for such toxic substances.

Furthermore, it has been observed that axonal degeneration can also occur in areas which have normal myelin [24] indicating that axonal damage can happen without demyelination. Contrary to this, selective loss of oligodendrocytes leads to myelin damage and axonal damage in the absence of T-cell and B-cell immune response [246] probably due to loss of metabolic support

discussed in section 1.2.3. Both of those studies indicate that axonal damage could occur by vastly distinct mechanisms. The exact interplay between inflammation, axonal degeneration, and myelin and oligodendrocyte loss and their relative contribution is still unclear and may be heterogeneous between patients.

### **Axonal death causes clinical deterioration**

Acute axonal damage is most prominent in the early stage of the disease (<1 year) when active demyelination happens but persists throughout the disease when the lesions are often chronic [163] [155]. Moreover, comparison of magnetic resonance spectroscopy imaging and clinical disability and progression in 88 MS patients revealed that axonal damage happens before symptoms manifest clinically and contributes significantly to disability [68]. The continuous axonal damage has been proved to be directly correlated to multiple sclerosis disability by many different groups using different techniques [155] [69] [64] [311] [304]. This is one of the few cellular events that have been found to significantly contribute to clinical presentation and course [90]. In fact, axonal loss is so well correlated to disease progression, it has led to the idea that MS is primarily a neurodegenerative disease discussed in section 1.2.1 [310].

Since axonal damage and death are so linked to disease symptoms and progression, it is natural that current therapies aim to prevent that. Therapies are mainly aimed at modulating the immune response to decrease its involvement in disease pathology and in managing the already existent symptoms.

## **1.3 Current MS therapies**

### **1.3.1 Relapse treatment and treatment of symptoms**

During a relapse, corticosteroids can be used to shorten the duration of a relapse and to speed recovery. They diffuse into the cell and bind cytoplasmic glucocorticoid receptors which then modulating gene expression by inducing expression of anti-inflammatory cytokines and inhibiting expression of pro-inflammatory cytokines [279]. Although corticosteroids reduce the chance of worsening or non-improvement of relapse 5 weeks after it has started, they do not influence the relapse frequency [54] and cannot be used long-term due to their side effects.

Moreover, numerous therapies exist to aid specific multiple sclerosis symptoms. Although those are important to improve the quality of life for the patients, they do not have long term benefits on the disease course [56] which is what the next class of drugs aims to do.

### **1.3.2 Disease-modifying therapies**

Another, very promising class of drugs is aiming to modify the disease course via suppressing inflammation and thus further immune infiltration as well as BBB permeability [230]. Decreasing the autoimmune attacks has the potential to be beneficial in the early stages of the

relapsing-remitting form of multiple sclerosis. There are numerous immunomodulatory therapies including interferon $\beta$ , glatiramer acetate, fingolimod, dimethyl fumarate, teriflunomide, natalizumab and alemtuzumab which all aim to dampen the inflammation using a variety of mechanisms. While they improve the disease course and reduce disability, the drugs are constantly superceded by more effective treatments making all the available literature out of date and therefore are out of the scope of this thesis.

The emerging theme is that although those drugs are effective in the initial inflammation-dominated stage of the relapsing-remitting disease, they are not effective in the progressive stage or the primary progressive form of the disease. Therefore, what is really missing is a neuroprotective treatment for the progressive part of the disease which could limit the axonal damage and therefore halt the accumulation of disability (discussed in subsection 1.2.3). Ensheathing the axons with new myelin sheaths, called remyelination, is believed to have the great potential to limit their damage and restore normal function.

The only immunomodulatory therapy which might have pro-remyelination properties is fingolimod. In LPC-demyelinated cerebellar slice cultures, it was found that fingolimod increased remyelination and process extension of oligodendroglia [207]. The same effect on process extension was observed in human OPCs and fingolimod also modulated their survival [206]. However, other articles have not found an improve in remyelination in animal models [7] [128] and it remains to be seen if this is true in humans.

Nonetheless, there are some oligodendrocyte maturation promoting drugs currently in clinical trials (anti-Lingo-1, clemastine) which have the potential to fill the existing gap for pro-remyelination therapies. The logic behind the development of these pro-remyelination drugs will be described in the next section.

### 1.4 Remyelination

The axon dysfunction and subsequent death as well as the disability which stem from it could be prevented by restoring the myelin wrap before axon damage has occurred. An extended research debate culminated in the recognition that the remyelination process is carried out by newly formed oligodendrocytes from oligodendrocyte precursor cells [324] and not by mature oligodendrocytes already present producing new sheaths [91]. To remyelinate, OPCs migrate into the area of damage and differentiate into myelinating oligodendrocytes which contact and ensheath axons with new myelin. The occurrence of remyelination after demyelination was confirmed by electron microscopy study of the cat spinal cord where initially all axons were demyelinated and after 64 days all had acquired thin new myelin [32] arguing against these remaining from incomplete demyelination. What is most important about remyelination is that it protects the axons and restores conductivity and function.

### 1.4.1 Remyelination leads to functional recovery

Numerous animal models are used to study remyelination and are discussed in detail in the introduction to chapter 4. In short, they are separated into models which primarily represent the immune response of MS with some demyelination (EAE, viral) and primarily demyelinating models with limited immune response (cuprizone and LPC). Using variety of those models, direct evidence that remyelination restores function has been found. For example, after a LPC-demyelination in the cat spinal cord [280], remyelination lead to recovery of conduction. Moreover, demyelination was found to produce measurable behaviour effects which were recovered after remyelination in a rat demyelination model [138] which indicates that upon remyelination the recovery of conduction leads to behavioural recovery. Similarly, in cats fed irradiated diet which lead to extensive demyelination and neurological symptoms, endogenous remyelination resulted in full functional recovery after 3–4 months [78]. Both in demyelination and in an immune-mediated chronic progressive demyelination mouse models, remyelination was associated with recovery of motor function which was lost due to demyelination [177] [214]. Finally, remyelination significantly decreases the enhanced mitochondria content associated with denuded axons [347] indicating that it can restore the energy imbalance which normally leads to the death of the axon (section 1.2.3), though admittedly these levels never reach normal.

All of those studies show how remyelination is directly responsible for recovery of function both at the cellular and at the organism level. However, remyelination does not necessarily result in complete recovery as cuprizone treated mice which have completely remyelinated after demyelination still have more acutely damaged axon and decreased locomotor performance compared to untreated controls 6 months after cuprizone was stopped [189], although cuprizone is also known to damage axons directly. Even though it does not offer complete recovery identical to the undamaged CNS, remyelination is an immense improvement over demyelination. In addition to functional recovery, remyelination offers physical protection from further damage to the axon.

#### Remyelination protects the denuded axons

The evidence that restoring the myelin sheath on denuded axon protects them from death is also strong. In a cuprizone-demyelination model, OPC depletion by X-ray irradiation resulted in significant increase in axonal loss which could be prevented by introduction of neural progenitors which differentiate into OPCs and remyelinate the axons [133]. Moreover, in human studies, axonal damage was lower in remyelinated lesions compared to active lesions [163] and chronic lesions [155]. Similarly, axonal damage in an animal EAE demyelination model is less in remyelinated areas than it is in demyelinated areas [155]. Those studies indicate directly and indirectly that remyelination has a protective effect on the axon and this protection might be increasingly more important with age. Following cuprizone-demyelination, adult mice (6–7 months) exhibited more axonal transections and axonal loss than younger mice (2–3 months) [132] suggesting that once demyelinated, older adult axons are more prone to damage and remyelination is more important for them. In people, the first evidence that remyelination is associated with

functional improvement comes from PET scans using a ligand reporting myelin [27]. Here, patients with higher levels of PET tracer in their MS lesions over time have less disability [27]. Conversely, the number of MS lesions does not correlate with disability [27].

### Role of the axon in remyelination

The denuded axon is not an innocent bystander in remyelination. It is known that myelination can be prevented by inhibition of electrical activity and increased by increase in electrical activity in animal models [74]. The same might be true for remyelination. Fish studies suggest that before remyelination can happen, connectivity of axons needs to be maintained or re-established [225] which might also be a requirement in MS. The axons are known to be able to modulate myelination as learning new tasks in humans creates structural changes in the white matter [349].

Increasing evidence shows that in addition to the involvement of OPCs and neurones in remyelination, various components of the immune system are also required.

### 1.4.2 The dual role of inflammation in MS

As discussed in section 1.2.1, the immune system is believed to be primary responsible for the pathology of MS with T cells, B cells and macrophages/microglia mediating the damage. However, numerous experiments have shown that the same molecules and cells which induce the damage are instrumental in repair as well.

Knock down of genes involved in the immune system such as  $TNF\alpha$  as well as one of its receptors,  $TNFR2$ , delay remyelination after demyelination because of delayed OPC recruitment and maturation [12]. This was further supported by a phase II clinical trial of a drug aiming to neutralise  $TNF\alpha$  which unfortunately resulted in increased relapse frequency and severity [171] which indicates that loss of  $TNF\alpha$  is detrimental in MS. Similarly, knock out of interleukin- $1\beta$ , a pro-inflammatory cytokine, in mice results in reduced remyelination following normal demyelination [190]. Moreover, knock down of the  $TNF\alpha$ -controlled MHC II has been shown to retard remyelination because its loss results in impaired recruitment of oligodendrocytes [13]. Overall, knockout of inflammatory cytokines has resulted in impaired OPC recruitment. In line with this, in a recent transcriptome study it was found that activated OPCs increase transcription of pro-inflammatory cytokines which play an important role in supporting OPC migration [210].

This means that inflammation is important for repair and losing key components of the inflammatory cascade can impede remyelination. To support this, administration of minocycline, an anti-inflammatory drug, reduced OPC recruitment and remyelination following ethidium bromide lesions in rodents [175]. Moreover, it is important to note that in genetic studies MHC has the strongest association with MS, including MHC II [98] (section 1.2.1).

In addition to individual inflammatory molecules being involved in remyelination, different immune cell types are also essential. For example, knockdown of T cells, the main offenders in the pathology of MS, reduces remyelination in animal models [22]. This may in part be due to the importance of the regulatory T cells [348]. Similarly, loss of macrophages/ microglia

has been shown to impede remyelination [158] because of transient delay in recruitment and impairment in maturation of OPCs into the lesion [159]. This OPC impairment was because of less efficient myelin debris clearance [159] which is essential step of the remyelination process [28]. Myelin debris is known to negatively impact OPC maturation in vitro [262] and remyelination in vivo [157]. In fact, less efficient clearance of myelin debris by old macrophages/microglia is one of the proposed reasons why remyelination is slower with age [274]. However, loss of macrophages/microglia also induced changed in the mRNA levels for different growth factors [159].

Furthermore, the same cell type can be both beneficial and detrimental in MS depending on their environment-induced activation state. Some microglia and macrophages/microglia have a pro-inflammatory phenotype which is responsible for antigen presentation [39], secretion of pro-inflammatory cytokines and reactive oxygen and nitrogen species while others have an anti-inflammatory phenotype and secrete anti-inflammatory cytokines essential for immunomodulation and repair [80] [205]. In a demyelinated lesion, pro-inflammatory cells are predominant while pro-repair cells take over around the time of initiation of remyelination to create a beneficial remyelination microenvironment [205]. Moreover, remyelinated lesions in MS patients were observed to have high density of the pro-repair phenotype [205] and to express predominantly pro-repair markers [243]. It has been shown that repeated insult in a mouse EAE model leads to dysregulation of the pro-repair and pro-inflammatory macrophages/microglia compared to the initial insult with an impaired pro-repair response [202] which correlates with the lower chance of repair in a chronic lesion.

Induction of inflammation increases the myelination of transplanted OPCs in the adult retina compared to normal non-inflamed retina [9]. Similarly, in a chronic rat model of demyelination, induction of inflammation after failure of remyelination resulted in remyelination [89].

There is some further indication that the same dual role is true in human as well. For example, in spinal cord MS lesions, the number of immature oligodendrocytes (O4+) in lesions was positively correlated with the number of debris-containing macrophages [336].

Those studies overwhelmingly indicate that remyelination and inflammation are intertwined and for remyelination to happen, inflammation has to be present. This can be partly because 'inflammation' covers wide spectrum of helpful and detrimental T cells, B cells, microglia/macrophages and even perhaps astrocytes. The timing of arrival of these cells and their types may be important or detrimental in successful repair. This observation is particularly important because all current MS therapies are immunomodulatory (as discussed in subsection 1.3.2). If inflammation is required for remyelination, is an anti-inflammatory therapy impeding remyelination in humans?

### 1.4.3 Remyelination occurs in multiple sclerosis

Studies presented so far which exemplify the importance of remyelination have been conducted in animal models of MS. Studying *post-mortem* tissue from MS patients has definitively revealed that remyelination also occurs in MS.

Remyelination was initially confirmed by electron microscopy in human [244] [251]. It has the characteristic features of thinner myelin (even after months of remyelination thickness does not go back to normal [181]), shorter internodes [107], and wider nodes of Ranvier [334]. Moreover, in one histological study, 42% of the investigated 161 human lesions showed signs of remyelination [16]. A study of 2 MS patients with long lasting disease showed that 22% of their lesions were fully remyelinated, 73% were partially remyelinated and 5% completely demyelinated [240] indicating that in the majority of lesions some remyelination happens.

On the contrary, remyelination is dependent on the disease chronicity with patients with early stage MS remyelinating better (80% of lesions showing signs of remyelination) than patients with chronic MS (60% of lesions showing signs of remyelination) [109]. Remyelination is also dependent on the anatomical location of the lesion [242] [109], age [274] and sex [174]. Females remyelinate better [174] while age is negatively correlated with the speed of remyelination [274].

When remyelination happens in MS, it is in active lesions where there is still a strong immune reaction [249] and demyelination and remyelination often coexist [250]. This again indicates the importance of inflammation in remyelination as discussed in section 1.4.2.

However, remyelination is often insufficient to overcome the damage. Moreover, there is great difference between the remyelination potential of different patients. In a *post-mortem* study of 51 patients with relapsing-remitting and progressive MS, it was found that around 20% of them were efficient remyelimators with more than 60% of the total lesion area being remyelinated [242] while the rest were not. Moreover, the extent of remyelination was positively correlated with longer disease duration and older age at death [242]. This means that remyelination happens at any stage of the disease (although the earlier in the disease, the better the remyelination [109]) and the better a patient is at remyelinating, the higher the chances for survival.

For remyelination to happen, OPCs need to be recruited into the area of damage, differentiate and ensheath the axons.

## 1.5 OPCs

As discussed in subsection 1.2.2, upon demyelination, oligodendrocytes are killed. For remyelination to happen, new cells with remyelination potential are required. After extensive debate in the literature, it was found that those remyelinating cells come from the OPC progenitor population [104] [324] and not from mature oligodendrocytes that are already present.

### 1.5.1 OPC recruitment and maturation are required for remyelination

For a lesion to remyelinate, OPCs need to be activated and recruited into the area of damage by migration and proliferation. OPCs that remyelinate axons either come from the lesion or from the immediately surrounding NAWM. In fact, in rat, it was shown that OPCs can be recruited only from a 2 mm rimm around the lesion [94]. Furthermore, the OPCs need to mature into

myelinating oligodendrocytes, engage the axons, ensheathe them, and finally create compact myelin. Remyelination could be ineffective because of failure of the OPC to carry out any of those processes.

### 1.5.2 OPCs: discovery, detection and heterogeneity

OPCs were identified around 50 years ago by their distinct electron microscopy features from the previously characterised oligodendrocytes, astrocytes and microglia [320] (Figure 1.1), OPCs are extensively spread throughout the brain and found throughout life [173] and constitute around 5–8% of all the glial cells in the CNS [172].

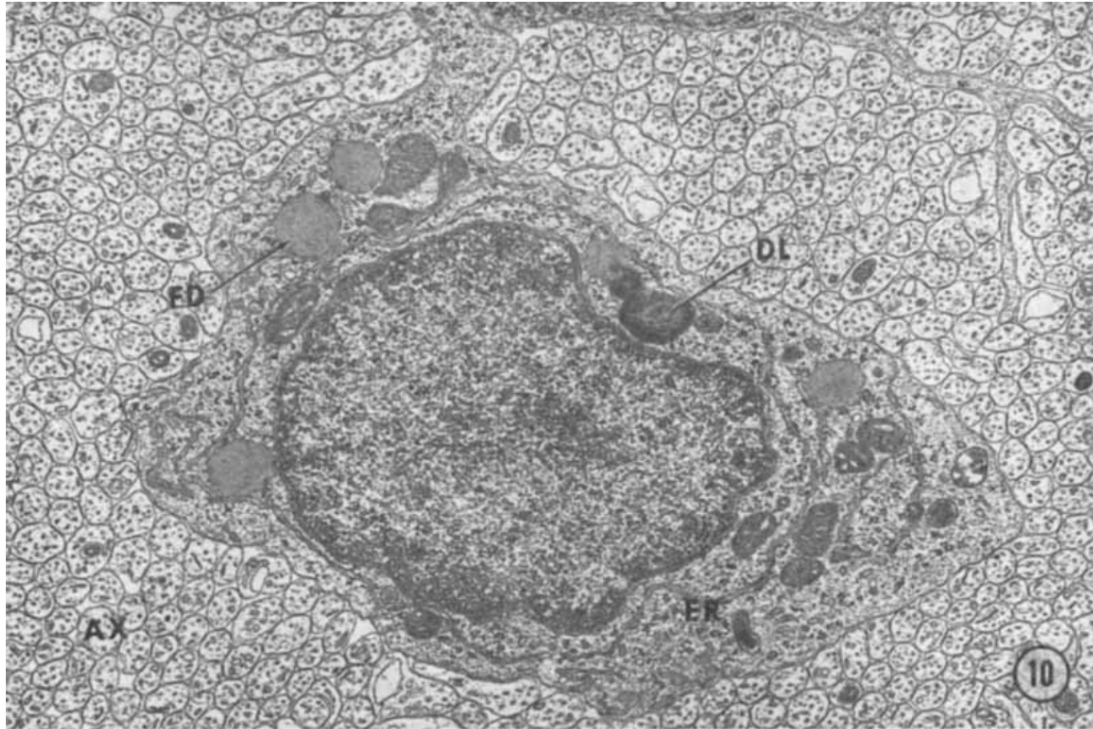


Figure 1.1: Electron microscopy image of OPC surrounded by unmyelinated axons in an optic nerve (postnatal day 1). Cell identification used to be performed by electron microscopy features of the nucleus and surrounding organelles — a skill which we have now lost. Magnification is x14800. Image from [320]

OPCs are often labelled by antibodies against the proteoglycan NG2 [289]. When OPCs start differentiating into immature oligodendrocytes, they express O4 sulfatide [286] and mature oligodendrocytes express myelin basic protein, MBP.

#### Origin

Although all OPCs express those markers, they are not all the same. OPCs have distinct positional (dorsal and ventral neuraxis) and time origin (early vs late development) [316] giving rise

to a inherently heterogeneous population [307]. OPCs can also arise from the subventricular zone stem cells both in normal homeostasis and following LPC-lesion in the corpus callosum and contribute to the remyelinating oligodendrocytes [215] [340] [197]. There is also evidence that SVZ stem cells are proliferating more in MS than control and were also found in active lesions next to the SVZ [216] indicating that the same could be true in human. To add to this heterogeneity, OPCs from young and old animals are different as well.

### Young and old

OPCs from adult and neonatal animals appear to be different in terms of their cell cycle as well as migration, differentiation and myelination capacity with adult OPCs being inferior [352] [48]. The same is true for adult purified human OPCs which have a reduced proliferation rate and survival and process outgrowth compared to neonatal cells [267]. Comparison of remyelination between young and old rats revealed that particularly the OPC recruitment but also the maturation into oligodendrocytes was slower in the older animals [277]. This is important in MS because of its prolonged duration and suggests that human OPCs will be recruited and mature worse with age as well. However, isolated adult human OPCs can migrate and extensively remyelinate brain of *shiverer* mouse, which completely lacks myelin [333]. This shows that even in adulthood, OPCs have an impressive potential to repair, but it is less than it has been in youth.

### 1.5.3 Oligodendroglial roles

Oligodendrocytes are known for their role in myelinating axons during development and OPCs are known as a dormant cell type in the CNS with the potential to differentiate into oligodendrocytes which then can repair. However, this is not the only role for either of those cell types. For example, OPCs primarily differentiate into oligodendrocytes. However, OPCs are also known to be have a limited ability to differentiate into astrocytes [255], Schwann cells [350], and controversially neurones [59] [60]. Oligodendrocytes also contribute to the axonal energy supply.

### Trophic support

Trophic support has been emerged as a new role for oligodendrocytes in addition to wrapping axons with myelin sheaths. Loss of myelin sheath protein PLP in mice resulted in overall normally appearing myelin; however, the mice exhibit axonal degeneration [114]. Similarly, an oligodendrocyte phosphodiesterase, CNP1, was also shown to be essential for axon support without involvement in the myelin formation [167]. Furthermore, knockout of MAG, a minor myelin constituent, also resulted in axonal degeneration with little effect on the myelin itself [235]. In the same way, ablation of oligodendrocytes leads to axonal injury without obvious demyelination [232]. Finally, it has been found that loss of PLP1, a myelin protein, in mouse leads to axonal degeneration which is length-dependent without evident myelin effects [103] supporting the same hypothesis. Similarly, patients with PLP mutations also show overall structurally

normal appearing myelin but accumulate axonal loss with time [103] indicating that the same mechanisms are probably active in human.

All of those studies indicate that oligodendrocytes support axons with more than just a myelin sheath. Therefore, it was proposed that myelinating oligodendrocytes support axons by trophic support [221] by secreting local factors. Deletion of MCT1, a transporter for lactate, pyruvate, and ketone bodies, in mature oligodendrocytes resulted in axonal damage and death [170] indicating the importance of the metabolic support of the oligodendrocytes for axonal integrity. Similarly, BDNF and NT3 neurotrophic factors, produced by oligodendrocytes *in vitro* and *in vivo* were able to enhance neural function [63]. Furthermore, myelinating oligodendrocytes are proposed to be able to remove organelles from axons [288] in order to help them cope with stress. Finally, following neuronal activation *in vitro*, nonmyelinating oligodendroglia were observed to release supportive exosomes with protein and RNA which are taken up by neurones [96]. Therefore, oligodendrocytes can support neurones by providing metabolic support, neurotrophic factors as well as transporting organelles, protein and mRNA.

While oligodendrocytes are involved in supporting the axon, axons are believed to be able to regulate OPCs via electrical signals.

### **Part of the electrical system**

OPCs were found to receive synaptic input [21] and some OPCs are able to integrate the synaptic input and generate action potentials [145]. In the developing brain, there is evidence that glutamatergic synapses regulate OPC proliferation [187] essentially linking experience and electrical activity of neurones to OPC numbers. The synaptic input is lost when the cells transition to premyelinating oligodendrocytes [65].

### **Repair**

When demyelination happens, oligodendrocytes die and OPCs are responsible for remyelination. Although OPCs are the major remyelinating cell of the CNS, there have been reports of Schwann cell remyelination in the human spinal cord lesions [134]. In addition to remyelination, oligodendrocytes express a wide variety of immunomodulatory molecules and are increasingly viewed as being able to influence the immune system [351]. This means that they might be involved not only in remyelination but also in attenuation of the immune attacks.

Even though they are supposed to be the cells maturing into myelinating oligodendrocytes to repair the damage, it has been found that OPCs are more susceptible to stress and TNF-induced cell death than oligodendrocytes [61]. The same is true for purified adult human OPCs which were found to be less able to survive than mature oligodendrocytes [267]. This indicates that any OPCs which will contribute to the remyelination process likely comes from an area slightly removed from the area of damage and it needs to migrate to get there.

Even though OPCs have the potential to remyelinate and repair the damage, remyelination in MS is often insufficient to overcome the constant damage by the immune system and eventually fails.

## 1.6 Why does remyelination fail in MS?

Even though remyelination eventually fails in all patients, there are multiple reasons for this failure connected to the processes that an OPC goes through leading to remyelination, discussed in section 1.5.1 [90].

### 1.6.1 OPC recruitment failure

One of the reasons remyelination fails in MS is because there are not enough OPCs in the lesion. To support this, some chronic inactive lesions were found to have significantly fewer OPCs than the surrounding NAWM [46]. Moreover, in a study of *post-mortem* tissue from 56 MS patients, in 30% of patient oligodendrocyte numbers were markedly reduced in chronic lesions [179] indicating that insufficient numbers due to failure of recruitment could be responsible for the chronic character of the lesion. This proportion of lesions lacking OPCs as well as chronic lesions which show failure in OPC recruitment was corroborated by another *post-mortem* study of 10 MS patients [29]. In it, 37% of the lesions were found to contain lower numbers of OPCs than white matter control brain and most chronic active lesions contained very few OPCs [29].

In another series of post mortem MS lesions, in active lesions, oligodendrocytes were confirmed to die but the majority of lesions failed to repopulate with OPCs. All 20 active lesions had reduced oligodendrocyte numbers compared to control [61] representing the result of the oligodendrocyte damage and death discussed in section 1.2.2. Some of the lesions (45%) had an increased OPC number compared to control indicating successful recruitment; however, the majority (55%) had less OPCs than control [61]. This decrease in OPC numbers is indicative of death of OPCs and failure of recruitment of new OPCs.

Finally, in a further study of 10 MS patients, 29% of the lesions did not contain pre-myelinating oligodendrocytes (as defined by antibodies to O4) [47] suggesting that there was not enough OPC migration into the lesions or that OPCs arrive but do not differentiate even into pre-myelinating oligodendrocytes. The majority (78%) of those lesions which lack pre-myelinating oligodendrocytes are from patients which have had the disease for more than 20 years [47] indicating that migration could be more prone to failure with prolonged disease. To support this, in cortical lesions, OPCs were found to decrease in number with disease progression [263].

Therefore, it is generally accepted that OPC recruitment fails in a third of MS cases/lesions while insufficient OPC maturation is responsible for the rest.

### 1.6.2 OPC maturation block

In human, the predominant reason for remyelination failure is believed to be a block in OPC maturation. Analysis of *post-mortem* tissue from MS patients revealed that in chronic lesions there were plenty of immature oligodendrocytes (O4+) which were neither dividing nor maturing into myelinating oligodendrocytes which suggested differentiation block as reason for impaired remyelination [335]. Mature oligodendrocytes (Olig2+ NogoA+) were rarely found in chronic

lesions while they were present in more active lesions and NAWM indicating further that remyelination could fail because of maturation block [162]. Moreover, in a study of *post-mortem* tissue from 56 MS patients, 70% of patients had marked oligodendrocyte destruction in active lesions but extensive oligodendroglial coverage in chronic lesions [179] indicating a maturation block of those present OPCs could be responsible. Finally, in a study of 10 MS patients, the majority of lesions (71%) were found to contain pre-myelinating oligodendrocytes [47] supporting the differentiation block hypothesis.

Overall, in around 70% of patients/lesions, oligodendroglia were present in the lesion but had not differentiated into myelinating oligodendrocytes while in the other 30%, oligodendroglia were absent or reduced in the lesion. These insights into the mechanism of the human disease are essential to guide development of new therapeutic targets to aid remyelination.

### 1.6.3 Novel therapeutic targets for MS

There two therapeutic options in promoting remyelination in MS — transplantation of remyelinating cells or enhancement of endogenous remyelination. Even though transplantation has been shown to enhance remyelination in animal models and transplanted cells are even proven to migrate better than endogenous cells [26], it would be extremely difficult to clinically deliver exogenous cells in a multifocal disease like MS.

Therefore, central to the current therapeutic efforts in multiple sclerosis is the aim to improve endogenous remyelination. Maturation is the primary reason for remyelination failure and it has been the focus in remyelination research for a long time. There are numerous compounds which have been developed to either promote maturation or to inhibit endogenous maturation blockers. For example, LINGO-1 has been shown to be upregulated in MS and disease models and inhibition of this Nogo receptor interacting protein has been proven to be beneficial in variety of animal models [200]. A blocking antibody against LINGO-1 has been tested in a Phase II clinical trial (AFFINITY) as an add on to disease modifying therapies in relapsing MS patients to determine if it can slow down accumulation of disability. The results have not been formally published yet, but the trial did not reach its primary endpoint. There were small improvements in neurophysiological measures reported in some patients, but clinical benefit has not yet been seen.

Moreover, even drugs which are already clinically approved for other conditions have been found to increase maturation of OPCs. For example, anti-muscarinic compounds were found to induce oligodendrocyte differentiation and thus remyelination in a variety of animal models [75] [196]. Clinically approved drugs should find their place in the multiple sclerosis clinic faster as their safety is already established in humans. Furthermore, there are numerous drug targets in pre-clinical development (e.g. retinoic X receptor  $\gamma$ , bexarotene, clemestine [112]). Therefore, we hope that there will be a maturation enhancing drug in the clinic soon.

Even though OPC recruitment in the developing brain is a carefully regulated and well studied process involving many secreted and contact dependent cues [66], OPC recruitment in MS is not as well studied. Moreover, enhancing recruitment of oligodendrocyte precursor cells

(OPCs) to the areas of damage is a clinically unexplored target and could add another class of drugs to the multiple sclerosis therapeutics. OPC recruitment will be explored in more detail before concentrating on the molecules I have modulated to promote OPC migration.

### 1.6.4 Recruitment and proliferation of OPCs

The repopulation of OPCs in an area of damage involves their activation, proliferation and migration.

#### Activation of OPCs

In recent years, the idea that OPCs have to be activated before they start remyelinating has emerged. Transcriptome studies of purified mouse OPCs from normal and cuprizone treated condition have revealed that upon activation, the transcriptome of adult OPCs resembles that of neonatal OPCs more than non-activated adult OPCs [210]. Numerous factors have been found to be upregulated in the activated OPCs which will eventually form oligodendrocytes which remyelinate the denuded axons after demyelination including proliferation markers and transcription factors such as sonic hedge hog (Shh) [93]. Shh, which is important in neonatal and adult oligodendrogenesis, is upregulated in oligodendrocytes in demyelinating disease models and increases survival, proliferation and differentiation of oligodendroglia [87]. Activated OPCs migrate and differentiate faster than non-activated OPCs [210]. The OPC activation is driven by the immune response [108] again pointing to the importance of inflammation in repair discussed in section 1.4.2.

#### Repopulation of OPCs

OPC migration into the area of damage is a necessary step for remyelination. Using fate tracing of proliferating NG2+ cells in a demyelination model, OPCs were initially found exclusively at the lesion periphery (day 2 post lesion) and then decreased from the periphery and increased in the lesion centre (day 7 post lesion) before they matured into myelinating oligodendrocyte [324]. After OPCs are recruited into the lesion to remyelinate, this leaves the zone around the lesion with less OPCs than before demyelination for 2 months [148]. Moreover, upon demyelination, OPCs also undergo extensive proliferation in vivo [37] [257] [148] which aids repopulation of the demyelinated areas with OPCs.

Normally, in the cuprizone model of demyelination, mice are fed cuprizone for 6 weeks and then this diet is stopped to allow for repair to happen. When mice are fed cuprizone for longer than 12 weeks endogenous remyelination fails [191]. OPCs continuously migrated into the lesion but then underwent apoptosis and this resulted in progressive depletion of the OPCs in the lesion [191]. This chronic cuprizone model may be a better representation of the repeated damage in a chronic disease like MS and recapitulates the remyelination failure of MS which other models do not. However, it does produce global rather than focal demyelination.

In a different model of repeated cuprizone administration mimicking recurrent demyelination insults, remyelination was slower and less efficient due to decrease in oligodendrocyte repopulation [140]. Both of those studies indicate that it is possible that recruitment only fails after certain threshold of repeated insults. This is supported by the observation discussed in section 1.6.1 that OPC depopulated lesions were primarily from patients with disease duration over 20 years [47].

However, this recruitment failure is not true in every chronic/repeated damage model. Four rounds of experimental demyelination in the subpial cortical region via EAE were not enough to deplete OPCs [263]. On the other hand, OPCs are depleted in the subpial cortical region lesions in *post-mortem* MS tissue [263]. This indicates the great discrepancy between different animal models as well as animal models and human disease.

The idea that recruitment fails upon chronic/repeated damage is further supported by the comparison of two studies involving PDGF-A, a well known chemoattractant and mitogen. PDGF-A did not improve remyelination in an acute model of demyelination (6 weeks cuprizone) [337] but it did in a chronic model of demyelination (12 weeks cuprizone) [319]. Therefore promoting OPC migration is much more important in a chronic/repeated damage than in acute damage. To further support the effectiveness of pro-recruitment modulators, in a rat LPC-model of demyelination, PDGF injection improved remyelination 10 fold [6]. While injecting growth factors in the brain is not a therapeutic option for people, it clearly shows that therapy which improves recruitment could be highly beneficial.

To further investigate the therapeutic potential of OPC recruitment modulators, I have looked at 2 different targets involved in OPC migration: NDST1/HS and Sema3A/NP1.

## 1.7 ECM and NDST1/HS

The extracellular matrix (ECM) was once thought to be a mesh providing mechanical support but it is now increasingly clear that the heterogeneous molecules in the ECM are involved in a variety of functions such as signalling, cell behaviour, and pathogenicity.

### 1.7.1 Role of ECM

ECM consists of a mesh of immobile secreted molecules which surrounds the cells in all tissues and provides the microenvironment in which they thrive. It is secreted by most cells in the central nervous system and can be remodelled or degraded by matrix metalloproteases (MMP) [318]. ECM has a structural role such as maintenance of the BBB but can also be involved in signalling, primarily via the integrin family of cell surface proteins connecting the intracellular cytoskeleton with the extracellular tissue architecture. For example, heparan sulfate proteoglycans on the plasma membrane surface are required to induce an activation conformation change of fibroblast growth factor-2 (FGF-2) before it can signal via the FGF receptor [102]. FGF-2 is a well known regulator of OPC survival and recruitment which is strongly implicated in remyelination [198] which means that heparan sulfate is involved in OPC behaviour and repair.

In a disease state the ECM changes and often makes the environment more or less permissive for repair.

### 1.7.2 ECM changes in MS

In multiple sclerosis, pro-inflammatory cytokines from activated immune cells have the potential to regulate the transcription of MMP [186] to modulate the integrity of the BBB but would also change the ECM composition. ECM changes have been widely observed in MS. Bioinformatic analysis of the proteome of active vs chronic active MS lesions revealed that ECM components (including heparan sulfate proteoglycans) and ECM signalling (primarily via integrins) were part of the molecular pathways responsible for transition into chronic lesions [271]. For example, heparan sulfate proteoglycans, which are normally found only in the basal membrane around blood vessels, are also found accumulated in human active MS lesions without blood vessel contact [317]. Moreover, TNF $\alpha$  expressing immune cells were in immediate proximity to those areas with ECM dysregulation and are believed to be responsible for it [317]. This is obviously different than heparan sulfate's normal function.

### 1.7.3 Heparan sulfate

Heparan sulfate and heparan sulfate proteoglycans are sulfated linear polysaccharides found on the ECM, basal membrane and cell surface and are part of glycosaminoglycan (GAG) family. Heparin, which is a highly sulfated form of heparan sulfate, is expressed in mast cells and is used as an anticoagulant. Heparan sulfate and heparin initially consist of alternating D-glucuronic acid and N-acetylglucosamine residues [178] as shown in figure 1.2. Those residues are then extensively modified in a variety of different ways resulting in diverse geometries to execute different functions [178]. The sulfation pattern is the strongest functional determinant.

In normality, heparan sulfate binds numerous ligands such as growth factors and signalling molecules including Sema3A and VEGF<sub>165</sub> as discussed in section 1.12 and this binding has functional consequences. Due to those ligand interactions, heparan sulfate is involved in numerous processes including leukocyte development and migration, cytokine and chemokine function as well as immune processes [278].

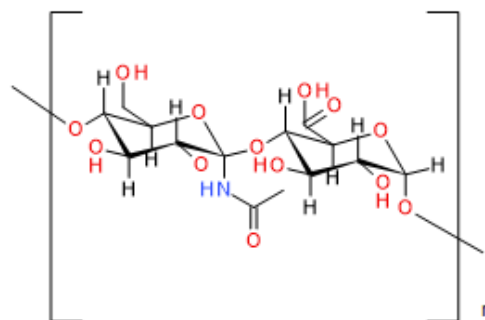


Figure 1.2: Heparan sulfate is a polymer of alternating D-glucuronic acid and N-acetylglucosamine. Figure drawn on ChemDraw by Scott Webster.

### 1.7.4 NDST1

N-deacetylase N-sulfotransferase1 (Ndst1) is the first enzyme which modifies heparan sulfate and is part of the 4 NDST enzymes. The human NDST1 was cloned following association of this region of the genome with Treacher Collins Syndrome, a craniofacial development disorder [76]; however, its causative role in this syndrome is under scrutiny [106]. In rat, NDST1 was already identified as the enzyme responsible for the initial and rate limiting steps in heparan sulfate synthesis — N-deacetylation and N-sulfation [327] shown in figure 1.3.

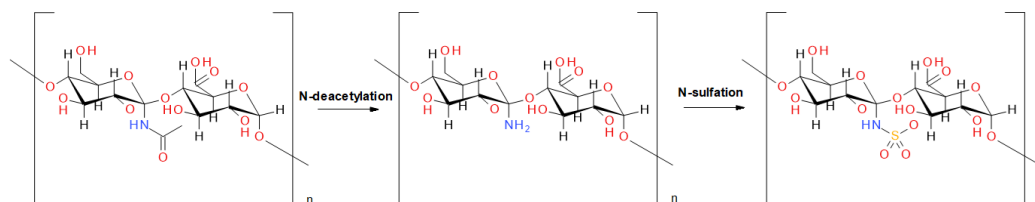


Figure 1.3: NDST1 enzyme catalyses the N-deacetylation and N-sulfation of heparan sulfate. Figure drawn on ChemDraw by Scott Webster.

As the first step in HS synthesis, NDST1 is a regulator of the subsequent enzymatic reactions because they depend on NDST1's modifications. NDST1 and the other HS modifying enzymes are found in specific parts of the Golgi apparatus to ensure proper sequential HS synthesis and modification [130]. The crystal structure of the sulfotransferase domain of NDST1 has been solved and revealed a spherical protein with an open cleft (shaped like the packman character) where the heparan sulfate chain resides [142] and is shown in figure 1.4.

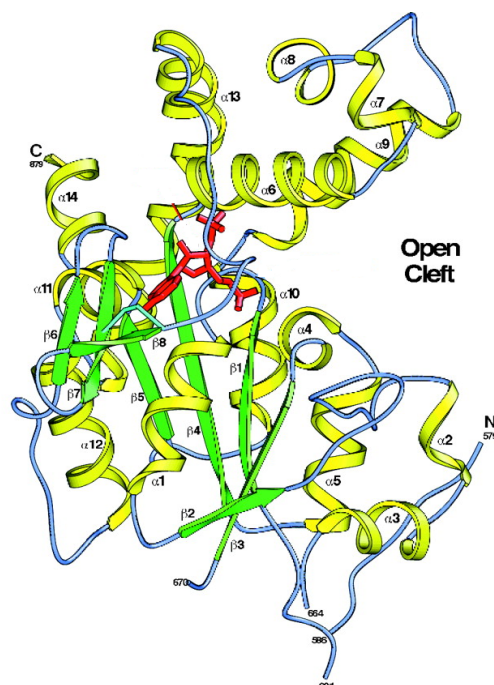


Figure 1.4: NDST1 sulfotransferase domain is spherical with an open cleft [142].

Heparan sulfate and NDST1 are so important for normal physiology that NDST1 KO mice have reduced sulfation of HS and die shortly after birth [261]. The reason for the lethality is insufficient surfactant production by their lung epithelial cells [261] but there are many other abnormalities.

NDST1 is also upregulated in femoral artery wire injury model where NDST1 mRNA is upregulated 20 times in the damaged blood vessels [4]. NDST1 deletion in vascular smooth muscle cells revealed that it is involved in their proliferation, vessel size, and vascular remodelling after injury [3]. This upregulation in injury might be important in disease state such as MS.

## 1.8 Neuropilin 1 and Semaphorin3A

The other molecular targets to modulate OPC recruitment are Neuropilin 1 and Sema3A. Sema3A is a soluble chemorepellent for OPCs in development and MS while Neuropilin 1 is its receptor found on OPCs and many other cells.

### 1.8.1 Semaphorin3A

Semaphorin3A is part of the semaphorin family. The family consists of secreted and membrane-bound proteins which contain sema domain (dimerisation and receptor binding) and cysteine-rich plexin-semaphorin-intergrin (PSI) domain and are involved in cell proliferation, survival, differentiation as well as chemorepulsion and chemoattraction of cells and neuronal neurites [141]. Even though NP1 is the primary receptor for Sema3A [330] [245] [29], plexins are the primary receptor for the majority of semaphorins [141].

Sema3A was the first mammalian semaphorin to be discovered and is therefore a prototype of the secreted members of the family. Sema3A was isolated and characterised by purification of a protein with the ability to collapse the tip of the growing axon called the growth cone from chick brain [182]. The 100kDa glycoprotein was named collapsin and even then it was suggested that it is a secreted protein with a basic region for binding ECM and an immunoglobulin-like domain with adhesive properties [182] which we now know is true. It was found to collapse neuronal growth cones with high potency [182] due to loss of actin polymerisation at the leading edge of the growth cone [83]. It was later found to also repel axons of dorsal root ganglion neurones [199] and also be able to steer growth cone away from a Sema3A source [84]. Therefore, Sema3A is able to induce growth cone collapse and steer growth cones away in order to navigate neurites and it is important for the development of proper nervous system connections.

This was confirmed by genetic knockout of Sema3A which manifested in abnormal projections in the CNS [20] and PNS [306] as well as bone and cartilage abnormalities and heart defects [20]. The phenotype and survival of the KO was dependent on the genetic background of the mice and one of the mouse KO lines survived well into adulthood [306] while the other one survived only a few days postnatally [20]. Therefore, Sema3A's role in the correct connection pattern for specific neuronal populations was confirmed but also new roles in the cardiovascular system, bone and cartilage emerged due to the patterns of the defects in the KOs.

Even though *Sema3A* is a repellent for cortical axons, *Sema3A* is a chemoattractant for the apical dendrites of pyramidal neurones because of different signal transduction machinery in the dendrites and the axon [247]. *Sema3A* also promotes the growth of cortical dendrites and this growth is dependent on MMP-2 [110] indicating the importance of ECM remodelling for this to happen. Moreover, it is involved in cell behaviour of many non-neuronal cells. For example, *Sema3A* negatively regulates oligodendrocyte process outgrowth [259], maturation [296] and migration [287].

*Sema3A* can be regulated by miRNA and can regulate the translation of its downstream signalling molecules [141]. Moreover, *Sema3A*'s downstream signalling response depends on its concentration — it depends on local protein synthesis at low *Sema3A* concentrations and does not depend on local protein synthesis at high *Sema3A* concentrations [188]. *Sema3A* can also be regulated by post-translational protease cleavage. In the initial study which discovered *Sema3A*, it was suggested that collapsin (*Sema3A*) splice variants exist [182]. *Sema3A* is expressed as inactive precursor which is processed by a protease such as furin into its potent isoform (95 kDa) and can be further processed to a much less potent isoform (65 kDa) [2] giving a post-transcriptional way to regulate *Sema3A* expression. Moreover, *Sema3A* dimerises via cysteine-cysteine disulphide bonds and this dimerisation is necessary for its activity [154]. For exerting their activity, semaphorins often depend on their receptors and coreceptors [141].

### 1.8.2 NP1

Neuropilin 1 is a transmembrane tyrosine kinase receptor and the primary receptor for *Sema3A*. Neuropilin 1 was identified and characterised in a series of studies due to its recognition by a monoclonal antibody (A5) in neurones of the *Xenopus* frog [298]. NP1 is a 140 kDa transmembrane protein consisting of a1 and a2 CUB domain, b1 and b2 (coagulation factor V and VIII homology domain) and c (MAM) extracellular domain, followed by transmembrane domain and a short 40 aa cytoplasmic tail with no obvious domains [298]. Those domains are shown in the recently solved crystal structure of NP1 [136] in figure 2.1. Neuropilin 2 was also identified by its 44% homology to Neuropilin 1 [153]. NP2 was found not to be a receptor for *Sema3A* although it binds other semaphorins [52].

NP1 could be post-translationally modified by O-linked glycosylation [345] but the prevalence and importance of this modification is still unknown. There are soluble truncated NP1 variants which consists of the a1,a2,b1,b2 domains [264] which could antagonise the full length receptor by sequestering its ligands without exerting any effects. The expression level of NP1 is known to be regulated not only by transcription factors but also by faster mechanisms including control by miRNA and cAMP [141]. NP1 can be regulated by sulfated polysaccharide-induced internalisation in endothelial cells [219]. Neuropilin 1 is involved in many different processes and systems.

Neuropilin-1 KO mice have severe abnormalities in the projections of the peripheral neural system [152] and are embryonic lethal [152] due to vascular defects [147]. Neuropilin-1 KO dorsal root ganglion neurones do not show growth cone collapse by *Sema3A* [152] which

strongly suggested that NP1 is indispensable for Sema3A signalling. The abnormality in the projections in the Sema3A and NP1 KO mice are very similar and stem from the inability of those two molecules to bind and guide the developing neurites. To support this, in development, NP1 is upregulated in axons and growth cones during the process of axon development and then is downregulated upon the completion of neuronal circuitry [299].

NP1 is a receptor for many different factors and it often uses another signalling coreceptors to transduce its effects [253] because its small intracellular domain does not contain any signalling motifs. One of the few NP1 dependent effects solely mediated by the intracellular domain of NP1 is vascular permeability via CendR peptides [265]. The NP1 intracellular domain can often be involved in modulation of the signalling of other receptors — for example it can promote kinase activation while in a receptor complex with VEGFR2 [86].

### **NP1 is a receptor for Sema3A and other semaphorins**

Neuropilin 1 was identified from two independent screens for Sema3A-binding proteins in a cDNA expression library obtained from mRNA from DRG and spinal cord tissue [153] or DRG tissue [125]. Neuropilin 1 was found to bind Sema3A directly and with high affinity ( $K_D = 1.5nM$ ) [153] and ( $K_D = 0.3nM$ ) [125]. Sema3A's repellent effect on DRG axons could be decreased two fold but not abolished by addition of anti-neuropilin antibodies [153]. Similarly, Sema3A's repellent effect on DRG axons and growth cone collapse could be decreased almost completely in a dose-dependent manner by addition of anti-neuropilin antibodies in an other study [125].

In addition to this direct binding, NP1's in vivo expression in Sema3A sensitive neurones and the similarity in the projection and vascular abnormalities in the phenotypes of the NP1 KO [152] and Sema3A KO mouse [306] [20] further strengthened the view that NP1 is Sema3A's endogenous receptor [153] [125]. NP1 was further shown to mediate the Sema3A mediated growth cone collapse in DRG neurones [188] and sympathetic nervous system neurones [51]. Moreover, there are indications that NP1 mediates Sema3A's effects in other cells as well. For example, Sema3A's negative effect on oligodendrocyte process outgrowth mentioned in sub-section 1.8.1 was partly inhibited by addition of anti-neuropilin1 antibodies [259]. While those papers clearly show NP1's involvement in Sema3A signalling, they do not exclude involvement of other receptors [125].

Neuropilin 1 is also shown to be able to bind other semaphorins [253]. NP1 expressing COS cells bind to Sema3A, Sema3C and Sema3F in vitro [52]. Similarly, in another study, NP1-expressing COS cells were found to bind Sema3A, Sema3B, and Sema3C with similar affinity ( $K_D = 0.8nM$ ,  $K_D = 0.6nM$  and  $K_D = 1.4nM$  respectively) [301]. To support this, Sema3C acts through NP1 in vivo to modulate angiogenesis in the retina [343]. Moreover, Sema3A and Sema3B compete with Sema3A for NP1 binding and excess of either can reduce the Sema3A's repulsive action of DRG axons in vitro [301] indicating that they bind the same binding site. Finally, regulatory T cells express NP1 which has been found to interact with class IV of semaphorins, particularly Sema4A, in order to modulate some T cell functions as well as

their stability [73].

In addition to those semaphorins, NP1 is also a receptor for  $VEGF_{165}$ .

### **NP1 is a receptor for $VEGF_{165}$**

Neuropilin 1 was later identified as a novel receptor able to bind  $VEGF_{165}$  directly and with high affinity ( $K_D = 32nM$ ) but also to enhance  $VEGF_{165}$  binding to other VEGF receptors and their effects by its presence [284].

Sema3A and  $VEGF_{165}$  are the classical NP1 ligands but recent research has shown that NP1 is a receptor for increasing amount of other ligands.

### **Non-classical NP1 ligands**

The reason for the numerous ligands of NP1 is the adhesive property of its immunoglobulin-like extracellular domain [182]. For those ligands, NP1 is not essential but acts as a coreceptor enhancing their responses in normal and cancer cells including  $TGF\beta$ , HGF and integrins [253]. This is similar to NP1's effect of enhancing  $VEGF_{165}$  action via its other VEGF receptors discussed in the previous section. One of those ligands is PDGF-D which binds directly to NP1 and NP1 acts as its co-receptor together with  $PDGFR\beta$  [211]. Furthermore, NP1 is also reported to be able to bind miRNA, short non-coding RNA which regulates genes, and the miRNA binding protein, AGO2 [252]. NP1 is involved in their internalisation in the cell which allows them to fulfil their gene regulatory function [252]. The variety of non-classical NP1 ligands further expands the functional importance of NP1 because it enhances the effect of many signalling molecules.

### **NP1 mediates Sema3A and VEGF effects**

It has long been debated whether Sema3A and VEGF bind to overlapping or distinct sites on NP1. Functional and binding studies have suggested that Sema3A and  $VEGF_{165}$  compete for NP1 binding and therefore have overlapping binding sites [201]. Furthermore, Sema3A's negative effect on oligodendrocyte process outgrowth mentioned in subsection 1.8.1 was partly inhibited by addition of  $VEGF_{165}$  [259]. Similar results were found in mutation studies where the a1,a2 and b1,b2 domains were found to be important for Sema3A binding and the b1,b2 domains important for VEGF binding [115].

However, NP1 blocking antibodies specific for Sema3A-NP1 binding and VEGF-NP1 binding suggest that the binding sites might be separate [236]. The anti-NP1(Sema3A) antibody disrupted Sema3A's functional effect on growth cone collapse while anti-NP1(VEGF) antibody did not and conversely anti-NP1(VEGF) antibody prevented VEGF binding to NP1 while the anti-NP1(Sema3A) antibody did not [236]. The separate binding sites and the lack of competition between VEGF and Sema3A was further confirmed by crystal structure of the a1,a2,b1,b2 domains together with the same blocking antibodies [10]. The fact that the 7 amino acid change

in the  $\alpha 1$  domain in the NP1(Sema3A-) mice only prevents Sema3A binding without affecting VEGF binding further corroborates this idea [116].

The observed antagonistic effect of the two NP1 ligands could be because when each ligand is occupying NP1, its conformation is not permissive for the other ligand to bind. Also, ligand-induced NP1 internalisation is suggested as functional way to antagonise the other ligand [220] since the available NP1 receptors are reduced. Finally, in endothelial cells it has been shown that the functional competition of Sema3A and  $VEGF_{165}$  is independent of NP1 binding competition but instead dependent on the downstream signalling cascades from NP1 activation by either ligand as well as VEGFR activation by  $VEGF_{165}$  [118].

Sema3A and  $VEGF_{165}$  mediate different and overlapping signals via NP1. Using the NP1(Sema3A-) mouse line in which the Sema3A signalling via NP1 is disrupted while the  $VEGF_{165}$  signalling is intact, it was shown that VEGF-NP1 signalling in endothelial cells is essential for angiogenesis while Sema3A-NP1 signalling is required for proper CNS and PNS projections and both ligands are vital for heart development [116]. Those overlapping signals can also be mediated in a different ways. For example, the cytoplasmic domain of NP1 is important for  $VEGF_{165}$ -induced vascular permeability but not for Sema3A-induced vascular permeability [86]. What is common for both ligands is the overall requirement for coreceptors to mediate signalling together with NP1.

### 1.8.3 Coreceptors

Different coreceptors are known to mediate downstream signalling of Sema3A via NP1 including Plexins, L1, and Unc-33-like phosphoprotein/collapsin response mediator protein (Ulip/CRMP) while  $VEGF_{165}$  signalling via NP1 is mediated interaction by its VEGF receptors. This section will focus on the NP1 binding partners mediating Sema3A signalling.

#### Plexin

Following the discovery of NP1 as a receptor to Sema3A, the transmembrane domain and the cytoplasmic tail of NP1 were shown not to be important for Sema3A signalling in vitro [218]. At the same time, plexins were discovered to be able to bind other semaphorins [332]. The plexin family has 9 members characterised by an extracellular sema domain and intracellular GTPase-activating protein (GAP) domain [141]. The dispensable intracellular and transmembrane domain indicated that another transmembrane receptor mediates the downstream signalling.

Now it is known that the Plexin-Neuropilin 1 complex forms the functional receptor for which Sema3A has higher affinity than to Neuropilin-1 only [300] [136]. The crystal structure of the NP1, Sema3A, and PlexinA2 functional receptor complex was shown to include NP1, Sema3A, and PlexinA dimers [136] as shown in figure 1.5. Only the  $\alpha 1$  domain of NP1 (refer to full length NP1 in figure 2.1) was crystallised in the complex because the rest of the receptor was found in numerous conformations [136]. The  $\alpha 1$  domain of NP1 locks together two molecules which do not normally interact, Plexin and Sema3A [136].

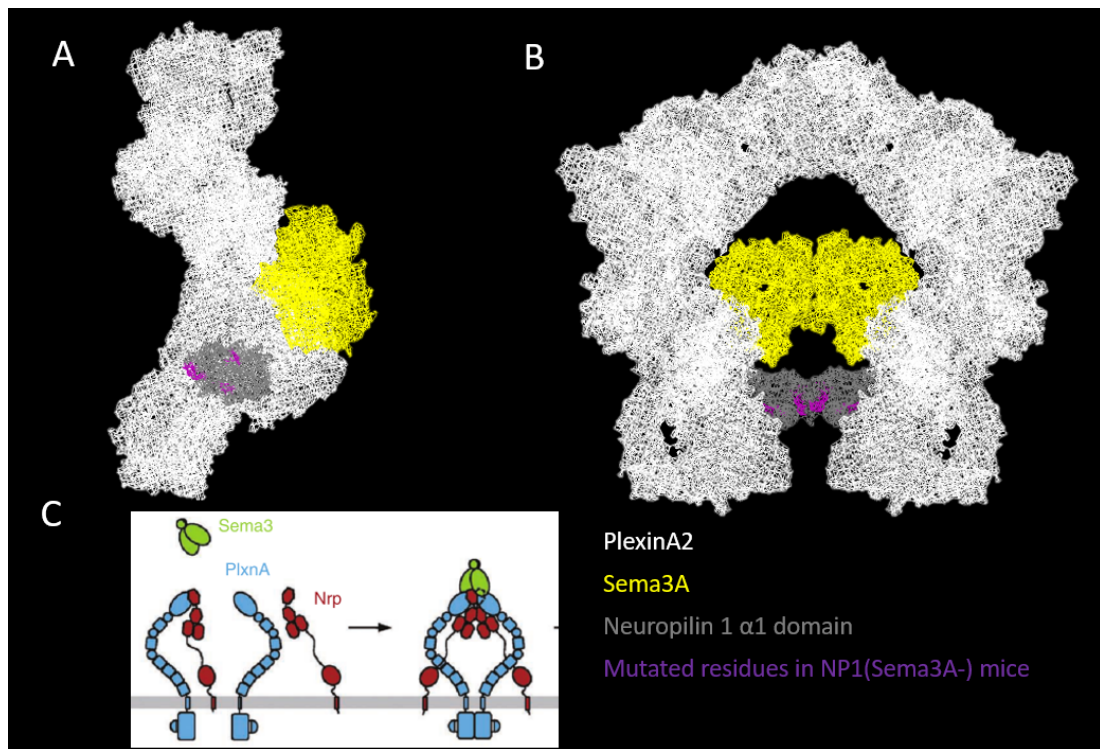


Figure 1.5: Structure of Sema3A, NP1 and Plexin in a complex. Crystal structure of full length plexin, full length Sema3A and  $\alpha$ 1 domain of NP1 (A). Proposed organisation of the molecules in a complex (B). To get these images, the crystal structure from [136] was coloured on Pymol. The location of the 7 mutated amino acids in NP1(Sema3A-) mice at the  $\alpha$ 1 domain of NP1 are highlighted on the wild type crystal structure of NP1. Cartoon of the proposed interaction of Sema3A, Np1, and Plexin from [136]

Sema3A signals are believed to be able to be transduced by NP1 in combination with any of the PlexA1-4 depending on the cell type. Sema3A's chemorepellent effect on neonatal OPCs are primarily mediated via PlexA4 [227]. The mRNA and protein expression of PlexA4 was validated in OPC cell line as well as OPC and immature oligodendrocytes in brain slices [227]. Cytoplasm truncated PlexinA4 greatly reduced but did not abolish the Sema3A-induced process shortening in the OPC cell line. OPCs also express PlexA3 which is important for another semaphorin, Sema3F and this mediated chemoattraction via NP2 [339]. Furthermore, Sema3A's rounding effect on transfected cell morphology was observed only if NP1 and full length Plexin were present but not if NP1 was present on its own or with NP1 and no cytoplasmic plexin-A1 [300] [305]. Finally, mitral cells from the olfactory bulb express NP1 but are insensitive to Sema3A; however, expression of Plexin-A4 results in growth cone collapse by Sema3A [294] indicating that plexin is absolutely required and NP1 is not enough for Sema3A signalling. Those effects are not due to direct binding as Sema3A does not bind Plexins directly [300] [136].

The involvement of plexins in Sema3A/NP1 signalling was further confirmed by plexin-A3 KO mice in which the repulsion of dorsal root ganglion axons by Sema3A is partially reduced

compared to WT [53]. This suggested that plexin is important but other plexins can probably compensate for the loss of one. Moreover, the phenotype of the plexin-A3 KO mouse [53] is similar to the Sema3A KO and the NP1 KO mice which indicates that they are all involved in the same signalling pathway [239]. Plexin is normally autoinhibited by its sema domain and binding of NP1 and Sema3A to it releases the inhibition and allows signal transduction [302].

Plexin has been implicated in CNS diseases. PlexinA2 has been associated with schizophrenia susceptibility and Sema3A has been found to be upregulated in schizophrenia patients [184] as well as amyotrophic lateral sclerosis (ALS) [156].

### L1

Another binding partner involved in the Sema3A/NP1 signalling is L1. L1 is a glycoprotein with 6 immunoglobulin-like domains and 4 fibronectin type 3 domains. Three different L1 KO models as well as human patients having CRASH syndrome caused by L1 mutations [342] show abnormal neuronal track development [143] which has suggested that it might be involved in signalling of neuronal guidance molecules.

Dorsal root ganglion axons and cortical axons from L1-deficient mice are insensitive to Sema3A [40] even though they still express NP1 and Plexins. L1 was shown not to interact with Sema3A directly but instead is suggested to modulate the Sema3A response via NP1 interaction as coimmunoprecipitation shows that NP1 and L1 form a stable complex [40]. Both Plexin and L1 with truncated cytoplasmic domain reduce the response to growth cone collapse by Sema3A indicating that they are both required and suggesting that signalling cascades from Plexin and L1 cooperate to induce the growth cone collapse characteristic for Sema3A [19]. To support this, coimmunoprecipitation with L1 or Plexin finds the other protein as well as NP1 indicating that they are probably all in a complex together [19]. Therefore, L1 is involved in a complex with NP1 and Plexin and removal of any of those components abolishes Sema3A signalling.

In addition to mediating Sema3A repulsion, L1 can also convert Sema3A repulsion to an attraction depending on the way it binds to NP1 [41]. Moreover, L1 mediates NP1 internalisation upon Sema3A binding [42] which would render any cell less sensitive to Sema3A and by this modulates signalling from its other ligands. To make matters even more complicated, Plexin and L1 are not the only 2 known coreceptors involved in Sema3A signalling.

### Other coreceptors

Other coreceptors such as members of the Unc-33-like phosphoprotein/collapsin response mediator protein (Ulip/CRMP) are also believed to be involved in Sema3A signalling [260] [259]. The previously reported Sema3A-induced inhibition of OPC process outgrowth [260] was inhibited by addition of anti-Ulip2/CRMP2 and anti-Ulip6/CRMP5 blocking antibodies [259].

There are numerous other receptors with which NP1 associates to mediate the signalling of the non-classical ligands discussed in section 1.8.2 as well as VEGF receptors to mediate  $VEGF_{165}$  signalling [252].

The numerous coreceptors involved in Sema3A signalling and the numerous NP1 ligands leads to variety of different potential roles in different systems.

### 1.9 Sema3A and Np1 role

Sema3A and NP1 are involved in many processes including injury and repair, and the immune response as well as in the development of neuronal connections, cartilage and bone as well as the cardiovascular system. Those different roles will be discussed below with emphasis on their role in MS models and oligodendroglia.

#### 1.9.1 Sema3A and NP1 in injury, repair and MS models

NP1 and Sema3A KO mice have revealed they have a variety of functions in the developing CNS; however, they are also involved in adult disease and injury.

##### Injury

Sema3A and NP1 are upregulated in many injury models and impairs repair. Removal of the olfactory bulb in rat results in progressive increase of Sema3A mRNA positive cells in the olfactory nerve lesion and contributes to regenerative failure because it repels NP1+ axons away from the lesion [237]. Similar upregulation of Sema3A and NP1 mRNA was observed in a rat stroke model [97]. Moreover, following rat spinal cord injury, Sema3A mRNA is highly upregulated in fibroblasts surrounding the lesion and then downregulated after 56 days [70]. Therefore, the glial scar after injury consists of many cells including fibroblasts which express Sema3A which contributes to the glial scar inhibition by inhibiting neurite growth [223]. The neurones in the lesion did not express NP1; however, NP1 upregulation was observed in the motor cortex [70]. Finally, Sema3A can cause the apoptosis of some neurones in vitro [101] [276] via NP1 and PlexinA3 [326] contributing to its impairment of repair. Sema3A blocking antibodies were able to reduce retinal ganglion cell death after axotomy of the rat optic nerve [275] indicating that Sema3A can induce neuronal death in vivo as well.

Therefore, Sema3A is upregulated in injury and repels NP1+ axons and contributes to neuronal death. Those properties make it a molecule of interest in multiple sclerosis models

##### MS animal models

The expression of Sema3A and NP1 in normal adult white matter of the NS is very limited and extensive upregulation is observed in multiple sclerosis animal models. Sema3A mRNA or protein is not found in the white matter in untreated mice [330]. After LPC lesion in adult rat spinal cord, Sema3A mRNA was upregulated primarily by astrocytes, followed by microglia/macrophages and oligodendroglia as well as neuronal cell bodies whose axons were in the lesion area [123] [330]. 18% of the oligodendroglia express NP1 mRNA which is also expressed in astrocytes, microglia, and neurones [330]. Overall, in the white matter Sema3A

mRNA is expressed by glia and its expression is dependent on inflammation while in the grey matter it is expressed by neurones and believed to be dependent on demyelination and axonal damage [330]. This Sema3A mRNA upregulation was also seen after adult rat CNS lesion but not neonatal rat CNS lesion and this correlates with the neonatal ability to fully regenerate axons in the lesion while the adult fails [238]. Therefore, the mRNA expression of Sema3A and NP1 in astrocytes, macrophages/microglia and oligodendroglia in lesions suggests that it might be negatively involved in repair.

Sema3A protein upregulation was later confirmed in an LPC mouse model of spinal cord demyelination and peaked at 14 days post demyelination [245]. At that time point, more than 50% of the OPCs express NP1 and varying proportions of OPCs express PlexinA1-3 but not PlexinA4 [245]. After ethidium bromide lesion in rat, Sema3A mRNA and NP1 protein were found to be upregulated in astrocytes, microglia/macrophages, and OPCs [296]. In LPC-demyelination corpus callosum mouse model, Sema3A protein is detected at 3 days post lesion but reduces at 7 days post lesion and disappears at 14 days post lesion [29]. In this study Sema3A expression was found on primarily on astrocytes and microglia/macrophages and NP1 was expressed in astrocytes, OPCs and microglia/macrophages [29]. Therefore 3 independent studies have confirmed Sema3A overexpression at the protein level in lesions and NP1 upregulation in astrocytes, macrophages/microglia, and oligodendroglia.

In an EAE model, Sema3A and NP1 were found in surrounding grey matter neurones [117]. In the damaged area astrocytes expressed Sema3A, microglia/macrophages expressed both Sema3A and NP1 and T cells and B cells expressed neuropilin 1 [117]. However, contrary to the LPC and ethidium bromide lesions in the previous paragraph [29] [296] [245], neither oligodendroglial nor astrocytes in this EAE model expressed NP1 [117]. Upon EAE induction, the expression of Sema3A, NP1, and plexin decreased in the peripheral immune system and increased in the resident CNS cells as well as the inflammatory infiltrate [117] suggesting that Sema3A/NP1 might be involved in the immune response.

In addition to the observation of the mRNA and protein level of Sema3A and NP1, modulation of their levels using different techniques and tools helps elucidate their role in MS-like repair and pathogenicity. Increasing the level of Sema3A by lentivirus or recombinant protein injection reduced the number of OPCs in the lesion. Lentiviral mediated gene transfer of Sema3A primarily in astrocytes and in some OPCs resulted in less OPCs recruited to the lesion at 2 days and 7 days after demyelination and this effect was not due to apoptosis and did not affect remyelination [245]. Similarly, injection of recombinant Sema3A into the lesion 6 days after demyelination resulted in fewer OPCs in the lesion at 2, 3, and 4 weeks after demyelination [29]. This resulted in decrease in the numbers of mature cells at the 3 and 4 week time points [29]. This effect was not due to proliferation or apoptosis [29].

Moreover, this decrease in recruitment translated to a decrease in remyelination at 4 weeks as the percentage of the myelinated fibres in the Sema3A treated mice was around 3 times lower than control [29]. The remyelinated myelin in those mice was also thinner than the remyelinated myelin in control [29]. Therefore, increasing the level of Sema3A in a lesion impairs OPC migration resulting in less OPCs in the lesion which impairs remyelination.

In reverse, decreasing the level of Sema3A enhances remyelination. In a Sema3A knockdown mouse, OPC migration and remyelination was improved compared to control as there was a higher percentage of myelinated fibres at 2 and 3 weeks after lesion [29]. The remyelinated myelin in those mice was also slightly thicker (not significant) than the remyelinated myelin in control [29]. Those studies show that the Sema3A level in a lesion negatively correlates with OPC migration and remyelination.

Impairing the ability of NP1 to bind Sema3A also modifies OPC migration indicating that NP1 is the receptor responsible for Sema3A's effect. In NP1(Sema3A-) mice, in which Sema3A cannot bind NP1 while VEGF binding is unaffected, there were increased number of OPCs in the lesion 7 days after demyelination compared to WT mice [245]. Moreover, deletion of NP1 in endothelial cells results in decreased EAE severity because of BBB preservation, altered immune infiltration and decreased demyelination [323]. This indicates again that NP1 is involved in the immune response and that inhibition of NP1 could enhance OPC migration and remyelination as well as reduce the immune damage. The effect of Sema3A and NP1 on OPCs and the immune system will be discussed in further detail.

### 1.9.2 Sema3A and NP1 on oligodendroglia

OPCs and oligodendrocytes express Sema3a and NP1. Sema3A's expression is present in the cell body in OPCs, and is found in the cell body and processes in oligodendrocytes. NP1 expression is present in the cell body and processes in OPCs but is only found in the cell body in oligodendrocytes in cultured mouse oligodendroglia [117]. Moreover, OPCs purified from adult mice express NP1 and PlexinA1-3 but not PlexinA4 [245]. OPCs express NP1 and Sema3A mRNA in vivo which decreases with their differentiation [55]. In MS disease models, after demyelination, in vivo, Sema3A and NP1 mRNA is upregulated in oligodendroglia and NP1 was upregulated in OPCs as discussed in section 1.9.1. Sema3A is reported to impair OPC migration, and inhibit growth of their processes as well as their maturation.

### OPC migration

Sema3A was initially found to repel a subtype of glial precursors in the optic nerve [293]. In embryonic development, Sema3A is a chemorepulsive for the OPC population of the optic nerve [287]. COS cells secreting Sema3A redistribute OPCs in optic nerve explants with more OPCs found away from the Sema3A source [287]. In development, NP1 was found to be expressed on OPCs in vitro and in vivo and blocking antibody against NP1 was able to abolish the Sema3A migratory effect on OPCs in optic nerve explants [287]. In another study, Sema3A coated on a culture surface was found to be a substrate which OPCs avoid in a stripe assay [55]. Those studies together with the in vivo studies discussed in section 1.9.1 indicate that Sema3A is a chemorepellent for OPCs in development and in disease.

The other classical NP1 ligand that might also be involved in OPC migration is VEGF-A, the precursor of  $VEGF_{165}$  which has been found to increase OPC migration in a scratch assay without affecting proliferation and differentiation [124].

### OPC process growth

In addition to their migration, Sema3A affects OPC's process outgrowth. Sema3A released in solution by transfected HEK cells reversibly inhibits process outgrowth of purified rat oligodendrocytes in a dose dependent manner [260] [259]. However, since this study was done with transfected HEK cells, the Sema3A concentration which causes this effect is unknown. Similar inhibition of process formation in vitro was observed in another study where Sema3A was coated on the bottom of a culture well [296].

### OPC maturation

In addition to OPC migration and morphology, Sema3A was also suggested to be an inhibitor of OPC maturation. Sema3A was found to be an dose-dependent inhibitor of OPC differentiation in vitro. Moreover, addition of 450 nM Sema3A 10 days after ethidium bromide lesion resulted in less mature oligodendrocytes and impaired remyelination 28 days after the lesion [296]. Sema3A did not affect the macrophages or the OPC present after 28 days [296]. This discrepancy with previous studies indicating Sema3A's effect on migration is likely because the injection time point was after OPC and immune recruitment. Moreover, Sema3A was found not to significantly affect OPC survival in vitro [296] excluding the possibility that those effects are mediated by oligodendroglial cell death.

### 1.9.3 Sema3A and NP1 effects on immune response

Sema3A and NP1 are also involved in controlling the immune response. NP1 is expressed in a subset of T cells,  $T_{Reg}$  cells, dendritic cells, and Sema3A is expressed in T cells [166].

#### Anti-inflammatory

Sema3A suppresses T cell function while NP1 is important in mediating cell contact in a Sema3A independent manner. Sema3A can suppress T cell proliferation and cytokine production [44] and also sensitise T cells to apoptosis [209]. On the other hand, NP1 is essential for the dendritic cell induced proliferation of T cells independent of Sema3A because it mediates contact between those cell types via homophilic interactions (NP1 on one cell with NP1 on another cell) and a blocking antibody against NP1 on either of those cell types abolished this response [308]. Dysregulation of Sema3A and NP1 expression in T cells in patients with rheumatoid arthritis is thought to contribute to the disease chronicity [43]. NP1, Sema3A, and  $VEGF_{165}$  are overexpressed in arthritic cartilage [228] [297].

On the other hand, Sema3A is involved in promoting the function of helper T cell and  $T_{Reg}$  cells. Namely, Sema3A is believed to be able to directly act on the CD4+NP1+ (helper or  $T_{Reg}$  cells) T cell subset which then suppresses the immune response [43]. Moreover, in a conditional KO of NP1 in CD4+ T cells, EAE is more severe indicating that NP1 is important in preventing autoreactive responses [285]. The same increased sensitivity to EAE was observed

in Plexin-A4 deficient mice [341] further strengthening the idea that the Sema3A-NP1-PlexinA complex decreases autoreactive immune responses. As for  $T_{Reg}$ , NP1 is overall involved in their stability and interaction with dendritic cells further promoting immune suppression. As mentioned in section 1.8.2, NP1 is involved in the modulation of their stability and survival [73]. In the absence of pro-inflammatory signals, NP1 on  $T_{Reg}$  cells prolongs their interaction with dendritic cells instead of T cells and promoting suppression of immune response [270].

Sema3A and NP1 influence the immune system in cancer. Sema3A reduces the proliferation of the protumoral M2 macrophages and promotes proliferation of the antitumoral M1 macrophages [322] and therefore plays important role in the immune suppression of tumor growth. Moreover, NP1 is also important for macrophage antibody-dependent cellular cytotoxicity and antitumoral cytokine secretion as NP1 knockdown or use of a NP1 function blocking antibody suppress both [146].

### Pro-inflammatory

On dendritic cells, NP1 and Sema3A have quite the opposite effect as they promote their transmigration and pro-inflammatory response which would promote immune activation. Sema3A promotes the lymphatic system entry and exit of dendritic cells [303] by enhancing their passing through gaps via binding to NP1 and Plexin-A1 [229]. Plexin-A1 KO in dendritic cells had impaired transmigration across the lymphatics [229]. Anti-NP1 antibody also blocked the pro-inflammatory response of dendritic cells to virus or nucleic acids [111]. Finally, Sema3A promotes the migration of human dendritic cells [62].

Sema3A and NP1 also influence microglia/macrophage/monocyte migration and apoptosis. In a transwell assay, Sema3A impaired the migration of monocytes [72]. Sema3A, NP1, and Plexin-As are upregulated during the differentiation of human monocytes into macrophages [139]. Pro-repair macrophage phenotypes have more Sema3A, NP1, and Plexin-As than pro-inflammation phenotypes and Sema3A induces their apoptosis [139]. To support this, activated microglia by lipopolysaccharide in vivo upregulate Neuropilin 1 and Plexin-A1, and Sema3A induces apoptosis in activated microglia in vitro by interferon $\gamma$  (pro-repair) [185]. Apoptosis of microglia/macrophages could promote or suppress inflammation depending on their polarisation [205]. From the data available so far it appears that NP1 can promote apoptosis of the pro-repair phenotype better as one study indicates a higher level of Sema3A receptors (and possibly apoptosis susceptibility) in the pro-repair type [139] and the other showed apoptosis in the pro-repair type [185].

Overall, Sema3A and NP1 have a variety of pro-inflammatory and anti-inflammatory actions depending on the context and the cell type they act on.

### 1.9.4 Other Sema3A and NP1 effects

In addition to their functions in repair, remyelination, immune response, and OPC behaviour, Sema3A and NP1 are also involved in variety of other processes which are briefly listed here.

### **Cardiovascular**

NP1 is important for VEGF-induced angiogenesis. Sema3A is an inhibitor of this and both Sema3A and VEGF induce NP1-dependent vascular permeability [1] and remodelling [236]. Sema3A was shown to modulate cell migration by inhibiting integrin activation and thus cell adhesion in endothelial cells during vascular development [273]. si-RNA mediated NP1 KO in endothelial cells disrupts their cell adhesion [213]. On the other hand, NP1 is involved in filopodia formation in endothelial cells during blood vessel sprouting [85].

### **Cancer**

Sema3A is known to have pro-tumor and anti-tumor effects in variety of cancers due to angiogenic, vascular permeability, metastatic, and immune effects [338]. Sema3A has also been associated with cancer-induced bone pain [183].

### **Bone and cartilage**

Sema3A regulates the development of sensory innervation of bone and thus is important in bone remodelling [99] as well as pathological bone loss [268]. In cartilage, Sema3A is believed to antagonise  $VEGF_{165}$  induced chondrocyte migration [228].

### **Neural progenitors**

Sema3A repels and induces apoptosis in a neural progenitor cell line via NP1 while  $VEGF_{165}$  promotes their survival, proliferation, and migration [14] indicating that the balance of the two NP1 ligands is important for the fate of neural progenitors.

### **Regulation of gonadotropin releasing hormone**

Sema3A has been shown to be involved in the migration of GnRH releasing cells during animal development [36] [121]. Moreover, the expression of the 65 kDa isoform of Sema3A is important for GnRH axon sprouting via NP1 [105]. Blocking antibodies against Sema3A or NP1 disrupt the ovarian cycle probably by changing GnRH secretion [105].

### **Other**

This is by no means an extensive list of all roles of Sema3A and NP1 but it illustrates their involvement in variety of different developmental and pathological processes. There might be more roles of semaphorins which we have not discovered yet. For example, Sema3F was found to modulate neuronal excitatory post synaptic potentials (EPSCs) and both NP1 and NP2 have been shown to be localised to synapses [269].

## 1.10 Sema3A and NP1 in human

All of the various roles discussed so far are suggested by animal studies. Studies of *post-mortem* human tissue as well as blood samples can give indications whether those observations are relevant in human.

### Sema3A mutations in human

Kallmann syndrome is characterised by insufficient gonadotropin-releasing hormone (GnRH) and 6.2% of 386 screened patients were shown to have mutations in the Sema3A gene in the heterozygous state [121]. This indicates that in human, Sema3A might also be involved in the migration and axon sprouting of GnRH releasing cells as suggested in section 1.9.4. Moreover, there are 2 identified cases of homozygous mutations in the Sema3A gene which leads to multiple congenital abnormalities [18] indicating its importance in development.

Another similarity between the role of Sema3A and NP1 in animal models and human disease is their involvement in cancer.

### Cancer

In animal models, Sema3A and NP1 appear to be either beneficial or detrimental depending on the cancer and the cells they act on. In human, Neuropilin1 is often found in human cancers and correlates with severe disease [344] and is believed to mediate metastasis, immune invasion, and tumor growth [253]. This indicates that Sema3A/NP1 might be predominantly detrimental in human cancers.

### Disregulation of blood Sema3A level in immune diseases

Sema3A and NP1's multiple roles in immunity in animal models might be at least in part translated similarly into human as disregulation of the blood Sema3A level has been found in multiple immune diseases in human. Reduced blood Sema3A levels have been observed in patients with the autoimmune disease systemic lupus erythematosus [315]. Similarly, the Sema3A serum level is decreased in asthma patients and this is believed to decrease its immunomodulatory effect and lead to asthma pathogenesis [58]. On the other hand, Sema3A serum levels are higher in patients with celiac disease than control [149]. Therefore upregulation or downregulation of Sema3A could be a result or cause of altered immune response.

#### 1.10.1 Sema3A and NP1 in MS

This connection between dysregulation of Sema3A and immune response might also be important in an autoimmune disease such as MS.

### Dysregulation of blood Sema3A level in MS

Recently, comparison of blood Sema3A levels in 160 MS and 70 control patients found that Sema3A levels were significantly higher in MS [135]. Gender separation of all patients showed that this Sema3A increase was true for females but not males [135]. Furthermore, blood Sema3A level in females was correlated with MS progression as measured by the expanded disability status scale (EDSS) [135]. Contrary to this, another study found that the Sema3A concentration in blood of 15 MS patients was much lower than that of 15 control patients [258]. One of the studies was looking at newly diagnosed relapsing-remitting patients [258] while the other one was looking at MS patients with disease duration longer than 2 years [135] so this difference can indicate genuine fluctuation of Sema3A with disease progression. This confirms that dysregulation of Sema3A level is found in MS patients' blood.

### Upregulation of Sema3A and NP1 in MS

Sema3A mRNA was not detected in normal white matter in human brain [330] and Sema3A protein was found only in grey matter neuronal bodies and axons but not in the white matter [29] indicating that in normality Sema3A is only confined to grey matter neurones and absent from white matter.

However, in MS, Sema3A mRNA was upregulated in active lesions [330]. Moreover, a higher proportion of Sema3A mRNA expressing cells was found in less inflammatory active lesions than more inflammatory active lesions [330] suggesting that Sema3A mRNA expression in the glial cells of the lesion is negatively correlated to inflammation. Active lesions with strong immune components had a high proportion of cells containing mRNA for another semaphorin, Sema3F, which is a chemoattractant for OPCs [330]. Therefore, active lesions with a stronger immune component are suggested to be more permissive for OPC migration than active lesions with a less strong immune component.

This was later confirmed at the protein level as Sema3A was primarily expressed in chronic active lesions followed by chronic inactive lesions, remyelinated lesions, and minimally expressed in active lesions and NAWM, and Sema3F followed the reverse pattern [29]. Therefore, the more active/likely to repair a lesion is, the less likely it is to express Sema3A and more likely to express Sema3F.

Another *post-mortem* study also correlated Sema3A expression to the immune response; however, in a positive direction. The Sema3A expression was higher when the immune activity in the MS lesion was high [34] indicating that it is either involved in or dependent on the immune response. It is suggested that the high Sema3A expression in highly active lesions is an attempt to control the immune response [34]. Regardless of the direction of the correlation, the 3 studies indicate that Sema3A expression is correlated with the immune response and as mentioned in section 1.4.3, remyelination happens in active lesions with strong immune reaction [249]. This indicates an indirect connection between Sema3A/NP1 and remyelination.

### Cells expressing Sema3A and NP1

Similarly to the expression in LPC spinal cord lesions described in section 1.9.1, Sema3A mRNA is expressed primarily in astrocytes, followed by microglia/ macrophages, oligodendroglia and rarely neurones in and around the lesion as well as neurones in all grey matter [330]. Another study also detected Sema3A in grey matter neurones, macrophages/microglia, and astrocytes in MS; however, it did not find Sema3A in oligodendroglia [34]. This expression pattern was very similar to an EAE study [117] described in section 1.9.1, indicating that the expression of Sema3A might depend on the demyelination method in animal models and possibly on the disease mechanism in humans.

It is possible that this difference, as well as the different association between Sema3A and immune response between the studies, was due to technical differences in antibody detection ability in the human tissue.

For NP1 expression, 24% of all oligodendroglia express NP1 mRNA which is also found in astrocytes, microglia/macrophages, and neurones [330]. The expression of NP1 in OPCs, astrocytes, and microglia was also confirmed by staining for NP1 protein in MS lesions [29]. The NP1 expression was only detected in microglia/macrophages in another study of MS tissue [34]. NP1 is also upregulated in endothelial cells of MS patients [323]. From section 1.9.1, we would expect that this would lead to worse demyelination, BBB permeability and less favourable immune infiltration.

In human tissue, it is hard to prove that a signal is causative of a cell behaviours because we see a snapshot in a timeline and we cannot modulate protein levels. Therefore, the best indication that Sema3A is involved in OPC migration in human is that the number of OPCs in the lesion negatively correlated with the number of Sema3A+ cells [29]. Therefore further proof that Sema3A is involved in OPC migration after demyelinating lesion can only sought via in vitro and in vivo animal studies modulating either protein and examining the effect.

## 1.11 Inhibitors

Luckily, because of Sema3A's roles in repair, the immune system and cancer, it is a putative target for development of inhibitors [331] which means that tools to modulate NP1 and Sema3A already exist and will be briefly discussed below.

### 1.11.1 SICHI

From a peptoid library screen for a Sema3A inhibitor, SICHI was identified as potent ( $IC_{50} = 0.039\mu g/ml$ ) and specific inhibitor of Sema3A axon repulsion and growth cone collapse [208]. Addition of SICHI increased the number of axons growing into a lesion after axotomy in mouse brain slices [208]. This effect was proposed to be because SICHI impairs the binding of Sema3A to its receptor complex Neuropilin1/PlexinAs [208].

### 1.11.2 Xanthofulvin

Another Sema3A inhibitor is naturally occurring and was isolated from *Penicillium* fungus [165]. The structure of xanthofulvin was determined and it was shown that it could inhibit the growth cone collapse of chick DRG neurones with high potency ( $IC_{50} = 0.09\mu g/ml$ ) [165]. In vivo, Sema3A increased axon regeneration, Schwann cell migration and remyelination, and cell survival and angiogenesis after spinal cord transection in rats [144]. This resulted in improved functional recovery [144]. Xanthofulvin could also increase peripheral nerve regeneration and functional outcome in corneal transplantation mouse model in vivo [233]. Moreover, nerve regeneration could be improved by the addition of Xanthofulvin in a rat olfactory nerve axotomy [150]. This indicates that Xanthofulvin can improve nerve regeneration in the peripheral nervous system as well as central nervous system including spinal cord and olfactory nerve. Those effects are mediated by direct binding of Xanthofulvin to Sema3A [150] thus preventing Sema3A binding to NP1.

### 1.11.3 L1

Another way to modulate the Sema3A effect is through its coreceptors. In vitro, L1 mimetic peptide blocks Sema3A's inhibition of axon growth and growth cone collapse by 20% and 50% respectively [204]. However, it failed to stop Sema3A's inhibition of axon regrowth into a spinal cord contusion lesion [204] probably due to limited neuronal responsiveness to Sema3A (Limited NP1 expression), the limited effect of L1 in this system or the tiny effect of the inhibitor in vitro.

### 1.11.4 anti-NP1 antibodies

An excellent way to study and differentiate the contribution of Sema3A and  $VEGF_{165}$  are the recently developed function blocking antibodies against the Sema3A and  $VEGF_{165}$  binding sites on NP1. A phage library screen for antibodies binding NP1 found two antibodies which specifically bound to the Sema3A binding site of NP1 and the VEGF site of NP1 respectively [176]. The anti-NP1(Sema3A) blocking antibody bound the a1a2 NP1 domains and blocked Sema3A's mediated DRG growth cone collapse while the anti-NP1(VEGF) blocking antibody bound the b1b2 NP1 domain and inhibited  $VEGF_{165}$  binding to NP1 [176]. Anti-NP1(VEGF) blocking antibody further inhibited  $VEGF_{165}$  mediated HUVEC migration in a Boyden chamber [176]. Both antibodies bound to NP1 with high affinity as shown in table 1.1.

Table 1.1: Affinity of anti-NP1(Sema3A) and anti-NP1(VEGF) blocking antibodies [176].

		anti-NP1(Sema3A) [YW63.4]	anti-NP1(VEGF) [YW107.4.87]
human	K <sub>D</sub>	0.9 nM	0.4 nM
	IC <sub>50</sub>	0.5 nM	6 nM
murine	K <sub>D</sub>	7.8 nM	1.3 nM
	IC <sub>50</sub>	3.4 nM	38 nM

An anti-NP1(VEGF) antibody for the VEGF site of NP1 is currently being tested as treatment for solid tumors [241] indicating that therapeutic inhibition of NP1 is possible.

## 1.12 The connection between NDST1, heparan sulfate, and Sema3A and NP1

The two pairs of OPC migration targets chosen for this study, NDST1/HS and Sema3A/NP1, appear to not to be associated in any way because a ECM component and its modification enzyme and a soluble signalling and its signalling receptor have little in common.

However, this is not the case as heparan sulfate binds both of the classical NP1 ligands.  $VEGF_{165}$  isoform was shown to be almost entirely bound to heparan sulfate proteoglycans and to be released by heparinase, heparan sulfate cleaving enzyme [127]. Similarly, removal of heparan sulfate by heparinase decreased the binding of Sema3A reduced Sema3A binding to NP1-expressing cells by 40% in vitro [71]. Therefore, both Sema3A and  $VEGF_{165}$  bind to heparan sulfate and removal of HS impairs Sema3A binding to NP1.

Moreover, both ligands also interact with heparin, a highly sulfated form of heparan sulfate. Heparin enhances  $VEGF_{165}$  binding to NP1 expressing cells [284]. Similarly, heparin potentiates the binding of Sema3A to NP1 as well as its DRG neurones growth cone collapse activity [71]. Moreover, secreted Sema3A from cells binds to the surface on which the cells are grown and could be mopped up either by adding heparin or heparan sulfate [71] because Sema3A binds to them. Therefore heparin enhances binding of Sema3A and  $VEGF_{165}$  to NP1 and so enhances Sema3A's activity. Overall, it is suggested that despite Sema3A being a secreted factor it heavily interacts with ECM including heparan sulfate and its proteoglycans [71].

In turn, Sema3A and  $VEGF_{165}$  can modulate the ECM composition by controlling the expression of matrix metalloproteases(MMPs). In the study of the effects of  $VEGF_{165}$ -Sema3A-NP1 in arthritic cartilage discussed in section 1.9.3, one of the  $VEGF_{165}$  effects antagonised by Sema3A is overexpression of matrix metalloproteases(MMPs) [228]. MMPs are involved in remodelling of the ECM including heparan sulfate and its proteoglycans.

Finally, there are indications that HS/NDST1 and Sema3A/NP1 might be involved together in development of areas of the CNS. HS deficient mice have defects in the corpus callosum tracts [131] which is similar to the neuronal tract defects in the Sema3A KD and the corpus callosum defect in the NP1(Sema3A-) mouse [116]. Therefore, it was suggested that heparan

sulfate, Sema3A, and NP1 might interact in the development of the corpus callosum [71].

### 1.13 Rationale for study

The requirement for OPC recruitment modulating drugs is clear in order to aid the 30% of MS patients in which remyelination fails because of insufficient OPC migration. In addition to this, a recruitment modulator would provide a different class of drugs to complement existing immunotherapy drugs and maturation enhancers which will hopefully enter the clinic soon.

#### Sema3A/NP1

The evidence that Sema3A negatively regulates OPC migration is overwhelming in animal models (section 1.9.2 and as strong as it can be in human studies (section 1.10.1)). However, the majority of migration studies have modified Sema3A using lentivirus, genetic KD, or addition of recombinant protein and those are obviously not suitable for therapeutic intervention in humans. The ball like shape of Sema3A (see figure 1.5) makes it also very hard to target with a small drug inhibitor.

Therefore the best therapeutic option may be to inhibit the interaction between Sema3A and NP1 with a inhibitor of NP1. Blocking NP1 in OPCs suggested has already been suggested as a therapeutic strategy for increasing remyelination in MS [81]. Moreover, inhibition of NP1 is expected to further benefit remyelination as it increases OPC maturation (section 1.9.2). However, only one study has attempted to answer the question whether inhibiting NP1 would have the same beneficial effect in MS animal models as decreasing the level of Sema3A discussed in section 1.9.1. The study used NP1(Sema3A-) mice, in which the Sema3A binding site on NP1 is disrupted but VEGF is unaffected and found that there were increased number of OPCs in the lesion after demyelination compared to WT mice [245]. This suggested that inhibiting NP1 could have the same beneficial effect of increased OPCs migration but its effect on remyelination is still unclear. This is why we aimed to answer the question of whether impairing Sema3A signalling via NP1 would have the expected beneficial effect on remyelination in vivo and OPC behaviour in vitro.

In addition to this, systemic administration of a therapeutic NP1 inhibitor would affect all NP1 expressing cells in the body. Even though Sema3A's role in OPC migration in MS animal models is clear and well studied, Sema3A and NP1's involvement in a variety of pro- and anti-inflammatory processes makes it hard to speculate what the immune effect of systemic inhibition of NP1 in an adult would be. To illustrate, CD4+ T cells specific NP1 KO mice have increased severity in an EAE model of MS [285] as discussed in section 1.9.3 while deletion of NP1 in endothelial cells results in decreased EAE severity [323] as mentioned in section 1.9.1. Therefore, NP1 inhibition is expected to have immune effects relevant in MS-like pathology which are currently unclear and require examination.

## **NDST1/HS**

NDST1 and HS have no published connection to OPC migration and remyelination; however, unpublished data from our collaborators from Pascale Durbec's group, which will be detailed in chapter 3 indicates that they play an important role in those processes in animal models. Therefore we strove to examine whether they are important in human MS tissue.

## 2 Materials and Methods

### 2.1 In vivo methods

All animal experiments were done under Home Office regulations under Elitsa Peeva's personal licence (PIL 70/26059) and Anna Williams' project licence 60/4524. All experimental plans and procedures were approved by university's veterinary scientific services before they were carried out. All animals were housed at the University of Edinburgh under Home Office regulations.

#### 2.1.1 Animal genotype

NP1(Sema3A-) mice have a mutation in the Semaphorin3A binding site of Neuropilin 1 which prevents Semaphorin3A binding. This is a 7 amino acid mutation in the  $\alpha 1$  domain of Neuropilin 1 which has been previously described and characterised [115] [116]. The NP1(Sema3A-) mice were extensively characterised [116]:

- NP1 expression remained the same
- $VEGF_{165}$  binding remained the same
- Sema3A binding was reduced in the tissue of NP1(Sema3A-) mice
- Sema3A does not induce DRG axon repulsion in DRG neurones from the NP1(Sema3A-) mice
- 15% of the mice from homozygous and wt crosses were homozygous at P7

The mice were obtained from Jackson Laboratories with strain name B6.129(C)-Nrp1tm1Ddg/J and strain ID JAX005245. Those animals were from a mixed background so for control, wild type (WT) animals from the colony were used. The colony was maintained as heterozygous/heterozygous or heterozygous/homozygous breeding pairs as homozygous/homozygous breeding pairs rarely produced offsprings. From heterozygous/heterozygous breeding pairs, only 3.8% of the mice at P21 were homozygous instead of the expected 25%.

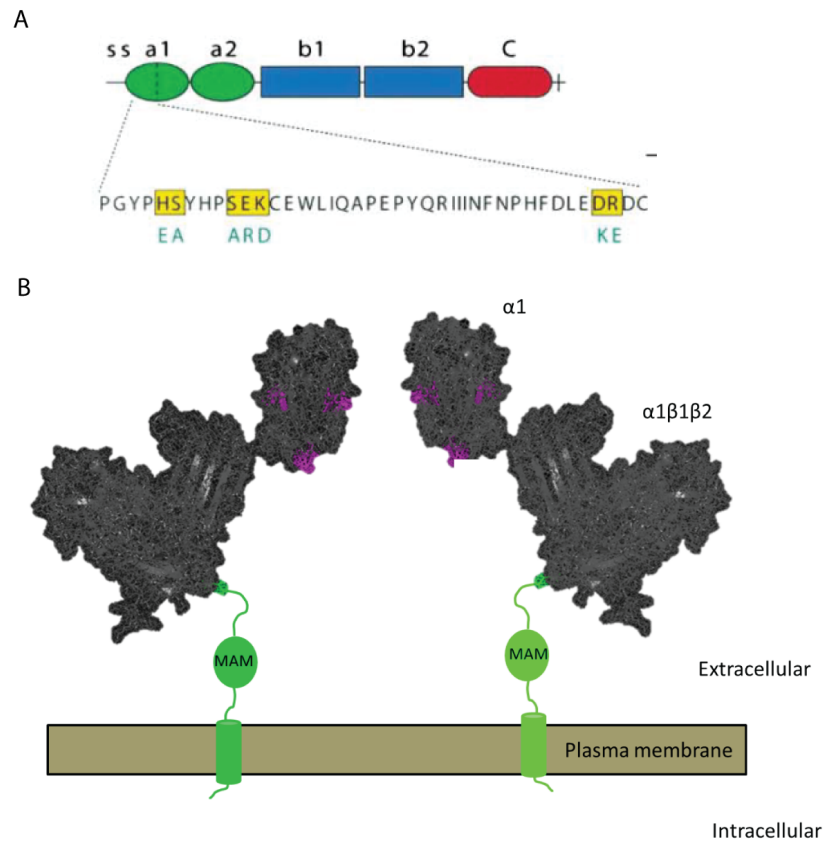


Figure 2.1: The 7 amino acids which were mutated in the a1 domain of NP1 are shown in yellow (A). Figure adapted from [116]. The location of the mutated amino acids are highlighted on the wild type crystal structure of NP1 which was discovered by [136]

PDGFR $\alpha$ -Cre x flx-NP1-flx mice have a Cre under the PDGFR $\alpha$  promoter which excises the floxed exon 2 of the Neuropilin 1 gene. This ensures knock down of Neuropilin 1 in PDGFR $\alpha$ + cells which are primarily oligodendrocyte precursor cells and the oligodendrocytes they differentiate to. However, PDGFR $\alpha$  is also expressed in pericytes. This line was derived by a cross of PDGFR $\alpha$ -Cre and flx-NP1-flx lines. The PDGFR $\alpha$ -Cre line was obtained from Jackson laboratories with strain name C57BL/6-Tg(Pdgfra-cre)1Clc/J and strain ID JAX013148. The flx-NP1-flx line was also obtained from Jackson laboratories with strain name B6.129(SJL)-Nrp1 tm2 Ddg/J and strain ID JAX005247. The PDGFR $\alpha$ -Cre x flx-NP1-flx colony was maintained as homozygous/ homozygous breeding pairs and C57Bl/6J animals were used as wild type controls.

Ear clips were taken from new born pups at P21 both for identification and genotyping. Genotyping was done using TransnetYX's services.

### 2.1.2 Animal surgery

Surgery was performed to produce a focal lesion in the corpus callosum of both mutant mice as well as their respective controls in order to study remyelination and cellular composition of the

## 2 Materials and Methods

lesions. One previous study has looked into the number of OPCs in lesions of NP1(Sema3A-) mice compared to control [245] and it was used to estimate the sample size calculation. The equation below was ( 2.1) used to calculate the sample size [328]:

$$n = \frac{2}{d^2} * c_{p, power} \quad (2.1)$$

Where n is the sample size number, d is the standardised difference and is is a constant dependent on the power of the study and cutoff for statistical significance. Assuming cutoff for statistical significance (p value) of 0.05 and power of the study of 80%, c = 7.9. The standardised difference is represented by the equation below ( 2.2):

$$\text{Standardized difference} = \frac{\text{Target difference}}{\text{Standard deviation}} \quad (2.2)$$

In the previous study [245], the difference between the means was around 0.7 and the standard deviation around 0.3. Standard difference for our experiment is calculated below ( 2.3)

$$\text{Standardized difference} = \frac{0.7}{0.3} = 2.3 \quad (2.3)$$

Therefore the sample size required to detect this difference of the size of the previous study [245] is 3 per group (refequ:finalpowercalc):

$$n = \frac{2}{d^2} * c_{p, power} = \frac{2}{2.3^2} * 7.9 = 2.99 \quad (2.4)$$

LPC-injected animals sometimes do not exhibit a lesion and any difference in remyelination is expected to be smaller than this, therefore we were aiming to have 4 or 5 animals per group. In practice, because of the breeding problems of those mice, we initially struggled to get this number for LPC-injected and control animals. However, later on both mouse lines needed to be terminated to keep costs down when I went on maternity leave which allowed for more mice than originally planned to be used in experiments. Moreover, because of the breeding and survival problems of the mice, both male and female mice of varied adult age but at least 2 months old were used.

Anaesthesia was introduced by placing the animal in an induction chamber with 4% isoflurane. Anaesthesia was then maintained by inhalation of 2% isoflurane for the duration of the surgery via a nose mask. Since isoflurane has no analgesic action, animals were given analgesia by subcutaneous injection of vetergesic (0.05mg/kg) and rimadyl (4mg/kg). After a incision was made to expose the skull, a tiny hole in the skull of the mouse was drilled at stereotactic coordinates 1.2 mm posterior, 0.5 mm lateral to the bregma. 2µl of 1% lysophosphatidyl choline/lysolecithin (LPC) was injected 1.4 mm deep at the same position over 4 minutes. Injection was controlled by KD scientific Nano pump and done with a 30 gauge needle and Hamilton syringe. The needle was left for another 4 minutes before removal to prevent LPC backflowing into the needle tract. The incision was stitched, animals were left to recover on a warm pad and carefully monitored.

### 2.1.3 Animal termination and tissue preparation

For electron microscopy (EM), animals were anaesthetised by intraperitoneal injection of ketamine (75 mg/kg) and medetomidine (1 mg/kg) and terminated by intracardiac perfusion fixation with 4% paraformaldehyde/2% glutaraldehyde in 0.1 M phosphate buffer 17 days after surgery. The brain was dissected out and postfixed in 1% glutaraldehyde in 0.1 M phosphate buffer for at least two weeks. The brain was cut in 1-mm thick coronal section samples. The sections anterior and posterior from the anatomical place of the lesion were further dissected to only include the cortex and corpus callosum (CC) on the lesion side. Those were processed into resin blocks using TAAB812 (Epon, TO24/1) resin embedding kit with BDMA as per manufacturer's guidelines.

Blocks were trimmed to expose the tissue and sagittal 1  $\mu$ m semi-thin sections were cut. The sections were stained with toluidine blue in order to determine which had a lesion. The ones which appeared to have a lesion based on cell accumulation and reduction of myelin staining were further cut into 60 nm ultra thin sections. Those were stained in uranyl acetate and lead citrate and imaged at a transmission electron microscope (TEM).

For immunohistochemistry (IHC), animals were anaesthetised by intraperitoneal injection of ketamine (75 mg/kg) and medetomidine (1 mg/kg) and terminated by intracardiac perfusion fixation with 4% paraformaldehyde (PFA) in PBS 10 days after surgery. The brain was dissected out and postfixed in 4% paraformaldehyde overnight and then incubated with 15% and then 30% sucrose for 24h each. Brains were embedded in optimal cutting temperature compound (OCT) and stored at -80°C. Brains were then cut in consecutive 10  $\mu$ m cryostat sections and stored at -20°C.

## 2.2 In vitro methods

OPC assays (apart from migration) were performed in optically clear bottomed 384 well plates (PerkinElmer, 6007460). Cells were seeded by an E1-ClipTip electronic adjustable 8 channel pipette (Thermo, 467060) while they were at room temperature and were grown in 100  $\mu$ l media. Cells were fixed by removing half of the media and replacing it with 8% PFA unless otherwise stated. Seeding cells at room temperature ensured even distribution of cells and this fixing protocol minimised loss of cells during fixation. Following fixation, cells were incubated in a volume of 20  $\mu$ l which is enough to cover the bottom of the well. All incubation steps were at room temperature unless otherwise stated. OPCs were grown in flasks and multiwell plates which were coated with Poly-D-Lysine (PDL) (Sigma Aldrich, P6407) or Poly-L-Lysine (PLL) (Sigma Aldrich, P4707) by incubation of enough 5  $\mu$ g/ml PDL or PLL in water to cover the bottom for at least 1 hour at 37°C.

### 2.2.1 OPC cultures

Oligodendrocyte precursor cells were obtained by the shake off method of mixed glial culture [192]. The brain was dissected out of euthanised P0-P2 rat pups. The meninges were removed and cortices separated from the rest of the brain. The cortices were minced by fine scissors and digested by mixture of 1.2 units/ml papain enzyme (Worthington Biochemical, LS003127), 0.1 mg/ml L-cysteine (Sigma Aldrich, C7477-25G) and 0.40 mg/ml DNase I for 1.5 h at 37°C. Digestion was stopped by addition of 10% fetal calf serum, 1% penicillin/streptomycin (Invitrogen 15140-122) in minimum essential media (MEM) (Gibco, 32360-026). Cells were collected by centrifugation at 1500 rpm for 5 min and then resuspended in the same media. A single cell suspension was obtained by passing the resuspended cells via a 19 gauge needle and then a 23 gauge needle several times. Cells were grown in vented PDL or PLL-coated flat bottomed flasks (Falcon (Corning), 353110) at 37°C and 7.5% CO<sub>2</sub>. Cells were fed new media every 2 days.

After 11 days microglia were separated from the mixed glial culture by shaking on a orbital shaker at 250RPM and 37°C for 1 h. After media was replaced, the OPCs were separated from the mixed glial culture by shaking on a orbital shaker at 250RPM and 37°C for 16 h. The media which contained the OPCs was removed and incubated on tissue culture untreated bacteriological plates at 37°C for 20 min to ensure any remaining microglia attach to the plastic. OPCs were then collected from the media by centrifugation at 1500 rpm for 5 min and then resuspended in SATO, 1% penicillin/streptomycin solution, 1% ITS supplement (Sigma Aldrich, 13146-5ml), 0.5% FCS in DMEM. This OPC SATO media which was used for growing OPCs from this point of the protocol onwards. Cells were counted using a haemocytometer. For proliferation, maturation, survival, motility and purity assays, 2000 cells in 100  $\mu$ l were seeded in wells of a 384 well plate. For migration, 12500 cells were seeded in in 100  $\mu$ l in a PDL-coated transwell insert of a 24 well plate.

Cells were subjected to the following treatments conditions in the assays:

- 22.5nM, 45 nM and 90 nM Semaphorin3A coated (R&D Systems, 5926-S3) (mixed with PDL/PLL and coated as normal)
- 22.5nM, 45 nM and 90 nM Semaphorin3A in media (R&D Systems, 5926-S3)
- 5  $\mu$ g/ml, 10 $\mu$ g/ml, 20 $\mu$ g/ml anti-NP1(Sema3A) blocking antibody against the Sema3A site of NP1 (Genentech, NRP1:9755)
- 0.001 mM, 0.002mM and 0.004 mM Xanthofulvin (Genzyme)
- 0.1g/ml recombinant human VEGFA 165 (Peprotech, 100-20)
- 10g/ml anti-NP1(VEGF) blocking antibody against the VEGF site of NP1 (Genentech, NRP-1, 9756)
- DMSO control (for Xanthofulvin which is dissolved in 10% DMSO)
- media only (negative) control

### 2.2.2 OPC proliferation assay

Proliferation was assessed by click-It EdU imaging kit from Life Technologies (Life Technologies, C10340). 10  $\mu$ M thymine analogue, EdU was added 24 h after the cells were plated. EdU was incubated for another 24 h and if the cells were replicating DNA for cell division, EdU would be incorporated. The cells were then fixed by 4% PFA for 10 min. Cells were incubated with 0.5 % Triton (Fisher Scientific, 10541754) in PBS (Sigma Aldrich, 70011-036) for 20 min and washed in 3% BSA in PBS. Cells were incubated with click-it reaction cocktail for 30 min as per manufacturer's guidelines (430  $\mu$ l Click-it reaction buffer, 20  $\mu$ l copper sulfate, 1.2  $\mu$ l Alexa Fluor 647 azide, 50  $\mu$ l Reaction buffer additive). This allowed the fluorescent azide to covalently bind the alkyne tag of EdU creating a fluorescent signal in the nuclei of dividing cells. Wells were washed, stained with 5  $\mu$ g/ml Hoechst for 1 min and washed again before imaging.

Positive control for this assay was 10ng/ml PDGF-AA (Peprotech, 100-13A) and 10ng/ml FGF (Peprotech, 100-18B) which showed increase in proliferation.

### 2.2.3 OPC survival assay

Survival was assessed by Click-iT TUNEL imaging kit from Life Technologies (Life Technologies, C10247). Cells were fixed by 4% PFA for 10 min 72 h after plating. Cells were permeabilised with 0.25 % Triton in PBS for 20 min and washed with distilled water. Wells were equilibrated with TdT reaction buffer for 10 min and then incubated with TdT reaction cocktail for 1 h at 37°C as per the manufacturer's guidelines (97  $\mu$ l TdT reaction buffer, 1  $\mu$ l EdUTP nucleotide, 2  $\mu$ l TdT enzyme). This step allowed the terminal deoxynucleotidyl transferase (TdT) enzyme to incorporate EdUTP on the edges of double stranded DNA breaks. The wells were washed in 3% BSA in PBS and then incubated with Click-it Reaction cocktail for 30 min (97.5  $\mu$ l Click-it reaction buffer and 2.5  $\mu$ l Click-it reaction buffer additive). This allowed the fluorescent azide to covalently bind the alkyne tag of EdU creating a fluorescent signal in the nuclei of dying cells. The wells were washed in 3% BSA in PBS, stained with 5  $\mu$ g/ml Hoechst for 1 min and washed again before imaging.

Positive control for this assay was the double stranded breaks created by the enzyme DNase I. Positive control wells were incubated with DNase I cocktail for 1 h as per the manufacturer's guidelines (89  $\mu$ l distilled water, 10  $\mu$ l DNase buffer, 1  $\mu$ l DNase enzyme) after permeabilisation. Almost all cells were positive after this treatment. Negative control was achieved by omitting the TdT reaction buffer step.

### 2.2.4 OPC motility assay

Motility was assessed by live imaging on the Operetta. Immediately after plating cells in different treatment conditions, plate was placed in the live imaging chamber at 37°C and 7.5 % CO<sub>2</sub>. Brightfield and digital phase contrast images were taken every 10 min for 19 hours.

### 2.2.5 OPC maturation assay

Maturation was assessed by immunohistochemistry staining with known markers for OPCs, immature oligodendrocytes and mature oligodendrocytes. Cells were fixed by 4% PFA for 10 min 72 h after plating. Wells were then blocked for 1 h with 10% heat inactivated horse serum (HIHS) (Gibco, 26050), 0.1% Triton in PBS. Wells were washed in PBS and incubated overnight at 4°C with primary antibodies (1:200 rabbit anti-NG2, 1:1000 mouse IgM anti-O4 and 1:300 rat anti-MBP in 10% HIHS, 0.1% Triton in PBS). Wells were washed with PBS and incubated with secondary antibodies for 1 h (1:1000 goat anti-rabbit Alexa 488, 1:1000 goat anti-rat Alexa 555 and 1:1000 goat anti-mouse IgM Alexa 647 in 10% HIHS, 0.1% Triton in PBS). The wells were washed in PBS, stained with 5 µg/ml Hoechst for 1 min and washed again before imaging.

Positive control for this assay was treatment with 100 units/ml LIF (obtained from in-house Cos7 transfected cells) which showed increase in MBP+ cell number and cell area.

### 2.2.6 OPC migration assay

Migration was assessed by quantity of cells which pass through pores on a membrane to reach the treatment compared to control. Cells were seeded on the top of PDL-coated poly-carbonate transwell culture inserts (6.5 mm diameter with 8 µm pore size (Corning, 3422) on a 24 well plate (Costar (Corning), 3524). Different treatments were placed in the media on the bottom of the transwell (in the 24 well plate wells). Cells were left at 37°C at 7.5% carbon dioxide and were fixed in 4% PFA after 16.5 h by removing the media on the top and bottom and replacing it with 4% PFA for 10 min. The wells were washed in PBS, stained with 5 µg/ml Hoechst for 1 min and washed again before imaging.

Positive control for this assay was 20ng/ml PDGF-AA (Peprotech, 100-13A) and negative control was 100 ng/ml netrin-1 (R&D, 1109-N1-025).

### 2.2.7 Purity of culture assay

Purity was assessed by immunohistochemistry staining with known marker for astrocytes, the major contaminant cell type. Cells were fixed by 4% PFA for 10 min 48 h after plating. Wells were then blocked for 1 h with 10% HIHS, 0.1% Triton in PBS. Wells were washed in PBS and incubated overnight at 4°C with primary antibodies (rabbit anti-GFAP (Covance, PCK591P-100) at 1:2000 or chick anti-GFAP (DAKO, Z0334) at 1:3000 in 10% HIHS, 0.1% Triton in PBS). Wells were washed with PBS and incubated with secondary antibodies for 1 h (1/1000 goat anti-rabbit 647 (Life Technologies, A212444) or 1/1000 goat anti-chick 568 (Life Technologies, A11041). The wells were washed in PBS, stained with 5 µg/ml Hoechst for 1 min and washed again before imaging. This assay allowed monitoring of quality of culture. Only cultures with purity of over 90% were used for data analysis. Cultures with purity of less than 90% were excluded.

## 2.3 Immunohistochemistry

### 2.3.1 Fluorescent IHC on fixed frozen mouse brain

Frozen sections were left to air dry for 3-4 minutes and then wax pen was used to mark around the tissue. This limited the spread of liquid and allowed lower volumes to be used. Slides were washed in PBS and incubated with 10% HIHS and 0.3% Triton in PBS for 2 h. Primary antibodies were incubated overnight in antibody diluent (Spring Bioscience, ADS-125) at 4°C. Primary antibodies used: rat anti-MBP antibody (Bio-Rad, MCA4095) at 1:200, rabbit anti-IBA1 (Wako, 019-19741) at 1:900, rabbit anti-NG2 antibody (Millipore, A135320) at 1:50, mouse IgG anti-CC1 (Abcam, ab16794) at 1:20, rat anti-PDGFR $\alpha$  (Biolegend, 135902) at 1:50, mouse IgG anti-NogoA (R&D, MAB3098) at 1:100, mouse IgG anti-iNOS (BD Bioscience, 610329) at 1:50, mouse IgG anti-CD68 (Abcam, ab53004) at 1:50, goat anti-Arginase-1 (Santa Cruz Biotechnology, sc-18355) at 1:25, mouse IgG anti-NP1 (R&D, MAB5661) at 1:50, rabbit anti-olig2 (Millipore, AB9610) at 1:50, rabbit anti-NP1 (CST, 3725 (D62C6)) at 1:50. Secondary antibodies were incubated for 2 h (anti-rabbit Alexa 488 (Life Technologies, A11008) at 1:1000, anti-rat Alexa 647 (Life Technologies, A21247) at 1:1000, anti-mouse Alexa 568 (Life Technologies, A11004) at 1:1000). Slides were stained with Hoechst for 1 min and mounted using fluoromount (Southern Biotech, 0100-01). PBS washes were performed between each treatment.

Initially, 5 slides from each mouse were stained with antibodies to MBP and IBA1 in order to determine if there was a lesion and its size. If there was a lesion, further staining was performed on slides around the slide with the biggest lesion size - assumed to be the centre of the lesion. Staining was done to identify OPCs, mature oligodendrocytes and macrophages/microglia in the lesions. For those experiments, control with no primary antibody was used to detect unspecific staining.

### 2.3.2 Colorimetric IHC on fixed frozen *post-mortem* human tissue

Frozen *post-mortem* human brain tissue was fixed in 4% paraformaldehyde in PBS for 30 min. Endogenous peroxidase and alkaline phosphatase activity was blocked by 10 min incubation with Vector Bloxall (Vector laboratories, SP-6000). Slides were blocked with ready-to-use 2.5% normal horse serum from Vector secondary antibody kits for at least 20 min. Primary antibodies were incubated overnight in antibody diluent (Spring Bioscience, ADS-125) at 4°C. Primary antibodies used: mouse anti-NDST1 (1/50; Abcam, ab55296), rabbit anti-NeuN (1/500; Abcam, ab104225), rabbit anti-IBA1 (1/500; Wako chemicals, 019-19741), rabbit anti-Olig2 (1/100; Sigma, HPA003254). HS staining with the mouse IgM anti-N-sulfated motifs on HS chains (10E4 antibody, Seikagaku, Japan) did not give any signal on human tissue. NDST1 intensity was evaluated after a short exposition (exactly 2 min). All other stainings were fully developed. To ensure antibody specificity, the NDST1 antibody was pre-absorbed with human NDST1 recombinant protein (Abcam, ab116875), and added to tissue sections, with no staining seen

(figure 2.2. Secondary antibodies were incubated at room temperature for 1h. Staining was developed with a DAB Peroxidase (HRP) Substrate Kit (with Nickel), 3,3-diaminobenzidine (Vector, SK-4100) and a VECTOR Blue AP Substrate Kit (Vector, SK-5300) as per manufacturers guidelines. Secondary antibodies used: ImmPRESS-AP Anti-Rabbit IgG Polymer Detection Kit (Vector, MP-5401) and ImmPRESS HRP Anti-Mouse IgG Polymer Detection Kit, made in Horse (Vector, MP-7402). PBS washes were performed between each treatment. For those experiments, control with no primary antibody was used to detect unspecific staining.

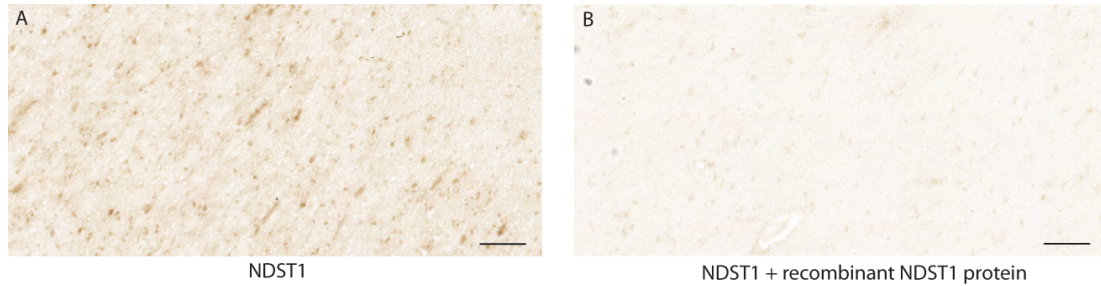


Figure 2.2: Immunohistochemical staining using antibodies to NDST1 on human tissue is absent after addition of recombinant NDST1. (A) NDST1 staining of MS WM (B) NDST1 staining of MS WM in the presence of recombinant NDST1. Scale bars: 100  $\mu\text{m}$

## 2.4 Imaging, analysis and statistics

### 2.4.1 Imaging

The colorimetric IHC on human *post-mortem* tissue and the fluorescent IHC on fixed frozen mouse brain slides were imaged using an Axio Scan.Z1 digital slide scanner(Carl Zeiss) at x20. OPC maturation, proliferation, survival, motility, purity and neural stem cell binding assays were imaged on an Operetta high-content imaging system(Perkin Elmer) at x20 with full well coverage. Migration assays were imaged on a confocal Leica SP8 microscope and images covered the top (seeded cells), membrane (migrating cells in pores) and bottom (migrated cells) of the transwell. Electron microscopy samples were imaged on TEM (Philips, CM120) and images collected on a Gatan Orius CCD camera or TEM (JEOL JEM-1400 Plus) and images collected on a GATAN OneView camera at x700. After the corpus callosum was identified, 10 images were taken starting at the centre the lesion area (the most demyelinated area in the CC).

### 2.4.2 Image analysis

For the human *post-mortem* tissue analysis, one researcher marked out the lesion sites and normal appearing white matter (WM) as regions of interest (ROIs), while another counted single positive (NDST1+ cells) and double positive cells (NDST+ cells and other brain cell markers combined as above) in these areas of interest (ensuring blinding of counting). If the ROIs were

## 2 Materials and Methods

small, the whole region was counted. If it was big, 5 smaller areas within the ROI were drawn. An example of both types of ROI is shown in figure 2.3. This approach was representative of the whole ROI because comparison between cell counts (per area) in the whole region of interest and the average of the smaller areas showed little difference. Those smaller areas were equally spaced and covered both the core and the outer edges of the ROI. NDST1+ staining did not show any spatial bias towards the core or edge of lesions/NAWM - it spanned the lesions in similar level and quantity (figure 2.3, top).

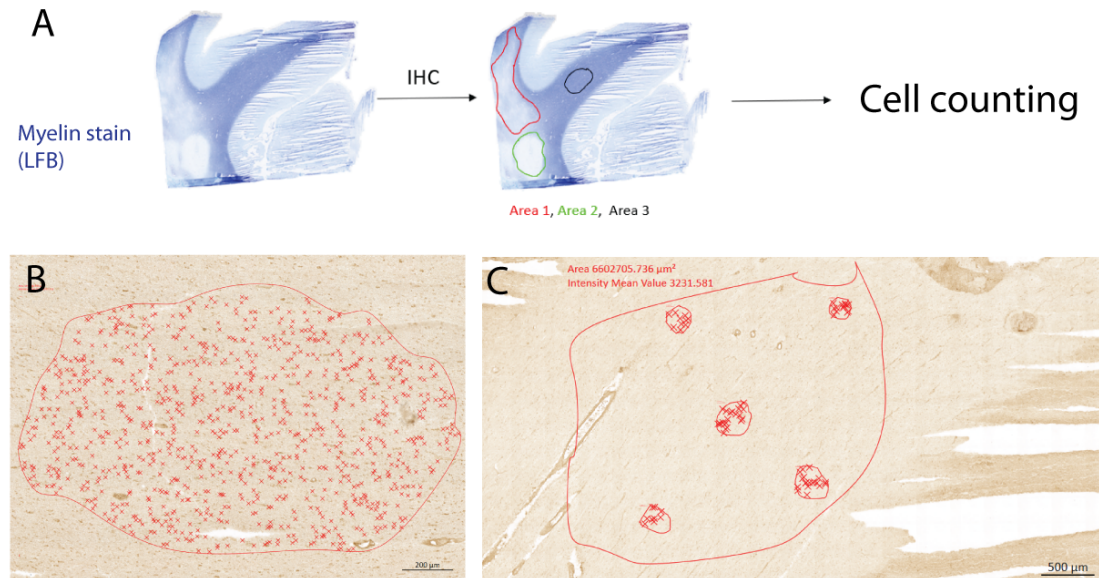


Figure 2.3: After IHC (here LFB staining is used as an example), regions of interest were drawn by a different researcher (marked here in different colours) (A). Cells were counted in the ROIs while blinded to the ROI's identity (different lesion types and NAWM) as well as the patient (control vs MS). Some ROIs were small and the whole area was counted such as the active lesion from MS154, A2D7 (B). In bigger ROI, 5 smaller areas were drawn within the ROI and only those were counted such as the NAWM from MS122. The cells/area from all 5 areas were then averaged. Red line shows the ROI outline and red crosses denote counted cells. Note scale bar is different in both images.

For the mouse tissue, lesions were determined by absence of linear myelin staining (MBP), presence of nuclei accumulation (Hoechst) and accumulation of immune cells (IBA1). Lesion outlines were drawn and lesion size measured. Cell counting was performed while blinded to the genotype of the animals. Cell counts were divided by the area of the lesion to give cell count/area.

For the mouse tissue electron microscopy analysis, the myelinated and unmyelinated axons were counted in all 10 fields of view and were averaged per each mouse. To determine the myelin thickness, the axon as well as the axon together with the myelin sheath were traced using a graphics tablet (Bamboo pad, Wacom) or (Huion, 1060 plus) on Image J to give axon

## 2 Materials and Methods

area and axon and myelin area respectively. From this, the diameter of the axon (inner) and diameter of the axon together with the myelin (outer) were estimated using the equation for area of circle ( 2.5):

$$A = \pi * r^2 \quad (2.5)$$

The g ratio was then calculated for each axon using the formula below ( 2.6)

$$g \text{ ratio} = \frac{\text{inner diameter}}{\text{outer diameter}} \quad (2.6)$$

Axons with thick myelin sheath have low g ratio (around 0.6) while axons with thin myelin sheath have higher g ratio (closer to 1). The g ratios of at least 250 axons were averaged for the mean g ratio per mouse. For the OPC migration assay, 3D reconstitution of the z-stack was created using Image J and the cells on the bottom (migrated cells) were counted while blinded to the treatment condition.

Images acquired on the Operetta were sent to the storage server Columbus which is also used to set analysis parameters. For all analysis pipelines, nuclei were detected by the Hoechst stain in the 405 nm channel. Their morphological properties were then calculated and the nuclei were further selected by area (30-150  $\mu m^2$ ) and shape (roundness) to exclude any non-nuclear Hoechst staining artefacts. This selection process was a starting point for each analysis. Further identification could then be made based on this population of selected nuclei depending on the assay. Result outputs were defined (such as cell numbers) and automatic batch analysis on the plate or multiple plates was run. The results file was an excel spreadsheet with the mean values per well (such as mean number of cells per well).

For proliferation and survival (TUNEL) assays, EdU or EdUTP incorporation was used to mark the proliferating and dying cells respectively as detailed in section 2.2.2 and 2.2.3. For both assay the EdU+ cells were visualised in the 647 nm channel. In the population of nuclei selected, the nuclear stain in the 647 nm channel was identified. The intensity properties were calculated and the EdU+ nuclei were further selected based on a threshold for the mean and maximum intensity of fluorescence. The results output was the ratio of EdU+ nuclei divided by all nuclei which gives the proportion of the proliferating or dying cells. This process is shown in figure 2.4.

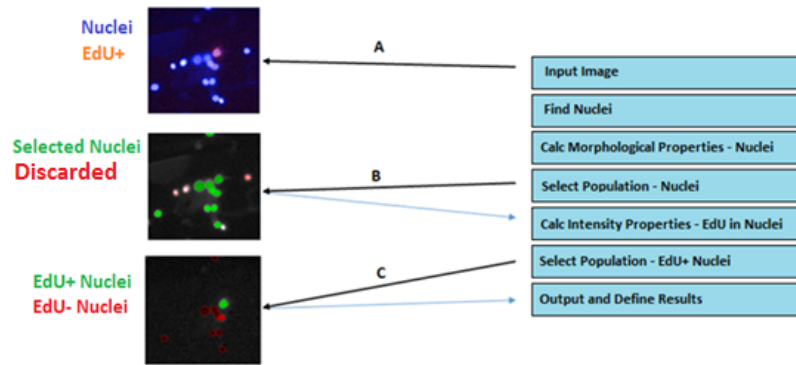


Figure 2.4: Analysis pipelines for proliferation and survival (TUNEL) assays were identical. Input image shows one EdU+ nucleus and several other nuclei (A). Nuclei were found in the 405 nm channel using Hoechst. Their properties were calculated and nuclei selected based on size and roundness (B). Nuclei which were too small, too bright or not round enough were excluded to avoid debris. The intensity in the 647 nm channel (EdU for proliferation or EdUTP for TUNEL) was calculated for the selected nuclei. Those nuclei were selected based on intensity threshold value (C). Finally, EdU+ cell were correctly identified among the other nuclei. Figure adapted from GS.

For motility analysis, cells were identified in the digital phase contrast channel. Their properties were calculated and they were selected based on texture, light intensity and morphology to exclude any debris. The selected cells were tracked by the software on the 114 subsequent time frames and tracks of their movement were generated. From those tracks, average velocity and accumulated distance could be calculated for cells in each well. The software required at least 1% overlap in the position of the cell from 1 time frame to another in order to detect continuous track. This informed the time between each frame (10 min). The software was able to identify cell division and exclude this. The Columbus pipeline is shown in figure 2.5.

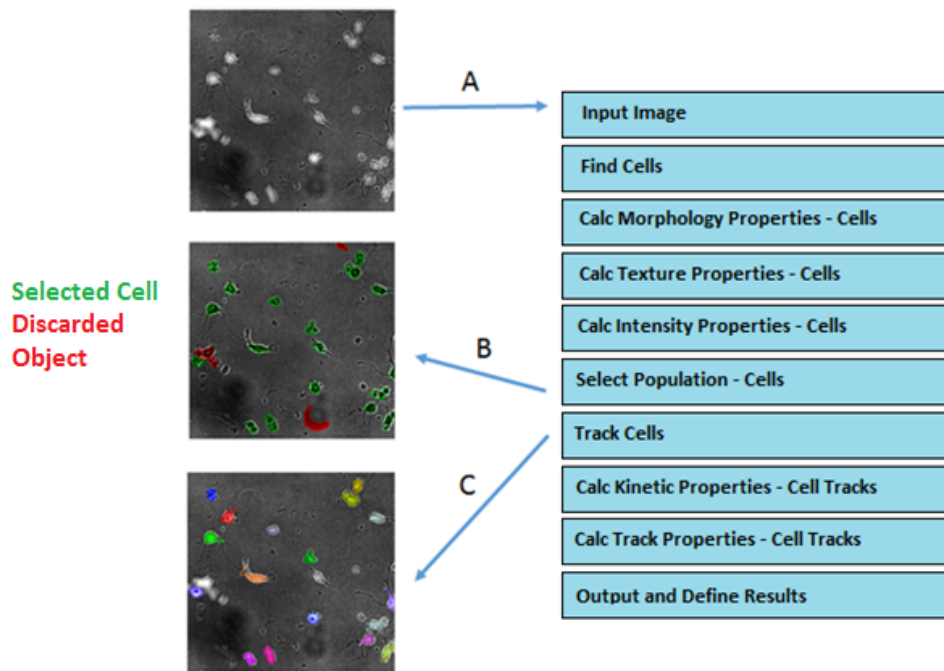


Figure 2.5: Analysis pipeline for motility. Input image (A) shows cells as bright objects on a dark background. Cells were found and their properties calculated. Population of cells was selected based on identified distinguishing properties (B). Debris is excluded at this point. Each individual cells was tracked over time (C). Figure adapted from Gregor Skeldon

For maturation assays, after identification of the selected nuclei, the cytoplasm was identified based on the NG2(488), O4 (568) and MBP (647) staining. Those 3 populations were further selected based on properties including: mean intensity of fluorescence, maximum intensity of fluorescence, intensity of cytoplasmic contrast and cytoplasmic texture to best identify the cells which were stained in each channel. NG2+ staining was variable and no parameters could detect NG2+ cells in all plates so those cells were manually counted in 3 fields of view in at least 3 wells per plate. The columbus pipeline is shown in figure 2.6. The results output was the proportion of MBP+ and O4+ cells divided by all cells. If a cell is O4+ and MBP+, it was included in both the MBP+ and O4+ cells proportion.

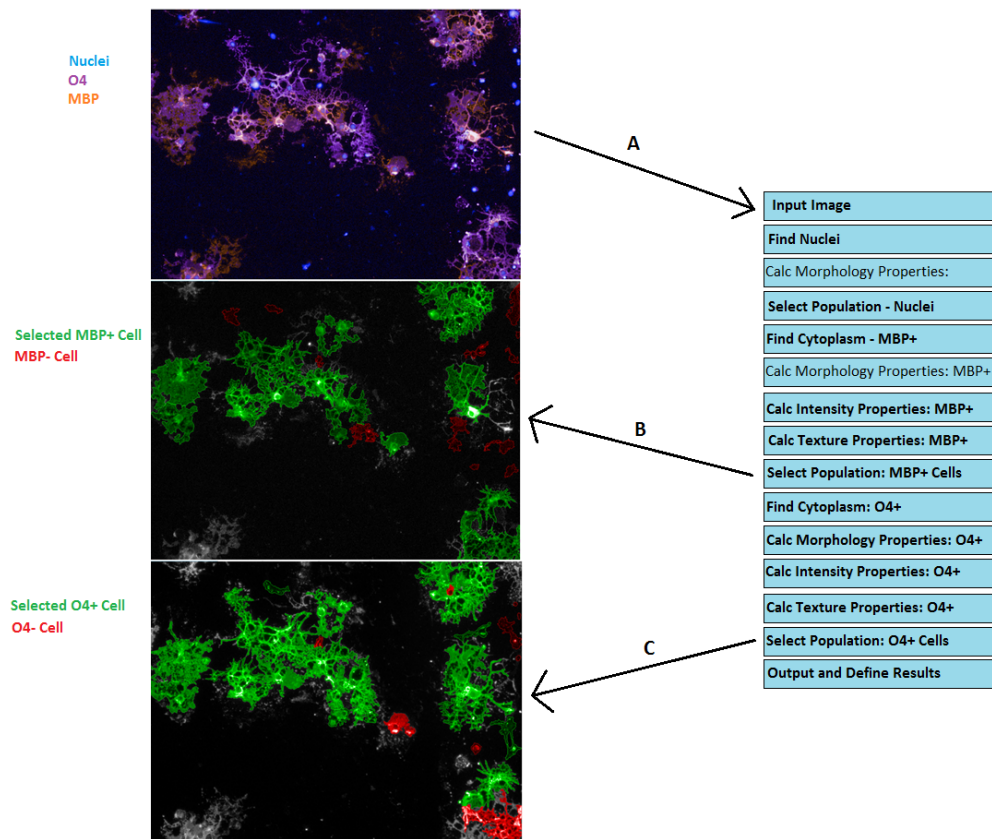


Figure 2.6: Analysis pipeline for maturation analysis. Input image shows O4 (purple) positive and MBP (orange) positive cells. After nuclei were selected, their cytoplasm was initially identified in the 647 nm channel (MBP). The properties of those cytoplasm were calculated including cytoplasm size, shape, intensity and the mean values for many properties were used to define parameters to select the MBP+ cells. The same process was repeated for O4+ cells. Finally, O4+ and MBP+ cells are correctly identified. Figure adapted from Gregor Skeldon

For purity analysis, in terms of calculating the number of contaminating astrocytes, after identification of the selected nuclei, the cytoplasm was identified based on GFAP (647) staining. The properties of the cytoplasm were calculated including size, intensity and morphology and used to define parameters to select the GFAP+ cells such as mean intensity of fluorescence and cytoplasmic morphology. The result output was the proportion of GFAP+ cells. The columbus pipeline is shown in figure 2.7

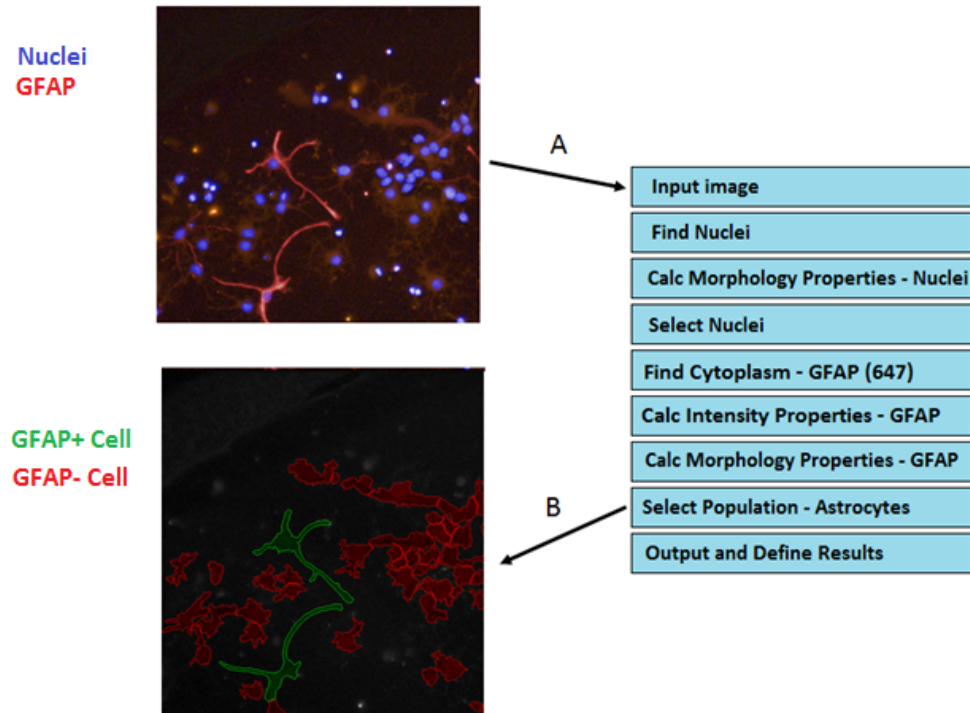


Figure 2.7: Analysis pipeline for purity assay. Input image shows two GFAP+ astrocytes (red). After nuclei were selected, their cytoplasm was found in the 647 nm channel (GFAP). The properties of the cytoplasm were calculated and used to define parameters to select the GFAP+ cells. Finally, GFAP+ cells are correctly identified. Figure adapted from GS.

### 2.4.3 Statistics

For all analysis, a d'Agostino and Pearson omnibus normality test was used to test whether the data fitted a normal distribution and a parametric test was done only if all compared data sets in an experiment passed the normality test. Otherwise, non parametric tests were performed. All statistical tests were performed using GraphPad Prism 5.

For human *post-mortem* staining, NDST1+ cells in control versus multiple sclerosis WM was compared using a two-tailed Mann Whitney U test. Multiple sclerosis lesions and their surrounding WM within one patient were compared using a paired two-tailed student's t test. The absolute numbers of NDST1+ cells and double positive NDST1+ OLIG2+ cells in individual lesions/normal appearing WM were compared by Kruskal-Wallis test. As MS tissue blocks contained more than one lesion, and we had several blocks from the same patients, we gave each patient an overall remyelination potential score corresponding to how many lesions in the blocks from that patient were remyelinated, or likely to remyelinate if the patient had survived.

Remyelinated lesions received an arbitrary 3 points, active lesions 2 points, chronic active lesions 1 point and chronic inactive lesions 0 points. This was divided by the number of lesions counted for each patient, to allow comparisons.

For the IHC on LPC-lesioned mouse brain, an unpaired two-tailed t test was used to compare between the transgenic animals and their wild type controls.

For the electron microscopy analysis, a two-factor ANOVA was used to identify the effects of treatment (LPC-surgery vs control) as well as the effects of genotype (transgenic vs wild type).

For the in vitro OPC assays, the Kruskal-Wallis test was used to compare between the different conditions and control and if significant difference was found, Dunn's multiple comparison test was used to identify the difference.

## 2.5 Materials

### 2.5.1 Human tissue

*Post-mortem* unfixed frozen tissues were obtained from the UK Multiple Sclerosis Tissue Bank via a UK prospective donor scheme with full ethical approval (MREC/02/2/39). Luxol fast blue (LFB) (staining myelin) and Oil Red O (staining lipids phagocytosed by macrophages) were performed to characterize and classify the lesion types. Active lesions have indistinct borders on LFB and lipid-laden macrophages/microglia. Chronic active lesions have a ring of lipid-laden macrophages/microglia and a core with few immune cells. Chronic inactive lesions have a distinct border on LFB and few immune cells. Finally, remyelinated lesions or shadow plaques have less intense staining on LFB. Cartoon representation of all lesion types is presented in figure 2.8. This classification was done by two independent researchers for a previous publication [29]. In this study, we used active (n=7), chronic active (n=4), chronic inactive (n=14) and remyelinated (shadow) MS plaques (n=21) from 14 blocks of brain tissue from 9 MS patients and 4 blocks of brain tissue from 4 controls with no neurological disease. These are summarised in the table 2.1.

## 2 Materials and Methods

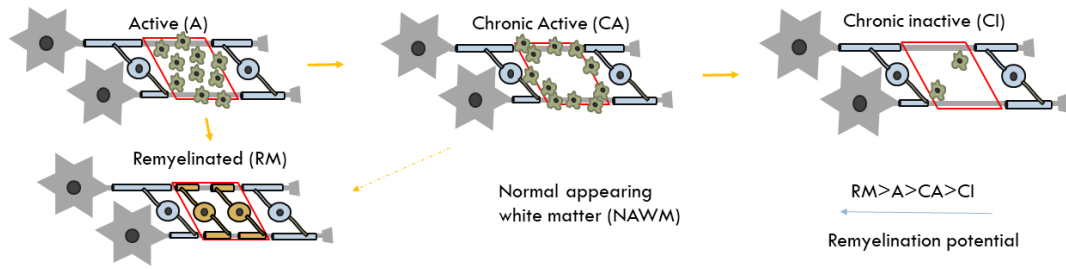


Figure 2.8: Schematic representation of different MS lesion pathological types and their hypothesised relationship to each other. Active lesions (red line) contain many immune cells (grey cells). Active lesions can repair if axons are ensheathed by new myelin sheaths (orange). However, if the lesion does not repair it may become a chronic active lesion. This type of lesion has many immune cells around its edge but not in the middle. This lesion may also repair to a fully remyelinated lesion however this is much less likely. Finally, chronic active lesions could in time turn into chronic inactive lesions which have barely any immune cells and very small chance of repair. Therefore, we propose that remyelinated lesions have the highest remyelination potential (already remyelinated), followed by active lesions, chronic active lesions and then chronic inactive lesions. All lesion types apart from the remyelinated lesions lack myelin staining. NAWM is also shown as it was counted and used as comparison.

Table 2.1: Classification and characteristics of human *post-mortem* samples

	Patient	Sex	Age (years)	MS type	Disease duration (years)	Time to post mortem (h)	Number of lesions	Active	Chronic active	Chronic inactive	Remyelinated
<b>MS</b>	MS100	M	46	SP	8	7	6	0	0	4	2
	MS121	F	49	SP	14	24	2	1	0	1	0
	MS122	M	44	SP	10	16	2	1	1	0	0
	MS136	M	40	SP	9	10	9	1	0	3	5
	MS154	F	34	SP	21	12	4	2	0	1	1
	MS176	M	37	PP	27	12	7	0	0	2	5
	MS187	F	57	SP	27	13	4	0	0	0	4
	MS207	F	46	SP	25	10	8	0	3	3	2
MS230	F	42	SP	19	31	4	2	0	0	2	
<b>Control</b>	CO14	M	64	-	-	26	-	-	-	-	-
	CO25	M	35	-	-	22	-	-	-	-	-
	CO28	F	60	-	-	13	-	-	-	-	-
	CO39	M	82	-	-	21	-	-	-	-	-
<b>Total</b>							46	7	4	14	21

## 2.5.2 Antibodies list

Table 2.2: List of primary and secondary antibodies used

<b>Primary antibodies</b>
chick anti-GFAP (DAKO, Z0334) at 1:3000
goat anti-Arginase-1 (Santa Cruz Biotechnology, sc-18355) at 1:25
mouse anti-NDST1 (1/50; Abcam, ab55296)
mouse IgG anti-CC1 (Abcam, ab16794) at 1:20
mouse IgG anti-CD68 (Abcam, ab53004) at 1:50
mouse IgG anti-iNOS (BD Bioscience, 610329) at 1:50
mouse IgG anti-NogoA (R&D, MAB3098) at 1:100
mouse IgG anti-NP1 (R&D, MAB5661) at 1:50
mouse IgM anti-O4 antibody (Immunosoty) at 1:1000
rabbit anti-GFAP (Covance, PCK591P-100) at 1:2000
rabbit anti-IBA1 (Wako, 019-19741) at 1:900
rabbit anti-NeuN (1/500; Abcam, ab104225)
rabbit anti-NG2 antibody (Millipore, A135320) at 1:200 (cells) and 1:50 (tissue)
rabbit anti-NP1 (CST, 3725 (D62C6)) at 1:50
rabbit anti-Olig2 (1/100; Sigma, HPA003254)
rabbit anti-olig2 (Millipore, AB9610) at 1:50
rat anti-MBP antibody (Bio-Rad, MCA4095) at 1:300 (cells) or 1:200 (tissue)
rat anti-PDGFRa (Biolegend, 135902) at 1:50
<b>Secondary antibodies</b>
anti-mouse Alexa 568 (Life Technologies, A11004) at 1:1000
anti-rat Alexa 647 (Life Technologies, A21247) at 1:1000
goat anti-chick 568 (Life Technologies, A11041) at 1:1000
goat anti-human IgG Alexa 568 (Life Sciences, A21090) at 1/1000
Goat anti-mouse IgM 647 (Life Technologies 21238) at 1:1000
Goat anti-rabbit 488 (Life Technologies, A11008) at 1:1000
goat anti-rabbit 647 ( Life Technologies, A212444) at 1:1000
Goat anti-rat 555 (Life Technologies, A21434) at 1:1000
ImmPRESS™ HRP Anti-Mouse IgG Polymer Detection Kit, made in Horse (Vector, MP-7402)
ImmPRESS™-AP Anti-Rabbit IgG Polymer Detection Kit (Vector, MP-5401)

## 3 NDST1 is upregulated in MS and correlates with remyelination

### 3.1 Introduction

Even though the importance of heparan sulfate and NDST1 in development is well recognised in the literature, their involvement in multiple sclerosis is less clear. There is increased risk of MS associated with a single nucleotide polymorphism in a gene for a heparan sulfate proteoglycan [15] mentioned in section 1.2.1. The same SNP was also associated with inefficient interferon $\beta$  therapy in MS patients [33]. Both of those effects are believed to be due to the ability of heparan sulfate proteoglycans to sequester cytokines. Moreover, heparan sulfate proteoglycans are expressed in active lesions and thought to contribute to lesion chronicity (section 1.7.2). The exact connection between NDST, HS and MS-like pathology and its mechanism were further elucidated by our collaborators in Pascale Durbec's group.

Pascale Durbec's group in France performed microarrays to compare SVZ progenitor gene expression between conditions of LPC-demyelination and control in a previous publication [45]. In addition to SVZ progenitors, they also isolated oligodendroglia and found that NDST1 is significantly upregulated (fold increase of 48.9 and 14.0 in two different trials) in conditions of demyelination compared to control (unpublished data). This prompted them to investigate the involvement of NDST1 and HS in vitro and in animal models of demyelination and remyelination. Their key findings are summarised below:

- After demyelination (caused by LPC injection), NDST1 is upregulated in mature oligodendrocytes in a rim around the lesion
- NDST1 KO in OLIG2+ cells increases demyelinated lesion size (again with LPC lesion) and delays OPC recruitment in vivo
- Removing heparan sulfate by heparinase impairs OPC migration in vitro
- Heparan sulfate controls the local enrichment of sonic hedgehog (Shh) which is important for remyelination [87]
- Heparan sulfate secretion by oligodendroglia in culture increases with their maturation

NDST1 and HS are therefore important for OPC migration in vitro and in vivo as well as prompt remyelination in LPC-demyelination animal models. However, their relevance to MS is unknown. Therefore, we aimed to investigate the expression of NDST1 and HS in human

*post-mortem* tissue from MS patients in collaboration with Pascale Durbec's group to find the relevance of their findings in human pathology.

The *post-mortem* tissue which was used for this study is summarised in section 2.5.1 and the staining method in section 2.3.2. In brief, tissue from 9 MS patients was previously characterised and classified into different lesion types: active, chronic active, chronic inactive, remyelinated. Normal appearing white matter (NAWM) and tissue from 4 patients which did not die from neurological disease were used as comparison. HS staining with the mouse IgM anti-N-sulfated motifs on HS chains which binds to the HS modification created by NDST1 (10E4 antibody, Seikagaku, Japan) did not give any signal on human tissue. On the other hand, NDST1 colourimetric staining was successful and allowed characterisation of the expression of this enzyme in different types of human lesions.

## 3.2 Results of tissue staining

To examine the relevance of the mouse findings for multiple sclerosis physiopathology, we examined the expression pattern of the NDST1 protein in human multiple sclerosis (MS) white matter (WM), ranging from normal appearing WM, remyelinated, active, chronic active or chronic inactive lesions. Observation that NDST1 staining was fainter in control tissue compared to MS tissue prompted us to investigate the level of expression of the enzyme after a short (exactly 2 min for each slide), incomplete development of the colorimetric stain.

### 3.2.1 NDST1 is upregulated in multiple sclerosis tissue

While NDST1 staining was very weak in control WM (no MS), we observed a significant increase of NDST1 labelling in MS patients WM (figure 3.1 A-B). Comparison of healthy control, MS normal appearing WM and MS lesions showed that there is a significant increase of NDST1 staining in multiple sclerosis lesions vs. control as measured by pixel count (Kruskal-Wallis test,  $H=13.09$ ,  $n=4,9,9$ ,  $p=0.0002$ ) (figure 3.1 C). Comparison of each MS lesion with its surrounding normal appearing WM using a paired t test, revealed that there is significantly more NDST1 labelling in MS lesions compared to their surrounding normal appearing WM (paired two-tailed t test,  $t_9=3.39$ ,  $p=0.0095$ ). If staining in control was fully developed, NDST1 positive cells were observed which indicates that NDST1 is expressed in control tissue as well, but it is over-expressed in MS brain and particularly in lesions.

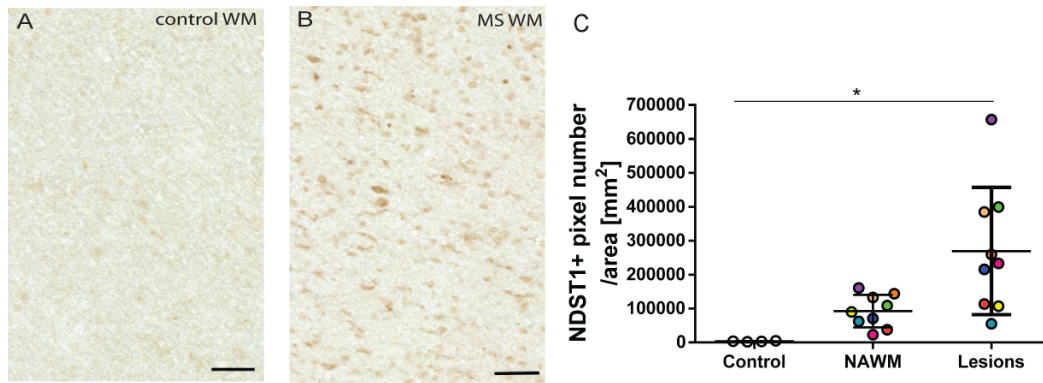


Figure 3.1: NDST1 is upregulated in MS. Representative images of NDST1 staining in control (A) and MS (B) WM. (C) Quantification of NDST1 labeling shows a significant over-expression of NDST1 in MS lesions compared to control tissue (Kruskal-Wallis test,  $H=13.09$ ,  $n=4,9,9$ ,  $p=0.0002$ ). The colours represent paired samples from the same patients. Graph shows means plus standard deviation. There are NDST1+ cells in control brain however NDST1 is overexpressed in MS brain. Scale bar is  $100 \mu m$ .

### 3.2.2 NDST1 is primarily expressed in oligodendroglial cells

I then performed double-labelling immunohistochemistry to determine which cells express NDST1. I characterized NDST1-positive cells in various types of lesions and normal appearing WM, defining their cellular type using the markers OLIG2 for oligodendroglia (figure 3.2 A), GFAP for astrocytes (figure 3.2 B), NEUN for neurons (figure 3.2 C) and IBA1 for microglia/macrophages (figure 3.2 D). A proportion of all of these cells expressed NDST1 but quantitative analysis showed that the majority of NDST1+ cells were oligodendroglia in all types of lesions (remyelinated, active, chronic active, chronic inactive), normal appearing WM and control tissue (figure 3.3). The NDST1+ cellular composition of control tissue, NAWM and lesions was slightly different with chronic lesions having more NDST1+ astrocytes and macrophages/microglia proportionally to control tissue.

3 *NDST1* is upregulated in MS and correlates with remyelination

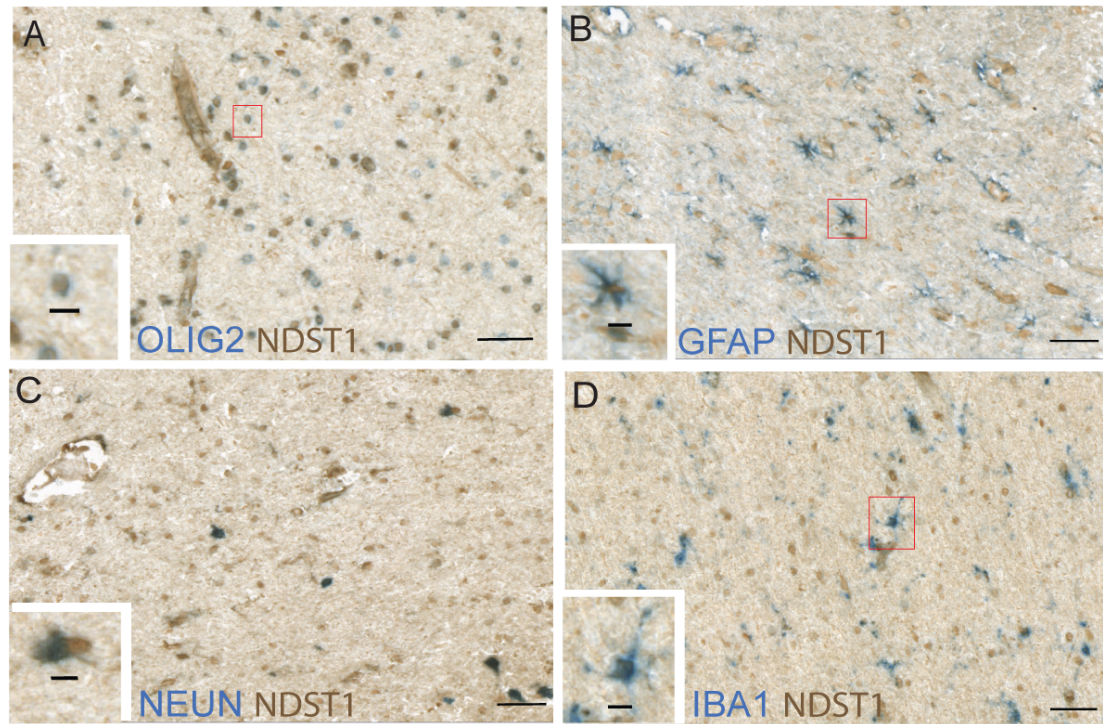


Figure 3.2: *NDST1* is expressed by oligodendroglia, astrocytes, microglia/macrophages and neurones. Representative images of immunohistochemistry using antibodies against *NDST1* successively co-labelled with antibodies for OLIG2 for oligodendroglia (A), GFAP for astrocytes (B), NEUN for neurones (C), and IBA1 for microglia/macrophages (D). Scale bars represent 50  $\mu\text{m}$  in low magnification and 10  $\mu\text{m}$  in high magnification.

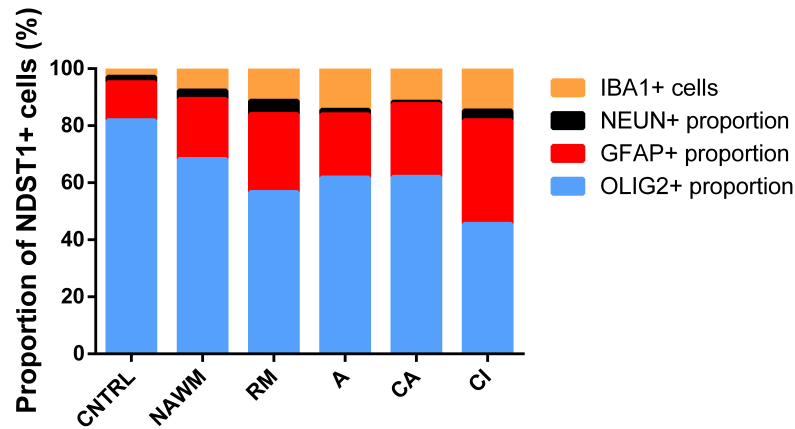


Figure 3.3: NDST1 is primarily expressed in oligodendroglia. Quantification of the proportions of different NDST1+ cell types in normal appearing WM and various MS lesions shows that NDST1 expressing cells are mainly oligodendroglia. This is followed by expression by astrocytes, microglia/macrophages and finally neurones. NAWM is normal appearing white matter, CNTRL is control, RM is remyelinated lesions, A is active lesions, CA is chronic active lesions, CI is chronic inactive lesions.

We also investigated the expression of NDST1 in cultured rat oligodendrocytes to investigate whether the increase in heparan sulfate extracellularly observed by Pascale's group can be attributed to increase in NDST1. We observed NDST1 expression in OPCs marked by antibody against NG2, immature oligodendrocytes marked by antibody against O4, pre-myelinating oligodendrocytes and oligodendrocytes with flat myelin sheaths marked with antibody against MBP (Figure 3.4). However, its expression level was unaffected by the maturity of the cells in culture. In immature oligodendrocytes and pre-myelinating oligodendrocytes the NDST1 staining was strongest in the perinuclear region consistent with its primary location in the Golgi apparatus [130] mentioned in section 1.7.4.

### 3 NDST1 is upregulated in MS and correlates with remyelination

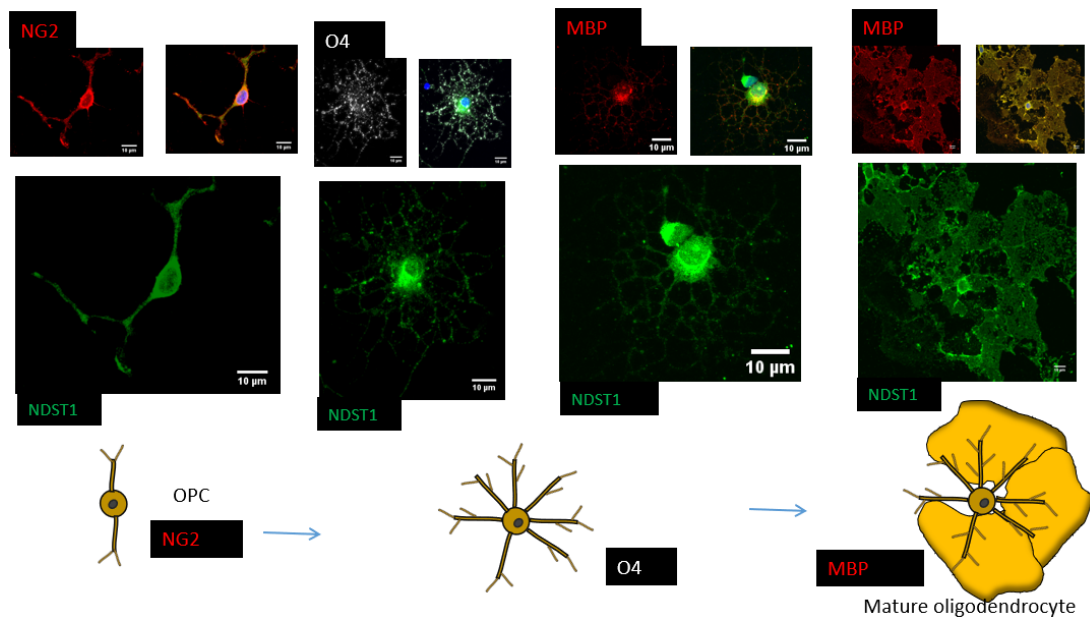


Figure 3.4: NDST1 is expressed in isolated rat oligodendroglia in vitro. The expression of NDST1 appeared independent of the maturation of OPCs. Scale bars represent 10  $\mu\text{m}$ .

#### 3.2.3 The majority of OLIG2+ cells in MS (but not control) are NDST1+

Since the majority of the NDST1+ cells were oligodendroglia, we looked at how many of the oligodendroglia were NDST1+. While the vast majority of OLIG2+ cells in multiple sclerosis patients (both the lesions and NAWM) expressed NDST1, less than half of the OLIG2+ cells in control tissue expressed NDST1 (figure 3.5). Particularly, there was a significantly higher proportion of NDST1+ oligodendroglia in active lesions compared to control tissue (Kruskal-Wallis test,  $H=13.92$ ,  $n=4,7,21,4,14,14$   $p=0.0162$  and Dunn's multiple comparison test). This means that in this disease state NDST1's level is upregulated and it is expressed by more oligodendroglia.

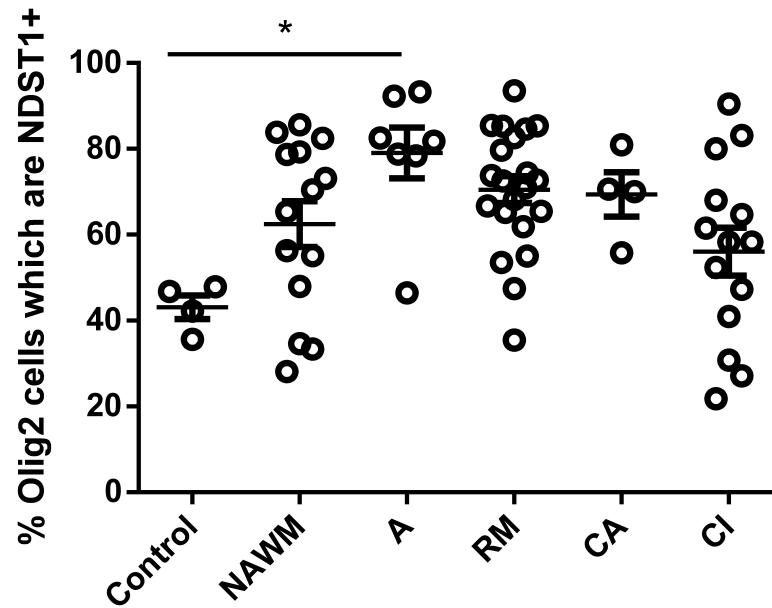


Figure 3.5: *NDST1* is expressed in around 2 times more oligodendroglia in MS than in control. Quantification of the proportion of the OLIG2+ cells which are *NDST1*+ shows that the percentage significantly increases in active lesions compared to control (Kruskal-Wallis test,  $H=13.92$ ,  $n=7,21,4,14,14$   $p=0.0162$  and Dunn's multiple comparisons test). Overall, the majority of the OLIG+ cells are *NDST1*+ in MS lesions and NAWM while this is not true in control brain tissue. Each dot is a lesion or NAWM/control region. NAWM is normal appearing white matter, CNTRL is control, RM is remyelinated lesions, A is active lesions, CA is chronic active lesions, CI is chronic inactive lesions.

So far, *NDST1* was found upregulated in primarily in oligodendroglia in MS which correlates very well with the animal model findings from Pascale Durbec's group. We then investigated whether any correlation exists with the lesion type and the number of *NDST1*+ oligodendroglia which appear to be important in repair in mouse.

### 3.2.4 OLIG2+ *NDST1*+ cell numbers are reduced in CI lesions and negatively correlate with lesion size

After we looked at the proportional relationships of oligodendroglia and *NDST1*, we analysed the the absolute number of double positive OLIG2+ *NDST1*+ cells in different types of lesion, NAWM and control tissue. We found a trend towards less absolute OLIG2+ *NDST1*+ cell numbers in more chronic lesions shown in figure 3.6. There were significantly less of those cells in CI lesions compared to NAWM (Kruskal-Wallis test,  $H=14.67$ ,  $n=4,22,21,7,4,14$   $p=0.012$  and Dunn's multiple comparisons test).

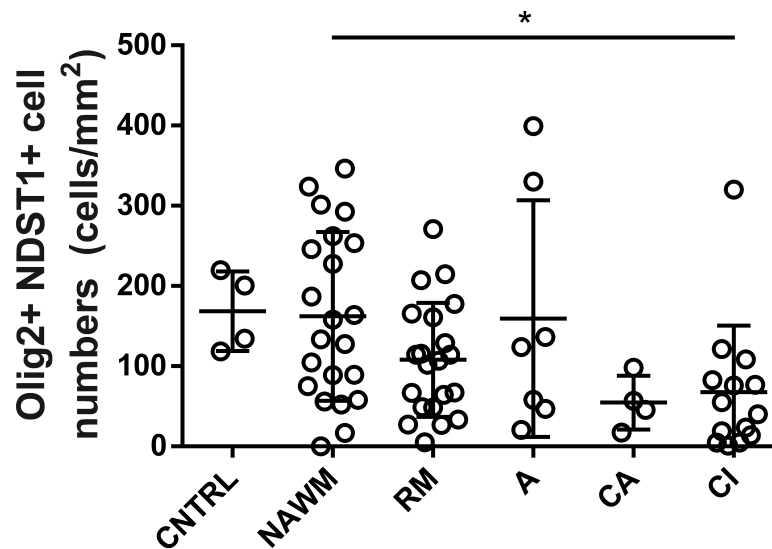


Figure 3.6: There are less absolute NDST1+ oligodendroglia numbers in CI lesions compared to NAWM. There is a trend towards less OLIG2+ NDST1+ cells in chronic active and chronic inactive lesions compared to control and NAWM. This trend reaches significance in the comparison of CI lesions and NAWM and there were significantly less of those cells in CI lesions compared to NAWM (Kruskal-Wallis test,  $H=14.67$ ,  $n=4,22,21,7,4,14$   $p=0.012$  and Dunn's multiple comparisons test).

Since loss of NDST1 in a mouse model results in increased demyelinated lesion size and having less NDST1+ OLIG2+ cells is correlated with chronic inactive lesions, we looked at the relationship between NDST1+ OLIG2+ cell number and lesion size. We found that the number of NDST1+ oligodendroglia in each lesion inversely correlated with the lesion size (figure 3.7). This gives an indication that there is similarity in the function of NDST1 between the mouse model and the human disease with the limitation that in human tissue we are observing a single time point and could only find correlation but not causation.

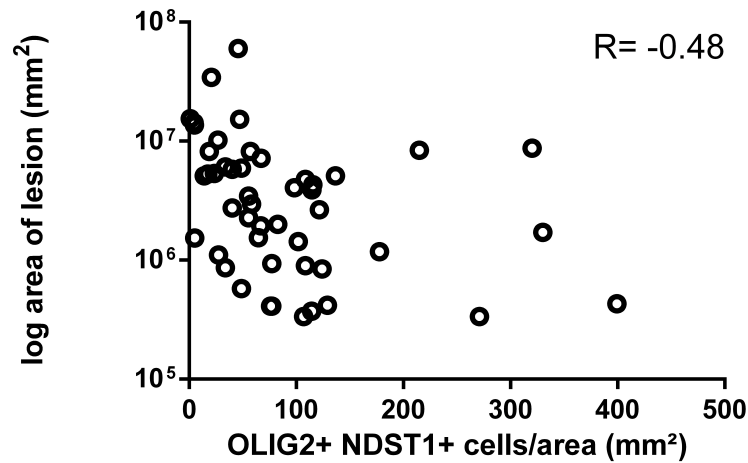


Figure 3.7: The number of oligodendroglia expressing NDST1 is inversely correlated to lesion size.

### 3.2.5 NDST1+ cells correlate with remyelination potential

We found that there was no difference in the average NDST1+ cell numbers in different lesions, NAWM and control (Kruskal-Wallis test,  $H=3.10$ ,  $n=4$  (CTL),  $n=22$  (NAWM),  $n=21$  (RM),  $n=7$  (A),  $n=4$  (CA),  $n=14$  (CI),  $p=0.54$ ) (figure 3.8). Moreover, we did not observe any correlation between NDST1+ cells and age, sex and disease duration in our small cohort. However, we noticed that the variation in the NDST1+ cell number between patients was very big. Moreover, some patients who had many chronic lesions had low NDST1+ numbers while others with multiple remyelinated lesions had very high NDST1+ cell numbers.

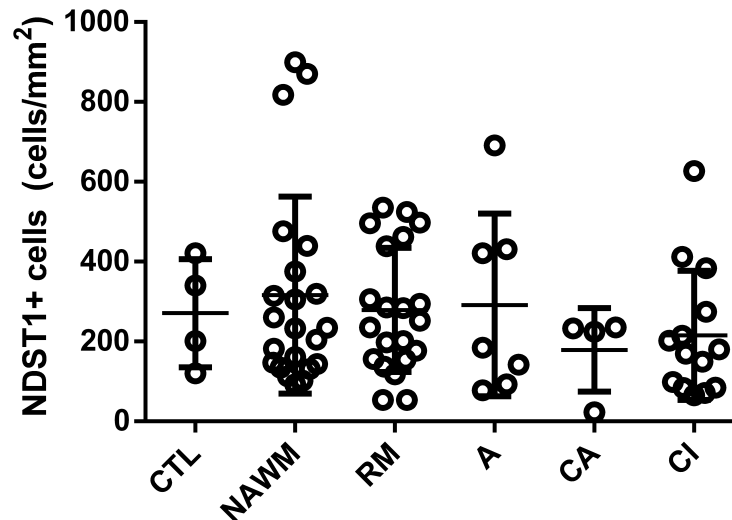


Figure 3.8: The number of NDST1+ cells is no different between lesion types, NAWM and control brain(Kruskal-Wallis test,  $H=3.10$ ,  $n=4,22,21,7,4,14$   $p=0.54$  )

We therefore wanted to check if there is any correlation between the lesion types a patient has and their NDST1+ cell numbers. As blocks of MS tissue had multiple lesions and sometimes we had multiple blocks from the same patient, we decided to assign an arbitrary score to each patient, correlating with the proportion of their lesions that were remyelinated (3 pts), active (2pts), chronic active (1 pt) and chronic inactive (0 pt). Here, we were aiming to see whether patients considered to be good remyelimators using this score may also have more NDST1+ cells. We showed that NDST1+ cell density positively correlated with patients' score of remyelination (figure 3.9). These data reveal that multiple sclerosis tissues with a higher repair potential (containing most active and remyelinated lesions) display a high number of NDST1+ cells therefore suggesting that higher numbers of NDST1+ cells in a lesion may provide a positive environmental support for myelin repair.

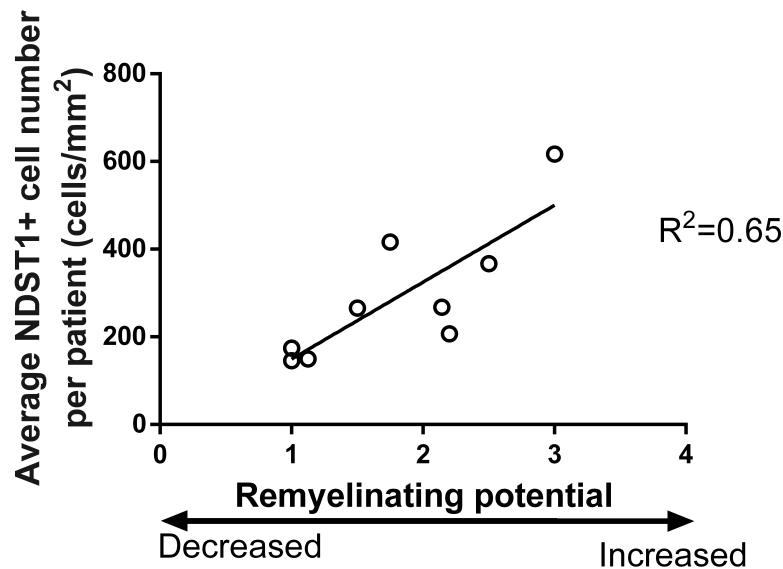


Figure 3.9: NDST1+ cell numbers positively correlate with remyelination score assigned to each patient, summing all lesions within blocks from the same MS patient.

### 3.3 Discussion

We have investigated the relevance of *in vivo* mouse findings to human disease. While *post-mortem* human tissue is currently one of the best tools to study human disease, it also has numerous limitations. The main limitation is that human tissue represents a snap shot of events at a specific time. Therefore, not only are we unable to track the progress of any process in time but we are also unaware what time point we are observing. To illustrate, we are unaware whether the active lesion in a *post-mortem* section originated a week, a month or a year before the death of the patient. Similarly, we are unaware if a chronic inactive lesion progressed from active to chronic active and finally to chronic inactive or not. Another caveat of using *post-mortem* human tissue is that we are looking at a small block of tissue in different brain regions in the different patients. Therefore, the part of the brain we study might not be representative of the whole brain and also regional differences might influence the results. Finally, the human tissue I used for my studies has the additional caveat that the MS patient and control cohorts are not age matched as the age of death of the the majority (3/4) of control patients is much higher than the age of death of the MS patients 2.1. Since age is known to influence remyelination, this age difference could influence the results. Regardless of these limitations, studying *post-mortem* human tissue is still on of the best way to study relevance to human disease.

Comparison of the NDST1 expression in *post-mortem* human tissue revealed remarkable but not complete similarity to the NDST1 expression and function in the LPC-demyelinated animal model (unpublished data from Pascale Durbec's lab).

### 3.3.1 Upregulation of NDST1 in MS

Investigation of *post-mortem* human brain for expression of NDST1 revealed that NDST1 is upregulated at the whole tissue level (figure 3.1) in MS patients compared to control. Moreover, in each patient, the expression of NDST1 was higher in lesions than in normal appearing white matter. Therefore, NDST1 is upregulated in MS brain compared to control brain and this upregulation is strongest in the lesions. This is in very good correlation with the upregulation observed after demyelination in an animal model. In addition to the increasing level of NDST1, NDST1 is expressed in more oligodendroglial cells in MS than in control (figure 3.5). This indicates that in addition to the increased protein level, NDST1 is expressed *de novo* in cells which have not expressed it before. Therefore, both in human and in mouse, NDST1 is upregulated as a result of demyelination insult.

What was different between our observations in human tissue and the observations of Pascale Durbec's laboratory in mouse was the spatial distribution of oligodendroglia (see figure 2.3 B). While they see NDST1 localised around the rim of the lesion, in human, NDST1+ cells were evenly spread throughout the lesion and NAWM with no obvious patterns. This difference could be because of timing of examination of the tissue after the lesion onset. In an animal model, the lesion is very acute and is examined only a few days/weeks following demyelination. On the other hand, the time between demyelination and examination in a human lesion is unknown and overall their repair is much less efficient. Therefore, this spatial rim could be characteristic only of a very acute lesions in their infancy which are not found in human *post-mortem* brain. These very young lesions may only be detected on biopsy of early lesions in CNS tissue from MS patients where Anna Williams has previously observed a travelling rim of cells at the edge of the active lesions which are available in some countries.

### 3.3.2 NDST1 is expressed in oligodendroglia in human

NDST1+ cells are predominantly OLIG2+ with the proportion varying from around 80% in control tissue to around 50% in CI lesions (Figure 3.3). As oligodendroglial cells were detected by using antibody against OLIG2, those cells could be OPCs, immature oligodendrocytes or mature oligodendrocytes. Moreover, our *in vitro* investigation on the expression of NDST1 in oligodendroglia during maturation revealed expression in all stages (Figure 3.4) indicating that the OLIG2+ NDST1+ cells likely consist of oligodendroglia in all stages of maturation. This is a limitation as no direct comparison is available with mouse data where NDST1 was expressed almost exclusively by mature oligodendrocytes. Unfortunately, detection of mature oligodendrocytes expressing NDST1 could not be performed due to limitations in double labelling using effective antibodies. In human tissue, mature oligodendrocytes are most commonly identified by positivity against the combination of antibodies against OLIG2 and NOGOA. However, the colourimetric detection is limited to two antigens and detection of OLIG2+ NOGOA+ NDST1+ cells is therefore not possible. For future studies, fluorescent detection of those antigens could be attempted if the problematic autofluorescence of adult human tissue could be overcome.

### 3.3.3 High NDST1 cell number is linked to smaller and less chronic lesions

I further showed that normal tissue and NAWM have more OLIG2+ NDST1+ cells than chronic lesions (figure 3.6). This is not surprising since demyelination selectively destroys the mature oligodendrocytes which are believed to be the main cell type expressing NDST1 according to the mouse studies. Overall, chronic lesions have less OPCs [29] which are the other population marked by antibodies against OLIG2. Therefore, this reduction in OLIG2+ NDST1+ in more chronic lesions is likely a result of the reduction of oligodendroglia in those lesions. However, bearing in mind the phenotype of the OLIG2-specific NDST1 KO mice (reduced OPC migration and remyelination) this reduction of OLIG2+ NDST1+ is also likely to have functional consequences.

Overall, human *post-mortem* tissue can have a very limited contribution to functional elucidation because studies on it are purely observational. However, luckily the OLIG2-specific NDST1 KO mouse gave a phenotype which could also be measured in human tissue - bigger lesion size. We therefore compared the size of the lesion and the content of OLIG2+NDST1+ cells and found a weak correlation. The more OLIG2+NDST1+ cells were in the lesion, the smaller the lesion. This data is in correlation with the transient increase of lesion size in the oligodendroglia-specific NDST1 KO mouse, indicating that OLIG2+NDST1+ cells are important for limiting lesion size. The next question is whether this effect on lesion size could contribute to better remyelination or its failure.

### 3.3.4 NDST1 and remyelination

Observation of the number of NDST1+ cells revealed that the inter-patient variation was much higher than the intra-patient variation. Great heterogeneity between patients but not within lesions of the same patient has previously been reported in the mechanism of demyelination [180] indicating that such observations of inter-patient variation are common and posing the question whether a single therapy can be effective in such a heterogeneous disease. With differences up to 4 times the number of NDST1+ cells and their possible importance for limiting lesion size, we could speculate that patients with increased number of NDST1 would be better at repairing. Although testing this hypothesis is impossible in human, I noticed that the patients which had higher number of NDST1+ cells tended to have more remyelinated and active lesions while those with low NDST1+ cell numbers had more chronic lesions. Therefore, we aimed to find a way to quantify this observation by assigning a score based on likelihood of the lesion to repair and taking the average of all lesions for each patient. Our finding that patients with higher NDST1+ cells also tended to have higher remyelination potential score indicated that NDST1 might be important in repair.

However, the remyelination potential is estimated in only a small tissue block (or a few blocks) and also in different brain regions in the different patients. Therefore, the remyelination potential in a part of the brain might not be representative of the whole brain and the inherent differences in the different brain regions might also influence the results. Regardless, together with the mouse data from Pascale Durbec's group, the correlation between NDST1+ cells and re-

myelination potential score is strong and indicative of NDST1's potential importance in human repair.

### 3.3.5 Summary

The NDST1 over-expression in human MS brain could be responsible for the previously observed de novo expression of heparan sulfate proteoglycans in active lesions [317] discussed in section 1.7.2. Even though heparan sulfate proteoglycans have been associated with the transition from active into chronic lesion [271], their overall function is unknown. Here we show that:

- NDST1 protein level is upregulated in MS
- NDST1 expression is significantly higher in MS lesions compared to surrounding normal appearing white matter (NAWM)
- NDST1+ cells are primarily oligodendroglia but do not form a ring around the lesion
- There is inverse correlation between lesion size and density of NDST1-expressing oligodendroglia
- NDST1 cell density is positively correlated with a score of potential remyelination ability in patients

Our data, in combination with Pascale Durbec's data in mouse, suggests that oligodendroglia are activated and respond to neighbouring demyelination by upregulation of NDST1. NDST1 and HS are involved in both limiting the size of the lesion and creating a permissive environment for myelin regeneration possibly by sequestering pro-repair signalling molecules.

### 3.3.6 Model

We postulate that in normal mice, mature NDST1+ oligodendrocytes deposit heparan sulfate in a rim around the lesion (Figure 3.10). Heparan sulfate deposition contributes to repair by making the environment around the lesion more permissive to OPC recruitment from surrounding tissue to the inside of the lesion.

In the OLIG2-specific NDST1 KO, the oligodendroglia around the lesion does not express NDST1 and cannot deposit heparan sulfate thus resulting in a bigger lesion, less OPC migration and less effective remyelination. In human, some patients have many NDST1+ cells which will deposit HS in the lesion and contribute to repair. On the other hand, other patients have less NDST1+ cells which will limit the heparan sulfate deposition and limit OPC recruitment and result in less effective remyelination.

### 3 NDST1 is upregulated in MS and correlates with remyelination

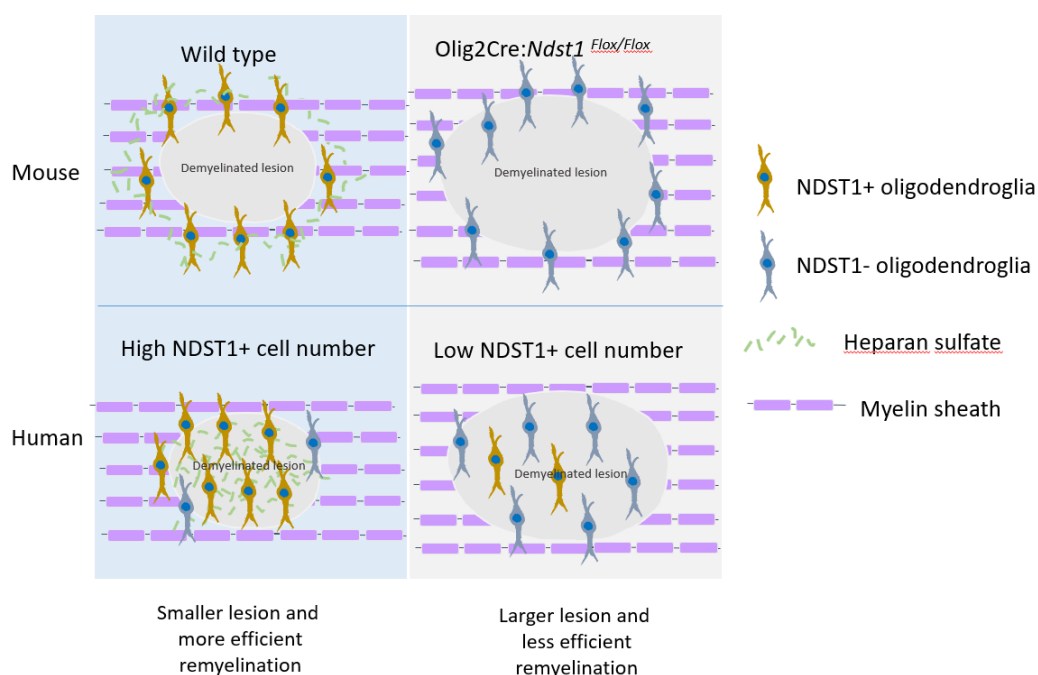


Figure 3.10: Comparison of mouse and human results.

The main limitation of our human study is that it only suggests correlation but cannot prove causation. The observed correlation between NDST1+ cell number and remyelination potential score as well as NDST1+ oligodendroglia number and lesion size could be just because another factor has caused these independently of each other. Moreover, human tissue shows us a snapshot of events [90] but not the transition and connection between those. Bearing those limitations in mind, our data in combination with the mouse data gives a strong case about the importance of heparan sulfate in repair.

Currently, HS is believed to be so important because it is a substrate for binding of pro-repair signalling molecules such as shh [87]. It is interesting to speculate that if the signalling molecule environment in MS is enriched in signalling molecules which impair repair, heparan sulfate would be involved in sequestering those as well and thus would have a negative effect. This hypothesis would have to be tested and the role of NDST1/HS would have to be elucidated on isolated primary human OPCs [195] or ES-derived human OPCs [217] in remyelination models before considering NDST1 enhancing as a therapeutic option in MS.

In addition to this, there often are multiple regulatory mechanisms for any signalling molecule which in turn have multiple downstream effects. To illustrate this complexity, both NDST1/HS and Sema3A/NP1 are involved in shh signalling with heparan sulfate sequestering it while NP1 is a positive regulator of shh and shh is a positive regulator of NP1 transcription [314]. Therefore, as discussed in section 1.12 heparan sulfate positively regulates Sema3A signalling via NP1 while NP1 positively regulates shh. Increasing the heparan sulfate content by enhancing NDST1 could be very beneficial for shh signalling which is important for remyelination [87] however it would also enhance Sema3A-mediated OPC repulsion via NP1. Conversely, block-

*3 NDST1 is upregulated in MS and correlates with remyelination*

ing NP1 would be beneficial for stopping Sema3A-mediated OPC repulsion but would also negatively impact shh.

## 4 Assessing remyelination in the NP1(Sema3A-) mice

### 4.1 Introduction

As summarised in section 1.13, Sema3A is a chemorepulsive molecule which is upregulated in demyelinated injury rodent models [29] [296] [245] [117] as well as multiple sclerosis lesions, particularly in OPC-depopulated chronic active lesions [330] [29] [34]. Research has consistently found that the level of Sema3A negatively correlates to remyelination because Sema3A hinders OPC migration(section 1.9.1). This has highlighted Sema3A as a potential target to improve OPC recruitment in MS however the size and shape of the molecule make it hard to design therapeutics against (Figure 1.5).

#### 4.1.1 Does NP1 inhibition aid remyelination?

Sema3A acts via its 'druggable' receptor, Neuropilin 1, which is a tyrosine kinase receptor for both Sema3A and vascular endothelial growth factor (VEGF) and is found on OPCs and many other cell types. Since decreasing the level of Sema3A is beneficial for OPC migration and remyelination and NP1 is Sema3A's receptor, we can hypothesise that disruption of Sema3A's signalling via NP1 would also be beneficial for OPC migration and remyelination. To support this, one study has shown that NP1(Sema3A-) mice which have mutations in the Sema3A binding site of NP1 show increased OPC migration after demyelination [245]. However, this study did not look at the effect of this increased migration on remyelination.

Therefore, we wanted to determine if inhibition of Sema3A signalling via NP1 had the same positive effect on remyelination as lowering the level of Sema3A. Embryonic lethality of the NP1 KO mice due to cardiovascular defects mediated by loss of VEGF signalling via NP1 [152] prevents using them as to assess adult remyelination. Therefore, we initially assessed remyelination in the NP1(Sema3A-) mice which have 7 amino acid changes in the Sema3A binding site on NP1 in all cells (highlighted in purple in Figure 1.5) which are the same mice which have been shown to exhibit increased OPC recruitment. We thought that this genotype was particularly suitable because it would mimick the effect of a potential therapeutic inhibitor of the Sema3A site of NP1 which will act on all cells of the body.

### 4.1.2 Animal models

Animals (other than humans) do not spontaneously develop multiple sclerosis. Therefore, numerous animal models exist which represent different parts of the complexity of multiple sclerosis. Largely, they are separated into models which primarily represent the immune response of MS with some demyelination (EAE, viral) and primarily demyelinating models with limited immune response (cuprizone and LPC). Therefore, animal models of the disease tend to represent only a part of it: EAE and viral mimic the inflammatory milieu while toxin models represent the demyelination [290]. Since we are interested in studying remyelination and migration of OPCs, for simplicity, we required a focal model which recapitulates primarily demyelination. A focal lesion is required to allow OPCs to migrate down a gradient of chemotactic factors between normal and abnormal tissue. This is why we used the LPC model of demyelination which results in a focal lesion in the area of injection in the CNS [120].

In this model demyelination and remyelination happen at fairly distinct times allowing separate investigation of the effect of a factor on either of them [95]. Demyelination is complete by 3 days post-lesion, followed by OPC migration around days 6-10 post lesion, differentiation around days 10-14 post lesion and remyelination which is complete by 4 weeks after lesion [29]. LPC-induced demyelination is characterised by myelin degradation, oligodendrocyte death, disruption of the BBB and immune infiltration by predominantly macrophages and microglia but also some T cells, neutrophils and monocytes [234].

### 4.1.3 Method

The methods used to induce demyelination and assess remyelination are detailed in section 2.1.2. In brief, stereotactic surgery was performed to inject LPC, a demyelinating toxin in the corpus callosum of adult WT and NP1(Sema3A-) mice (Figure 4.1). Repair was allowed for 17 days and then the tissue in the lesion was prepared for EM examination. To assess the remyelination efficiency, I determined the percentage of unmyelinated axons. The smaller the proportion of unmyelinated axons, the better the remyelination. In addition to this, the myelin thickness was determined by calculation of the g-ratio, the diameter of the axon over the diameter divided by the axon together with its myelin (equation 2.6). The smaller the g ratio, the thicker the myelin. In remyelination, the new myelin sheaths are thinner (section 1.4.3) and have a slightly bigger mean g ratio (thinner myelin). Therefore, detection of this in lesioned animals compared to unlesioned animals is evidence that the myelin in this area is remyelinated.

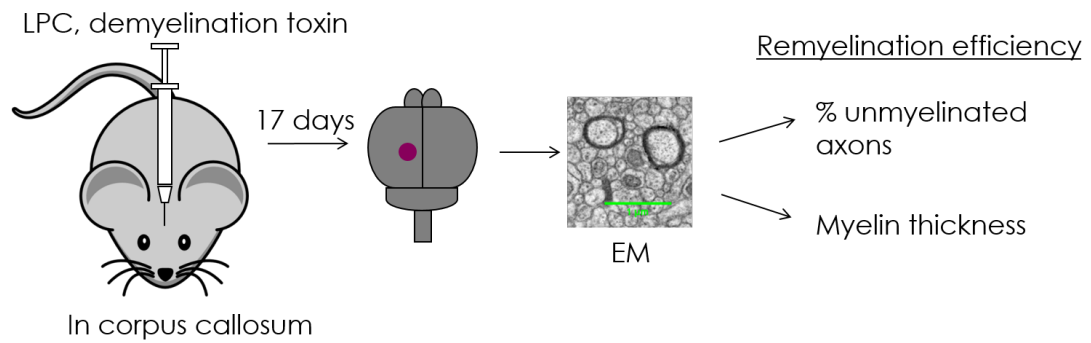


Figure 4.1: Summary of the in vivo methods used to assess remyelination. 17 days after LPC injection in the corpus callosum, the percentage unmyelinated fibres and myelin thickness were determined from electron microscopy images of the lesion area.

## 4.2 EM Results

In order to test whether NP1 could be a therapeutic target in multiple sclerosis, we compared the remyelination between NP1(Sema3A-) mice and their WT controls 17 days after LPC-induced demyelination in the corpus callosum. From all the extensive Sema3A literature (section 1.9.1), we expected that the TG mice would remyelinate better than WT because OPCs will not be chemorepelled by Sema3A, their migration into the lesion will be increased and remyelination would be enhanced. We thought that this experimental setup is particularly relevant to possible translation into therapeutics because a mutation in NP1 in all cells mimicks the effect of a possible NP1 inhibitor on the Sema3A site. The difference here being that in the mutant mouse this would be present throughout life including development while in a therapeutic setting this inhibitor would be transient.

### 4.2.1 NP1(Sema3A-) mice do not remyelinate better than WT mice

To assess remyelination, both TG and WT mice were given 17 days to repair before they were sacrificed. The number of myelinated and unmyelinated axons in 10 fields of view was counted and then averaged (methods in section 2.4.2). Representative images of a field from unlesioned and lesioned mice from the two genotypes are shown in figure 4.3 and it is clear that there are more unmyelinated axons in the lesioned samples. The quantification of the number of myelinated and unmyelinated axons was expressed as the proportion of unmyelinated axons by dividing the number of unmyelinated axons by the number of all axons and is shown in figure 4.3 top.

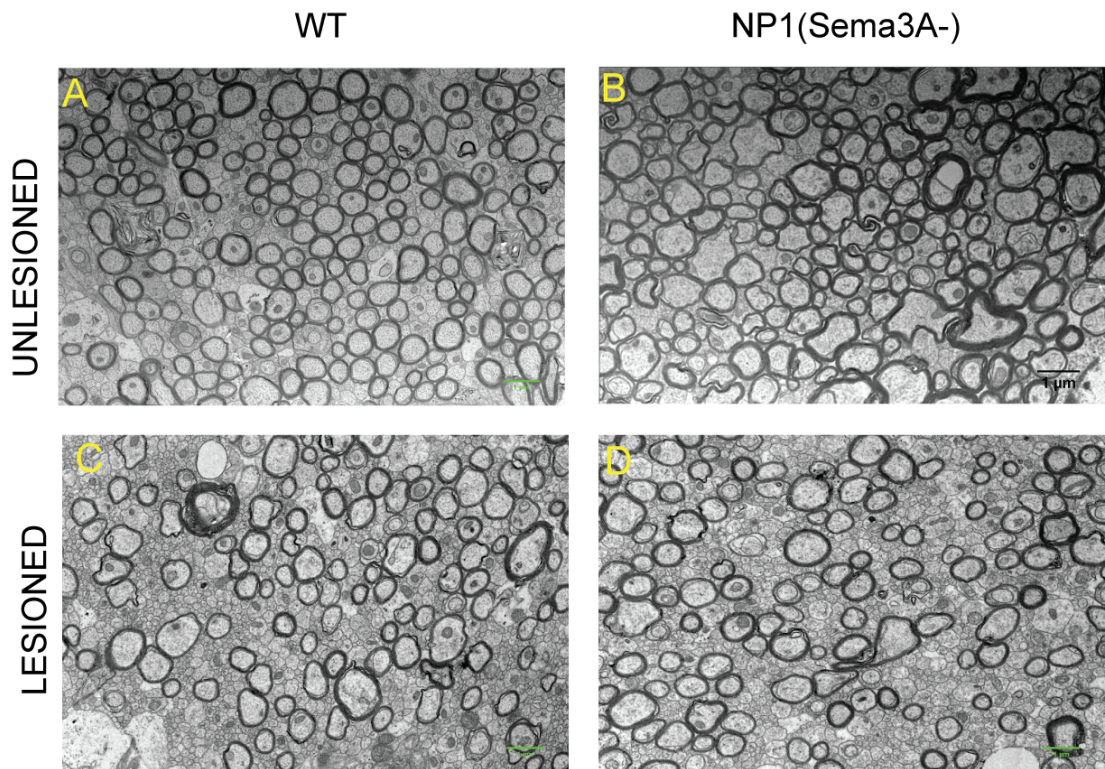
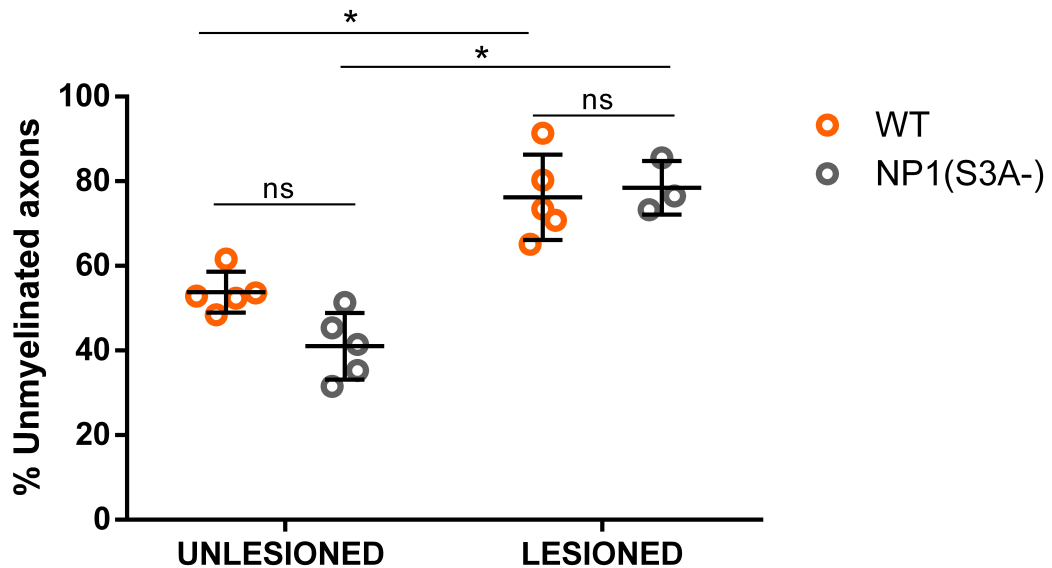


Figure 4.2: Representative EM images of unlesioned corpus callosum and areas of the lesion 17 days after lesion induction in WT and TG mice. Unlesioned WT (A), unlesioned TG (B), Lesioned WT (C) and lesioned TG (D). There are more unmyelinated axons in the lesioned animals. Scale bar is 1  $\mu m$

Comparison of the proportion of unmyelinated axons by a two-factor ANOVA showed that there was a significant effect of treatment ( $F_{(1,14)} = 64.83$ ,  $p < 0.0001$ ) but no significant effect on genotype ( $F_{(1,14)} = 1.997$ ,  $p = 0.1794$ ) and no significant interaction between those factors ( $F_{(1,14)} = 4.07$ ,  $p = 0.0632$ ). A posteriori Tukey's multiple comparisons test showed that there were significantly more unmyelinated axons in lesioned WT and NP1(Sema3A-) animals but no difference between the genotypes at any treatment (Figure 4.3 top). Therefore, LPC treatment causes demyelination in both genotypes but despite our expectations that the NP1(Sema3A-) mice will remyelinate better than WT, their remyelination is identical to WT.

We then looked at the total number of axons to ensure that the proportion is not biased by a different total number of axons. Comparison of the number of axons per field of view by a two-factor ANOVA showed there was no significant effect of treatment ( $F_{(1,14)} = 2.866$ ,  $P = 0.11$ ), genotype ( $F_{(1,14)} = 0.91$ ,  $P = 0.36$ ) and no significant interaction ( $F_{(1,14)} = 0.09$ ,  $P = 0.76$ ) (Figure 4.3 bottom) suggesting that this was not the case. Therefore, mice in which Sema3A cannot signal via NP1 do not remyelinate better than WT.



treatment significantly affects the results

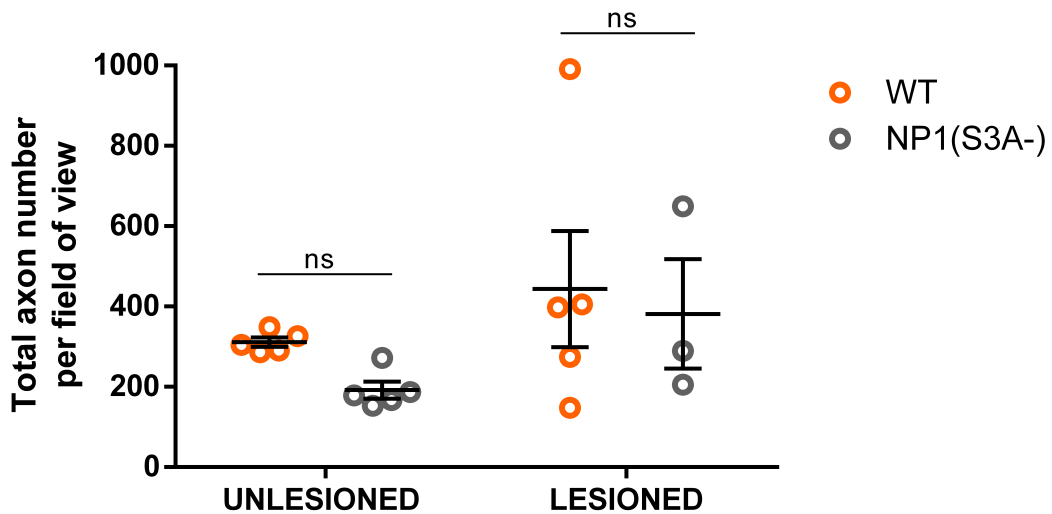


Figure 4.3: There is no difference in proportion of unmyelinated axons between TG and WT mice. Comparison of the proportion of unmyelinated axons by a two-factor ANOVA showed that there was a significant effect of treatment ( $F_{(1,14)} = 64.83$ ,  $p < 0.0001$ ) but no significant effect on genotype ( $F_{(1,14)} = 1.997$ ,  $p = 0.1794$ ) and no significant interaction between those factors ( $F_{(1,14)} = 4.07$ ,  $p = 0.0632$ ). A posteriori Tukey's multiple comparisons test showed that there were significantly more unmyelinated axons in lesioned WT and NP1(Sema3A-) animals, as we would expect after a demyelinated lesion, but no difference between the genotypes at any treatment (top). We also looked at the total number of axons to ensure that the proportion is not biased by a different total number of axons. There is no difference in axon number. A two-factor ANOVA showed there was no significant effect of lesion treatment ( $F_{(1,14)} = 2.866$ ,  $P = 0.11$ ), genotype ( $F_{(1,14)} = 0.91$ ,  $P = 0.36$ ) and no significant interaction ( $F_{(1,14)} = 0.09$ ,  $P = 0.76$ ). Each dot represents an average of data from an animal.

To ensure that the lack of better remyelination was not due to an inherent difference in number of myelinated or unmyelinated axons, we compared the absolute numbers of the myelinated and unmyelinated axons between treatments and genotypes shown in figure 4.4. Comparing the absolute number of myelinated axons, a two-factor ANOVA showed there was a significant effect of demyelinating treatment ( $F_{(1,14)}=13.61$ ,  $P=0.0024$ ) but no significant effect of genotype ( $F_{(1,14)}=0.963$ ,  $P=0.343$ ) and no significant interaction between them ( $F_{(1,14)}=0.0025$ ,  $P=0.96$ ) (Figure 4.4 top). This means that LPC treatment reduces the number of myelinated axons which is expected as it is a toxin which causes demyelination. What is important is that it does not decrease the number of unmyelinated axons which ensures that LPC does not cause axonal death. For absolute number of unmyelinated axons, a two-factor ANOVA showed there was no significant effect of treatment ( $F_{(1,14)}=4.575$ ,  $P=0.051$ ), genotype ( $F_{(1,14)}=0.465$ ,  $P=0.506$ ) and no interaction between those factors ( $F_{(1,14)}=0.025$ ,  $p=0.877$ ) (figure 4.4 bottom).

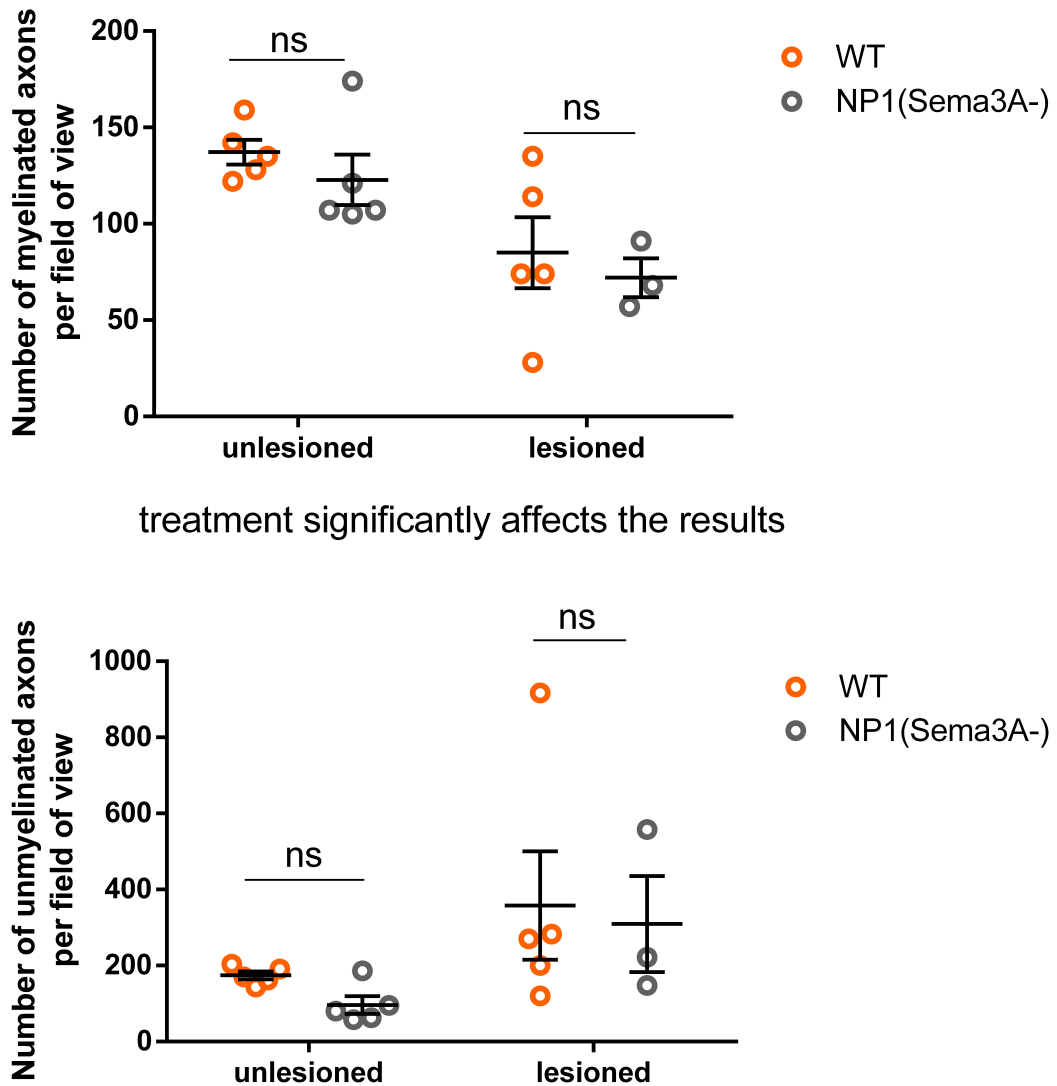
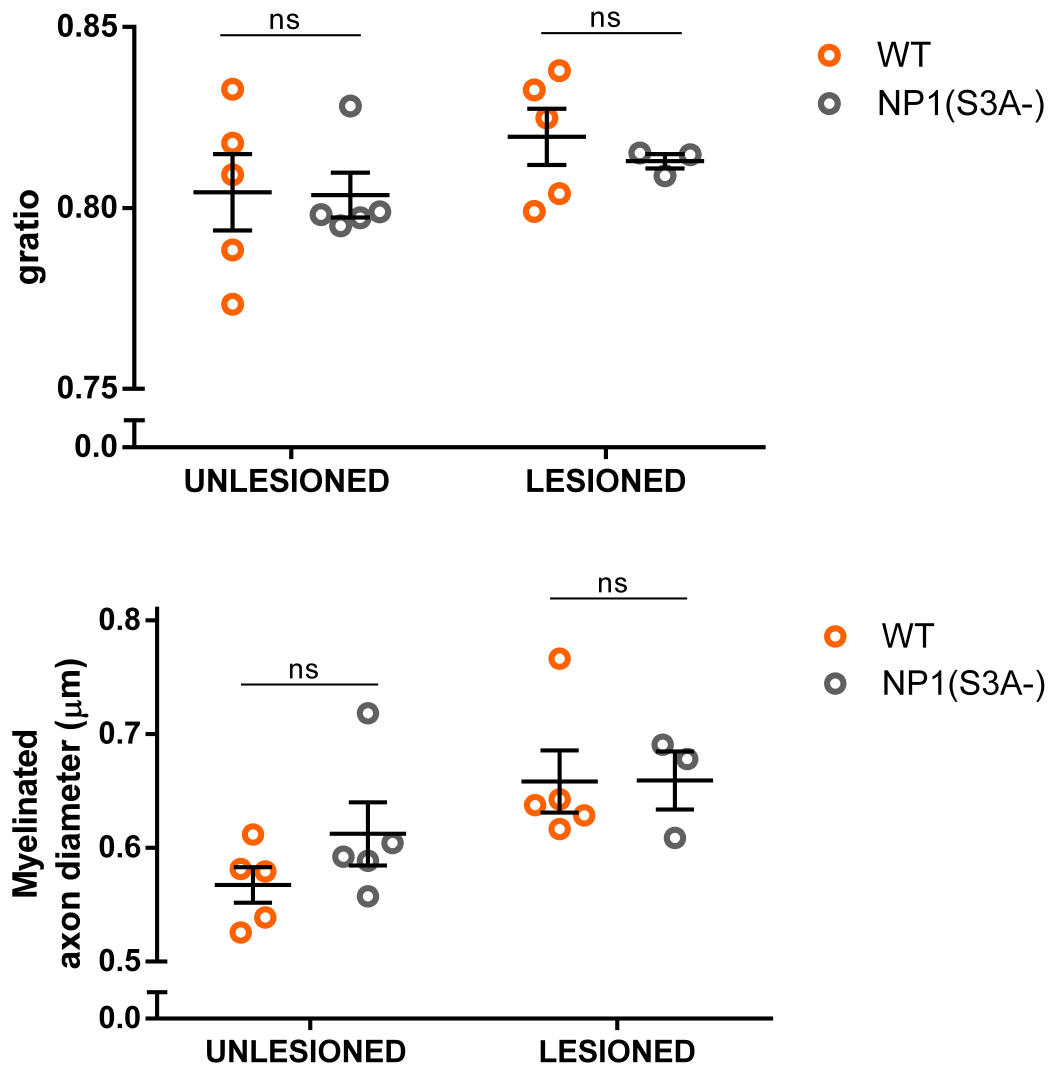


Figure 4.4: Absolute numbers of myelinated and unmyelinated axons before and after lesion induction in WT and TG mice. Comparison of the absolute number of myelinated axons by two-factor ANOVA showed that there was a significant effect of treatment ( $F_{(1,14)}=13.61$ ,  $P=0.0024$ ) but no significant effect of genotype ( $F_{(1,14)}=0.963$ ,  $P=0.343$ ) and no significant interaction ( $F_{(1,14)}=0.0025$ ,  $P=0.96$ ) (top). Comparison of absolute number of unmyelinated axon by two-factor ANOVA showed that there was no significant effect of treatment ( $F_{(1,14)}=4.575$ ,  $P=0.051$ ), genotype ( $F_{(1,14)}=0.465$ ,  $P=0.506$ ) and no interaction between those factors ( $F_{(1,14)}=0.025$ ,  $p=0.877$ ) (bottom). Each dot represents an average of data from an animal.

After we showed that the NP1(Sema3A-) mice do not remyelinate any better than WT and ensured that this was not because of inherent difference between the unmyelinated/myelinated or total axons, we looked at the thickness of the myelin in the unlesioned and lesioned animals.

#### 4.2.2 No difference between genotypes in myelin thickness and axon diameter

Comparison between WT and TG mice showed that there is no difference in the myelin thickness between the genotypes. Comparison of g-ratio by two-factor ANOVA showed there was no significant effect of treatment ( $F_{(1,14)}=2.18$ ,  $P=0.16$ ), genotype ( $F_{(1,14)}=0.20$ ,  $P=0.65$ ) and no significant interaction between those factors ( $F_{(1,14)}=0.13$ ,  $P=0.73$ ). However, there is a slight increase in g ratio in the lesioned animals in both genotypes which indicates that the myelin sheath is slightly thinner (figure 4.5 top). This is consistent with a small increase in g ratio characteristic of remyelination. We also looked at the average diameter of the axons because g ratio is dependent on axon diameter. A two-factor ANOVA showed there was a significant effect of treatment ( $F_{(1,14)}=7.31$   $P= 0.02$ ) but no significant effect of genotype ( $F_{(1,14)}=0.80$ ,  $P=0.39$ ) and no significant interaction ( $F_{(1,14)}=0.74$ ,  $P=0.40$ ). However, this difference was too small as a posteriori Tukey's multiple comparisons test showed that there no significant differences between unlesioned and lesioned WT and NP1(Sema3A-) animals (figure 4.5 bottom). This change in the diameter of myelinated axons after lesion is because the most predominant small caliber axons which were once myelinated are no longer myelinated and this results in a bigger average diameter of the myelinated axons.



treatment significantly affects the results

Figure 4.5: There is no difference in the myelin thickness between TG and WT mice. Comparison of myelin thickness by a two-factor ANOVA showed there was no significant effect of treatment ( $F_{(1,14)}=2.18$ ,  $P=0.16$ ), genotype ( $F_{(1,14)}=0.20$ ,  $P=0.65$ ) and no significant interaction ( $F_{(1,14)}=0.13$ ,  $P=0.73$ ). However, there is a slight increase in g ratio in the lesioned animals which indicates that the myelin sheath is slightly thinner (top), as expected after demyelination. We also looked at the average diameter of the axons because g ratio is dependent on axon diameter. Comparison of myelinated axon diameter by a two-factor ANOVA showed there was a significant effect of treatment ( $F_{(1,14)}=7.31$ ,  $P=0.02$ ) but no significant effect of genotype ( $F_{(1,14)}=0.80$ ,  $P=0.39$ ) and no significant interaction ( $F_{(1,14)}=0.74$ ,  $P=0.40$ ). However, this difference was too small as a posteriori Tukey's multiple comparisons test showed that there no significant differences between unlesioned and lesioned WT and NP1(Sema3A-) animals.

This difference in the diameter between treatments is best visualised in the frequency distribution of the myelinated fibres shown in figure 4.6. Unlesioned WT and TG are almost overlapping and after lesion the the frequency of myelinated axon diameter are shifted to the right for both genotypes. This is a result of the demyelination of fibres which used to be myelinated.

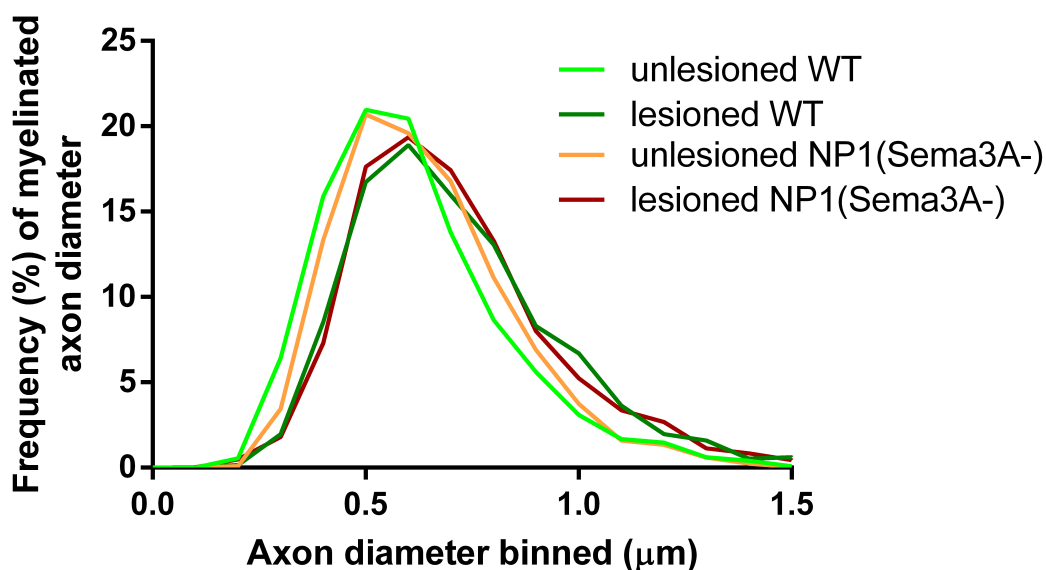


Figure 4.6: Frequency distribution (histogram) of axon diameter of myelinated axons. Lesioned WT and TG values are shifted to the right compared to unlesioned animals

Finally, we investigated the relationship between g ratio and diameter as myelin thickness depends on the diameter of the axon (Figure 4.7). G ratio vs diameter plots are often used to visualise the difference in myelin thickness as a result of remyelination. The data points from both genotypes in both treatments show good overlap indicating that the myelin thickness and axonal diameter are not profoundly different in any condition (Figure 4.7 top). Comparison of the WT axons (Figure 4.7 middle) shows the lesioned animal axons (dark green) are more prominent on the right which indicates that they are slightly bigger. This is the same shift in size which we observed in figure 4.6 partly because previously myelinated small fibres are now unmyelinated/not yet remyelinated. Moreover, the slope of a best fit line of the data becomes less steep following demyelination which is consistent with bigger g ratio (thinner myelin) for each axon diameter which is exactly what we would expect in remyelination. Finally, comparison of the NP1(Sema3A-) axons before and after lesion (Figure 4.7 bottom) shows the lesioned animal axons are shifted to the right, again because they appear slightly bigger. However, in the TG mouse the best fit lines are almost overlapping indicating that the change in the myelin thickness after remyelination is smaller which can also be observed in the average g ratio (figure 4.5 top). This is likely due to the slightly bigger shift in myelinated axon diameter evident in the TG mice which will overall have thicker myelin and would mask the small effect of remyelination.

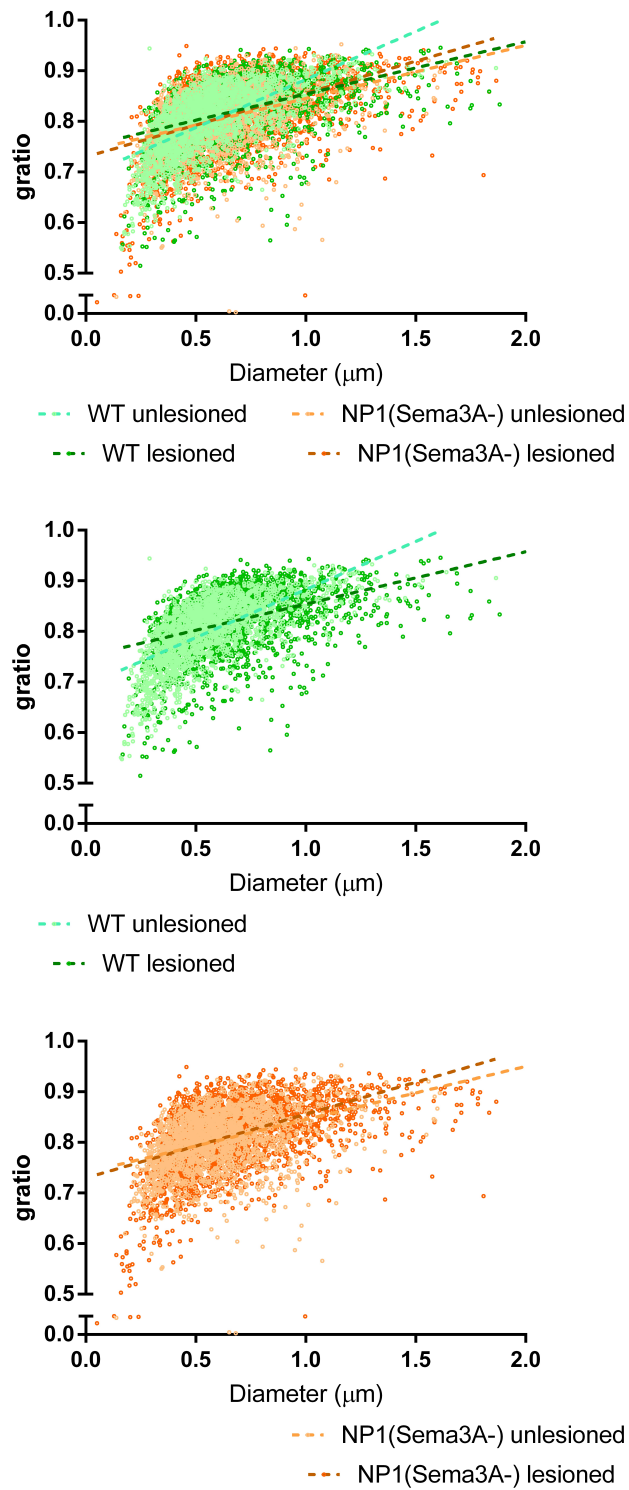


Figure 4.7: The relationship between myelin thickness and axon diameter. The top g ratio vs diameter plot shows both genotypes and treatments together. For clarity, those were separated and presented by genotype: WT (middle) and NP1(Sema3A-)(bottom). Dashed line is best fit line of the data and each dot is an axon

After we assessed remyelination and showed that the TG mice do not repair better than WT, we assessed the cellular composition of the lesion by immunohistological staining.

### 4.3 IHC

The lack of improved remyelination in the NP1(Sema3A-) mice was unexpected as previous LPC-induced lesions in the same mice have shown almost 2 times increase in OPC numbers [245]. To examine migration in our lesions and to investigate the immune response which might be affected by loss of Sema3A signalling via NP1 (because of Sema3A's immune effects discussed in section 1.9.3), we chose to examine the cellular composition of the lesions 10 days after LPC injection. At this time point, OPC migration occurs, maturation is starting and the immune response is extensively characterised in CC LPC-induced lesions [205]. Therefore, 10 days after LPC injection WT and TG mice were sacrificed and the lesion was examined by IHC on consecutive 10  $\mu$ m coronal sections.

#### 4.3.1 Finding lesions

Initial staining with antibodies against IBA1 to find macrophages/microglia and antibody against MBP for myelin were performed in different regions of the brain in order to determine if each brain had a lesion and its extent. Representative images of WT and TG lesions are shown in figure 4.8. Lesions were identified by accumulation of nuclei (Figure 4.8 A, E), macrophages/microglia (Figure 4.8 B, F) and loss of myelin (Figure 4.8 C, G).

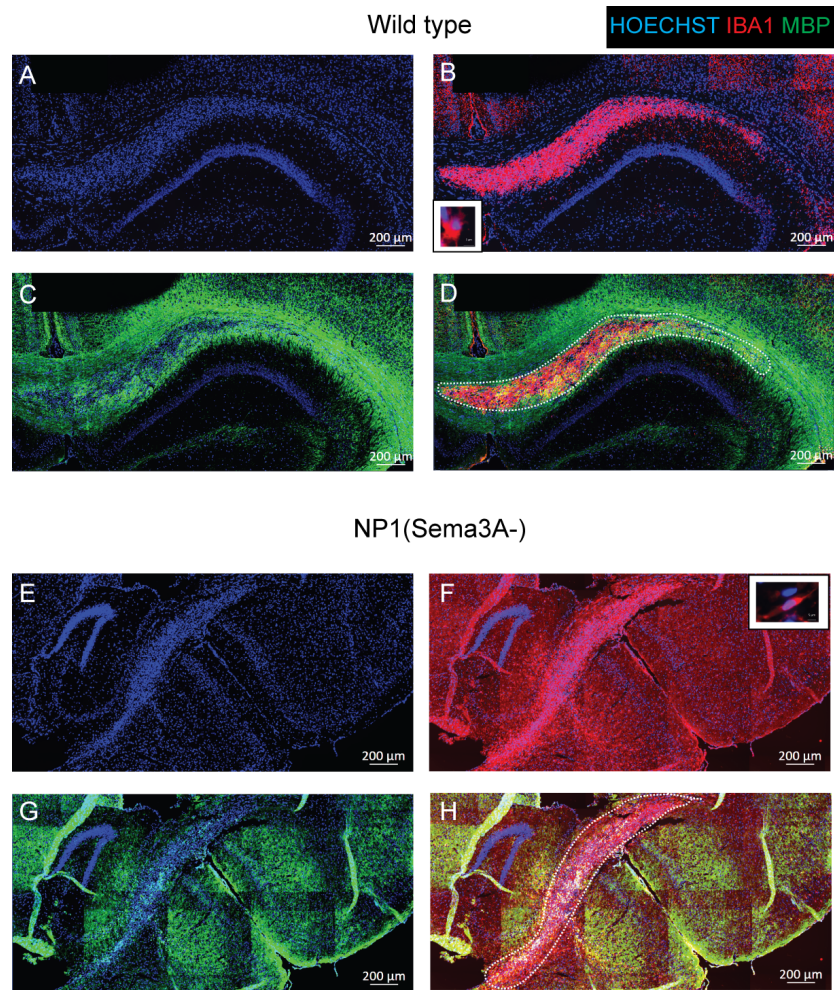


Figure 4.8: Representative images of initial staining with antibodies against MBP and IBA1 used to find lesions. Lesions are characterised by accumulation of nuclei (A/E), infiltration of immune cells (B/F) and loss of MBP (C/G). Scale bar is 200  $\mu\text{m}$

Using these criteria to define lesion outlines, we compared the lesion size as well as the content of macrophages and microglia. We found that the lesions were similar in terms of size and macrophages/microglia (non-activated and activated) which are marked by IBA1 (figure 4.9). If remyelination was enhanced in the NP1(Sema<sup>-</sup>) mice, then we would expect their lesions to be smaller than WT. However, since they are similar to WT size, this is another indication that the NP1(Sema<sup>-</sup>) mice do not remyelinate better than WT. Even though the numbers of all macrophages/microglia (non-activated and activated) marked by antibody against IBA1 were not significantly different, we wanted to look at the numbers of activated macrophages/microglia and attempt to determine their functional subtype.

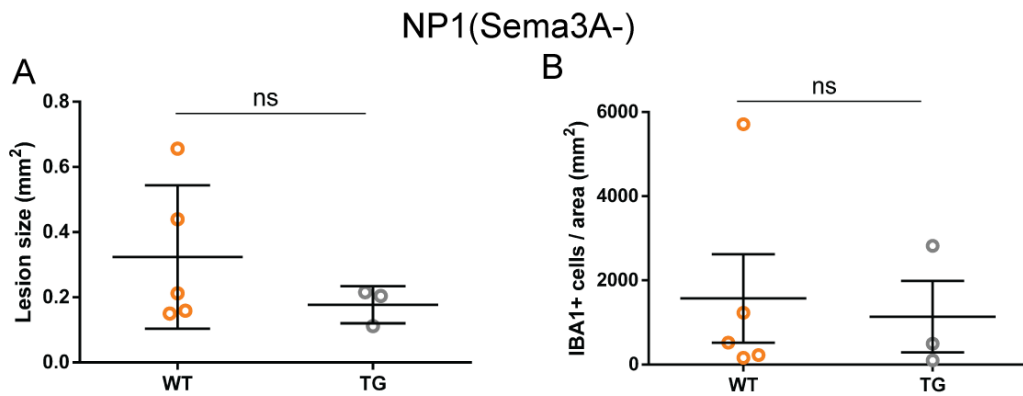


Figure 4.9: Lesions are a similar size between WT and TG mice and they have a similar amount of IBA1+ cells. Lesion size did not differ between genotypes (Mann-Whitney  $U = 5.0$ ,  $n=5,3$ ,  $p=0.57$ , two-tailed) (A). IBA1+ cell density in lesions did not differ between WT and TG mice (Mann-Whitney  $U = 6.0$ ,  $n=5,3$ ,  $p=0.68$ , two-tailed) (B)

### 4.3.2 The innate immune response is different

In order to look at the activated macrophages/microglia and determine if they belong to the pro-inflammatory or pro-repair subtype, we performed IHC against CD68 (activated macrophages/microglia), Arginase-1 (pro-repair subtype) and iNOS (pro-inflammatory subtype). At 10 days post CC LPC-induced lesion we would expect to have predominantly Arginase-1+ (pro-repair subtype) cells [205]. Representative images of WT and TG lesions are shown in figure 4.10 and figure 4.11 respectively. CD68+ cells were found extensively in the lesion in both genotypes however the CD68+ staining was denser in TG compared to WT Lesions (Figure 4.10 B and figure 4.11 B). In both genotypes, the iNOS+ cells appeared to be predominant compared to Arginase-1+ although the majority of the cells expressed both markers (Figure 4.10 D,C,E and figure 4.11 D,C,E). This is in sharp contrast to the expected predominance of pro-repair subtype of macrophages/microglia at 10 days and the exclusivity of iNOS or Arginase-1 expression in macrophages/microglia observed previously [205]. Due to the extensive overlap in subtype marker expression, I regarded pro-inflammatory macrophages/microglia as CD68+ iNOS+ (even if Arginase+) and pro-repair macrophages/microglia as CD68+ Arginase-1+ iNOS-.

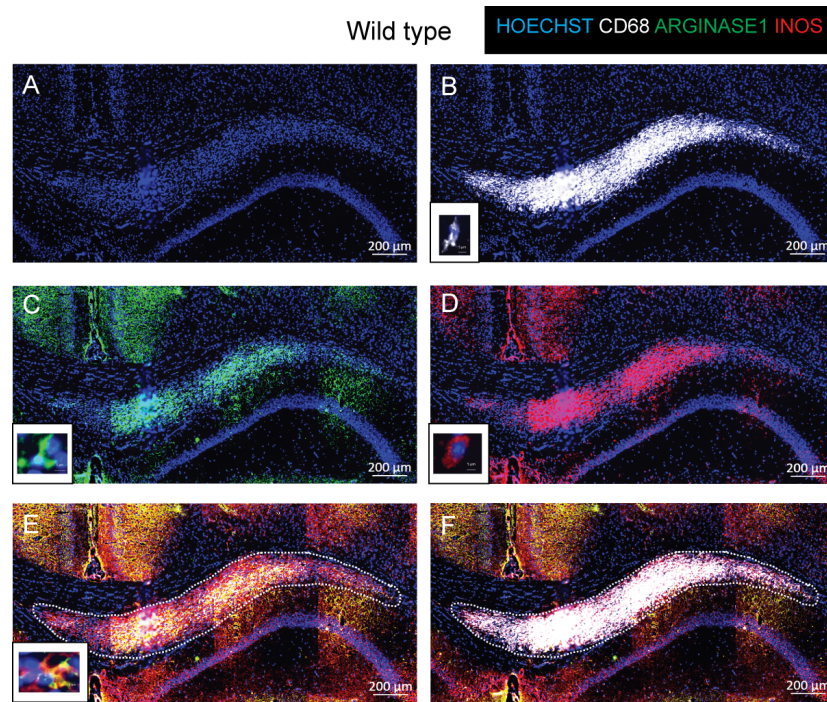


Figure 4.10: Representative images of staining using CD68, Arginase-1 and iNOS antibodies on WT tissue. CD68 (activated macrophages/microglia), Arginase-1 (pro-repair subtype) and iNOS (pro-inflammatory subtype) staining was extensively present in the lesions at 10 days after LPC injection. A high magnification of an example cell is shown in the bottom left panel. Scale bar is 200  $\mu\text{m}$

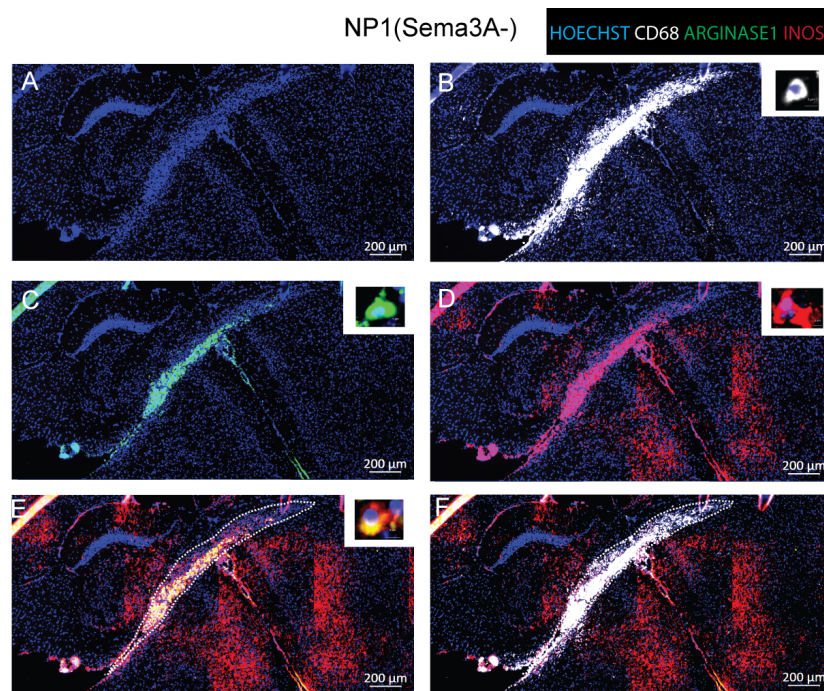


Figure 4.11: Representative images of staining using CD68, Arginase-1 and iNOS antibodies on TG tissue. CD68 (activated macrophages/microglia), Arginase-1 (pro-repair subtype) and iNOS (pro-inflammatory subtype) staining was extensively present in the lesions at 10 days after LPC injection. A high magnification of an example cell is shown in the top right panel. Scale bar is 200  $\mu m$

Quantification of the activated macrophages/ microglia, pro-inflammatory macrophages/ microglia and pro-repair macrophages/ microglia is shown in figure 4.12. The number of activated macrophages/ microglia was found to be significantly increased in the lesions of TG mice compared to WT (Figure 4.12 A) (Mann-Whitney  $U = 0.0$ ,  $n=5,3$ ,  $p=0.036$ , two-tailed). This increase was largely because of the increase in the number of pro-inflammatory macrophages/microglia (Figure 4.12 B) (Mann-Whitney  $U = 0.0$ ,  $n=5,3$ ,  $p=0.036$ , two-tailed). The number of pro-repair macrophages/microglia was not significantly different (Figure 4.12 C) (Mann-Whitney  $U = 3.0$ ,  $n=5,3$ ,  $p=0.25$ , two-tailed). Therefore, we have found that NP1(Sema3A-) genotype results in different immune response characterised by increase of activate macrophages/microglia in the lesions primarily because of increase in the pro-inflammatory phenotype.

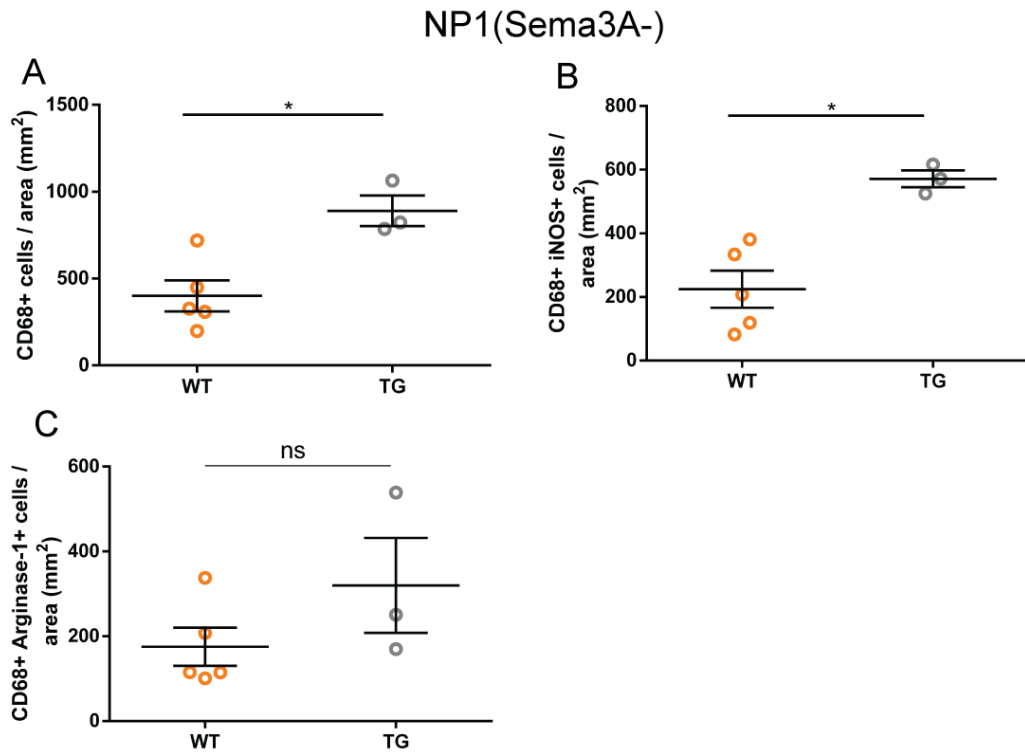


Figure 4.12: NP1(Sema3A-) mice have a different innate immune response. TG mice have significantly more activated microglia/macrophages in the lesions (Mann-Whitney U = 0.0, n=5,3, p=0.036, two-tailed) (A). This is because they have significantly more iNOS+ cells (Mann-Whitney U = 0.0, n=5,3, p=0.036, two-tailed) (B) and a similar amount of Arginase-1+ cells in the lesions (Mann-Whitney U = 3.0, n=5,3, p=0.25, two-tailed) (C)

Finally, we aimed to see if we can replicate the published increase in OPC recruitment in this genotype after LPC-induced lesion [245] in our lesions.

### 4.3.3 OPC recruitment is similar in WT and TG mice

In order to quantify the amount of OPC migration into the WT and TG lesions, we performed IHC using antibodies against OPC markers NG2 and PDGFR $\alpha$ . In addition to this, we wanted to quantify the number of mature oligodendrocytes in the lesion since Sema3A has been reported to be a maturation inhibitor [296] and because our chosen time point was late in the migration process and at the start of the maturation process. In order to do this, we performed IHC with antibodies against the mature oligodendrocyte markers NogoA and CC1. Representative images of IHC with antibodies against NG2 and CC1, and PDGFR $\alpha$  and NogoA in WT and TG lesions are shown in figure 4.13 and figure 4.14 respectively. We found that the majority of lesions contained many OPCs but few mature oligodendrocytes which is exactly what we would expect at day 10 after LPC-induced demyelination. While PDGFR $\alpha$  antibody worked well in all sections, the intensity of staining with the NG2 antibody was variable (see figure 4.13 B and

F). We then quantified the number of OPCs and mature oligodendrocytes present in the lesion expecting that TG mice will show an increase in the number of OPCs.

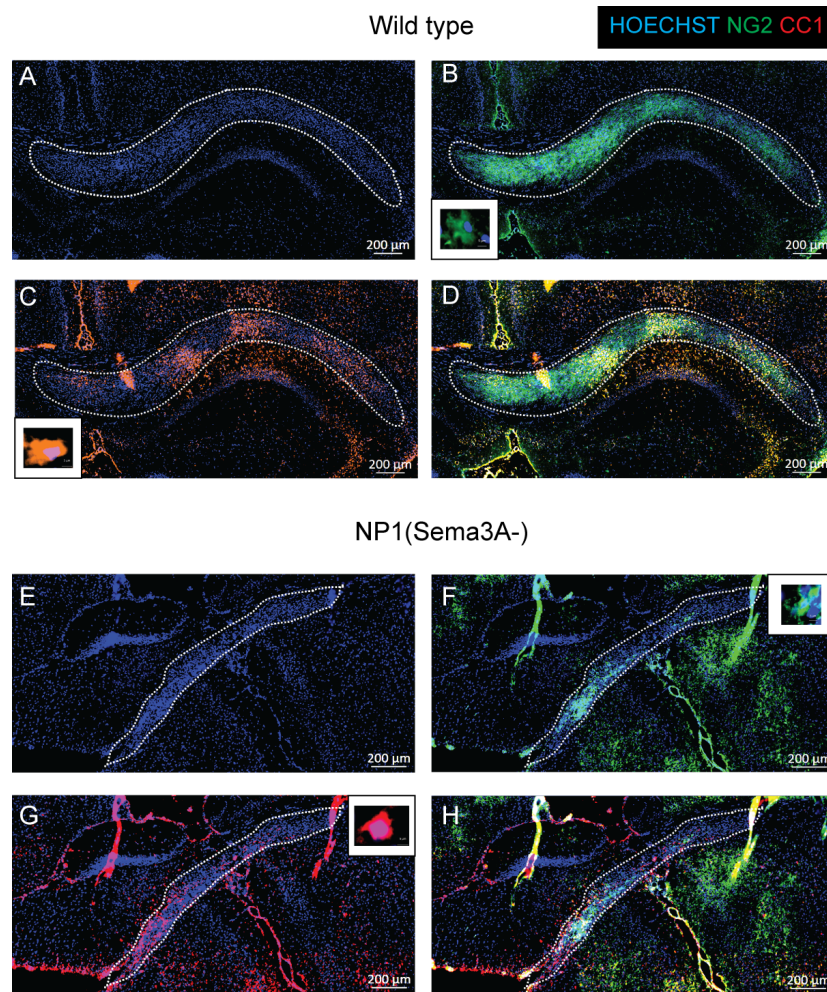


Figure 4.13: Representative images of IHC with antibodies against NG2 and CC1 on WT and TG tissue. A high magnification of an example cell is shown in the small panel. Scale bar is 200  $\mu m$

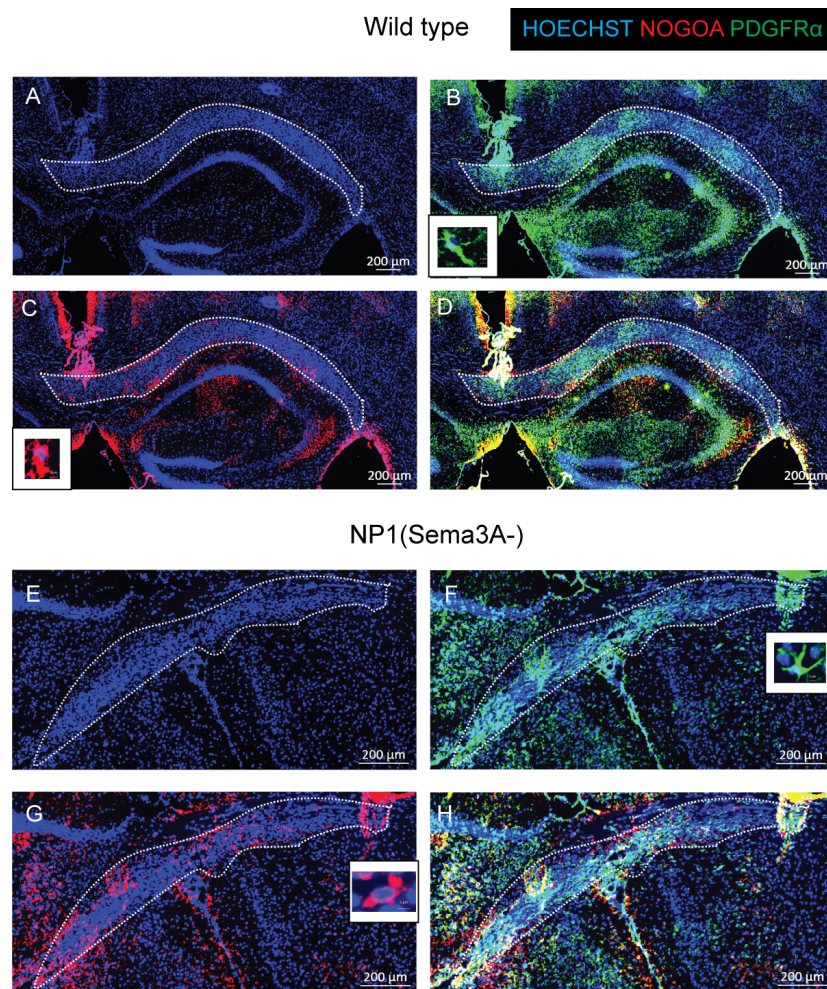


Figure 4.14: Representative images of IHC using antibodies against PDGFR $\alpha$  and NogoA on WT and TG tissue. A high magnification of an example cell is shown in the top right panel. Scale bar is 200  $\mu m$

Quantification of OPC numbers in the lesions using either NG2+ cells or PDGFR $\alpha$ + cells revealed that there was no difference in the number of OPCs in WT and TG mice (NG2:Mann-Whitney U = 5.0, n=5,3, p=0.57, two-tailed) (PDGFR $\alpha$ :Mann-Whitney U = 6.0, n=5,3, p=0.79, two-tailed) (Figure 4.15 A,C). Moreover, comparison of the mature oligodendrocyte numbers using CC1+ cells or NogoA+ cells in lesions also revealed that there was no difference between WT and TG mice (CC1:Mann-Whitney U = 2.0, n=5,3, p=0.14, two-tailed) (NogoA:Mann-Whitney U = 4.0, n=5,3, p=0.39, two-tailed) (Figure 4.15 B,D). Therefore, contrary to previously published results [245], loss of Sema3A signalling via NP1 did not improve OPC recruitment into the lesion at 10 days and moreover it did not affect the number of mature oligodendrocytes.

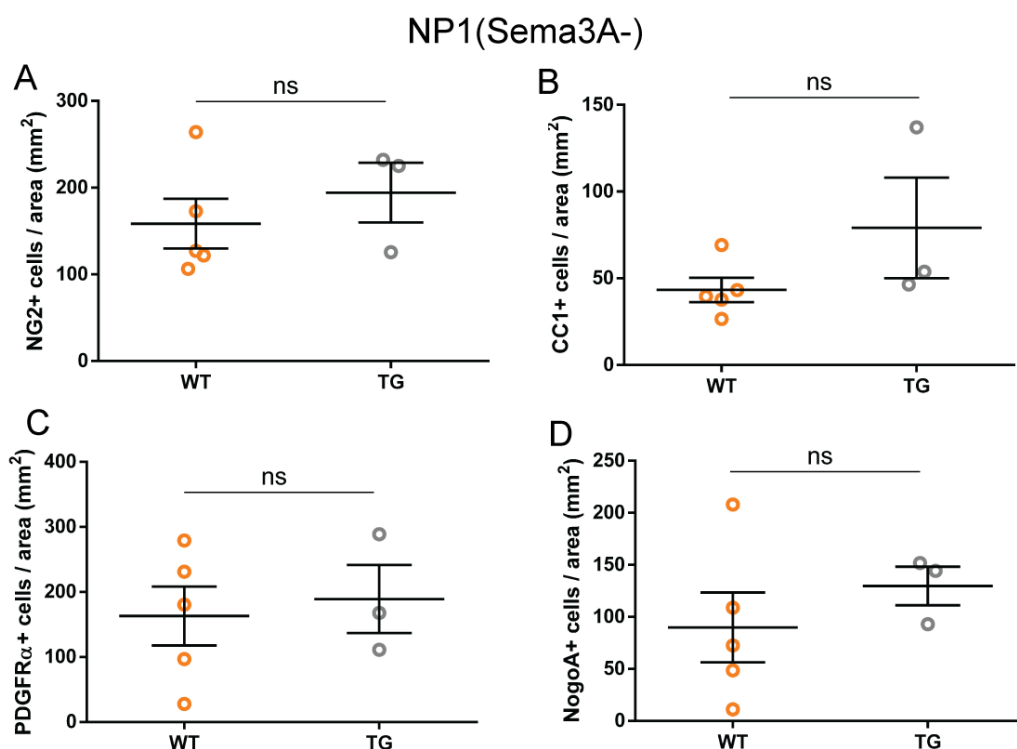


Figure 4.15: NP1(Sema3A-) mice do not have more OPCs in lesions. The NG2+ density in lesions of TG mice was not different to WT (Mann-Whitney U = 5.0, n=5,3, p=0.57, two-tailed) (A). The CC1+ density in lesions of TG mice was not different to WT (Mann-Whitney U = 2.0, n=5,3, p=0.14, two-tailed) (B). The PDGFR $\alpha$ + density in lesions of TG mice was not different to WT (Mann-Whitney U = 6.0, n=5,3, p=0.79, two-tailed) (C). The NogoA+ density in lesions of TG mice was not different to WT (Mann-Whitney U = 4.0, n=5,3, p=0.39, two-tailed) (C).

#### 4.3.4 Discussion

In this chapter, we aimed to compare the remyelination and the cellular composition of LPC-induced lesions between WT and NP1(Sema3A-) mice. Previous findings in the literature strongly suggested that we should see increase in remyelination and OPC migration in the TG mice since Sema3A will be unable to repel OPCs away from the lesion.

#### 4.3.5 Remyelination

First, to compare remyelination, we assessed the percentage of unmyelinated axons 17 days after lesion induction and compared it between the genotypes (Figure 4.3 top). Decrease in the proportion of unmyelinated axons would indicate better remyelination. Contrary to our expectations, there was no significant difference between genotypes after lesion which means that TG mice repair as well as WT but not better. Even though we have only compared remyelination at a single time point, 17 days, this time point is between the two time points which showed sig-

nificant increase in remyelination in Sema3A KD mice (2 weeks and 3 weeks) [29]. Therefore, if any difference existed in the remyelination of the transgenic mice, it should have been evident and persisted at 17 days.

Another indication that NP1(Sema3A-) mice do not repair better is that the lesion size is not different between the genotypes (Figure 4.9). If remyelination was improved in TG mice, lesions would be smaller. However, due to the breeding problems of the mice and the limited numbers of animals we had, we have not performed a full reconstruction of the lesion. A full reconstruction would require staining of serial sections with antibodies against markers for myelin and macrophages/microglia and then combining the volume of the lesion in all sections. Instead, we have averaged the area of the lesion in a few equally spaced sections in lesions of similar span throughout the brain to allow us to perform other IHC labelling on the rest of the slides. Although this approach can give us an indication that there is no big difference in the lesion size, a small difference could only be revealed by complete reconstruction of the lesion volume. Our measurement of lesion volume backed up by the lack of increased remyelination from our EM data provides strong evidence that NP1(Sema3A-) mice do not remyelinate better despite expectations.

In order to examine why remyelination was not improved in the TG mice, we examined the OPC migration into the lesions which has been previously shown to be improved in those mice after lesion [245].

#### 4.3.6 OPC migration

Previous data on LPC-induced lesions in NP1(Sema3A-) mice has shown a two fold increase in the OPCs numbers in the lesion as shown in figure 4.16. This is in sharp contrast with our findings that there was the same number of OPCs in WT and TG lesions (Figure 4.15 A,C).

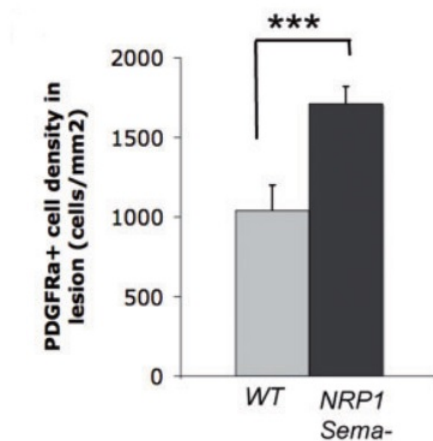


Figure 4.16: OPC migration in NP1(Sema3A-) mice has been shown to be increased in a previous publication [245]

Even though the genotype, the toxin used to induce lesions and the marker identifying OPCs

were identical between those experiments, our lesions were in the CC and were analysed 10 days after lesion induction while the lesions in the paper were in the spinal cord and were analysed 7 days after lesion induction. Therefore the difference in OPC migration could be due to the lesion location or timing of analysis. We have accounted for the different time of analysis to some extent by analysing the number of mature oligodendrocytes (Figure 4.15 C,D). Thus, OPCs which have migrated into the lesion before 10 days, would start differentiating and thus would be counted as mature oligodendrocytes. We did not see a difference in the number of mature oligodendrocytes in lesions between genotypes indicating that the lack of increased migration is genuine and not due to the day of analysis.

However, we cannot exclude the possibility that OPCs which have migrated in those lesions have matured only to immature oligodendrocytes (e.g. O4+) but not mature oligodendrocyte (e.g. NogoA+/CC1+/MBP+) since we have not counted immature oligodendrocytes in our lesions. A possible explanation as to why we are not seeing an increase in OPC migration is that in the TG lesions OPCs have migrated into lesions before 10 days and differentiated into immature oligodendrocytes and thus are 'invisible' for our analysis. While this possibility is unlikely as in our experience immature oligodendrocytes still express NG2/PDGFR $\alpha$  (but at lower level) and would be therefore counted in our analysis, in future studies this possibility could be excluded by staining the lesions with antibodies against O4 to mark the immature oligodendrocytes or Olig2 to mark all oligodendroglia.

We also looked at the number of mature oligodendrocytes (Figure 4.15 B,D) because Sema3A has been found to inhibit OPC maturation in vivo [296]. While we did not find a significant difference between the number of mature oligodendrocytes, the time point we have chosen is very early in oligodendrocyte maturation (in a previous study maturation was analysed at 21 days post lesion [296]). Therefore, we cannot exclude loss of Sema3A signalling via NP1 having an effect on maturation at a later time point. If TG mice numbers were not limited, examination of the mature oligodendrocyte numbers at a later time point (e.g. 21 days post lesion) could have been examined to address this.

Comparison of the NP1(Sema3A-) mice and WT mice has shown that TG mice do not remyelinate better or have enhanced OPC recruitment. However, comparison between the genotypes did show a different innate immune response.

#### 4.3.7 Immune response

Since the mutation in the Sema3A binding site of NP1 is present in all cells and Sema3A is involved in variety of immune processes(section 1.9.3), we also examined the immune response in the TG and WT mice. Even though we found that the number of all macrophages/microglia, non-activated and activated, was the same between the genotypes (figure 4.9), comparison of the activated macrophages showed that they were significantly increased in TG lesions compared to WT lesions (Figure 4.12). This suggests that loss of Sema3A signalling via NP1 increases the number of infiltrated immune cells. This finding is in agreement with unpublished finding that addition of Sema3A decreases the activated macrophages/microglia in lesions from a previous

MSc student in the lab shown in figure 4.17. Therefore, increasing Sema3A results in a decrease of activated macrophages/microglia while inhibiting its signals via the NP1 mutation increases activated macrophages/microglia. We wanted to investigate the mechanism of this effect.

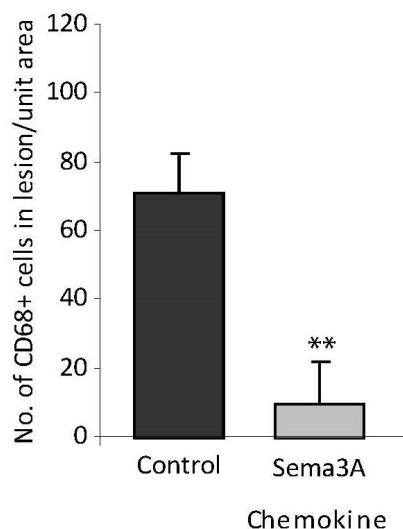


Figure 4.17: Addition of Sema3A decreases the number of activated macrophages/microglia in lesions. 10 days after LPC-induced lesion. Data is mean + standard error of the mean (SEM). Unpublished data from previous MSc student in the lab, Jonathan Murnane

To do this, we examined the macrophages/ microglia subtype by staining with antibodies against iNOS and Arginase-1 to differentiate between pro-inflammatory and pro-repair macrophages/ microglia respectively. Despite our expectations to find predominantly pro-repair macrophages /microglia and for individual macrophages/ microglia to express one of the used markers [205], we found that the majority of cells expressed both markers (Figure 4.10 E and figure 4.11 E) and the pro-inflammatory subtype dominated (Figure 4.12). Expression of iNOS and Arginase-1 was correlated to pro-inflammatory and pro-repair function in CC LPC-induced lesions however iNOS+ Arginase-1+ cells were not seen [205] and therefore their function is unclear. One possible explanation could be that those cells could be macrophages/ microglia in the process of switching their phenotype. Previously, intermediate activation state of microglia/macrophages which express both pro-inflammatory and pro-repair markers has been observed [243]. The quantification we performed was based on data that Arginase-1 is present in all infiltrating macrophages [113] and this is why we have used iNOS positivity as the differentiating factor for the pro-inflammatory phenotype. To determine whether the double positive cells truly represent pro-inflammatory functionality, IHC with further pro-inflammatory and pro-repair markers should be performed. However, it is clear that NP1(Sema3A-) mice have a different immune response to WT mice.

This is not unexpected as from the literature, Sema3A is expected to have an effect on macrophages/

microglia. As discussed in section 1.9.3, Sema3A mediates apoptosis of pro-repair macrophages/microglia [185] [139] so in the NP1(Sema3A-) mice a reduction in the apoptosis of pro-repair macrophages/microglia is expected. Moreover, Sema3A is a chemoattractant for tumor associated macrophages [38] which are primarily of the pro-repair phenotype. Therefore, in the NP1(Sema3A-) mice we would expect to have decrease in the pro-repair subtype of macrophages/microglia.

In addition to this, unpublished data from Jonathan Murnane on transwell migration of pro-inflammatory (M1) and pro-repair (M2) in vitro polarised microglia showed that Sema3A is a repellent for pro-inflammatory (M1) and an attractant for pro-repair (M2) subtype as shown in figure 4.18. Even though in vitro polarisation of the cells might not be representative of the in vivo subtypes present in a lesion, this data is in nice correlation with the previously published chemoattractant effect of Sema3A on pro-repair macrophages/microglia [38].

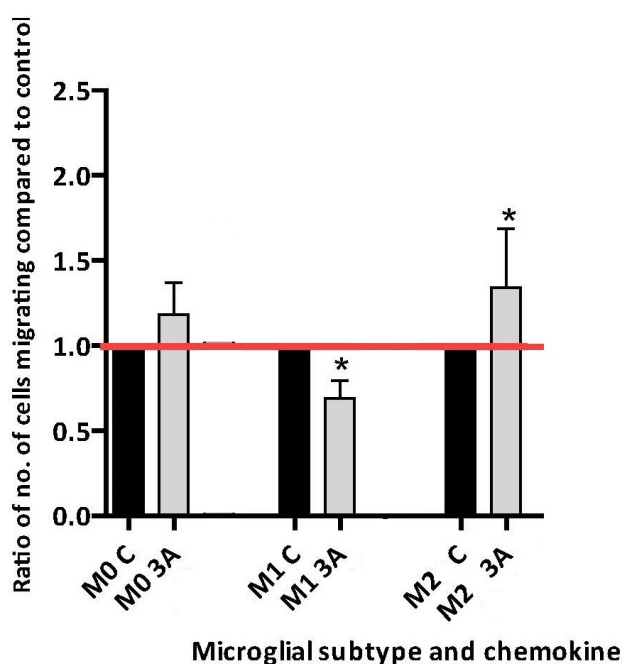


Figure 4.18: Sema3A affects the in vitro migration of pro-inflammatory (M1) and pro-repair (M2) differently. In a transwell, Sema3A is an repellent for pro-inflammatory (M1) and an attractant for pro-repair (M2) subtype. Recombinant 3A placed in lower well, microglia placed on the top of transwell and cells counted on the undersurface of membrane. Data shows as mean + SEM. Unpublished data from previous MSc student in the lab, Jonathan Murnane

Therefore, we would expect to have more pro-inflammatory cells in the NP1(Sema3A-) lesions since the chemorepulsive effect of Sema3A is lost which is exactly what we see our analysis (Figure 4.12). Moreover, we would expect less migration of pro-repair macrophages/microglia and but less apoptosis which would cancel each other out. Even though more experiments need to be performed to assign the iNOS+ Agrinase-1+ macrophages/microglia in our lesions to pro-

repair or pro-inflammatory function, there is clearly a difference in the innate immune response in the TG mice and this is most probably because of dysregulation of the proportion of the pro-repair or pro-inflammatory macrophages/microglia phenotypes.

#### **4.3.8 Summary**

This dysregulation of the proportion of the pro-repair or pro-inflammatory macrophages/microglia phenotypes in the NP1(Sema3A-) mice would have significant impact on the ability of OPCs to migrate into the lesion and remyelinate [205]. Next, we determined whether knockout of the NP1 receptor specifically in OPCs would have an effect on OPC migration by using a oligodendroglia specific NP1 KO mouse described in chapter 5.

## 5 Assessing remyelination in the PDGFR $\alpha$ -Cre x flx-NP1-flx mice

### 5.1 Introduction

The dysregulation in the proportion of the pro-repair and pro-inflammatory macrophages/ microglia phenotypes observed in the NP1(Sema3A-) mice discussed in chapter 4 would have significant impact on the ability of OPCs to migrate into the lesion and remyelinate [205]. Since the mutation of NP1 was present in all cells in the NP1(Sema3A-) mice, we wanted to look at a cell specific transgenic animal. We crossed PDGFR $\alpha$ -Cre mice with flx-NP1-flx mice (PDGFR $\alpha$ Cre:flxNP1flx by convention) in which Cre is expressed under the PDGFR $\alpha$  promoter and excises part of the NP1 gene effectively silencing it. This results in knock down of NP1 in OPCs (PDGFR $\alpha$  +) and the oligodendrocytes they differentiate into as well as other PDGFR $\alpha$  + cells such as pericytes. As with the NP1(Sema3A-) mice, we expected that the TG mice would remyelinate better than WT because their OPCs will not be chemorepelled by Sema3A and their migration into the lesion will be increased. Moreover, unlike the NP1(Sema3A- mice), we expected the microglia/macrophages response would be the same as WT. Therefore, this genotype would allow us to isolate the effect of losing NP1 signalling on OPC and we can investigate the hypothesis that NP1(Sema3A-) mice do not remyelinate better than WT because increased OPC migration is masked or cancelled out by the different microglia/macrophages response.

### 5.2 EM Results

The methods used to assess remyelination and the cellular content of the lesion are identical to the ones used in chapter 4 and are presented in the same way and order.

#### 5.2.1 PDGFR $\alpha$ -Cre x flx-NP1-flx mice do not remyelinate better than WT

Comparison of the representative EM images between the two genotypes and conditions (Figure 5.1) reveals that there is increasing proportion of unmyelinated axons in the lesioned animals which is expected after LPC treatment. Moreover, the myelin sheaths in the lesioned TG animals appears thicker than in the lesioned WT animals (Figure 5.1 C and D). Finally, looking at the myelinated axons in the unlesioned animals, the axons in the TG animals appear slightly bigger than the WT axons (Figure 5.1 A and B).

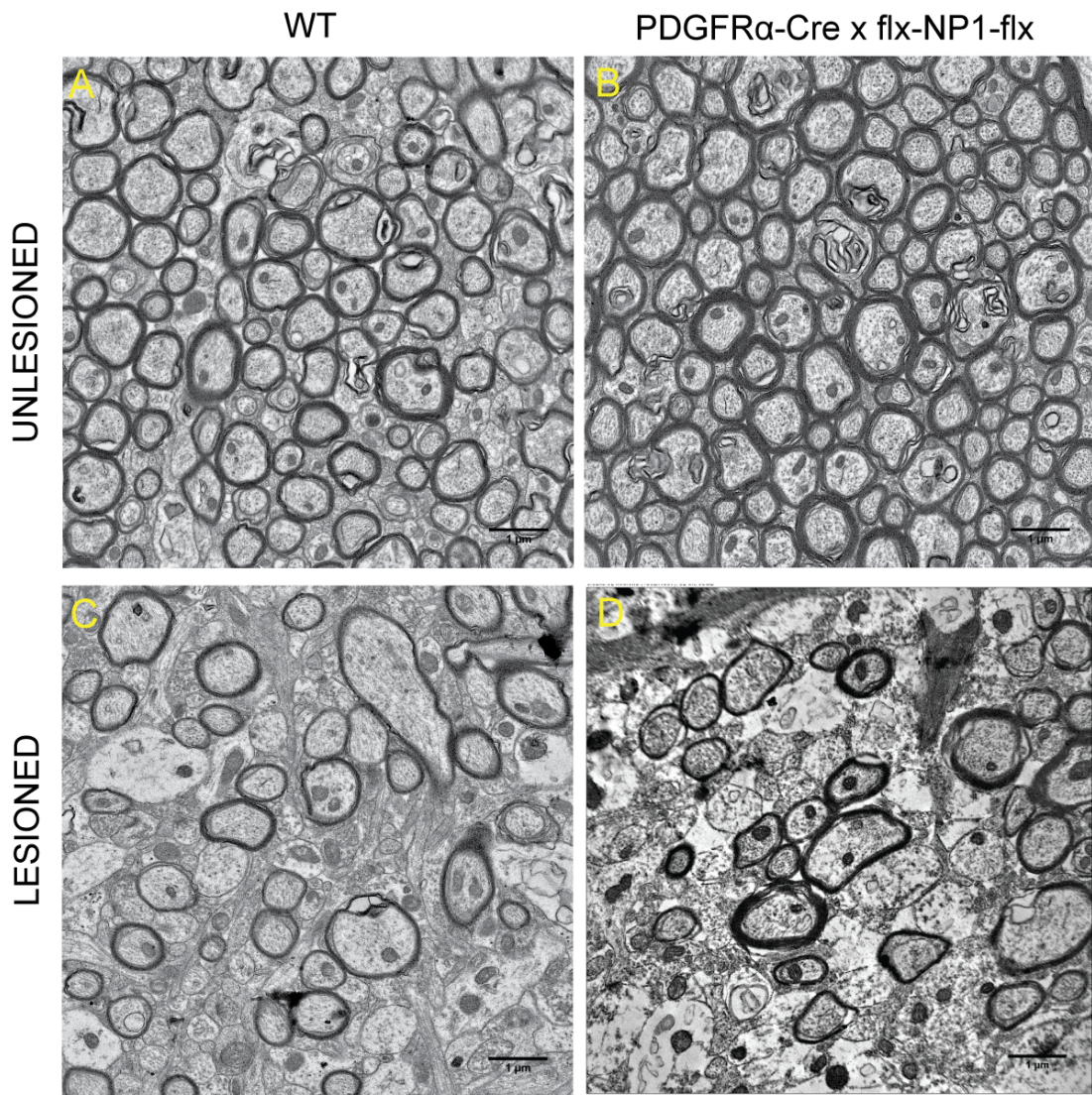
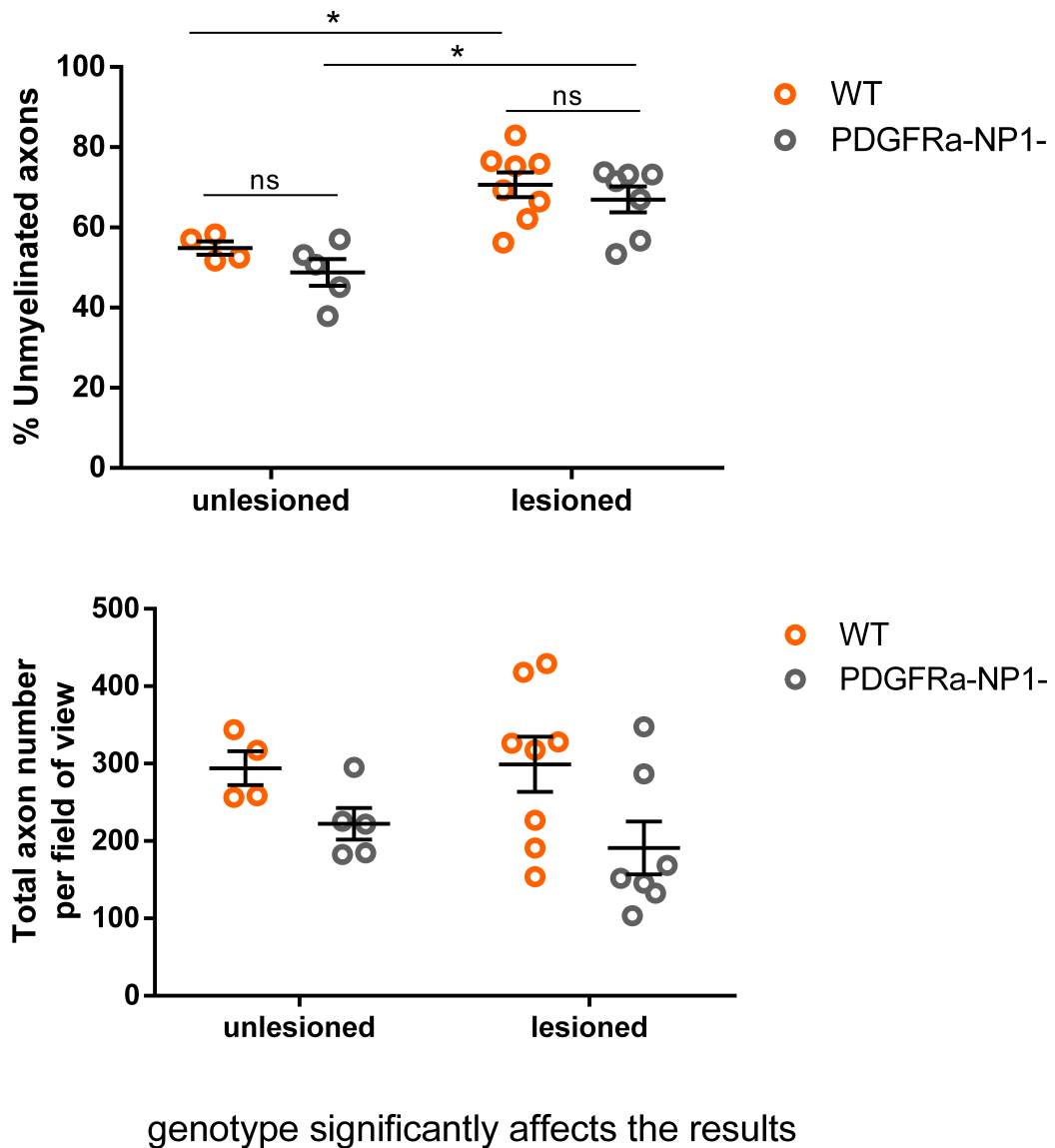


Figure 5.1: Representative EM images. Unlesioned WT (A), unlesioned TG (B), lesioned WT (C) and lesioned TG (D). There are more unmyelinated axons in the lesioned animals and the myelin in the lesioned TG mice is slightly thicker than WT.

Quantification of the proportion of unmyelinated axons by a two-factor ANOVA showed there was a significant effect of treatment ( $F_{(1,20)}=26.09$ ,  $P<0.0001$ ) but no significant effect of genotype ( $F_{(1,20)}=2.153$ ,  $P=0.158$ ) and no significant interaction between those factors ( $F_{(1,20)}=0.142$ ,  $P=0.711$ ). A posteriori Tukey's multiple comparisons test showed that there were significantly more unmyelinated axons in the lesioned counterpart of the each genotype but no difference between the genotypes (Figure 5.2, top). Therefore, LPC increases the proportion of unmyelinated fibres as we would expect. However, comparison of the proportion of unmyelinated axons between the lesioned WT and TG mice did not show any difference between the genotypes. This means that *PDGFR $\alpha$ -Cre x flx-NP1-flx* mice do not remyelinate better than WT mice despite our expectations that they would. Moreover, by using oligodendroglia specific KO animals, we have eliminated the possibility that the inability to repair is due to the dysregulation of the

immune response which we observed in the NP1(Sema3A-) mice.

As before, we then looked at total axon numbers since the proportion of unmyelinated axons depends on the amount of axons. Comparison of the number of axons per field of view by a two-factor ANOVA showed there was a significant effect of genotype ( $F_{(1,20)}=6.733$ ,  $P=0.017$ ) but no significant effect of treatment ( $F_{(1,20)}=0.144$ ,  $P=0.708$ ) and no significant interaction between those factors ( $F_{(1,20)}=0.271$ ,  $P=0.609$ ). However, this difference was small as a posteriori Tukey's multiple comparisons test found no significant differences between the genotypes (Figure 5.2, bottom). Therefore, *PDGFR $\alpha$ -Cre x flx-NP1-flx* mice do not remyelinated better than WT but have less axons per field of view compared to WT.



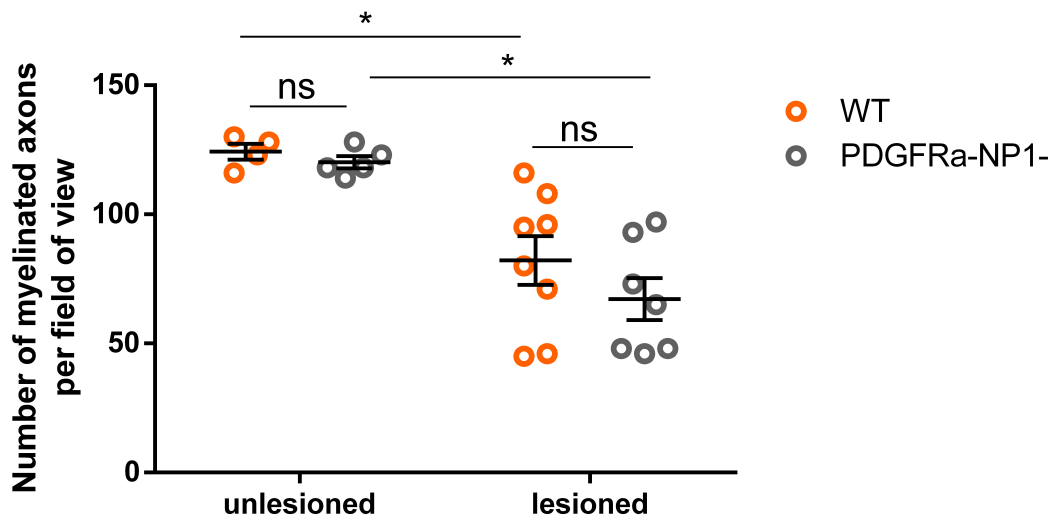
genotype significantly affects the results

Figure 5.2: There is no difference in proportion of unmyelinated axons between TG and WT mice. Comparison of the proportion of unmyelinated axons by a two-factor ANOVA showed there was a significant effect of treatment ( $F_{(1,20)}=26.09$ ,  $P<0.0001$ ) but no significant effect of genotype ( $F_{(1,20)}=2.153$ ,  $P=0.158$ ) and no significant interaction ( $F_{(1,20)}=0.142$ ,  $P=0.711$ ). A posteriori Tukey's multiple comparisons test showed that there were significantly more unmyelinated axons in the lesioned counterpart of the each genotype but no difference between the genotypes (top). Comparison of the number of axons per field of view by a two-factor ANOVA showed there was a significant effect of genotype ( $F_{(1,20)}=6.733$ ,  $P=0.017$ ) but no significant effect of treatment ( $F_{(1,20)}=0.144$ ,  $P=0.708$ ) and no significant interaction between those factors ( $F_{(1,20)}=0.271$ ,  $P=0.609$ ). However, this difference was small as a posteriori Tukey's multiple comparisons test found no significant differences between the genotypes (bottom). Each dot represents the average of data from one animal.

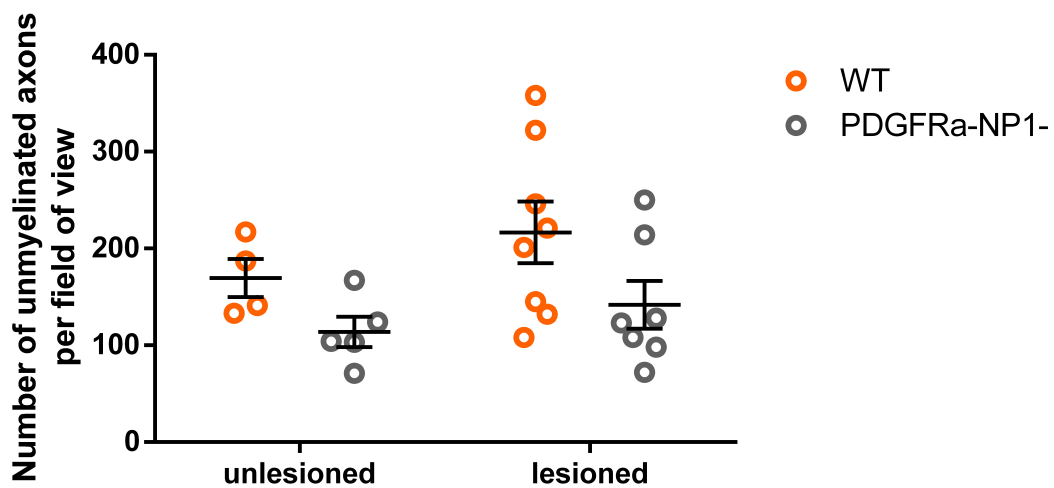
We then looked at the absolute numbers of myelinated and unmyelinated axons per field of view to investigate where this difference in total axons per field comes from. We found no significant difference between genotypes in the number of myelinated axons per field of view. Comparison of absolute number of myelinated axons by a two-factor ANOVA showed there was a significant effect of treatment ( $F_{(1,20)}=31.55$ ,  $P<0.0001$ ) but no significant effect of genotype ( $F_{(1,20)}=1.262$ ,  $P=0.275$ ) and no significant interaction ( $F_{(1,20)}=0.416$ ,  $P=0.52$ ). A posteriori Tukey's multiple comparisons test showed that there were significantly less myelinated axons per field of view in the lesioned counterpart of the each genotype but no difference between the genotypes (Figure 5.3 top). As expected, the number of myelinated axons decreased following LPC treatment for both genotypes. Although there was no significant difference, there was a clear trend towards less myelinated axons per field of view in the TG lesioned compared to WT lesioned animals. Therefore, one of the reasons we see less total axons is that there are slightly less myelinated axons per field of view.

Looking at the absolute number of unmyelinated axons per field of view we found a small but significant effect of the genotype on the results. A two-factor ANOVA showed there was a significant effect of genotype ( $F_{(1,20)}=5.189$ ,  $P=0.034$ ) but no significant effect of treatment ( $F_{(1,20)}=1.72$ ,  $P=0.204$ ) and no significant interaction of those factors ( $F_{(1,20)}=0.11$ ,  $P=0.743$ ) on absolute number of unmyelinated axons (Figure 5.3 bottom). However, this difference was too small as a posteriori Tukey's multiple comparisons test found no significant differences between the genotypes. Overall, there was a clear reduction in the absolute number of unmyelinated axons per field of view in the TG animals compared to WT. However, there was no significant effect of LPC treatment on the number of unmyelinated axons per field of view which indicates that it does not result in axon death.

So far, we have found that the *PDGFR $\alpha$ -Cre x flx-NP1-flx* mice have less axons per field of view and this is primarily because they have less unmyelinated axons but also because they have slightly less myelinated axons per field of view. We then investigated the axon diameter and myelin thickness in order to find clues as to the apparent reduction in axon numbers.



treatment significantly affects the results



genotype significantly affects the results

Figure 5.3: Absolute numbers of myelinated and unmyelinated axons per field of view are reduced in TG animals. Comparison of the absolute number of myelinated axons by a two-factor ANOVA showed there was a significant effect of treatment ( $F_{(1,20)}=31.55$ ,  $P<0.0001$ ) but no significant effect of genotype ( $F_{(1,20)}=1.262$ ,  $P=0.275$ ) and no significant interaction between the factors ( $F_{(1,20)}=0.416$ ,  $P=0.52$ ) (top). A posteriori Tukey's multiple comparisons test showed that there were significantly less myelinated axons per field of view in the lesioned counterpart of the each genotype but no difference between the genotypes. Comparison of absolute number of unmyelinated axons by a two-factor ANOVA showed there was a significant effect of genotype ( $F_{(1,20)}=5.189$ ,  $P=0.034$ ) but no significant effect of treatment ( $F_{(1,20)}=1.72$ ,  $P=0.204$ ) and no significant interaction of those factors ( $F_{(1,20)}=0.11$ ,  $P=0.743$ ) (bottom). However, this difference was too small as a posteriori Tukey's multiple comparisons test found no significant differences between the genotypes. Each dot is an average of data from one animal. 108

### 5.2.2 Myelin thickness and axon diameter

Comparison of the myelin thickness between the TG and WT before and after LPC treatment showed that there was no significant differences between the genotypes or treatments (Figure 5.4). Comparison of g ratio by a two-way ANOVA showed there was no significant effect of treatment ( $F_{(1,20)}=4.07$ ,  $P=0.057$ ), genotype ( $F_{(1,20)}=0.003$ ,  $P=0.958$ ) and no significant interaction between the factors ( $F_{(1,20)}=4.204$ ,  $P=0.054$ ). Although not significant, we see the characteristic bigger g ratio indicating thinner myelin after remyelination in WT mice however we do not see this after remyelination in the TG mice (Figure 5.4). Since the g-ratio does not change following remyelination in TG mice, this means that the myelin after remyelination is as thick as it was before demyelination. This is very interesting and unprecedented finding that the remyelinated myelin keeps normal thickness in the PDGFR $\alpha$ -Cre x flx-NP1-flx mice. It is also worth noting that in the unlesioned animals, the TG mice have slightly thinner myelin to begin with (bigger g ratio).

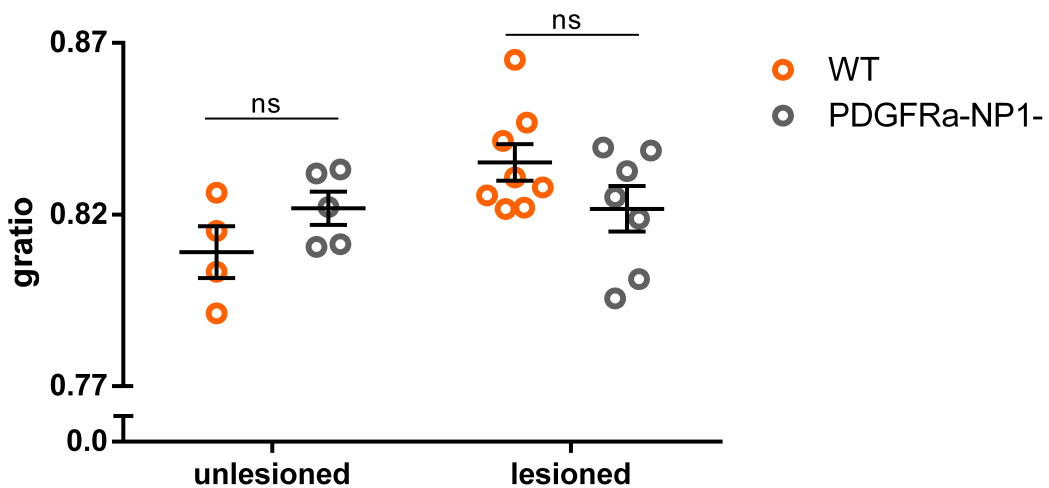
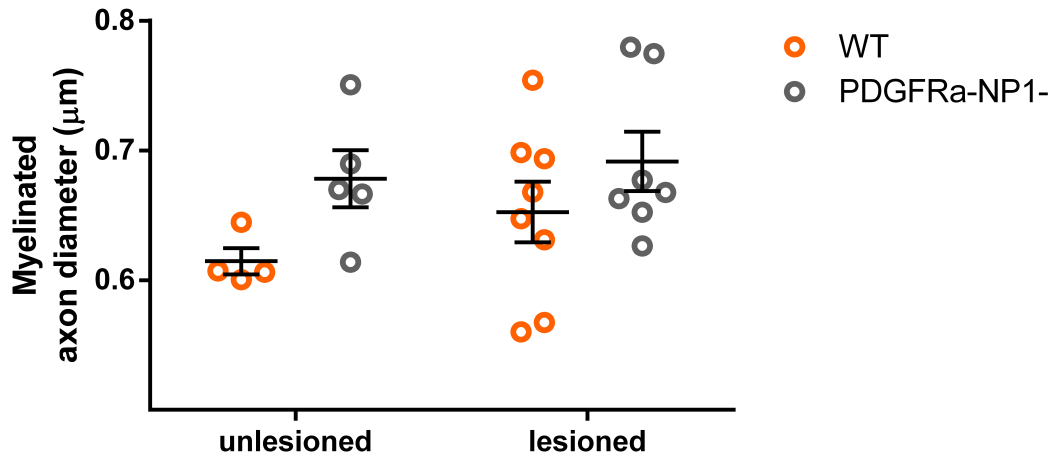


Figure 5.4: There is no difference in the myelin thickness between TG and WT mice. Comparison of g ratio by a two-way ANOVA showed there was no significant effect of treatment ( $F_{(1,20)}=4.07$ ,  $P=0.057$ ), genotype ( $F_{(1,20)}=0.003$ ,  $P=0.958$ ) and no significant interaction between the factors ( $F_{(1,20)}=4.204$ ,  $P=0.054$ ). However, myelin is slightly thinner after remyelination in the WT as expected but in the TG the myelin does not change its thickness after remyelination. Moreover, the unlesioned TG animals have slightly thinner myelin than the unlesioned WT animals.

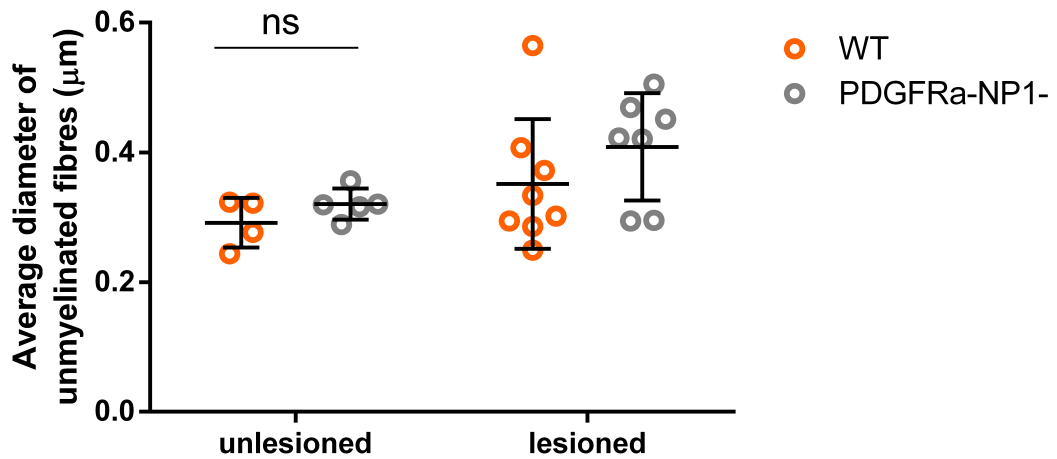
We then looked at the diameter of myelinated axons since the g ratio depends on the axon diameter. Comparison of average myelinated axon diameter by a two-way ANOVA showed there is a significant effect of genotype ( $F_{(1,20)}=4.60$ ,  $P=0.044$ ) but no significant effect of treatment ( $F_{(1,20)}=1.15$ ,  $P=0.296$ ) and no significant interaction between the factors ( $F_{(1,20)}=0.262$ ,  $P=0.614$ ) (Figure 5.5, top). However, this difference was small as Tukey's multiple comparisons test found no significant differences between the genotypes. The average myelinated axon di-

iameter in the TG mice is bigger than the WT mice in both unlesioned and lesioned condition. Therefore, the myelinated axons in the TG mice are bigger than the ones in the WT.

Seeing this difference in the diameter of the myelinated axons in the TG mice, we wanted to examine if the same is true for the unmyelinated fibres (Figure 5.5, bottom). Comparison of the average diameter of unmyelinated axons showed that there is a significant effect of treatment ( $F_{(1,20)}=5.19$ ,  $P=0.034$ ) but no significant effect of genotype ( $F_{(1,20)}=1.74$ ,  $P=0.20$ ) and no significant interaction between the factors ( $F_{(1,20)}=0.19$ ,  $P=0.67$ ). Therefore, there was no significant difference in the size of unmyelinated axons between WT and TG mice but after LPC treatment, the diameter of unmyelinated axons increases. This is because previously myelinated axons have lost their myelin after LPC treatment which increases the average diameter of unmyelinated axons. Even though the difference between the genotypes was not significant, there is clearly a trend towards increased axon diameter in the TG animals compared to control both in the unlesioned and lesioned condition.



genotype significantly affects the results



treatment significantly affects the results

Figure 5.5: Myelin and unmyelinated axon diameter. Comparison of average myelinated axon diameter by a two-way ANOVA showed there is a significant effect of genotype ( $F_{(1,20)}=4.60$ ,  $P=0.044$ ) but no significant effect of treatment ( $F_{(1,20)}=1.15$ ,  $P=0.296$ ) and no significant interaction between the factors ( $F_{(1,20)}=0.262$ ,  $P=0.614$ ). Comparison of the average diameter of unmyelinated axons showed that there is a significant effect of treatment ( $F_{(1,20)}=5.19$ ,  $P=0.034$ ) but no significant effect of genotype ( $F_{(1,20)}=1.74$ ,  $P=0.20$ ) and no significant interaction between the factors ( $F_{(1,20)}=0.19$ ,  $P=0.67$ ). The name of the PDGFR $\alpha$ -Cre x flx-NP1-flx mice is shortened to PDGFR $\alpha$ -NP1— in the graph.

Therefore, the myelinated axons in the TG animals are significantly bigger than in the WT animals. In addition to this, the unmyelinated axons are slightly bigger. A histogram of myeli-

nated (Figure 5.6 top) and unmyelinated (Figure 5.6 bottom) axons shows this change in axon diameter better. In the comparison of the NP1(Sema3A-) mice and WT the genotypes are almost overlapping in the unlesioned and the lesioned condition(see Figure 4.6). On the other hand, comparison of the myelinated (Figure 5.6 top) and unmyelinated (Figure 5.6 bottom) axons between PDGFR $\alpha$ -Cre x flx-NP1-flx mice and WT mice shows that the lesioned WT and the unlesioned and lesioned TG axons are shifted to the right with respect to the unlesioned WT. Shift to the right in the unlesioned TG axon distribution indicates bigger axons. The shift in the myelinated axons is much bigger than the shift in the unmyelinated axons and this is consistent with size of the changes in average axon diameter we observed in Figure 5.5.

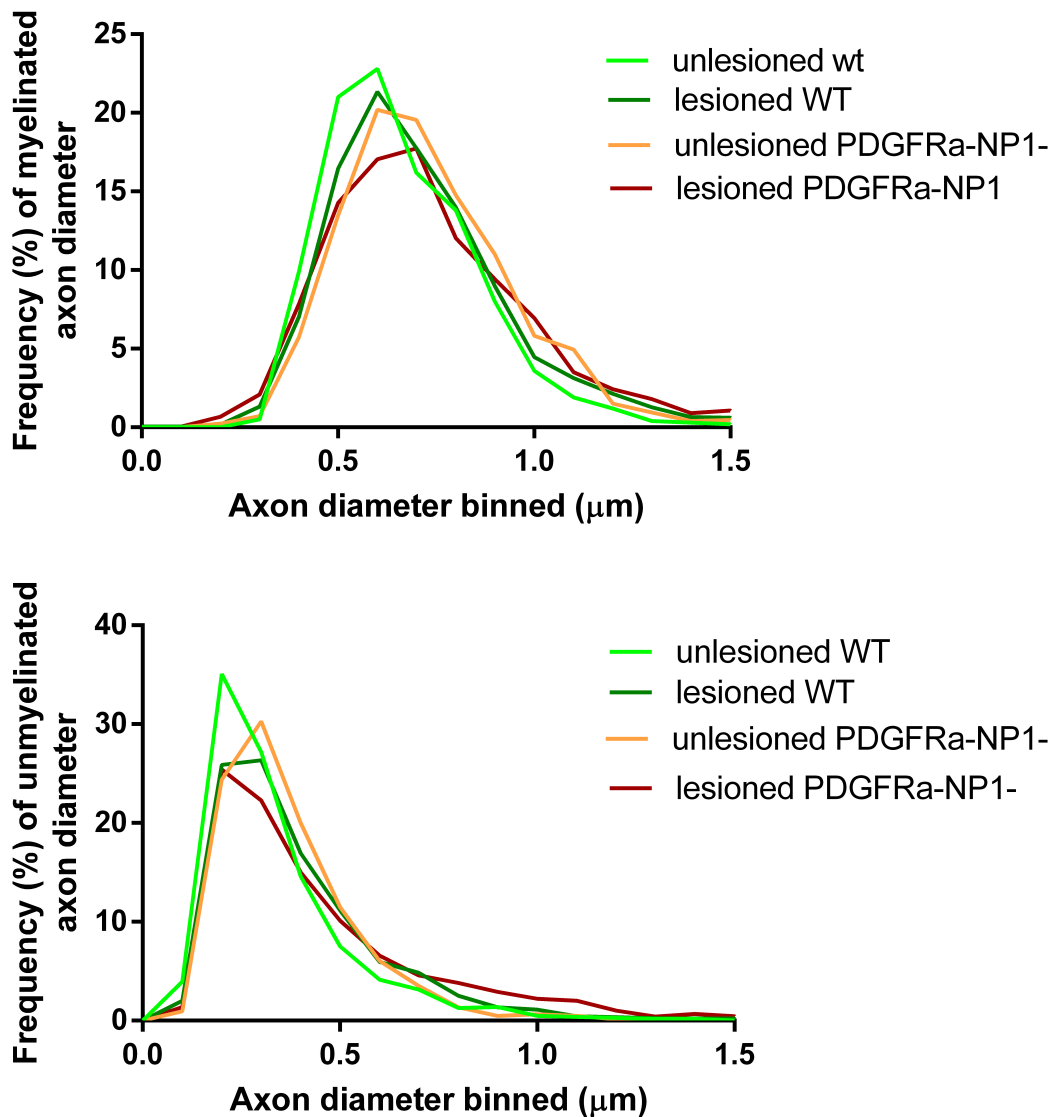


Figure 5.6: Frequency distribution (histogram) of axon diameter. Myelinated axons on the top, unmyelinated at the bottom. Unlesioned TG axons show a shift to the right compared to unlesioned WT indicating bigger axons which is more pronounced in myelinated axons than unmyelinated axons. The name of the *PDGFR $\alpha$ -Cre x flx-NP1-flx* mice is shortened to *PDGFR $\alpha$ -NP1-* in the graph.

Overall, *PDGFR $\alpha$ -Cre x flx-NP1-flx* mice have bigger axons than WT with the difference in the size of myelinated axons being much bigger than that of the unmyelinated axons. The bigger axons in *PDGFR $\alpha$ -Cre x flx-NP1-flx* mice provide an explanation for the observed decrease in total axon number per field of view in figure 5.2 (bottom) and figure 5.3.

Finally, we aimed to visualise the difference in myelin thickness as a result of remyelination in figure 5.7. The data points from both genotypes in both treatments show good overlap even though the average diameter of axons in the TG mice were shown to be bigger (Figure 5.7, top). In the WT animals, a slight shift to the right in the axons after LPC treatment (dark green) is

observed compared to the unlesioned animals (light green) (Figure 5.7, middle). This means that at any diameter, the g ratio is slightly higher indicating thinner myelin consistent with what we would expect in remyelination. However, this shift did not change the slope of the best fit curve at all. In the TG animals, the spread of the axons in the lesioned and unlesioned condition is undistinguishable which is consistent with the lack of any change in the myelin thickness observed in figure 5.4.

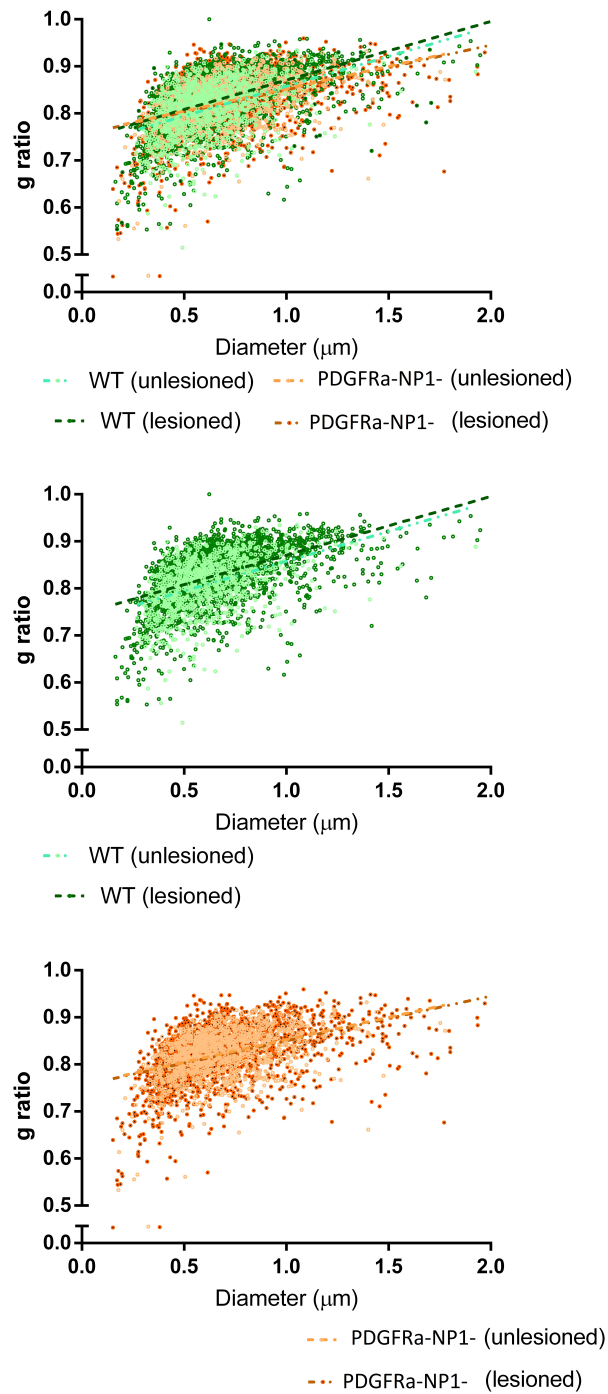


Figure 5.7: The relationship between myelin thickness and axon diameter. The top g ratio vs diameter plot shows both genotypes and treatments together. For clarity, those were separated and presented by genotype: WT (middle) and *PDGFR $\alpha$ -Cre x flx-NP1-flx* (bottom). Dashed line is best fit line of the data and each dot is an axon. The name of the *PDGFR $\alpha$ -Cre x flx-NP1-flx* mice is shortened to *PDGFR $\alpha$ -NP1-* in the graph.

So far we have found that:

- *PDGFR $\alpha$ -Cre x flx-NP1-flx* mice have bigger axons (which is also seen as having less axons per field).
- In unlesioned *PDGFR $\alpha$ -Cre x flx-NP1-flx* mice, the myelin is slightly thinner even though their axons are bigger
- *PDGFR $\alpha$ -Cre x flx-NP1-flx* mice do not remyelinate better than WT
- In *PDGFR $\alpha$ -Cre x flx-NP1-flx* mice, after remyelination, the thickness of myelin (g ratio) is maintained

Our expectation that *PDGFR $\alpha$ -Cre x flx-NP1-flx* mice would show improved repair was not correct and we also observed other unexpected changes in axon diameter and myelin thickness. To find why *PDGFR $\alpha$ -Cre x flx-NP1-flx* mice do not remyelinate better than WT, we investigated the cellular composition of the lesion by immunohistological staining. We were particularly interested to investigate if improved OPC recruitment was present in the TG mice.

## 5.3 Cryo IHC

As in chapter 4, we initially assessed whether the animals which have undergone LPC lesion have lesions and their extent.

### 5.3.1 Finding lesions

Initial staining with antibodies against IBA1 to find macrophages/ microglia and against MBP for myelin were performed and representative images are shown in figure 5.8. Lesions were identified by accumulation of nuclei (Figure 5.8 A, E), macrophages/ microglia (Figure 5.8 B, F) and loss of myelin (Figure 5.8 C, G).

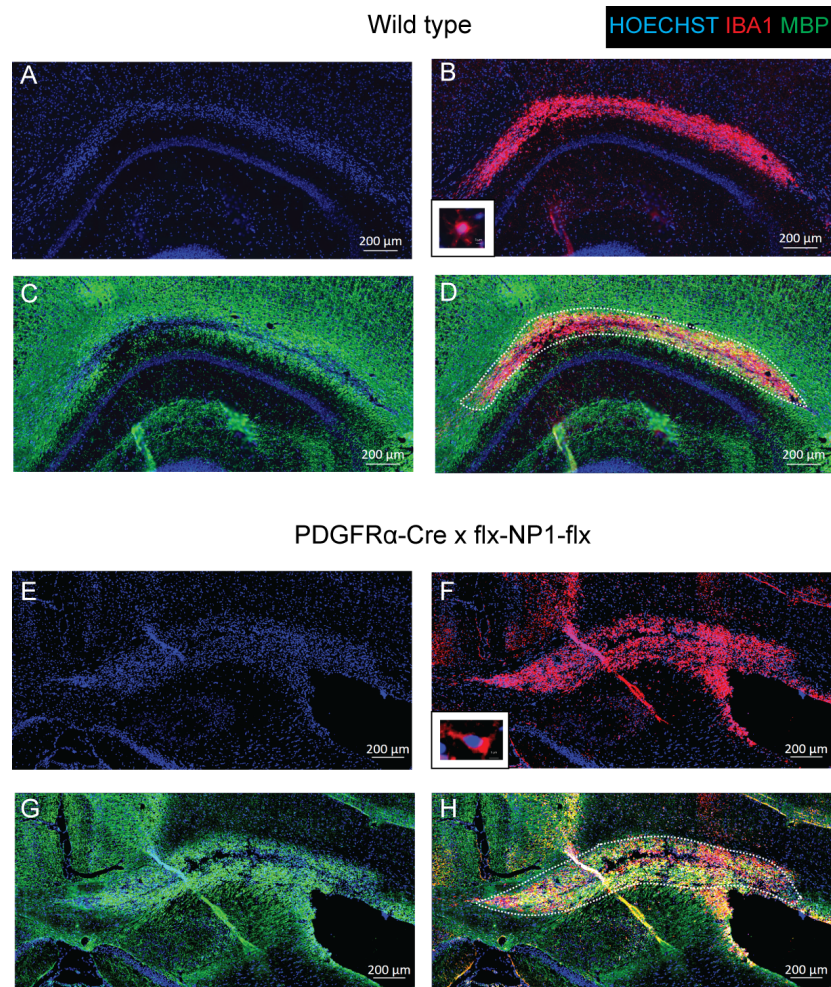


Figure 5.8: Representative images of initial staining with antibodies against MBP and IBA1 used to find lesions. Lesions are characterised by accumulation of nuclei (A,E), infiltration of immune cells (B,F) and loss of MBP (D,G). Scale bar is 200  $\mu$ m

Using these criteria to define lesion outlines, we then quantified and compared the lesion size between the genotypes and found that the lesions are of similar size (Figure 5.9 A) (Mann-Whitney  $U = 5.0$ ,  $n=3,4$ ,  $p=0.86$ , two-tailed). Therefore, based on lesion size, *PDGFR $\alpha$ -Cre x flx-NP1-flx* mice do not remyelinate better than WT mice. We then looked at the immune response and expected it to be identical between genotypes since the NP1 KO is oligodendroglial specific. Comparison of the activated and non-activated macrophages/microglia numbers (IBA1+ cells) revealed that there was not significant difference between the genotypes (Figure 5.9 B) (Mann-Whitney  $U = 4.0$ ,  $n=3,4$ ,  $p=0.63$ , two-tailed).

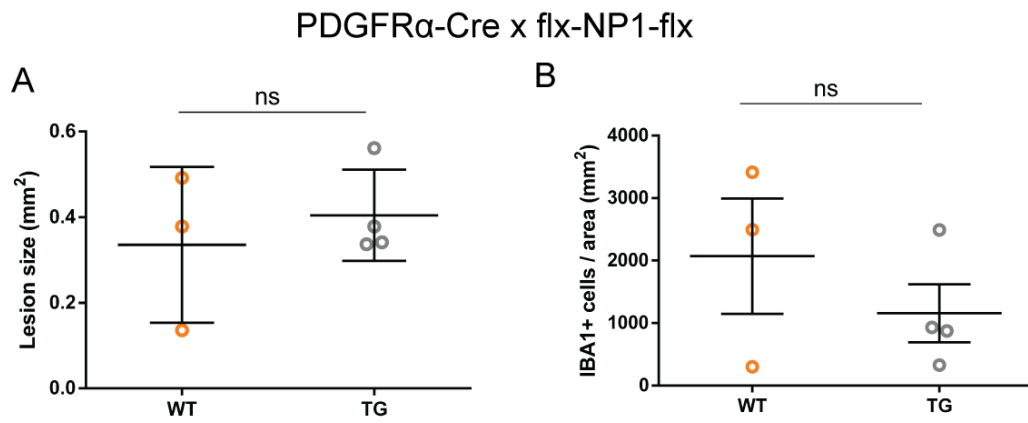


Figure 5.9: Lesions are similar size between WT and TG mice and have similar amount of IBA1+ cells. Lesion size did not differ between genotypes (Mann-Whitney U = 5.0, n=3,4, p=0.86, two-tailed) (A). IBA1+ density in lesions did not differ between WT and TG mice (Mann-Whitney U = 4.0, n=3,4, p=0.63, two-tailed) (B)

We then looked at the numbers of activated macrophages/ microglia as well as their subtype to insure that the immune response in the TG mice does not differ from the WT.

### 5.3.2 Innate immune response is the same

IHC with antibodies against CD68 (activated macrophages/ microglia), Arginase-1 (pro-repair subtype) and iNOS (pro-inflammatory subtype) revealed that in both WT and TG, CD68+ cells were extensively present throughout the lesions (Figure 5.10 B and figure 5.11 B). As we saw in the NP1(Sema3A-) mice, the pro-inflammatory subtype marked by iNOS+ cells was predominant to the pro-repair subtype marked by Arginase-1+ cells but there was some overlap in the expression of those markers (Figure 5.10 C,D,E and figure 5.11 C,D,E). While in the NP1(Sema3A-) mice and their WT counterpart the overlap of iNOS+ and Arginase-1+ cells was extensive in both genotypes, the overlap in the PDGFR $\alpha$ -Cre x flx-NP1-flx mice is much more extensive than in their WT counterpart (Figure 5.10 E and figure 5.11 E). As before, this predominance of the pro-inflammatory macrophages/ microglia subtype at 10 days after lesion is in contrast with previous reports [205] and further characterisation of the iNOS+ Arginase-1+ cells would be required to truly elucidate their functional phenotype.

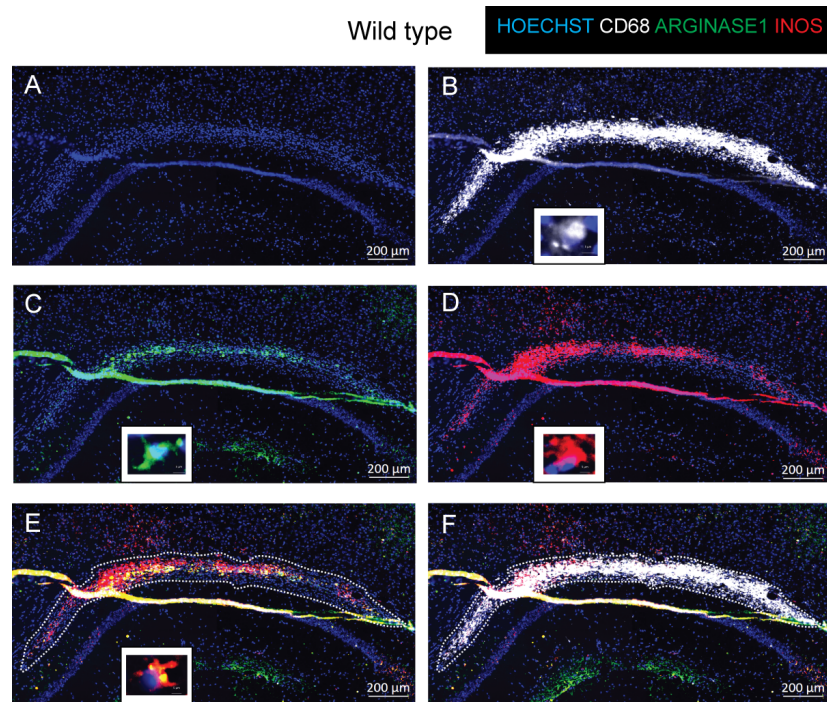


Figure 5.10: Representative images of staining using CD68, Arginase-1 and iNOS antibodies on WT tissue. CD68 (activated macrophages/microglia), Arginase-1 (pro-repair subtype) and iNOS (pro-inflammatory subtype) staining was extensively present in the lesions at 10 days after LPC injection. A high magnification of an example cell is shown in the bottom left panel. Scale bar is 200  $\mu\text{m}$

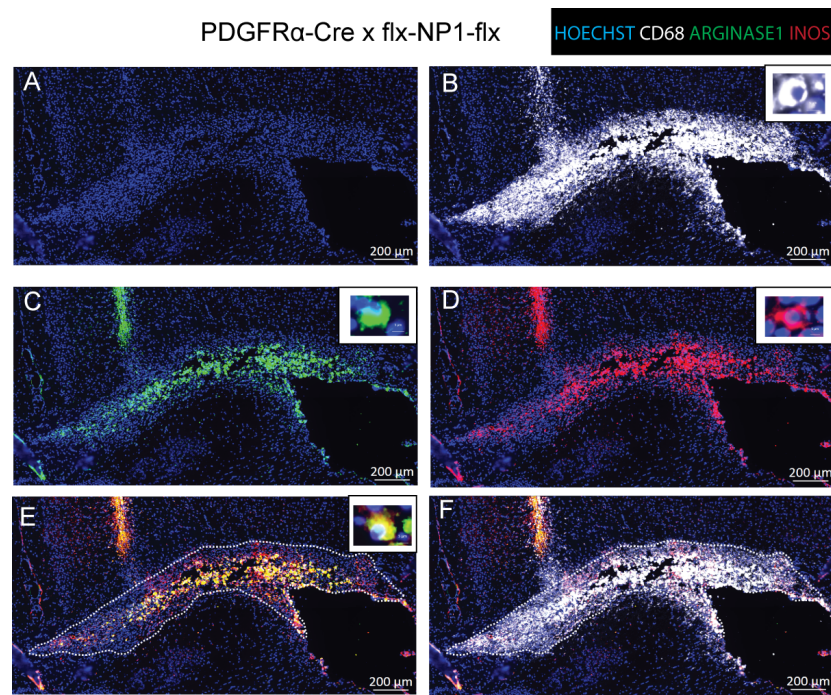


Figure 5.11: Representative images of staining using CD68, Arginase-1 and iNOS antibodies on *PDGFR $\alpha$ -Cre x flx-NP1-flx* tissue. CD68 (activated macrophages/microglia), Arginase-1 (pro-repair subtype) and iNOS (pro-inflammatory subtype) staining was extensively present in the lesions at 10 days after LPC injection. A high magnification of an example cell is shown in the bottom left panel. Scale bar is 200  $\mu\text{m}$

Quantification of the number of cells using the same criteria as in chapter 4, revealed that there was no difference between the genotypes in the number of activated macrophages/microglia (CD68+ cells) (Figure 5.12 A) (Mann-Whitney  $U = 2.0$ ,  $n=3,4$ ,  $p=0.23$ , two-tailed). They also have a similar amount of pro-inflammatory macrophages/microglia (iNOS+ cells) (Figure 5.12 B) (Mann-Whitney  $U = 1.0$ ,  $n=3,4$ ,  $p=0.11$ , two-tailed) and pro-repair macrophages/microglia (Arginase-1+ cells) (Figure 5.12 C) (Mann-Whitney  $U = 2.0$ ,  $n=3,4$ ,  $p=0.23$ , two-tailed). Therefore, the innate immune response in the *PDGFR $\alpha$ -Cre x flx-NP1-flx* mice does not significantly differ from the WT mice. This was expected as in the *PDGFR $\alpha$ -Cre x flx-NP1-flx* mice genotype, immune cells do not lose NP1 and therefore should migrate and survive in a pattern identical to WT cells.

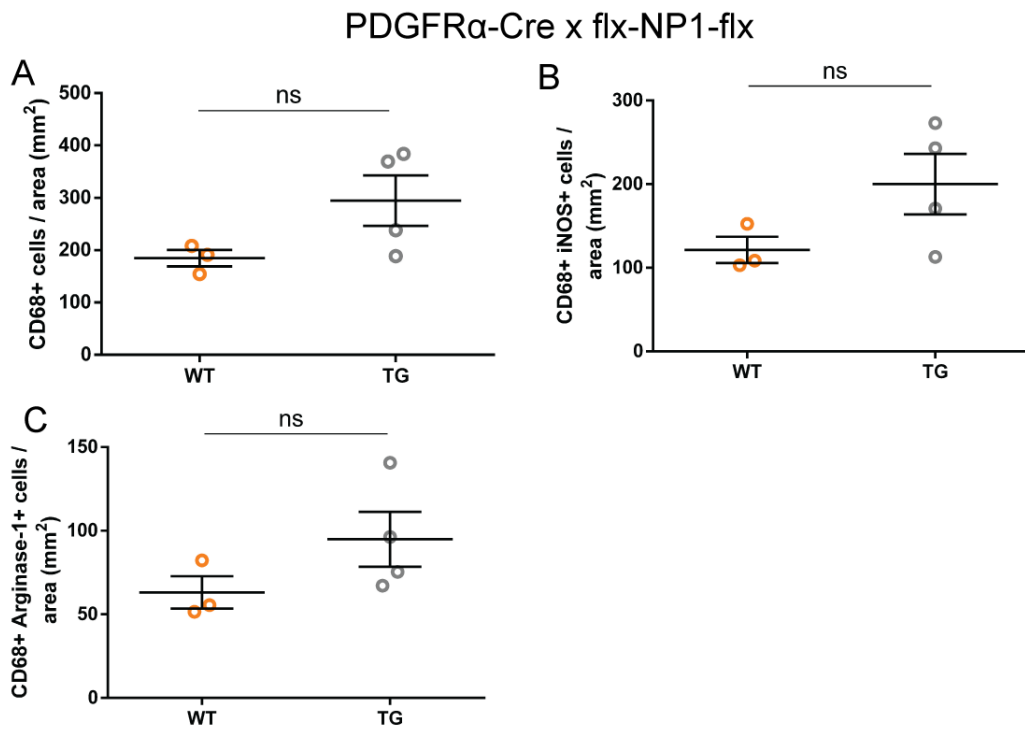


Figure 5.12: PDGFR $\alpha$ -Cre x flx-NP1-flx mice have a normal immune response. TG mice have the same amount of activated microglia/macrophages in the lesion as WT mice (Mann-Whitney U = 2.0, n=3,4, p=0.23, two-tailed) (A). Furthermore, they have a similar amount of iNOS+ cells (Mann-Whitney U = 1.0, n=3,4, p=0.11, two-tailed) (B) and a similar amount of Arginase-1+ cells in the lesions compared to WT (Mann-Whitney U = 2.0, n=3,4, p=0.23, two-tailed) (C)

After we have proven that the PDGFR $\alpha$ -Cre x flx-NP1-flx mice do not have a different response compared to WT as their genotype would predict, we compared their OPC and mature oligodendrocyte numbers in the lesion. Since we have eliminated the different innate immune response which we saw in the NP1(Sema3A-) mice, there was nothing to prevent the improved migration of OPCs into the lesions. Therefore, we strongly expected to see increased OPC numbers in the TG mice compared to WT.

### 5.3.3 Do not have more OPCs in lesions

As in chapter 4, we quantified OPCs using antibodies against NG2 and PDGFR $\alpha$  to ensure that the marker we have chosen does not bias our results. We also used antibodies against CC1 and NogoA to quantify the mature oligodendrocytes in the lesions. Representative images of IHC with those antibodies is shown in figure 5.13 and figure 5.14. The lesions in both TG and WT mice were extensively but not completely covered by OPCs (Figure 5.13 B, F and figure 5.14 B, F) and had very few mature oligodendrocytes (Figure 5.13 C, G and figure 5.14 C, G). As discussed in chapter 4, this distribution of OPCs and mature oligodendrocytes is what is expected at 10 days post lesion.

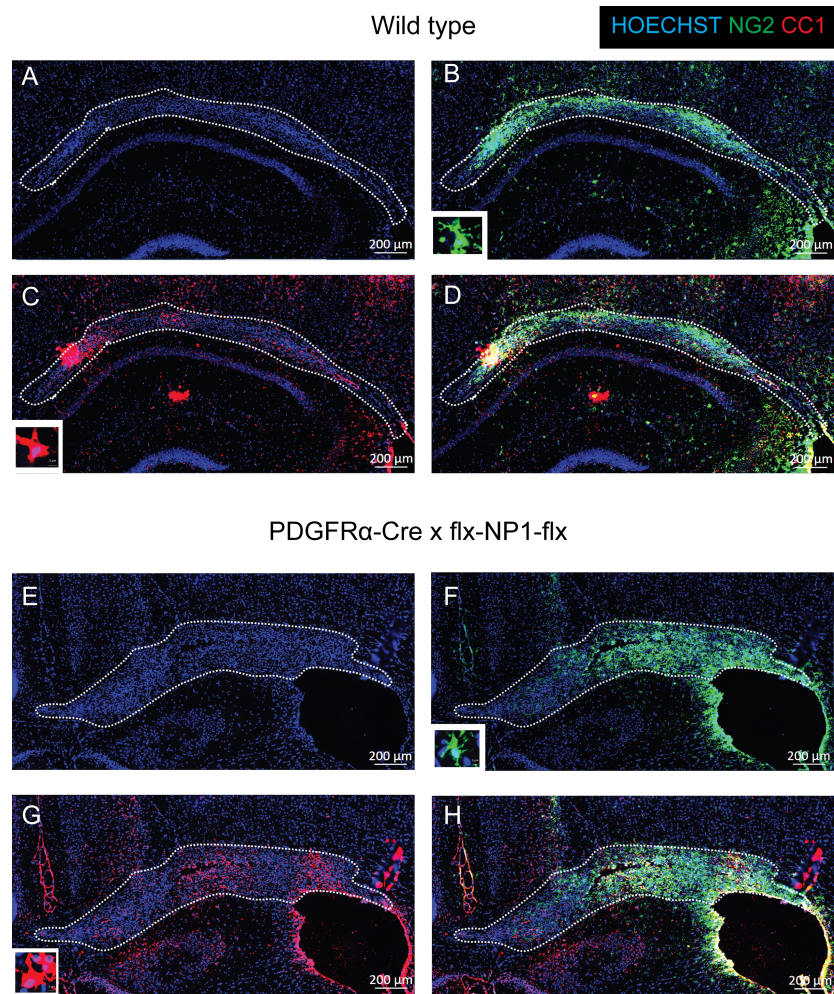


Figure 5.13: Representative images of IHC with antibodies against NG2 and CC1 on WT and TG tissue. A high magnification of an example cell is shown in the bottom left panel. Scale bar is 200  $\mu m$

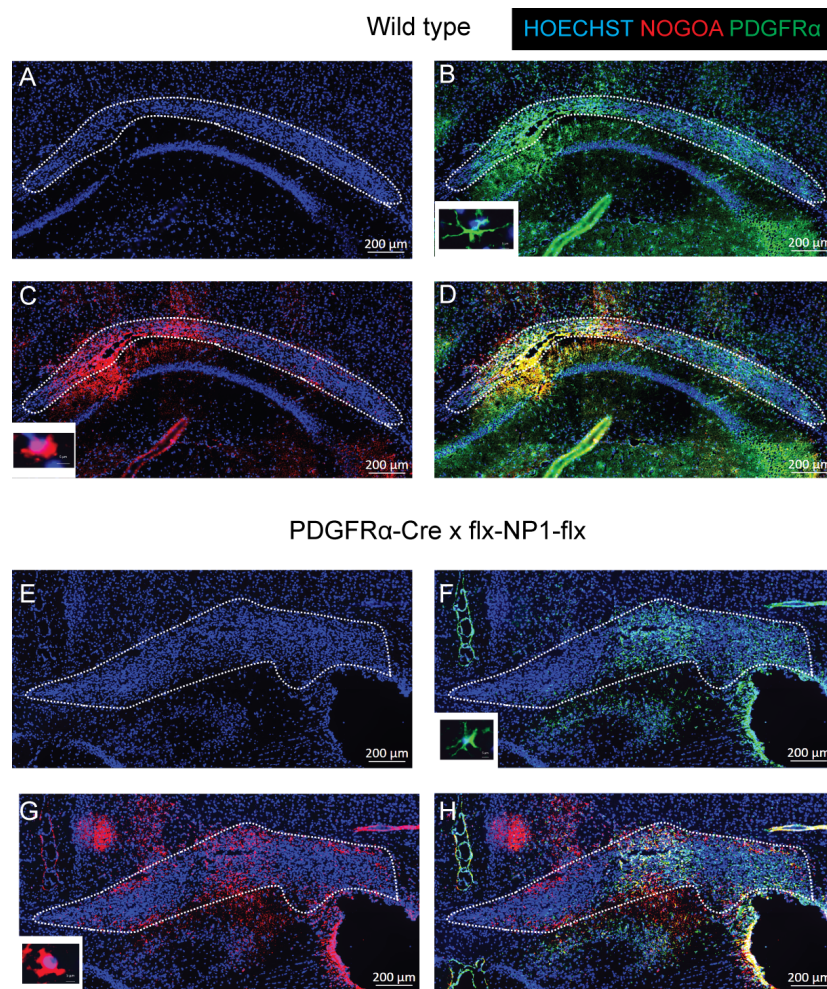


Figure 5.14: Representative images of IHC using antibodies against PDGFR $\alpha$  and NogoA on WT and TG tissue. A high magnification of an example cell is shown in the bottom left panel. Scale bar is 200  $\mu$ m

Quantification of OPCs as NG2+ cells or PDGFR $\alpha$ + cells revealed that despite our expectations PDGFR $\alpha$ -Cre x flx-NP1-flx mice do not have significantly more OPCs in the lesions (Figure 5.15 A, C). In the comparison of NG2+ cell numbers in figure 5.15 A, the OPC numbers in the TG animals appear increased because 2 of the analysed mice have more OPCs than WT but the other 2 analysed mice have identical amount of OPCs to WT. Addition of more TG animals to the analysis would aid in determining if there was any real difference in the NG2+ cell numbers between genotypes. However, the quantification of PDGFR $\alpha$ + cells in figure 5.15 C indicates that there is no significant difference suggesting that the observed NG2+ cell increase in the TG mice is due to chance.

Comparison of the mature oligodendrocytes by counting of CC1+ cells revealed that there was no significant difference between the genotypes (Figure 5.15 B). Despite this, the numbers of CC1+ cells in the TG mice were markedly lower than the in the WT. While this could have been an indication that Sema3A is preventing oligodendroglial maturation as previously observed [296], the same was not observed in the mature oligodendrocyte numbers counted as

NogoA+ cells (Figure 5.15 D). We observed that the numbers of NogoA+ cells were similar in both WT and TG mice. It is worth noting that both OPC and both mature oligodendrocyte markers give us slightly different results which emphasise the importance of using multiple markers to define the same cell type.

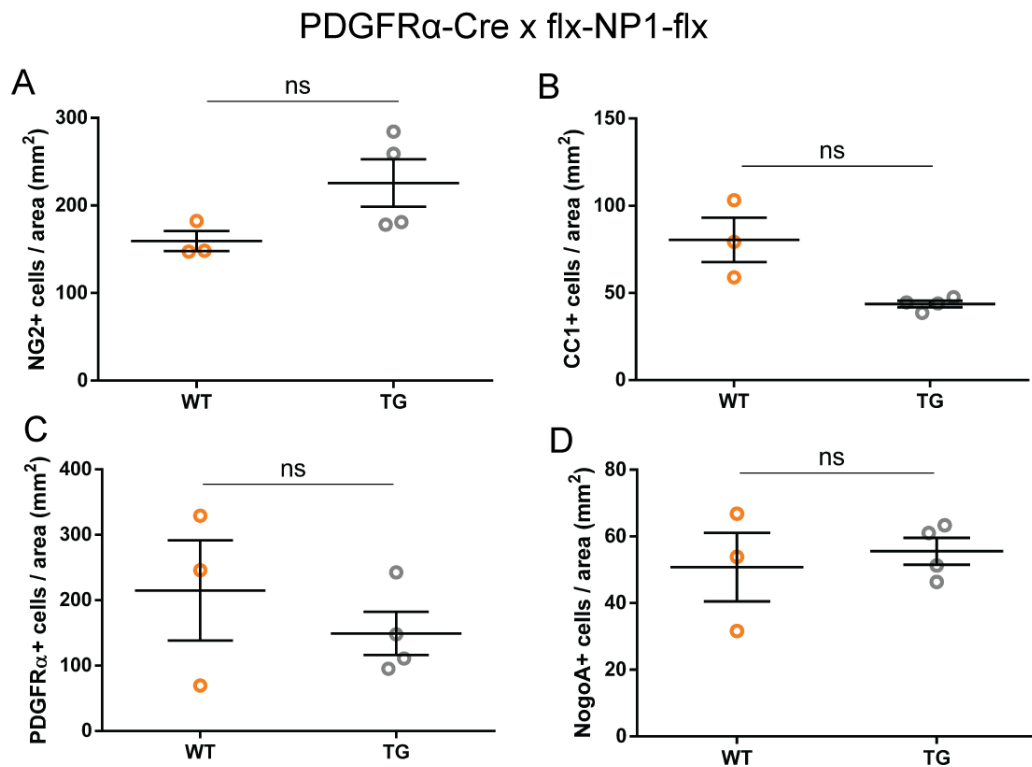


Figure 5.15: *PDGFR $\alpha$ -Cre x flx-NP1-flx* mice do not have more OPCs or mature oligodendrocytes in lesions. The NG2+ density in lesions of TG mice was not different to WT (Mann-Whitney U = 2.0, n=3,4, p=0.23, two-tailed) (A). The CC1+ density in lesions of TG mice was not different to WT (Mann-Whitney U = 0.0, n=3,4, p=0.057, two-tailed) (B). The PDGFR $\alpha$ + density in lesions of TG mice was not different to WT (Mann-Whitney U = 4.0, n=3,4, p=0.63, two-tailed) (C). The NogoA+ density in lesions of TG mice was not different to WT (Mann-Whitney U = 4.0, n=3,4, p=0.39, two-tailed) (C).

Therefore, despite no different innate immune response in the *PDGFR $\alpha$ -Cre x flx-NP1-flx* mice, we do not see improved migration of NP1 KO OPCs into the lesions or a difference in the mature oligodendrocyte numbers at 10 days.

## 5.4 Discussion

In the remyelination and cellular contents of the lesion analysis of *PDGFR $\alpha$ -Cre x flx-NP1-flx* mice we did not find the expected OPC recruitment enhancement or improved remyelination

but instead found increased axon diameter and dysregulation of myelin thickness. The only result we expected was the similarity of the innate immune response of the *PDGFR $\alpha$ -Cre x flx-NP1-flx* and WT to a LPC lesion.

## 5.5 Immune response

The failure of NP1(Sema3A-) mice to remyelinate better or exhibit enhanced OPC migration could be due to the dysregulation of the immune response because of the loss of Sema3A signalling via NP1 in immune cells. Therefore, we examined remyelination and OPC migration in the *PDGFR $\alpha$ -Cre x flx-NP1-flx* mice which do not have NP1 in oligodendroglia. Since in the mice the NP1 KO is specifically in oligodendroglia and not in immune cells, we expected the immune response to be unaffected by the genotype. Comparison of the activated and non-activated macrophage/ microglia numbers (Figure 5.9 B), activated macrophage/ microglia numbers as well as the pro-repair and pro-inflammation phenotype numbers (Figure 5.12 A, B, C) in the lesion between the TG and WT revealed that our expectation was indeed correct. Since this genotype does not affect the immune response but its OPCs do not express NP1, there is nothing to prevent the increase in OPC migration due to loss of Sema3A chemorepulsion. Therefore, we expected increased OPC migration in the TG compared to the WT lesions.

## 5.6 OPC recruitment

However, comparison of the OPC numbers at 10 days post lesion showed that the OPCs which do not have NP1 do not migrate better into the lesions (Figure 5.15). This is in sharp contrast to other reports which indicate that modulating the level of Sema3A results in a difference in OPC migration (section 1.9.1). Since the OPCs might have migrated into the lesions and started differentiating by this time-point, we compared the mature oligodendrocyte numbers between WT and TG mice and found that the amount of mature oligodendrocytes between both is similar (Figure 5.15). This excludes the possibility that the OPCs in the TG mice have migrated earlier and matured into oligodendrocytes since then we would see an increase in the number of mature oligodendrocytes even if there was no difference in OPC numbers. Although there are other limitations, those were discussed in section 4.3.6 and since the EM and IHC analysis were performed in the same way and at the same time points, they will not be repeated here.

Therefore, mice which lack Sema3A signalling via NP1 and mice whose oligodendroglia do not have NP1 both fail to show enhanced OPC migration after lesion. While increase in OPC number is transient and could be easily missed, the increase in OPC numbers in Sema3A KD mouse [29] has previously lead to increase in remyelination so we examined how well the TG mice remyelinate compared to WT.

## 5.7 Remyelination

Even though we expected an improvement in remyelination in the *PDGFR $\alpha$ -Cre x flx-NP1-flx* mice, comparison of the proportion of unmyelinated axons in lesioned WT and TG animals (Figure 5.2 A) revealed that mice which lack NP1 in oligodendrocytes do not repair any better than WT. In addition to this, their lesion size is not smaller than the lesion in the WT mice (Figure 5.9 A) which also suggests that the remyelination of the *PDGFR $\alpha$ -Cre x flx-NP1-flx* mice is not improved.

Therefore, both mice which lack *Sema3A* signalling via NP1 in all cells and mice which do not have NP1 in oligodendroglia do not show improved remyelination despite the extensively documented negative effects *Sema3A* has on remyelination. In addition to this, losing NP1 or the *Sema3A* site on NP1 does not result in increased OPC migration.

We have excluded the possibility that this lack of improved remyelination or OPC recruitment is because of a dysregulation in the immune response by looking at a oligodendroglia specific KO. Therefore, we aimed to find an explanation why OPCs which cannot signal via NP1 or do not have NP1 are still chemorepelled by *Sema3A*.

### 5.7.1 Is NP1 the only receptor for *Sema3A*?

A possible explanation for the lack of improved OPC recruitment and remyelination in both mutant mice is that *Sema3A* can signal via another receptor if NP1 is unavailable. Although *Sema3A* is believed to only bind to NP1 and its coreceptors as discussed in section 1.8, it is possible that the body can compensate for loss of NP1 since the mutation/loss of NP1 is present throughout life. This compensation could be upregulation of a protein already present in oligodendroglia, expression of a protein which is not normally found on oligodendroglia or different post-translational modification.

Although the literature is overwhelmingly convincing that NP1 is *Sema3A*'s only receptor, there are indications in different cell types that this might not be the case and those are listed below:

The *Sema3A* inhibition of monocyte migration in a transwell assay [72] discussed in section 1.9.3 is not mediated via NP1. The monocytes did not express NP1 either on the protein or the mRNA level [72] indicating that another receptor is mediating this effect.

Moreover, the effect of *Sema3A* on the gonadotropin-releasing hormone (GnRH) neuron system mentioned in section 1.10 is mediated redundantly via NP1 or NP2. In vivo, reduced migration of GnRH cells is observed in *NP1(Sema3A-)* mice as well as *NP2-/-* mice. In a double mutant *NP1(Sema3A-)/NP2-/-* it was completely abolished [36]. Since *Sema3F* was shown not to be important for this process [36], this indicates that the presence of one NP is enough to mediate *Sema3A*-driven migration but loss of both results in complete loss of migration. This study also showed that the *Sema3A* binding in the *NP1(Sema3A-)* mutant mice was indeed reduced but not completely abolished [36]. Finally, shRNA KD of NP2 in a cell line reduced its migratory response to *Sema3A* by about 30% [36] indicating that NP2 plays a role in *Sema3A*

signalling. This data indicates in vivo and in vitro that NP2 could be a receptor for Sema3A.

Finally, in tumors, hypoxia induced Sema3A attracts tumor-associated macrophages via NP1/PlexinA1 or 4 [38]. NP1 KO cells are resistant to the Sema3A induced increase in migration in vitro [38] suggesting that NP1 is Sema3A's binding partner. However, in hypoxia, NP1 is downregulated by 80% [38] and Sema3A induces a NP1 independent stop of migration. To investigate the binding partners responsible for this NP1 independent migration blockage, Sema3A binding was assessed in NP1 KO cells and was found to be present although reduced by about 50% [38]. PlexinA1 or PlexinA4 KO inhibited the Sema3A migration to the same extent as the NP1 KO [38] indicating their common involvement in Sema3A signalling via NP1. However, PlexinA1 or PlexinA4 KO in NP1 KO cells resulted in abolishment of the NP1 independent migration stop [38]. This suggests that Sema3A signals via NP1/Plexin complex to mediate migration by when NP1 is downregulated in the hypoxic core of the tumor, Sema3A signals via PlexinA1 or 4 to stop their migration.

Therefore, 3 independent studies with 3 different cell types have indicated that Sema3A can exert effects on cells without NP1. From these studies, NP2 and PlexinAs are set forward as possible binding partners of Sema3A which can mediate its signalling in the absence of NP1. This is in sharp contrast to previous reports that Sema3A does not bind NP2 [52] and that it does not bind PlexinAs directly but only in combination with NP1 [300] [136] (section 1.8). While NP1 might be the Sema3A's preferred receptor, investigation into Sema3A's binding partners in NP1 KO oligodendroglia could allow elucidation of Sema3A's signal transduction machinery in the absence of NP1.

To sum up, the OPC recruitment and remyelination studies after lesion in both mice have lead us to the hypothesis that NP1 is not solely responsible for Sema3A's effects on OPC recruitment and remyelination. There might be other receptors responsible for Sema3A's effects in the absence of NP1. Although the literature suggests NP1 and PlexinAs as possible receptors, further studies need to be carried out to confirm or exclude them.

Although we did not find a difference in the remyelination or OPCs migration in the TG mice, we found differences in the diameter of myelinated axons and that the myelin thickness in those mice.

### 5.7.2 Unexpected changes in *PDGFR $\alpha$ -Cre x flx-NP1-flx* mice

Investigation of the lesions in *PDGFR $\alpha$ -Cre x flx-NP1-flx* mice using electron microscopy showed that there were significantly less axons per field of view in the TG mice compared to WT (Figure 5.2 B). This reduction in total axons is primarily because of reduction in unmyelinated axons but also because they have slightly less myelinated axons (Figure 5.3). The reduction in the number of axons per field of view is explained by the observation that the average axon diameter of the axons was bigger in the TG mice. This was primary true for myelinated axons but the unmyelinated axons had the same tendency to be bigger in the TG compared to WT (Figure 5.5 and figure 5.6).

Therefore, loss of NP1 in oligodendroglia has resulted in bigger axons. This effect was not

seen in the NP1(Sema3A-) in which Sema3A signalling was lost via NP1. It was only seen in the *PDGFR $\alpha$ -Cre x flx-NP1-flx* mice in which Sema3A signalling and VEGF signalling via NP1 are lost in oligodendroglia. Therefore, we could hypothesise that the bigger axon diameter observed in those mice is due to the loss of VEGF signalling via NP1 as it was not seen when only Sema3A signalling via NP1 is interrupted.

Despite having bigger myelinated axons, the myelin in the TG mice is slightly thinner than the myelin in WT before lesion ( Figure 5.4). In addition to this, after lesion, the myelin remains the same thickness instead of being thinner as we expect after remyelination. Therefore, the *PDGFR $\alpha$ -Cre x flx-NP1-flx* mice also exhibit a dysregulation in the myelin thickness. The myelin is thinner before lesion and thicker after lesion compared to the WT. Since those mice have bigger myelinated axons and the g ratio is dependent on the axon diameter, it could also be said that the those mice have the same myelin thickness but on bigger axons (bigger g ratio) before surgery. After remyelination, the myelin thickness remains the same. Since this effect was not observed in the NP1(Sema3A-) mouse, it is likely due to the loss of VEGF signalling via NP1 as well.

To sum up, loss of VEGF signalling via NP1 results in bigger axons and myelin thickness dysregulation. As discussed in section 1.5.3, loss of myelin proteins, lactate transporters and enzymes in the oligodendroglia have previously lead to axonal injury or axonal death. Therefore, there is precedent for a loss of oligodendroglial protein resulting in axonal changes the same way that loss of NP1 in oligodendroglia results in bigger axons. In addition to this, Sema3A (via NP1 and Plexin) is known to promote ERK/MAPK activation which in turn is involved in myelin thickness [161]. Therefore, NP1 is known to be able to activate a downstream signalling pathway which has known function in regulation of myelin thickness which could further explain this unexpected result. However, the exact mechanism of the loss of VEGF signalling via NP1 resulting in axonal changes is unknown since the only known VEGF effect on oligodendroglia is in promoting OPC migration [124] (section 1.9.2). It is also unclear whether the cause of these axonal changes is loss of NP1 in OPCs, mature oligodendrocytes or myelinating oligodendrocytes since NP1 will be absent in all of those.

Loss of VEGF signalling via NP1 also results in dysregulation in the myelin thickness which is likely attributable to the loss of NP1 in myelinating oligodendrocytes. However, there is no known role of NP1 or VEGF in determining myelin thickness. Therefore, both the effect on axon diameter and myelin thickness should be further investigated and their mechanisms elucidated. This can be studied by assessing the myelin thickness which NP1 KO oligodendrocytes produce in vitro. It is worth noting that *PDGFR $\alpha$*  is not exclusively expressed on oligodendroglia and NP1 loss on pericytes could be responsible for some of these effects although there is no indication in the literature that NP1 is involved in pericyte behaviour. What is clear is that VEGF or the VEGF binding site of NP1 are involved in more than OPC migration and are regulators of axonal diameter and myelin thickness.

### 5.7.3 Summary

From the in vivo studies on the *PDGFR $\alpha$ -Cre x flx-NP1-flx* and *NP1(Sema3A-)* mice we can conclude that:

- *PDGFR $\alpha$ -Cre x flx-NP1-flx* and *NP1(Sema3A-)* mice do not remyelinate better than WT
- *PDGFR $\alpha$ -Cre x flx-NP1-flx* and *NP1(Sema3A-)* mice do not show enhanced OPC migration into lesions compared to WT
- *NP1(Sema3A-)* mice have different innate immune response compared to WT
- *PDGFR $\alpha$ -Cre x flx-NP1-flx* have bigger axons and dysregulation in the myelin thickness

Therefore, mutation in NP1 or loss of NP1 does not increase OPC migration and remyelination even though downregulating Sema3A does. This is likely due to Sema3A exerting its chemorepellent effect on OPC via another unknown receptor. Not only did the mutant mice not exert the expected increase in OPC recruitment and remyelination but also had 'side' effects. Loss of NP1 in immune cells resulted in dysregulation of the proportion of pro-repair and pro-inflammatory macrophage/ microglia while loss of VEGF signalling via NP1 lead to bigger axons and dysregulation in the myelin thickness.

### 5.7.4 Model

We propose a model in which NP1 normally mediates Sema3A's chemorepulsive effect on OPCs and therefore remyelination. However, if NP1 is lost, the same negative Sema3A effect on OPC recruitment and remyelination could be mediated by another receptor. While the aforementioned another receptor is labelled in the model as 'mystery receptor' as it could be any receptor, the literature suggests that is likely to be NP2 [36] or PlexinA [38]. NP1 is indispensable for macrophage/ microglia recruitment resulting in the different innate immune response in the *NP1(Sema3A-)* mice. Finally, VEGF or another ligand in the VEGF site of NP1 is responsible for determining axon diameter and myelin thickness. Therefore, NP1 is indispensable for some of its roles but could be replaced by other receptors for other roles.

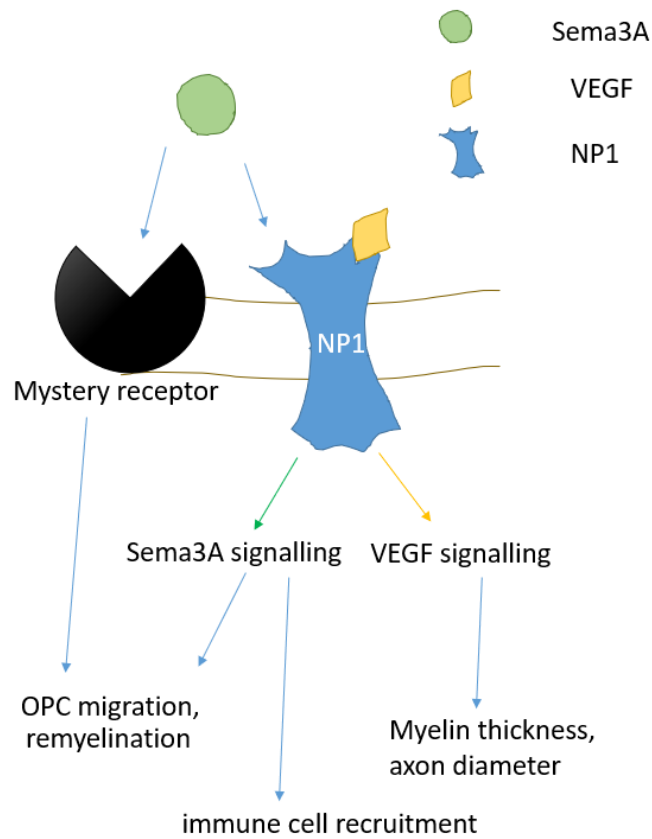


Figure 5.16: Model of roles of NP1 and its ligands

Moreover, these *in vivo* results show that modulating the ligand and the receptor is not necessarily identical. While reducing the level of Sema3A increased OPC migration and remyelination, effectively inhibiting NP1 does not have the same beneficial effect. Therefore, inhibiting NP1 is not a therapeutic option in humans for pro-remyelination therapies.

In order to get further insight to these *in vivo* findings, we then studied the effects Sema3A, VEGF, and NP1 inhibition exert on OPC behaviour in a simpler *in vitro* system.

## 6 In vitro work

### 6.1 Introduction

The in vivo experiments in the two different mutant mice revealed that genetically inhibiting NP1 does not improve OPC migration into lesions. On the other hand numerous experiments have shown that Sema3A is a chemorepellent for OPCs (section 1.9.2). Moreover, downregulation of Sema3A improves OPC migration into lesions and upregulation of Sema3A decreases OPC recruitment (section 1.9.1). To resolve this difference, I decided to use a simple in vitro migration assay and test the effect of NP1 ligands as well as inhibitors. In addition to this, I wanted to know if the NP1 ligands or inhibitors would affect other cell behaviours illustrated in figure 6.1.

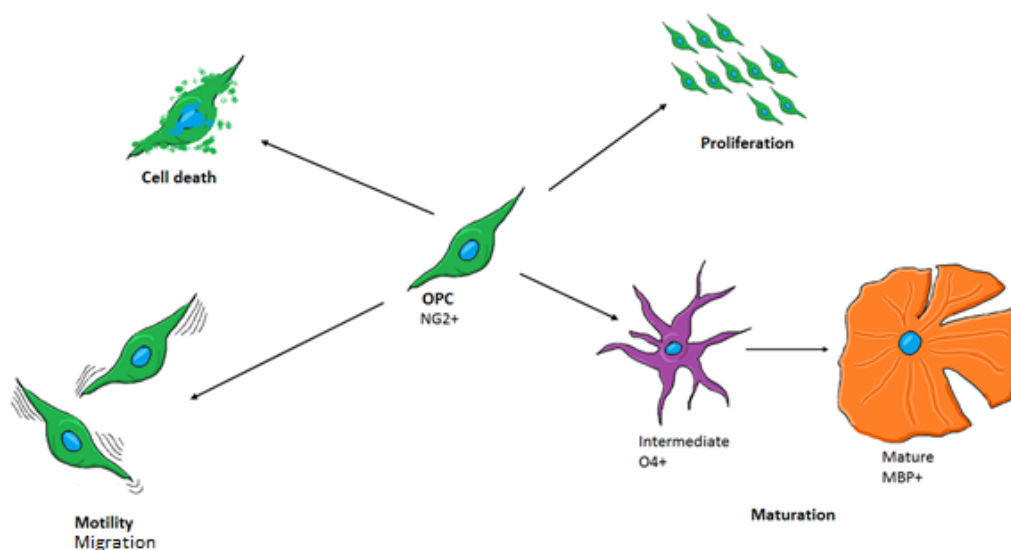


Figure 6.1: Summary of different OPC behaviours tested in the assays. Figure drawn by Gregor Skeldon.

This is particularly important as if inhibition of NP1 does enhance migration but also impairs proliferation or survival, this could explain the lack of increased OPC cell numbers or improved remyelination in the two mutant mice. In order to test the effect of NP1 ligands and inhibitors on OPC behaviour, we isolated OPCs from P0-P2 rats using the shake off method (Figure 6.2). The cells were then plated in 384 well plates in order to test proliferation, survival, maturation

and motility and in transwells in a 24 well plate to test migration.

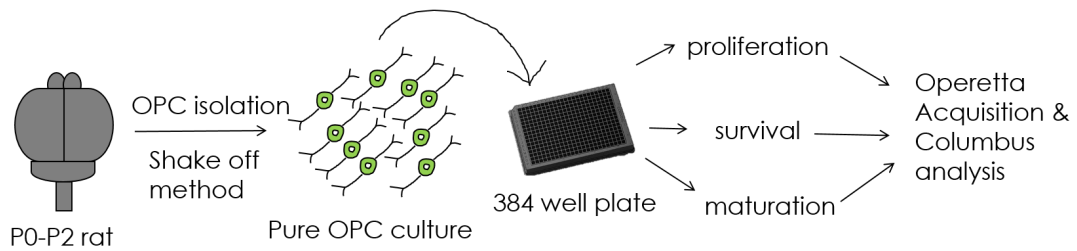


Figure 6.2: In vitro method summary. OPCs were dissected out from P0-P2 rat brain and then grown in 384 well plate to test different cell behaviours. The only assay which was not performed in 384 well plates was the migration assay using a transwell.

I have used different concentrations of VEGF, Sema3A, blocking antibodies against the VEGF and Sema3A binding sites and Xanthofulvin (Figure 6.3). VEGF binds NP1 but this could be prevented by anti-NP1(VEGF) blocking antibody binding to NP1. Similarly, Sema3A binds NP1 and this could be prevented by xanthofulvin which is a Sema3A inhibitor (section 1.11.2) or by anti-NP1(Sema3A) blocking antibody which binds to the Sema3A site on NP1(section 1.11.4). We also tested SICH1 which was believed to interfere with the binding of Sema3A to NP1 (section 1.11.1) but was later found to inhibit Sema3A action by preventing Sema3A's interaction with ECM [57]. Initially representative images are shown and then data is presented with each point being the average of an individual experiment. A representative image for control (no substance) has been repeated for each set of representative images to ease comparison. All data was analysed by Kruskal-Wallis test and a posthoc test if significant difference was found (apart from the first comparison of control and netrin-1 using Mann Whitney test)

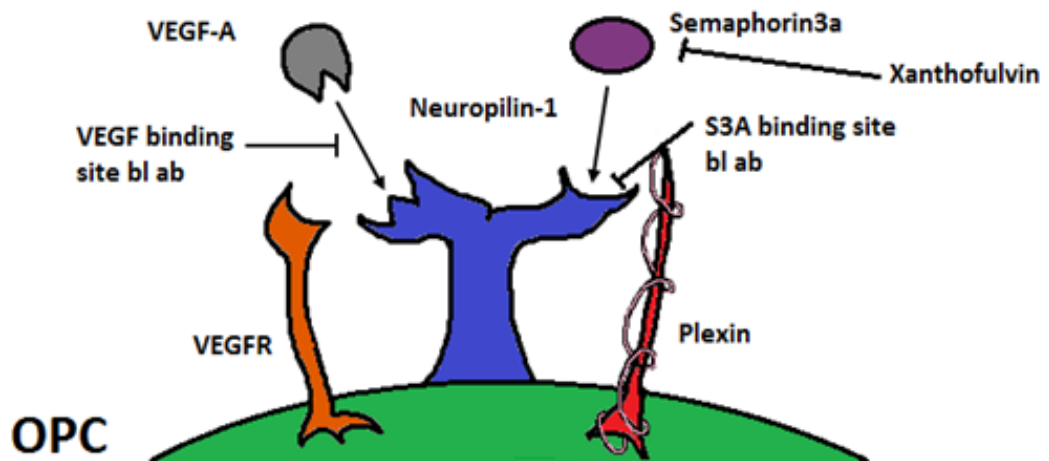


Figure 6.3: Summary of tools used in in vitro studies. Figure drawn by Gregor Skeldon.

## 6.2 Migration assay

Since Sema3A is a chemorepellent for OPCs, we initially investigated migration of OPCs in a transwell. The OPCs are placed on top of a porous membrane and the factor is diluted in media on the bottom of the membrane. If OPCs are attracted to the factor in question, more will pass through the pores while if they are repelled, less will pass through the pores.

### 6.2.1 Transwell assay can be used to detect chemorepulsion

There has been a lot of controversy about the effectiveness of the gold standard transwell migration assay. This is why, initially, we tested the rat OPCs in transwells in the presence of Netrin-1, a well-known chemorepellent at doses known not to be toxic to OPCs from the literature [137]. Comparison of the migration in the media only control (Figure 6.4 A) and 100 ng/ml Netrin-1 (Figure 6.4 B) conditions showed Netrin-1 significantly decreases the number of migrated cells (Mann Whitney test,  $p=0.029$ ) compared to control (Figure 6.4 C). Cells were counted from the 3D reconstruction of the z stack where a cell appears as a sphere and is easily to distinguish from cell debris. However, for simplicity representative images shown are the average projection of the flattened z stack images where a green arrow indicates a cell while a red arrow indicates cell debris which are excluded in image analysis.

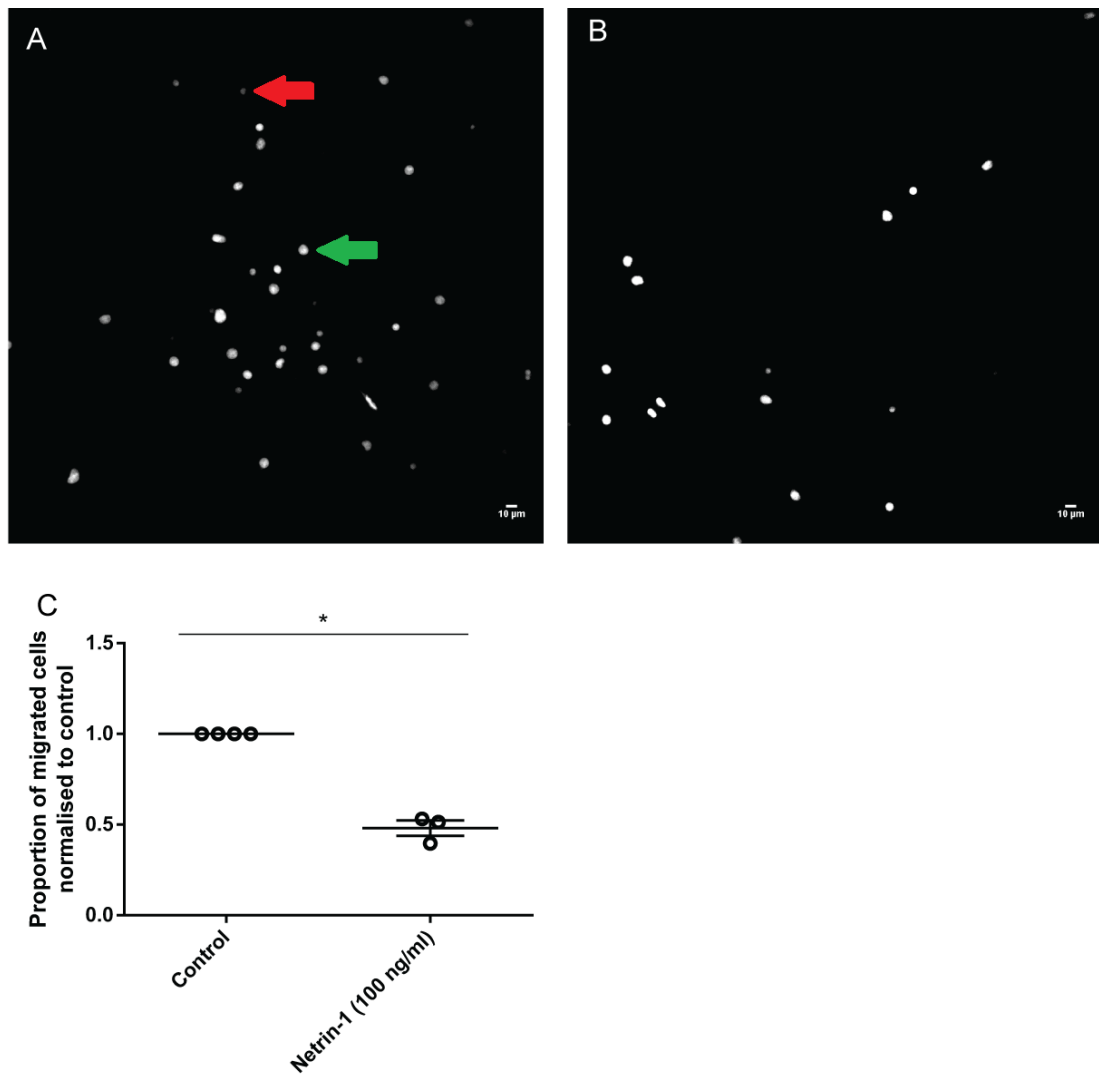


Figure 6.4: Transwell assays can be used to detect chemorepulsion. In control conditions, some cells migrate through the pores (A). The number of migrated cells is decreased by addition of 100 ng/ml Netrin-1 to the bottom of the transwell (B). Comparison of those 2 conditions showed that there is a significant difference in the number of migrated cells (Mann Whitney test,  $p=0.029$ ) (C). White is Hoechst stain. Scale bar is 10  $\mu\text{m}$ .

We have shown that the transwell assay can be used to detect chemorepulsive effects of molecules. Therefore, in our hands the transwell assay can be used to detect the chemorepulsive effects of Sema3A.

### 6.2.2 Sema3A is a chemorepellent but anti-NP1(Sema3A) antibody and xanthofulvin does not rescue OPC migration decisively

After establishing that the transwell assay can successfully be used to detect a chemorepulsive effect in our hands, we tested Semaphorin3A as well as the anti-NP1(S3A) blocking antibody

and both in combination. Semaphorin3A has been previously shown to have chemorepulsive action on OPCs (section 1.9.2). However, we wanted to test what effect the anti-NP1(Sema3A) blocking antibody would have on its own and whether it would be able to prevent Semaphorin3A's chemorepulsive effect. When compared to control (Figure 6.5 A), Semaphorin3A addition to the bottom of the transwell resulted in less cells which have migrated through the pores (Figure 6.5 B). When we tested the anti-NP1(Sema3A) blocking antibody on its own, we expected to see no effect on migration or a slight positive effect as it would block the effect of the endogenous Semaphorin3A which the OPCs produce. However, the anti-NP1(Sema3A) blocking antibody reduced migration alone (Figure 6.5 C) to a similar extent as Semaphorin3A. Moreover, a combination of Semaphorin3A and the anti-NP1(Sema3A) blocking antibody resulted in similar decrease of migration (Figure 6.5 D). Comparison of those 4 conditions showed that there is a significant difference in the number of migrated cells (Kruskal-Wallis test,  $H=8.77$ ,  $n=4,4,3,4$ ,  $p=0.014$ ) and Dunn's multiple comparison test showed that Sema3A significantly decreases the number of cells that have migrated through the pores compared to control (Figure 6.5 E). Since the only significant difference was between Sema3A and control, there was no significant difference between anti-NP1(Sema3A) blocking antibody or the combination of inhibitor and Sema3A to control. Despite not being statistically significant, these treatments seem to reduce the number of cells migrated through the pores by around 50% compared to control in a similar manner to Sema3A alone. Moreover, the combination of Sema3A and anti-NP1(Sema3A) blocking antibody does not reverse the Sema3A-induced chemorepulsion.

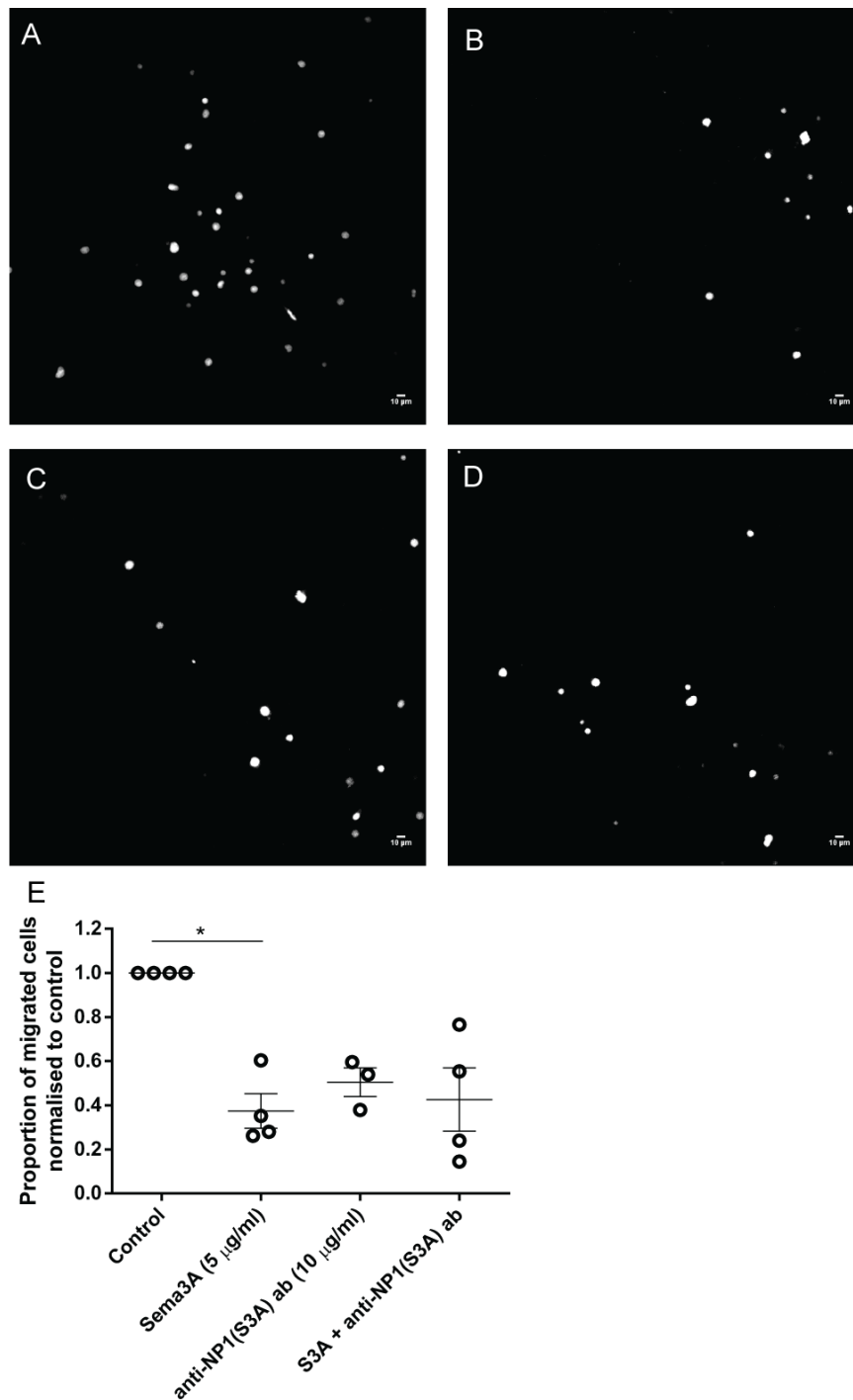


Figure 6.5: Sema3A is chemorepellent for OPCs but addition of anti-NP1(Sema3A) antibody does not rescue OPC migration. Compared to control (A), Sema3A addition to the bottom of the transwell decreased OPC migration (B). Similarly, the anti-NP1(Sema3A) blocking antibody reduced OPC migration on its own (C). Combination of Semaphorin3A and the anti-NP1(Sema3A) blocking antibody also resulted in fewer OPCs migrating through the pores (D). Comparison of these 4 conditions showed that there is a significant difference in the number of migrated cells (Kruskal-Wallis test,  $H=8.77$ ,  $n=4,4,3,4$ ,  $p=0.014$ ) and Dunn's multiple comparison test showed that Sema3A significantly decreases the number of cells that have migrated through the pores compared to control (E). White is Hoechst stain.

Since this result was unexpected, we conducted a similar experiment with Xanthofulvin because it is another NP1-Sema3A antagonist which works in a different way. Control (Figure 6.6 A) and Semaphorin3A example images (Figure 6.6 B) are shown again to ease comparison. Addition of Xanthofulvin also results in fewer migrated cells (Figure 6.6 C) and when Xanthofulvin is added together with Sema3A, OPC migration is less (Figure 6.6 D) than in control (Figure 6.6 A). Comparison of these 4 conditions showed that there is a significant difference in the number of migrated cells (Kruskal-Wallis test,  $H=10.47$ ,  $n=4,4,3,4$ ,  $p=0.003$ ) and Dunn's multiple comparison test showed that Sema3A significantly decreases the number of cells that have migrated through the pores compared to control (Figure 6.6 E). Since the only significant difference was between Sema3A and control, there was no significant difference between xanthofulvin or the combination of inhibitor and Sema3A to control. Despite not being statistically significant, these treatments seem to reduce the number of cells migrated through the pores compared to control in a similar manner to Sema3A alone with the combination not reversing the Sema3A-induced chemorepulsion. However, this experiment was really variable, making it difficult to interpret. If additional experiments were added to the analysis, it is possible that treatment with xanthofulvin and combination of xanthofulvin and Sema3A would be more similar to control which would indicate that xanthofulvin does not impair migration alone and it can reverse the Sema3A-induced reduction in migration. However, from the 3 conducted experiments, it appears that xanthofulvin reduces the migration of cells by around 40% compared to control and is unable to decisively reverse the Sema3A-induced chemorepulsion.

Sema3A significantly decreases the number of OPCs migrated through the pores. However, combination of Sema3A and an inhibitor does not statistically affect migration compared to Sema3A alone indicating that both tested inhibitors of the NP1-Sema3A interaction do not rescue Semaphorin3A's chemorepulsive action. The anti-NP1(Sema3A) blocking antibody and Xanthofulvin do not significantly affect migration compared to control but appear to have chemorepulsive properties when added alone.

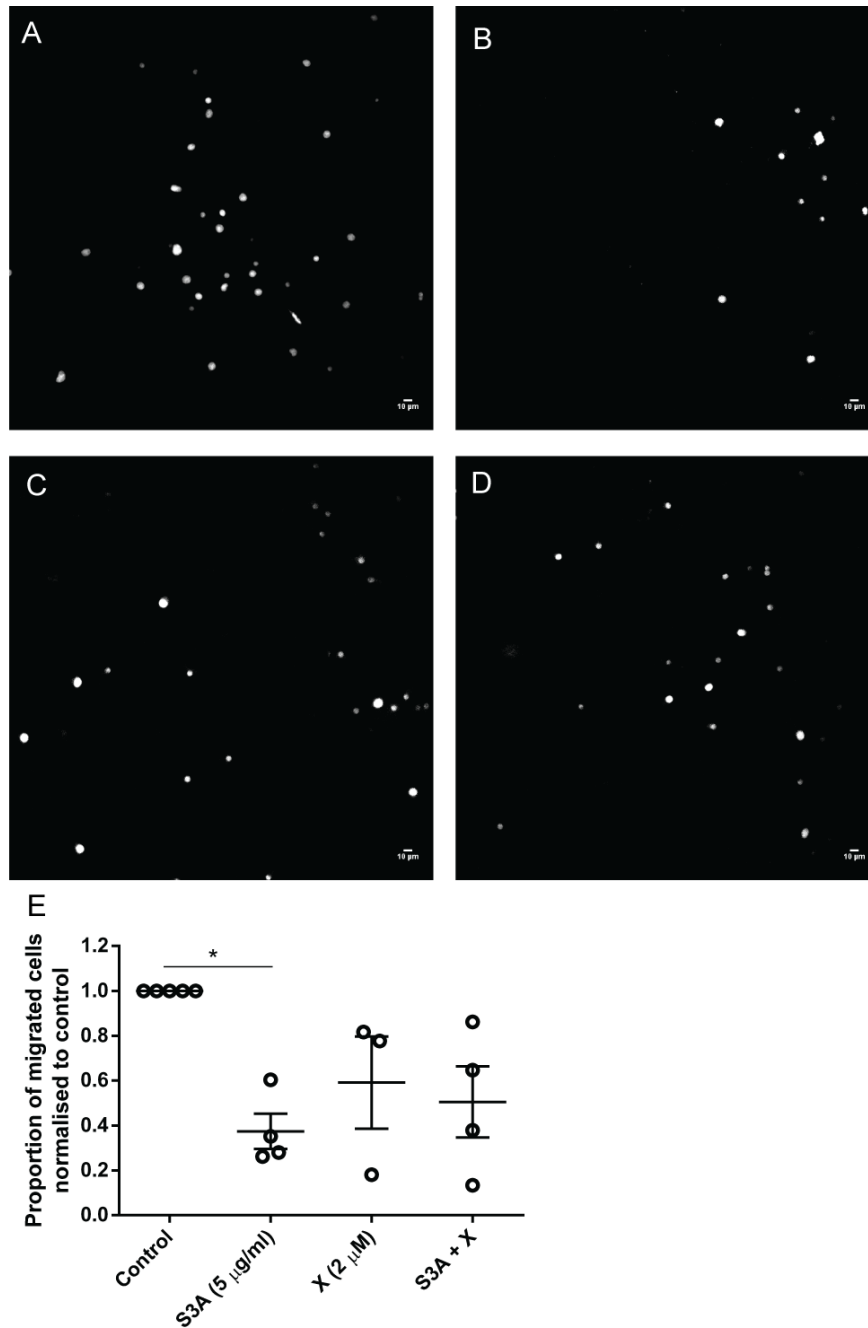


Figure 6.6: Xanthofulvin does not rescue migration. Compared to control (A), Sema3A addition to the bottom of the transwell resulted in decreased migration (B). Similarly, Xanthofulvin reduced migration (C). Combination of Semaphorin3A and Xanthofulvin also resulted in fewer cells migrated through the pores (D). Comparison of these 4 conditions showed that there is a significant difference in the number of migrated cells (Kruskal-Wallis test,  $H=10.47$ ,  $n=4,4,3,4$ ,  $p=0.003$ ) and Dunn's multiple comparison test showed that Sema3A significantly decreases the number of cells that have migrated through the pores compared to control (E). White is Hoechst stain.

### 6.2.3 VEGF increases OPC migration and anti-NP1(VEGF) blocking antibody reverses this

We then wanted to look at the other ligand of NP1,  $VEGF_{165}$ . This was particularly important because the  $PDGFR\alpha$ -Cre x flx-NP1-flx mice have lost the  $VEGF_{165}$  signalling via NP1 in oligodendrocytes. It has been previously reported that VEGF-A promotes OPC migration and VEGF-A is the precursor of  $VEGF_{165}$  which binds to NP1 [124]. Therefore, we wanted to investigate if  $VEGF_{165}$  (which will be referred to as VEGF from now on) influences OPC migration in a similar way to VEGF-A. Moreover, we wanted to investigate the effect of losing the VEGF receptor site on NP1 in OPCs would affect migration (by addition of anti-NP1(VEGF) blocking antibody). In comparison to control (Figure 6.7 A), addition of VEGF resulted in increased number of migrated cells (Figure 6.7 B). The anti-NP1(VEGF) blocking antibody appeared to reduce migration on its own (Figure 6.7 C) and the combination of VEGF and anti-NP1(VEGF) blocking antibody resulted in a even more pronounced reduction (Figure 6.7 D). Comparison of these 4 conditions showed that there is a significant difference in the number of migrated cells (Kruskal-Wallis test,  $H=11.71$ ,  $n=4,4,3,4$ ,  $p=0.0005$ ) and Dunn's multiple comparison test showed that the combination of VEGF and anti-NP1(VEGF) blocking antibody significantly decreases the number of cells that have migrated through the pores compared to VEGF (Figure 6.7 E).

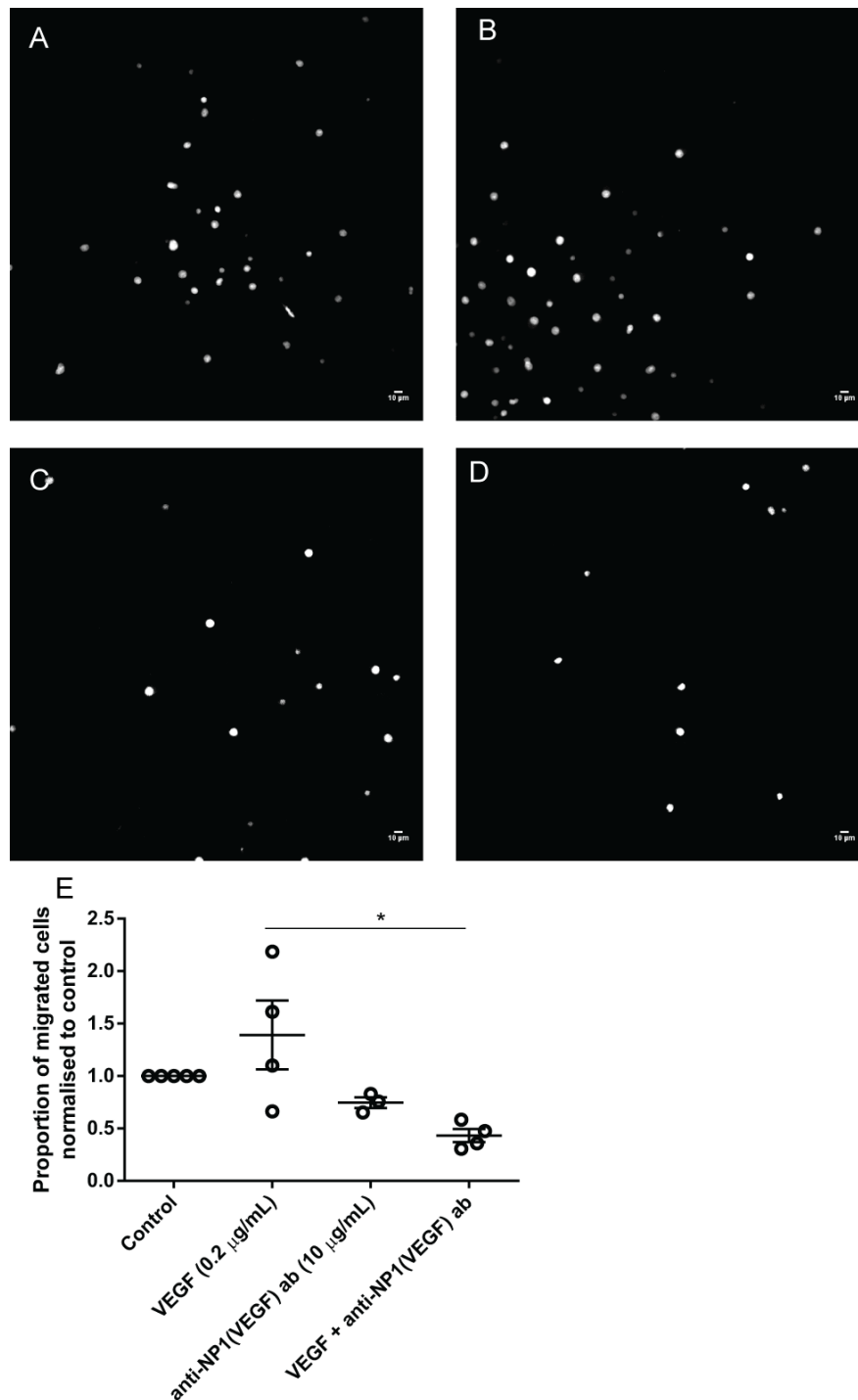


Figure 6.7: VEGF increases migration and anti-NP1(Sema3A) antibody reverses it. Compared to control (A), VEGF increases migration (B). The anti-NP1(VEGF) blocking antibody reduces migration (C). VEGF in combination with the anti-NP1(VEGF) blocking antibody also resulted in reduced migration (D). Comparison of those 4 conditions showed that there is a significant difference in the number of migrated cells (Kruskal-Wallis test,  $H=11.71$ ,  $n=4,4,3,4$ ,  $p=0.0005$ ) and Dunn's multiple comparison test showed that the combination of VEGF and anti-NP1(VEGF) blocking antibody significantly decreases the number of cells that have migrated through the pores compared to VEGF (E). White is Hoechst stain.

Therefore, VEGF stimulates OPC migration which can be blocked by addition of anti-NP1(VEGF) antibody. Since the comparison of VEGF and the anti-NP1(VEGF) blocking antibody is the only significant difference in this assay, the difference between the anti-NP1(VEGF) blocking antibody and control is not significant. However, the antibody results in around 20% decrease in migration on its own. Therefore, the anti-NP1(VEGF) antibody reverses the VEGF-induced increase in migration but it also appears to affect it on its own.

#### 6.2.4 Migration assay discussion

So far, we have shown that *Sema3A* is a chemorepellent and VEGF is a chemoattractant. In addition to this, all the tested *Sema3A* and VEGF inhibitors appeared to reduce migration but these effects were not significant. Despite the fact that these effects were not significant, it will be discussed because if true, they could contribute to the inability of the inhibitors to reverse the effects of the NP1 ligands. Therefore, it is essential to consider when aiming to improve OPC migration.

Xanthofulvin and the anti-NP1(*Sema3A*) blocking antibody are expected to increase migration when added to *Sema3A*, as they would block the *Sema3A*-mediated chemorepulsion by inhibiting *Sema3A* and the *Sema3A* binding site on NP1 respectively. Regardless of this, the NP1 inhibitor and the *Sema3A* inhibitor could decrease migration by themselves. A possible explanation for this unexpected decrease in migration by adding NP1 blocking antibodies or *Sema3A* inhibitors is that they reduce the ability of OPCs to squeeze through a pore.

This could be because their physical interaction with the cell surface makes the cell bigger and less easy to deform. Alternatively, it could be a functional effect of the inhibitors. In section 1.9.3, it was mentioned that *Sema3A* enhances dendritic cell passing through gaps for entry or exit to the lymphatics system via binding to NP1 and Plexin-A1 [229]. Since passing into the lymphatics system would require the same deformation as passing through a pore in the transwell, we would expect that *Sema3A* and therefore NP1 is important for this process. This would explain why blocking endogenous *Sema3A* and inhibiting the *Sema3A* site of NP1 would result in decreased migration. Their inhibition would result in decreased ability of the OPCs to squeeze through the pores. To support this, another semaphorin, *Sema3C*, increased the migration of dendritic cells in a transwell because of increased cell deformability [62]. Therefore, it is possible that *Sema3A* and NP1 are involved in cell deformability and their complete inhibition by Xanthofulvin or anti-NP1(*Sema3A*) blocking antibody would impair OPC migration.

The anti-NP1(VEGF) blocking antibody could also reduce migration alone. This might be explained by binding of the anti-NP1(VEGF) blocking antibody to NP1 inducing conformational change which impairs *Sema3A* signalling via NP1. This could decrease OPC deformability because of the possible NP1 and *Sema3A* importance for cell deformability discussed above and thus impair migration. However, the anti-NP1(VEGF) blocking antibody has previously been shown not to impair *Sema3A* induced growth cone collapse [176].

In the combination of VEGF and the anti-NP1(VEGF) blocking antibody, if the blocking antibody was indeed antagonising the VEGF-induced migration effect, we would expect mi-

gration to be restored to approximately control levels. However, this was not the case and the response was much more similar to the response of the blocking antibody alone. This could be explained by the mismatch of concentrations of the ligand and the blocking antibody which we have chosen due to their previously published effectiveness *in vitro* [176] [284]. In essence, at these concentrations the blocking antibody is much more likely to occupy NP1 than VEGF which is shown by the calculated receptor occupancy detailed below. Receptor occupancy is determined by equation 6.1 where [A] is the concentration of the agonist and  $K_A$  is the dissociation constant (affinity) of the agonist and [B] is the concentration of the antagonist and  $K_B$  is the dissociation constant (affinity) of the antagonist.

$$P_{AR} = \frac{[A]}{K_A * (1 + \frac{[B]}{K_B}) + [A]} \quad (6.1)$$

Since we have used 0.2  $\mu\text{g/ml}$  VEGF and its mass is 38.2 kDa (Peprotech,100-20), we can calculate its concentration in molar (M) as detailed below in equation 6.2:

$$VEGF \text{ conc} = \frac{\frac{0.2 * 10^{-6}}{10^{-3}} \text{g/l}}{38.2 * 10^3 \text{g/mol}} = \frac{1 * 10^{-4} \text{g/l}}{38.2 * 10^3 \text{g/mol}} = 5.2 * 10^{-9} \text{mol/l} = 5.2 \text{nM} \quad (6.2)$$

Therefore [A]=5.2 nM. Similarly, we have used 10  $\mu\text{g/ml}$  of the anti-NP1(VEGF) blocking antibody and the mass of an antibody is roughly 150kDa. Therefore its concentration in molar (M) is calculated in equation 6.3

$$\begin{aligned} \text{anti - NP1(VEGF) conc} &= \frac{\frac{10 * 10^{-6}}{10^{-3}} \text{g/l}}{150 * 10^3 \text{g/mol}} = \frac{1 * 10^{-2} \text{g/l}}{150 * 10^3 \text{g/mol}} \\ \text{anti - NP1(VEGF) conc} &= 4.44 * 10^{-7} \text{mol/l} = 444 \text{nM} \end{aligned} \quad (6.3)$$

Therefore, [B]= 444 nM. Since the dissociation constant of the VEGF for NP1 is 0.32 nM [284] ( $K_A = 0.32 \text{nM}$ ) and the dissociation constant of the anti-NP1(VEGF) blocking antibody for NP1 is 1.3 nM [176] ( $K_B = 1.3 \text{nM}$ ), we can use equation 6.1 to calculate the receptor occupancy of NP1 with VEGF at those concentrations.

$$\begin{aligned} P_{AR} &= \frac{[A]}{K_A * (1 + \frac{[B]}{K_B}) + [A]} = \frac{5.2 \text{nM}}{0.32 \text{nM} * (1 + \frac{444 \text{nM}}{1.3 \text{nM}}) + 5.2 \text{nM}} \\ P_{AR} &= \frac{5.2 \text{nM}}{0.32 \text{nM} * 342.5 \text{nM} + 5.2 \text{nM}} = \frac{5.2 \text{nM}}{114.8 \text{nM}} = 0.045 = 4.5\% \end{aligned} \quad (6.4)$$

Therefore at the concentration we have chosen only 4.5% of the receptors will be occupied by VEGF. Even though this calculation only takes into account the affinity of the ligand and antagonist and not the efficacy of the ligand, it gives good indication that at those concentrations the the anti-NP1(VEGF) blocking antibody is surmounting VEGF binding to NP1. A dose response curve with the same concentration of VEGF but increasing concentration of anti-NP1(VEGF) blocking antibody peaking at a maximum of 10  $\mu\text{g/ml}$  should be able to answer whether this inhibitor can gradually reduce VEGF induced migration. This explains why the effect of the combination of VEGF and its blocking antibody is much more similar to blocking

antibody alone than to VEGF.

It is interesting to note that all tested inhibitors possibly resulted in reduction of OPC migration. The same was true for antibodies against PDGFR $\alpha$  (data not shown) which indicates that there is a possibility that migration could be reduced by physical interaction of inhibitors with the cell surface making the cell bigger and less easy to deform. This effect was not due to cell death since neither of the tested conditions significantly decreased OPC survival (Section 6.5).

### 6.3 Motility

We wanted to test whether the same inhibitors which reduce migration do so because they reduce motility. In addition to this, since Sema3A is a chemorepellent, we asked whether it affects the motility of the cells as well. For the motility assay, we plated the cells in 384 well plate and imaged every 10 min for 19 hours. From the live images, we extracted both mean accumulated distance and mean velocity per well to determine if the cells moved in a different manner. An example of a cell moving in the motility assay and the automatic detection of its movement are shown in figure 6.8.

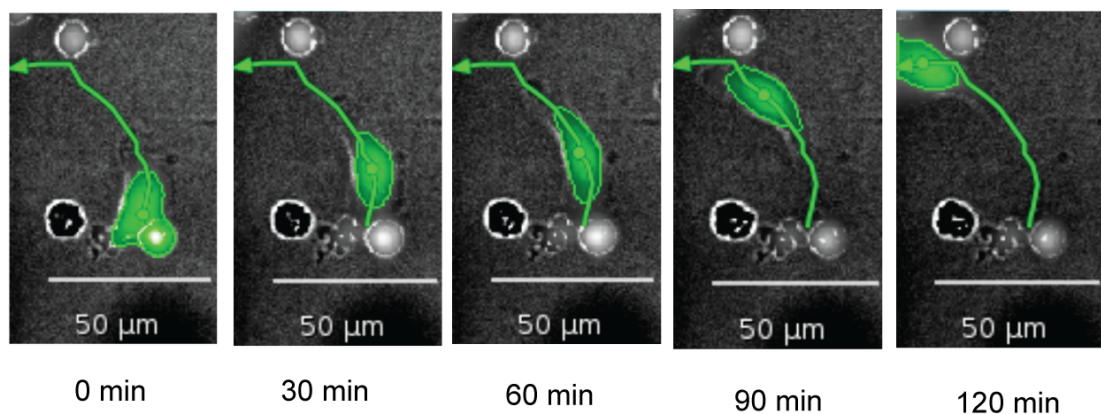


Figure 6.8: A representative example of a cell in the motility assay. The same cell is shown every 30 min and highlighted in green and the track it takes for the whole 120 min is shown as a green arrow. Scalebar is 50  $\mu\text{m}$

We tested 22.5 nM, 45 nM and 90 nM coated Sema3A, 45 nM Sema3A in solution, 10 ng/ml anti-NP1(Sema3A) blocking antibody, 2  $\mu\text{M}$  Xanthofulvin, VEGF and 10 ng/ml anti-NP1(VEGF) blocking antibody. None of the treatments significantly affect the accumulated distance or the velocity and this data is presented in section 6.7.1 of the appendix.

#### 6.3.1 Motility discussion

Therefore, neither the chemorepellent Sema3A, nor the chemoattractant VEGF affect motility on a flat surface. This excludes one of the possible explanations for observing a different number of cells on the bottom of a transwell - that cells have different motility. If cells move more, they

would be more likely to travel to the other side of the pore. Conversely, if they are less mobile, they are less likely to find a pore and go through it. Therefore, a chemorepellent effect could be explained by decreased motility and chemoattractant effect by increased motility. Since neither VEGF or *Sema3A* affect motility, this ensures that our transwell assay observations are because of real chemoattraction or chemorepulsion and not because of motility differences.

In addition to this, none of the inhibitors affected motility even though they appeared to decrease migration. While this shows that addition of antibodies or big molecules does not impede motility on a flat surface, it cannot exclude the possibility that they decrease the physical ability of a cell to squeeze through a pore. The migration and motility assay used together are very powerful to uncouple motility and migration.

### 6.3.2 Motility and migration discussion

To sum up, the migration assay showed that *Sema3A* and VEGF are a chemorepellent and a chemoattractant respectively as the literature would suggest [287] [55] [124]. However, none of the tested inhibitors could significantly oppose the action of their ligand and instead appeared to reduce migration (non significant effect). While this was not because they reduced motility on a flat surface, it could be because they physically or functionally impair the cell's ability to squeeze through a pore. This may suggest that none of the tested inhibitors would be a suitable therapeutic strategy. Alternatively it may suggest that the transwell system is not the best system for examining chemotaxis.

Our *in vivo* studies already suggested that functional inhibition of NP1 via knockdown or mutation does not improve OPC migration and proposed alternative receptors could be mediating the *Sema3A* effect. The migration and motility assays described here add another possible explanation for the lack of positive effect on migration in the mutant mice - inhibition of NP1 could impair the ability of OPCs to pass through pores. This is further supported by the published observation that *Sema3A* is important for a dendritic cell's passing through gaps via binding to NP1 and Plexin-A1 [229] and that another semaphorin, *Sema3C* increases the migration of dendritic cells in a transwell because of increased cell deformability [62].

Thus, it is possible that a low concentration of *Sema3A* and thus NP1 activation is important for OPC deformation and a higher concentration of *Sema3A* is chemorepulsive for OPCs. In this case, complete loss of the *Sema3A* binding to NP1 (in NP1(*Sema3A*-) mouse) or NP1 KO (in PDGFR $\alpha$ -Cre x flx-NP1-flx mice) would impair cell deformation and thus the ability of cells to squeeze through the tissue. Therefore, even though the OPCs would not be repelled by *Sema3A*, their ability to migrate through the tissue would be impaired resulting in identical migration to WT. On the other hand, *Sema3A* KD which was shown to effectively increase OPC migration and remyelination [29] only resulted in around 60% knockdown of *Sema3A*. This incomplete knockdown as opposed to losing all *Sema3A* binding sites on NP1 could provide a low concentration *Sema3A* which is enough to maintain a cell, deformation ability but not to cause chemorepulsion.

In addition to suggesting that low level activity of NP1 via *Sema3A* binding might be im-

portant for cell deformation ability, our migration and motility assay indicate that none of the tested modes of inhibition would be beneficial in increasing OPC migration. While this might not be a surprise for the anti-NP1(Sema3A) blocking antibody after the *in vivo* effects of the NP1(Sema3A<sup>-</sup>) mice which the antibody effectively mimicks, it is unexpected for Xanthofulvin.

Xanthofulvin is an inhibitor of Sema3A and therefore it closely mimicks the Sema3a KD mouse *in vivo* experiments [29]. However, instead of having positive effect on OPC migration as expected based on the improved OPC migration in the Sema3A KD mouse [29], it impairs OPC migration *in vitro*. This could be attributed to the complete inhibition of Sema3A-NP1 signalling by Xanthofulvin and the incomplete inhibition of the Sema3A-NP1 signalling in the Sema3A KD mouse [29]. As discussed above, a low level of NP1 activation by Sema3A might be important for cell deformation ability which in itself is important for cell migration in a transwell or *in vivo*. It is also possible that the the transwell assay is poor and therefore unable to detect these effects.

After we determined that both NP1 ligands influence migration in opposite directions and that all tested inhibitors impair migration, we looked at their effect on proliferation.

## 6.4 Proliferation assay

We then aimed to investigate whether any of the ligands or inhibitors of NP1 influence proliferation. Even though Sema3A has been reported to not affect OPC proliferation *in vitro* and *in vivo* [29] [296], we decided to test this in our assay as a comparison for the NP1-Sema3A inhibitors' effect. We aimed to investigate if inhibition of the Sema3A or VEGF site of NP1 affects proliferation.

### 6.4.1 Sema3A

Initially we looked at different concentrations of Sema3A in solution. We found that in comparison to control (Figure 6.9 A), 90 nM Sema3A in solution increased the proportion of proliferating cells (Figure 6.9 D). On the other hand, 22.5 nM and 45 nM Sema3A in solution (Figure 6.9 B and C) did not have a significant effect on the number of proliferating cells. Comparison of the 3 concentrations of Sema3A and control showed that there is a significant difference in the number of proliferating cells (Kruskal-Wallis test,  $H=9.21$ ,  $n=9,3,9,3$ ,  $p=0.026$ ) and Dunn's multiple comparison test showed that 90 nM Sema3A in solution significantly increases the number of proliferating cells compared to control (Figure 6.9 E).

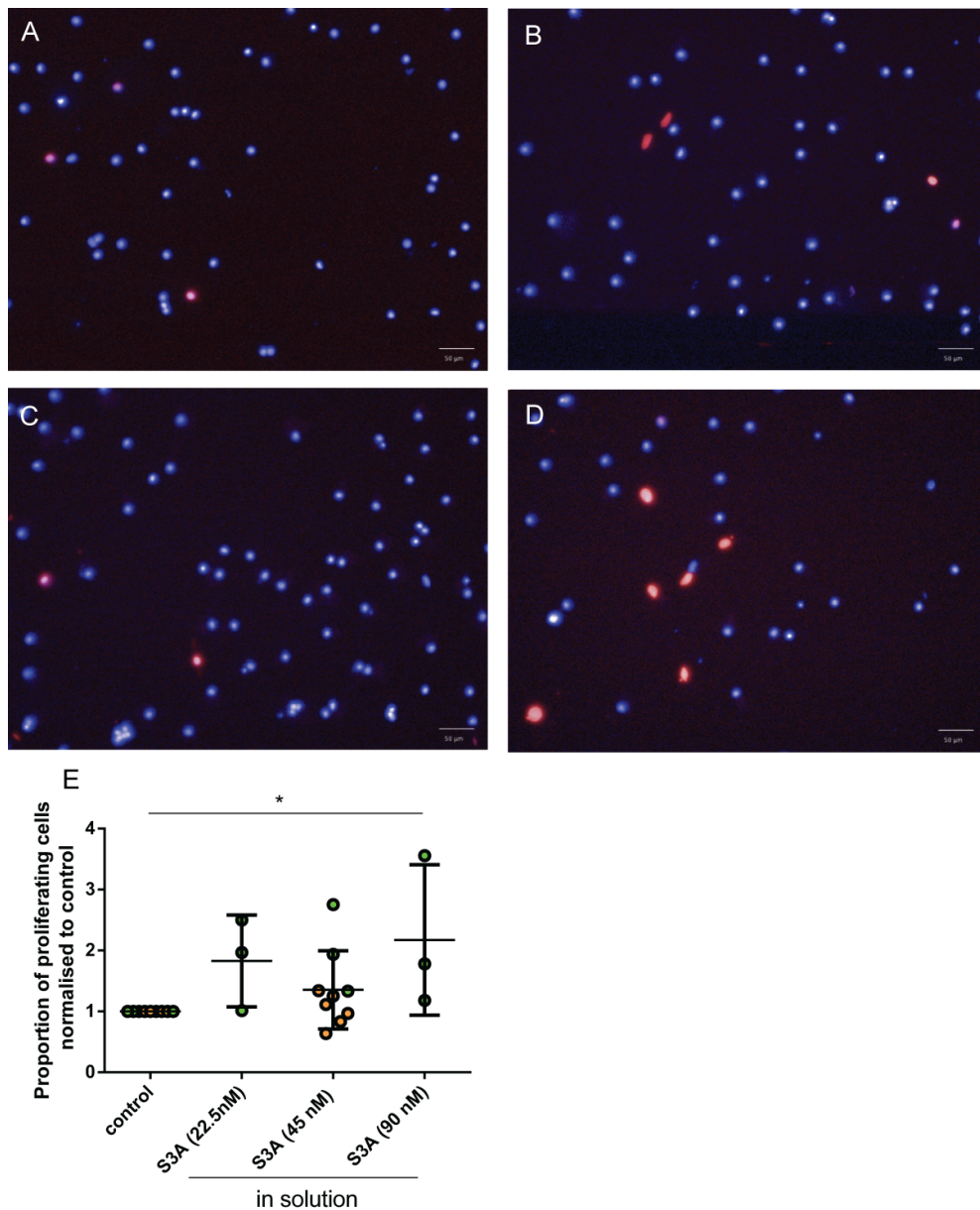


Figure 6.9: High concentration of Sema3A increases proliferation of rat OPCs in vitro. In comparison to control (A), 22.5 nM Sema3A in solution (B) and 45 nM Sema3A in solution (C) do not significantly affect OPC migration. However, at the highest tested concentration, 90 nM Sema3A in solution, there was a significant increase in the number of proliferating cells (D). Comparison of the 3 concentrations of Sema3A and control showed that there is a significant difference in the number of proliferating cells (Kruskal-Wallis test,  $H=9.21$ ,  $n=9,3,9,3$ ,  $p=0.026$ ) and Dunn's multiple comparison test showed that 90 nM Sema3A in solution significantly increases the number of proliferating cells compared to control (E). Each dot is an experiment. Green and orange dots are experiments performed by two different researchers. Blue is Hoechst and red is EDU+ cells.

We also tested the same concentrations of Sema3A coated onto the coverslip, rather than in solution and found that none of them influences proliferation. Data is shown in section 6.7.2 of the appendix.

#### 6.4.2 Sema3A-NP1 inhibitors

We then tested proliferation in the presence of different concentrations of the 3 available NP1-Sema3A inhibitors. We found that in comparison to control (Figure 6.10 A), 5  $\mu\text{g/ml}$  (Figure 6.10 B) and 20  $\mu\text{g/ml}$  anti-NP1(Sema3A) blocking antibody (Figure 6.10 D) increase the number of proliferating cells. Contrary to that, the 10  $\mu\text{g/ml}$  anti-NP1(Sema3A) blocking antibody (Figure 6.10 C) did not increase proliferation. Comparison of the 3 concentrations of anti-NP1(Sema3A) blocking antibody and control showed that there is a significant difference in the number of proliferating cells (Kruskal-Wallis test,  $H=12.55$ ,  $n=9,3,9,3$ ,  $p=0.006$ ) and Dunn's multiple comparison test showed that both 5  $\mu\text{g/ml}$  and 20  $\mu\text{g/ml}$  anti-NP1(Sema3A) blocking antibody significantly increases the number of proliferating cells compared to control (Figure 6.10 E)

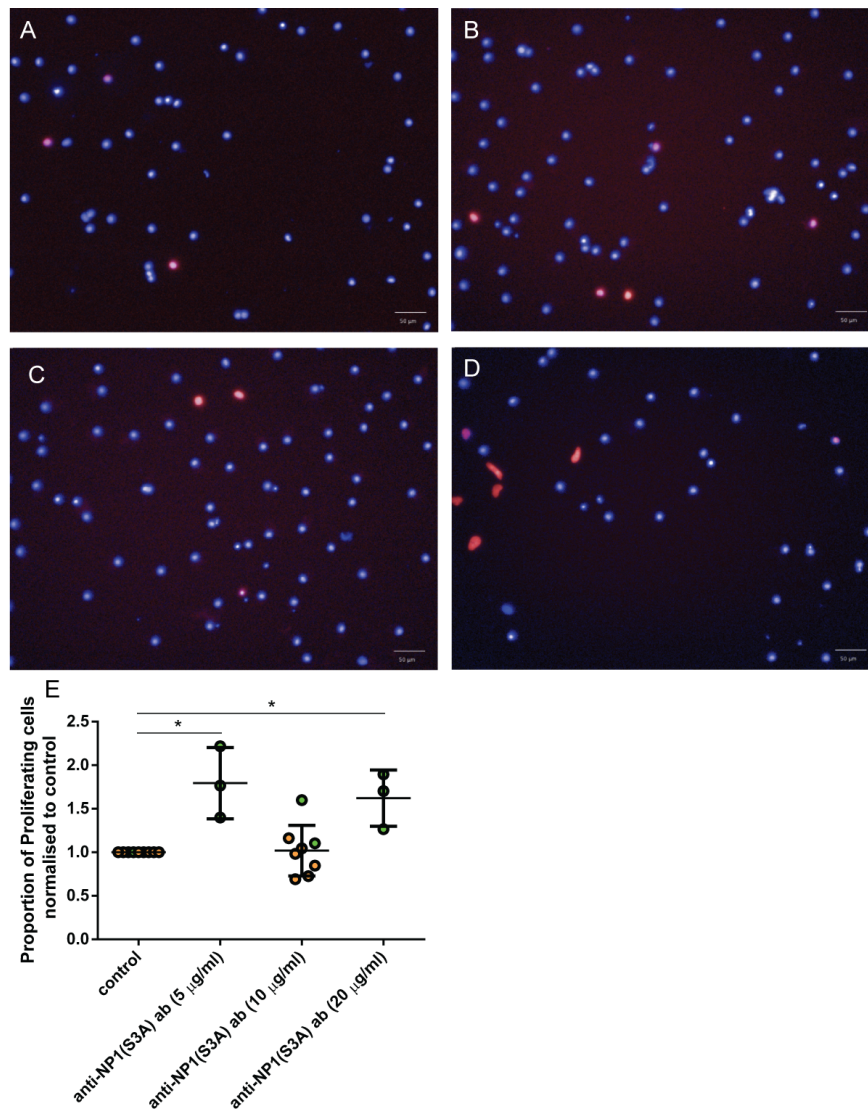


Figure 6.10: anti-NP1(Sema3A) blocking antibody increases proliferation at some concentrations. Compared to control (A), 5  $\mu\text{g/ml}$  anti-NP1(Sema3A) blocking antibody increases the proportion of proliferating cells (B). Similarly, the highest tested concentration of anti-NP1(Sema3A) blocking antibody (20  $\mu\text{g/ml}$ ) increases proliferation (D). However, the middle concentration, 10  $\mu\text{g/ml}$ , does not have this effect (C). Comparison of the 3 concentrations of anti-NP1(Sema3A) blocking antibody and control showed that there is a significant difference in the number of proliferating cells (Kruskal-Wallis test,  $H=12.55$ ,  $n=9,3,9,3$ ,  $p=0.006$ ) and Dunn's multiple comparison test showed that both 5  $\mu\text{g/ml}$  and 20  $\mu\text{g/ml}$  anti-NP1(Sema3A) blocking antibody significantly increases the number of proliferating cells compared to control (E). Each dot is an experiment. Green and orange dots are experiments performed by two different researchers. Blue is Hoechst and red is EDU+ cells.

Therefore, both Sema3A and the anti-NP1(Sema3A) blocking antibody increase proliferation even though they are supposed to have opposite actions as a ligand and a receptor inhibitor.

We then tested other NP1-Sema3A inhibitors to check if this effect was true for all of them. We found that neither Xanthofulvin nor SICHI influence proliferation indicating that the proliferation enhancement effect of the anti-NP1(Sema3A) blocking antibody was specific to it and not observed with other NP1-Sema3A inhibitors. This data is shown in section 6.7.2 and section 6.7.2 of the appendix.

Finally, we tested whether VEGF and the anti-NP1(VEGF) antibody influence proliferation and we found that neither of these changes the proportion of proliferating cells (section 6.7.2 of the appendix).

### 6.4.3 Proliferation assay discussion

Previous studies have concluded that Sema3A does not influence proliferation as addition of Sema3A protein into a lesion or Sema3A KD genotype does not result in significantly increased proliferation after two weeks [29] or because cell counts are not decreased after addition of Sema3A in vitro [296]. Here we show that addition of 90 nM Sema3A in solution and 5  $\mu\text{g}/\text{ml}$  or 20  $\mu\text{g}/\text{ml}$  of the anti-NP1(Sema3A) blocking antibody result in increased proliferation. All concentrations which have shown significant difference compared to control are two times lower or two times higher than previously used in publications [296]. This is clearly a concentration dependent effect as no consistent effect with increased concentration is observed. Therefore, it is possible that the difference in concentration used in our study and previous studies is the reason for the different results.

It is also worth noting that the middle concentration of each of the tested conditions has experiments conducted by two independent researchers and it is not significantly different to control. Since for the high and the low concentrations only 3 experiments were conducted, additional experiments could be performed to further ensure that the observed data is real and not due to chance.

What is most interesting about this observation in proliferation is that both high concentration of Sema3A in solution and an inhibitor for the Sema3A site of NP1 improve proliferation. Sema3A and inhibitors of NP1 are expected to have opposing effects. A possible explanation for this could be that both Sema3A and the blocking antibody result in activation of NP1. While this is a possibility, previous studies with the anti-NP1(Sema3A) blocking antibody have shown that it is a potent blocker of Sema3A-induced growth cone collapse in axons [176] indicating that this is probably not the case.

An alternative explanation is that high concentration of Sema3A and the anti-NP1(Sema3A) blocking antibody cause internalisation of NP1. NP1 is known to be internalised after binding a ligand [220] as mentioned in section 1.8.2. It would be expected that the same internalisation would follow an antibody binding to NP1. Therefore, the effect of increased proliferation could be due to decrease of NP1 on the surface of OPCs and therefore loss of signalling via any of its other ligands. This is consistent with the lack of proliferation by the other inhibitors which do not bind NP1 - Xanthofulvin and SICHI. If the internalisation hypothesis is correct, we would expect that VEGF and the anti-NP1(VEGF antibody) at low and high concentrations would also

increase proliferation. Unfortunately, we have only tested the standard middle concentration of both.

Therefore, both high concentration of Sema3A as well as low and high concentrations of anti-NP1(Sema3A) blocking antibody promote proliferation. The mechanism of this is unknown but could be due to NP1 internalisation and loss of signalling of other ligands of NP1. After we determined this effect on proliferation, we aimed to see if inhibition of NP1 would influence survival.

## 6.5 Survival assay

As with proliferation, studies have shown that Sema3A does not influence survival by measuring apoptosis after Sema3A protein injection or in the Sema3A KD genotype 2 weeks after lesion induction [29] or by measuring apoptosis after culturing with Sema3A coated on the culture surface *in vitro* [296].

### 6.5.1 Sema3A

When we cultured cells on different concentrations of coated Sema3A, we found that indeed it does not affect survival (section 6.7.3 in appendix). However, the same was not true for Sema3A in solution. Compared to control (Figure 6.11 A), 22.5 nM Sema3A in solution (Figure 6.11 B) improved survival. However, 45 nM Sema3A and 90 nM Sema3A in solution did not have a significant effect on the number of dying cells (Figure 6.11 C, D). Comparison of the number of dying cells between control and the 3 different concentrations of Sema3A in solution and control showed that there was a significant difference between the conditions (Kruskal-Wallis test,  $H=10.39$ ,  $n=3,7,3$ ,  $p=0.015$ ) and Dunn's multiple comparison test revealed the difference between 22.5 nM Sema3A in solution and control was significant (Figure 6.11 E).

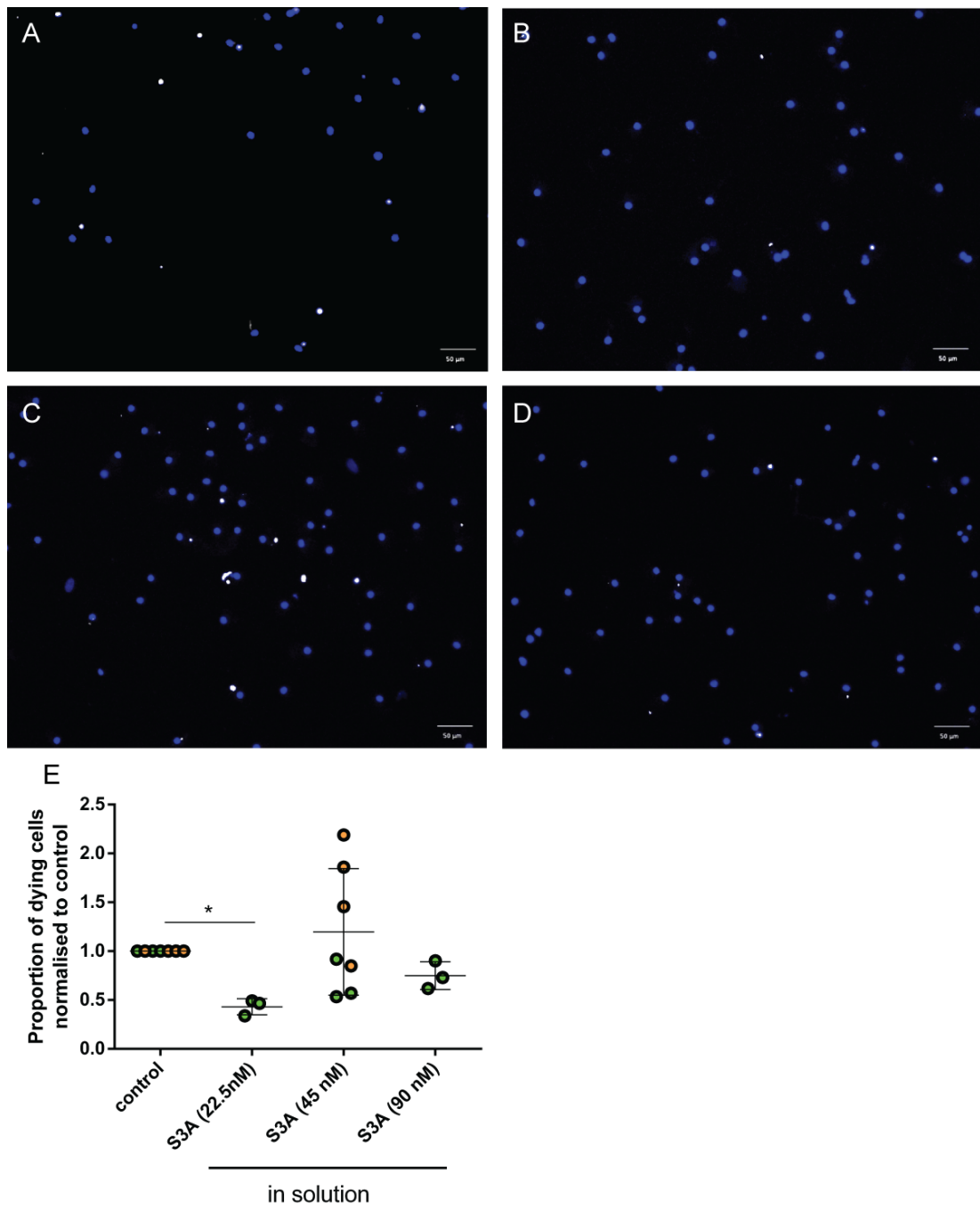


Figure 6.11: Low concentration of Sema3A in solution improves survival. Compared to control (A), 22.5 nM Sema3A in solution (B) reduced the number of dying cells. This effect was not seen with higher doses — 45 nM Sema3A in solution (C) and 90 nM Sema3A in solution (D). Comparison of the number of dying cells between control and the 3 different concentrations of Sema3A in solution and control showed that there was a significant difference between the conditions (Kruskal-Wallis test,  $H=10.39$ ,  $n=3,7,3$ ,  $p=0.015$ ) and Dunn's multiple comparison test revealed the difference between 22.5 nM Sema3A in solution and control was significant (E). Blue is Hoechst and white is TUNEL+ cells.

Therefore, at the lowest concentration of Sema3A, 22.5 nM it has a protective effect on cells and reduces the cell death.

### 6.5.2 NP1-Sema3A inhibitors

We also wanted to test whether the NP1-Sema3A inhibitors affect survival as well. Since Sema3A reduces the proportion of dying cells, inhibition of NP1 is expected to increase cell death. This is particularly important since it would contribute to the failure of both mutant mice to remyelinate better than WT and because it would mean that the NP1 inhibitors are not suitable for therapeutic use.

We initially tested the anti-NP1(Sema3A) blocking antibody at different concentrations and found that it does not significantly affect survival (section 6.7.3 in appendix). Similarly, SICHI does not affect survival significantly (Section 6.7.3 in appendix). Finally, we tested Xanthofulvin which inhibits Sema3A and found that it does not significantly affect survival (Section 6.7.3 in appendix).

Therefore, all tested inhibitors did not significantly affect the survival of OPCs. We then went on to test combination of Sema3A and NP1-Sema3A inhibitors and found that neither combination significantly affects survival (Section 6.7.3 in appendix).

Finally, we tested the effect of VEGF and the anti-NP1(VEGF) blocking antibody on survival and found that neither of them affects survival (Section 6.7.3 in appendix).

### 6.5.3 Survival discussion

Despite the literature indicating that Sema3A does not influence survival in vivo [29] or in vitro [296], we have found that 22.5 nM Sema3A in solution increases survival. In section 6.3.1, we hypothesised that a low concentration of Sema3A might be important for the ability of cells to deform. A low concentration of Sema3A might also be important in promoting survival. In vivo, such low concentration of Sema3A might be found around the edge of the lesion and prime cells for survival and better ability to squeeze their way into the lesion. The proliferation enhancing effect of Sema3A was only seen when Sema3A was in solution instead of coated at the bottom of the culture plate. Since Sema3A interacts heavily with ECM (Section 1.12), it is more likely that the condition when Sema3A is coated on the bottom of the culture plate is more representative of in vivo than Sema3A in solution. Therefore, this proliferation enhancing effect of Sema3A might not be observed in vivo.

Since low concentration of Sema3A improves survival, the NP1-Sema3A inhibitors would be expected to decrease it. However, the anti-NP1(Sema3A) blocking antibody, Xanthofulvin, SICHI or combinations of Sema3A did not significantly affect survival compared to control. Therefore, the loss of NP1 in the PDGFR $\alpha$  x flx-NP1-flx mice or the NP1 mutations in the NP1(Sema3A-) mice are not expected to negatively impact OPC survival.

## 6.6 Maturation assay

Finally, we wanted to determine if any of the NP1 ligands or their inhibitors influence maturation since it has been previously reported that treatment of OPCs with Sema3A reduced their maturation into O4+ cells [296]. Therefore, the NP1-Sema3A inhibitors would be expected to increase OPC maturation. To test maturation, we seeded the cells in 384 well plates and incubated for 3 days in each condition. After that we performed IHC with antibodies against NG2 to mark OPCs, O4 to mark immature oligodendrocytes and MBP to mark mature oligodendrocytes. The intensity of the NG2+ staining was very variable throughout the experiments and therefore NG2+ cells were counted manually. Brightness and contrast of the image were adjusted to show NG2+ cells as clear as possible without compromising the background and therefore the visibility of the O4+ and MBP+ cells. However, this resulted in the NG2+ cells not being clearly visible in some of the images even though they were present. The O4+ and MBP+ cells were counted automatically by Columbus software which does not change brightness or contrast of the images for analysis. However, to increase clarity of images, brightness and contrast were adjusted to better show the O4+ and MBP+ cells in the representative images. Quantification of all cells expressing each of those markers as well as the cytoplasmic size of MBP+ cells gives an stepwise indication of how well the cells matured.

### 6.6.1 Sema3A

We initially looked at whether Sema3A in solution influences the maturation of rat OPCs and we found that neither of the concentrations influence maturation significantly (Section 6.7.4 in appendix). However, the previously reported reduction in O4+ cells was seen when Sema3A was coated [296]. Therefore, we performed the same experiment with coated Sema3A (Section 6.7.4 in appendix). We found that coated Sema3A changes the morphology of the cell and causes a small but not statistically significant reduction in OPC maturation ( increased NG2+ cells, decreased O4+ cells and reduced MBP+ cell size) which is in concert with previous report [296] but the effect is much smaller.

### 6.6.2 NP1-Sema3A Inhibitors

We then moved onto investigation of whether the NP1-Sema3A inhibitors influenced maturation of OPCs. We expected that they may improve maturation since Sema3A has been reported to decrease it [296]. We first looked at the anti-NP1(Sema3A) blocking antibody. Compared to control (Figure 6.12 A), 5  $\mu\text{g/ml}$  anti-NP1(Sema3A) blocking antibody (Figure 6.12 B), 10  $\mu\text{g/ml}$  anti-NP1(Sema3A) blocking antibody (Figure 6.12 C) and 20  $\mu\text{g/ml}$  anti-NP1(Sema3A) blocking antibody (Figure 6.12 D) did not have obvious effect on maturation.

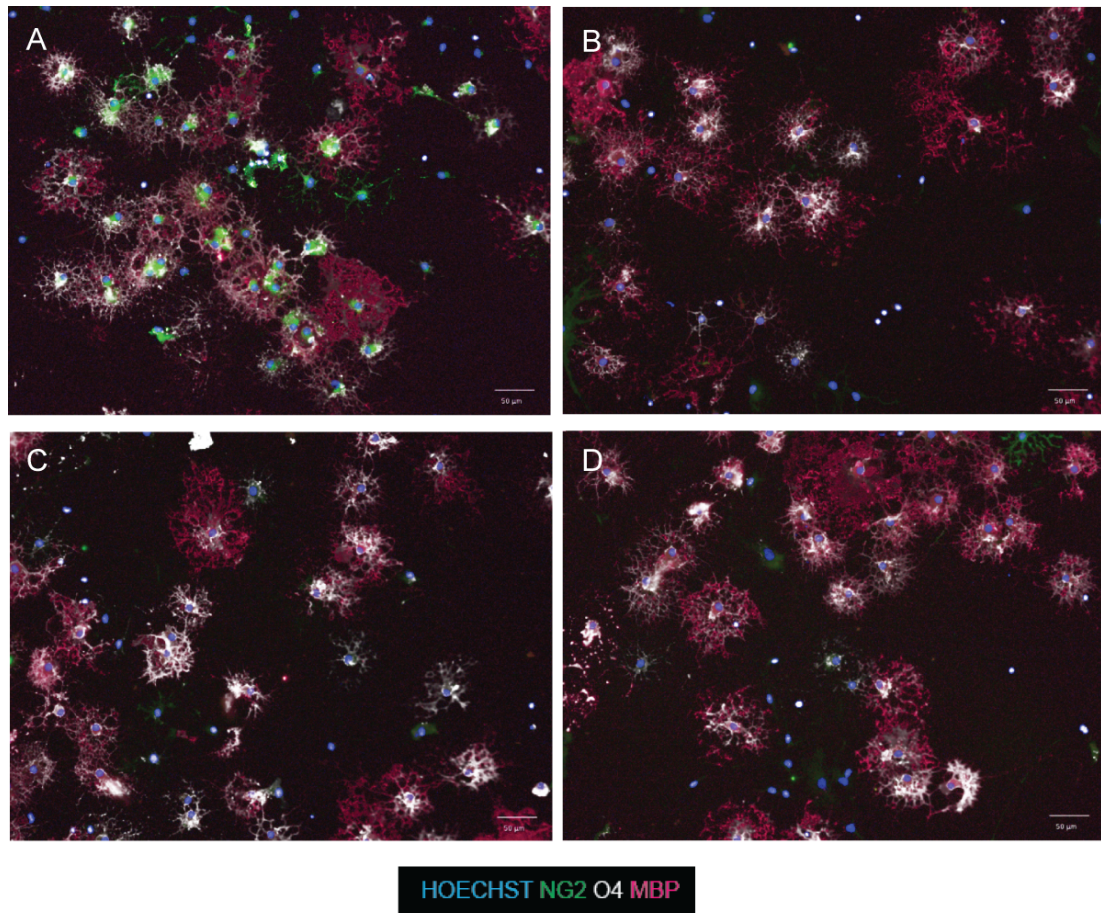


Figure 6.12: anti-NP1(Sema3A) blocking antibody has no effect on maturation. Images shown are control (A), 5  $\mu\text{g/ml}$  anti-NP1(Sema3A) blocking antibody (B), 10  $\mu\text{g/ml}$  anti-NP1(Sema3A) blocking antibody (C) and 20  $\mu\text{g/ml}$  anti-NP1(Sema3A) blocking antibody (D). Scale bar is 50  $\mu\text{m}$ . Blue is Hoechst, green is NG2+ cells, white is O4+ cells and red is MBP+ cells.

Quantification of the results showed that the anti-NP1(Sema3A) blocking antibody has no significant effect on the number of NG2+ cells, O4+ cells or MBP+ cells (Figure 6.13 A,B,C). However, comparison of the size of mature oligodendrocytes showed that 5  $\mu\text{g/ml}$  anti-NP1(Sema3A) blocking antibody significantly increases the size of MBP+ cells.

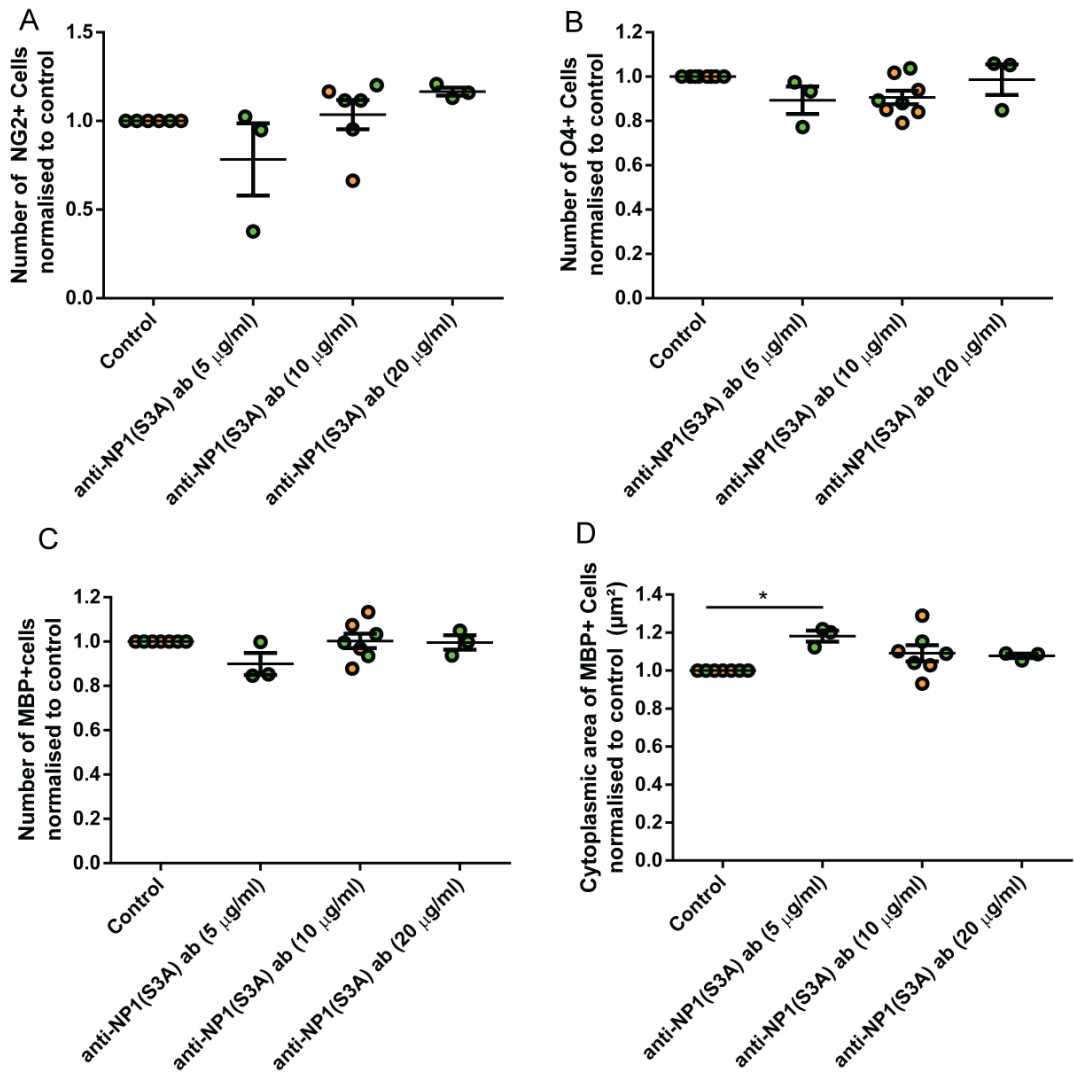


Figure 6.13: anti-NP1(Sema3A) blocking antibody significantly increases the area of MBP+ cells. Graphs represent quantification of NG2+ cells (A), O4+ cells (B), MBP+ cells (C) and size of MBP+ cells (D). There was a significant difference between concentrations of anti-NP1(Sema3A) blocking antibody and control in NG2+ cells (Kruskal-Wallis test,  $H=7.54$ ,  $n=6,3,6,3$   $p=0.04$ ). However, those differences were small as Dunn's multiple comparison test revealed no significant differences to control (A). There is no significant difference in the number of O4+ cells (Kruskal-Wallis test,  $H=6.46$ ,  $n=8,3,8,3$   $p=0.091$ ) however lower concentrations of the blocking antibody show a slight decrease in O4+ cells(B). Similarly, there was no significant difference in the number of MBP+ cells (Kruskal-Wallis test,  $H=5.51$ ,  $n=7,3,7,3$   $p=0.138$ ) (C). However, there was a significant difference in MBP+ cell area (Kruskal-Wallis test,  $H=11.78$ ,  $n=6,3,6,3$   $p=0.008$ ). Dunn's multiple comparison test revealed that 5 g/ml anti-NP1(Sema3A) blocking antibody increases the cytoplasmic area of MBP+ cells compared to control.

Therefore, the anti-NP1(Sema3A) blocking antibody significantly increases the size of MBP+ cells at 5  $\mu\text{g/ml}$ . This might indicate that these cells are more mature as they are more complex. To sum up, the anti-NP1(Sema3A) blocking antibody may promote some aspects of maturation.

We then tested Xanthofulvin and found that it does not significantly affect oligodendroglial maturation (Section 6.7.4 in appendix). We then looked at the effect of SICHI on maturation and found that it does not significantly affect the maturation of OPCs (Section 6.7.4 of the appendix).

Finally, we looked at the combination of Sema3A and inhibitors on maturation. Comparison of control (Figure 6.14 A) and 45 nM Sema3A (Figure 6.14 B) to 45 nM Sema3A and 10  $\mu\text{g/ml}$  anti-NP1(Sema3A) blocking antibody (Figure 6.14 C), 45 nM Sema3A and 2  $\mu\text{M}$  Xanthofulvin (Figure 6.14 D) and 45 nM Sema3A and 2  $\mu\text{g/ml}$  SICHI (Figure 6.14 E) revealed that the morphology of the OPCs changes in the presence of Sema3A and antagonist.

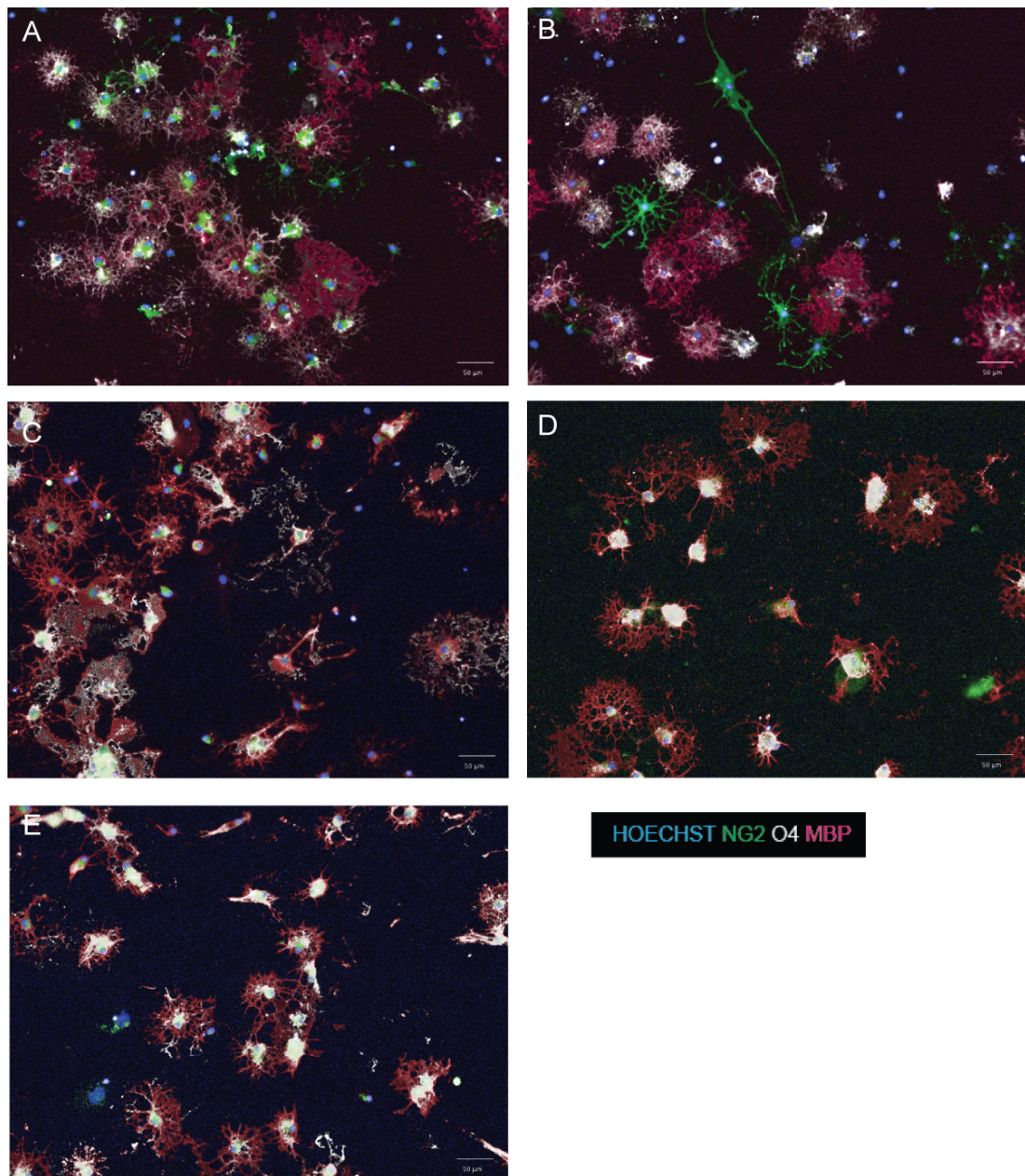


Figure 6.14: Example images of Sema3A and inhibitors on maturation. Images shown are control (A), 45 nM Sema3A in solution (B), 45 nM Sema3A in solution and 10  $\mu$  g/ml anti-NP1(Sema3A) blocking antibody (C), 45 nM Sema3A in solution and 2  $\mu$  Xanthofulvin (D) and 45 nM Sema3A in solution and 2 ng/ml SICHI (E). Scale bar is 10  $\mu$ m. Blue is Hoechst, green is NG2+ cells, white is O4+ cells and red is MBP+ cells.

Quantification of the data showed that the none of the tested combinations affect the number of NG2+ cells or MBP+ cells (Figure 6.15 A, C). However, Sema3A in combination with Xanthofulvin significantly decreases the proportion of O4+ cells (Figure 6.15 B). Those effects in combination of the change in morphology observed in all ligand-inhibitor combination might

## *6 In vitro work*

indicate that a combination of Sema3A and inhibitors might reduce maturation because it is toxic to the cells.

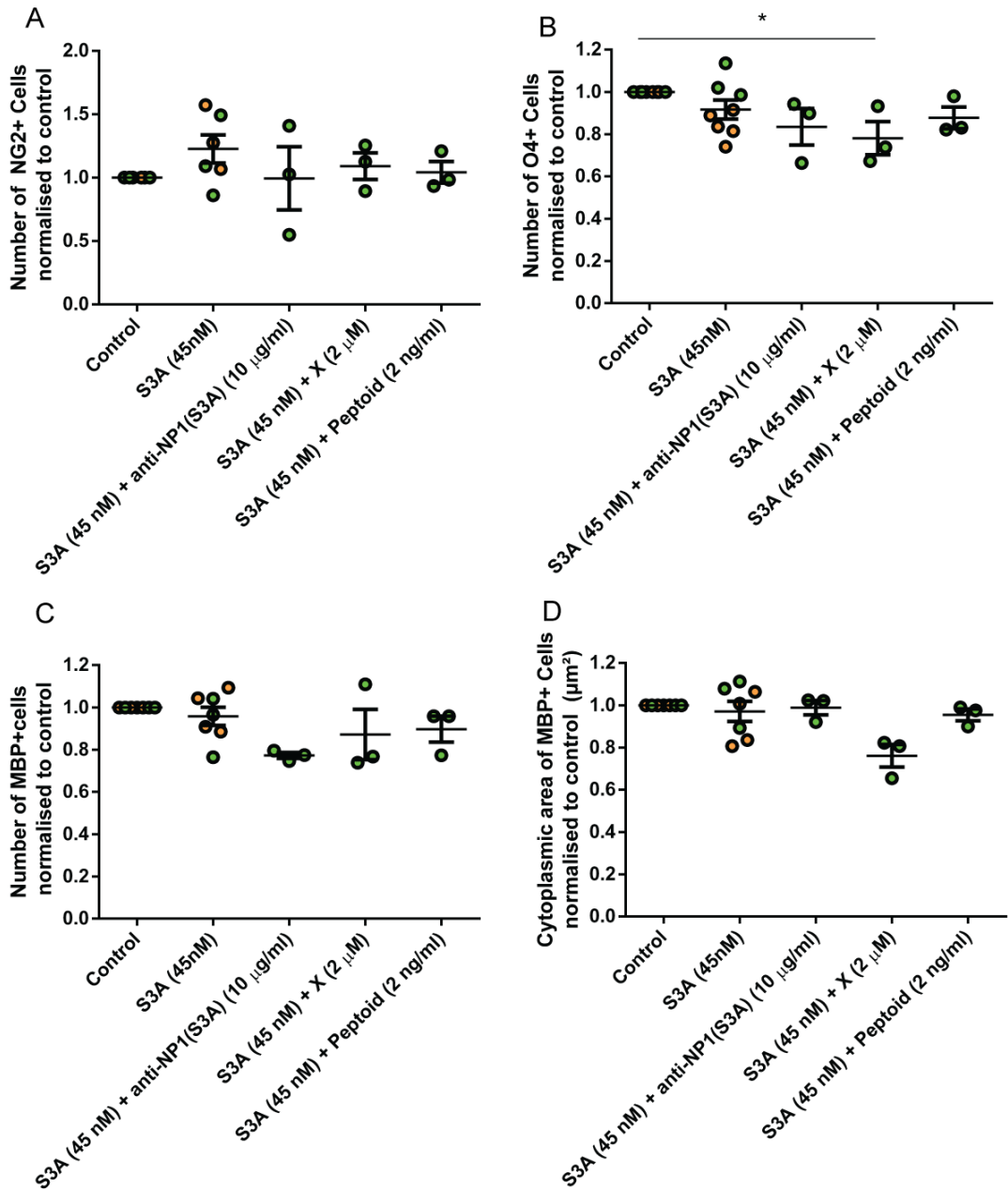


Figure 6.15: Combinations of Sema3A and NP1-Sema3A inhibitors influence maturation. Comparison of the effect of the Sema3A, the combination of Sema3A and the inhibitors as well as control showed that there is no significant difference in the number of NG2+ cells (Kruskal-Wallis test,  $H=3.75$ ,  $n=6,6,3,3,3$   $p=0.441$ ) (A). Further, comparison of the conditions showed that there is a significant difference in the number of O4+ cells (Kruskal-Wallis test,  $H=11.89$ ,  $n=8,8,3,3,3$   $p=0.018$ ) and Dunn's multiple comparison test showed that there is significantly less O4+ cells when Sema3A is added together with Xanthofulvin compared to control (B). Conversely, no significant difference was found in the number of MBP+ cells (Kruskal-Wallis test,  $H=7.40$ ,  $n=7,7,3,3,3$   $p=0.116$ ) (C) and the area of MBP+ cells (Kruskal-Wallis test,  $H=9.17$ ,  $n=7,7,3,3,3$   $p=0.057$ ) (D). Peptoid refers to SICHI as it is a peptoid drug.

### 6.6.3 VEGF

Finally, we looked at the effect of VEGF and anti-NP1(VEGF) blocking antibody on maturation. There is no indication that VEGF or blocking the VEGF site for NP1 should affect maturation in the literature. Comparison of the control (Figure 6.16 A), 0.1  $\mu\text{g/ml}$  VEGF (Figure 6.16 B) and 10  $\mu\text{g/ml}$  anti-NP1(VEGF) blocking antibody (Figure 6.16 C) revealed that both VEGF and the anti-NP1(VEGF) blocking antibody induced a change in morphology.

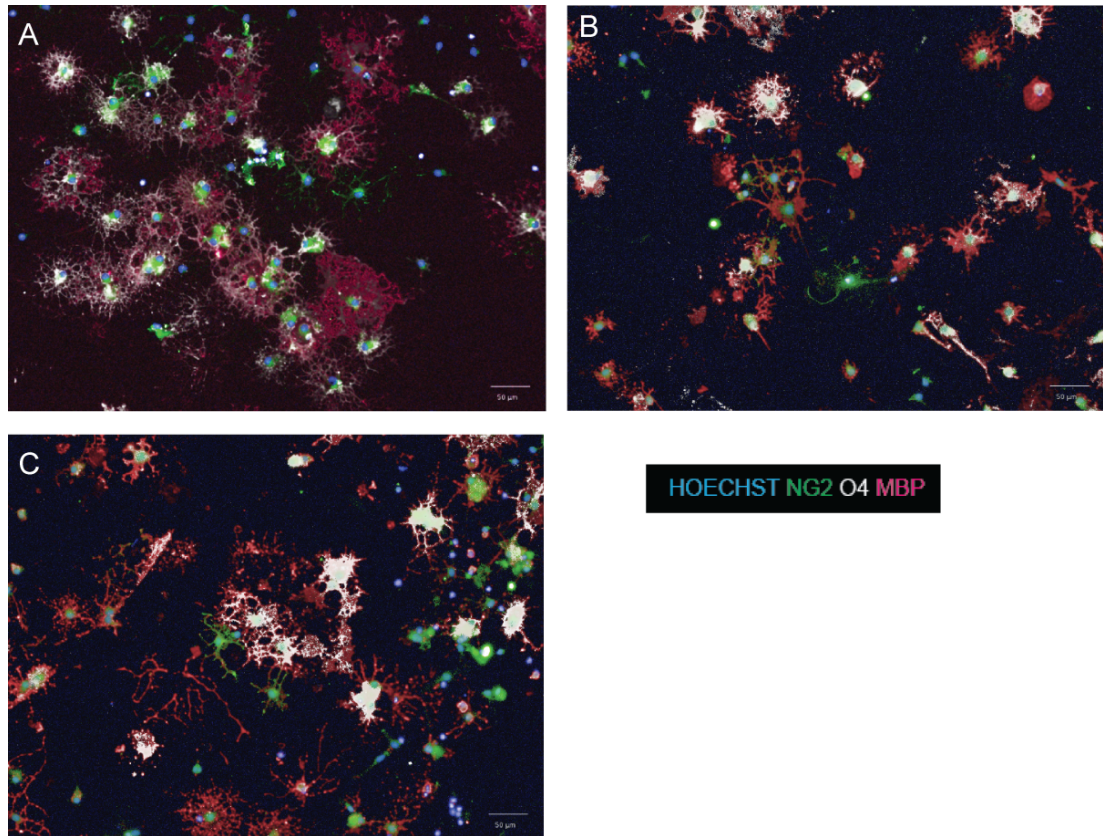


Figure 6.16: Example images of the effect of VEGF and anti-NP1(VEGF) on maturation. Images shown are control (A), VEGF (B) and anti-NP1(VEGF) blocking antibody (C). Blue is Hoechst, green is NG2+ cells, white is O4+ cells and red is MBP+ cells.

Quantification of the data revealed that neither VEGF nor anti-NP1(VEGF) on maturation influence the proportion of NG2+, MBP+ and the size of MBP+ cells (Figure 6.17 A,C,D). However, the anti-NP1(VEGF) blocking antibody reduced the proportion of O4+ cells (Figure 6.17 B).

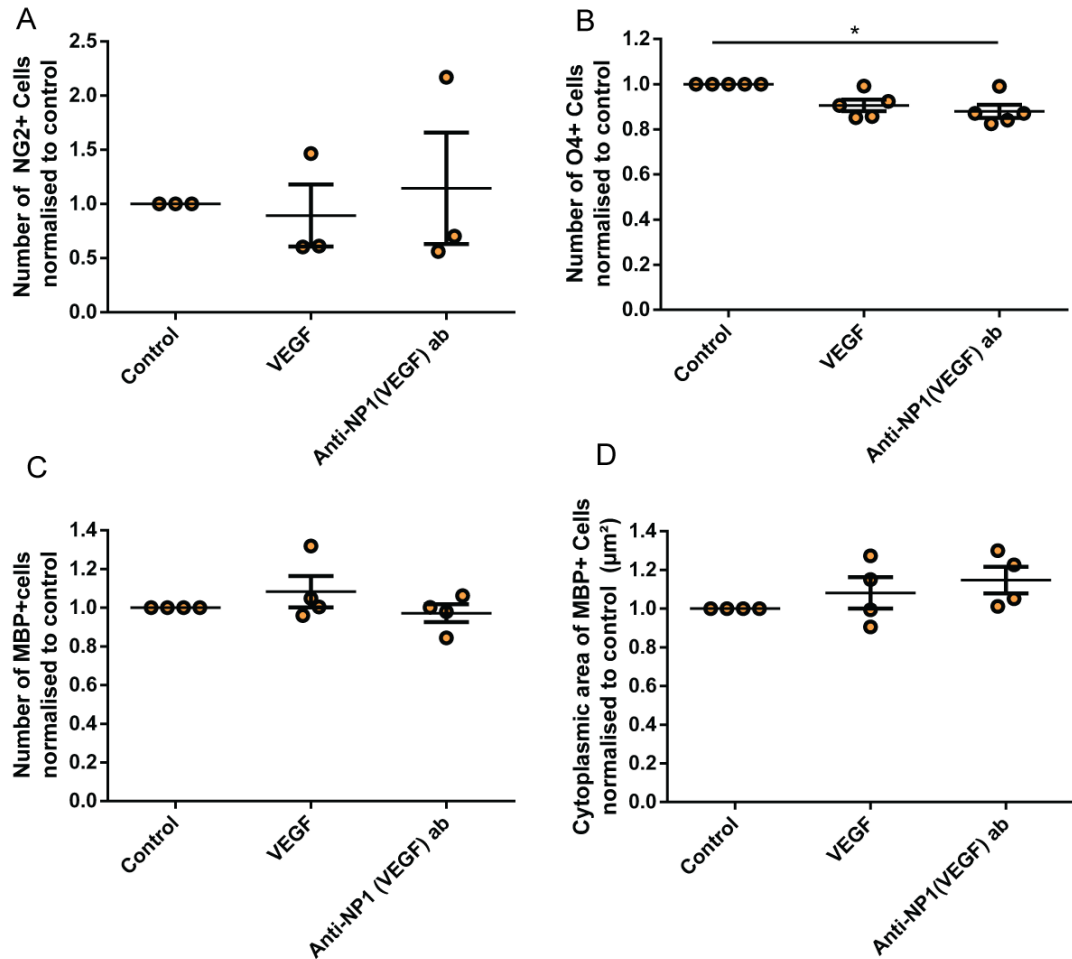


Figure 6.17: Anti-NP1(VEGF) blocking antibody influenced maturation while VEGF did not. Comparison of VEGF, anti-NP1 (VEGF) blocking antibody and control showed that there is no significant difference in the proportion of NG2+ cells (Kruskal-Wallis test,  $H=0.64$ ,  $n=3,3,3$   $p=0.818$ ) (A). However, there was a significant difference in the proportion of O4 + cells (Kruskal-Wallis test,  $H=10.14$ ,  $n=5,5,5$   $p=0.001$ ) and Dunn's multiple comparison test showed that the anti-NP1(VEGF) blocking antibody significantly reduces the number of O4+ cells compared to control (B). Furthermore, there was no significant difference in the proportion of MBP+ cells (Kruskal-Wallis test,  $H=1.48$ ,  $n=4,4,4$   $p=0.509$ ) (C) and the area of MBP+ cells (Kruskal-Wallis test,  $H=3.87$ ,  $n=4,4,4$   $p=0.152$ ) (D).

#### 6.6.4 Maturation discussion

##### Sema3A

As discussed in section 1.9.2, Sema3A has been previously found to be inhibitor of OPC maturation on the bottom of the culture well [296]. Culturing rat OPCs on a substrate of PLL and  $2.5 \mu\text{g}/\text{cm}^2$ ,  $5 \mu\text{g}/\text{cm}^2$  and  $10 \mu\text{g}/\text{cm}^2$  Sema3A resulted in a dose-dependent decrease of the

proportion of O4+ cells after 4 days [296].

In our hands, culturing OPCs in 2.5  $\mu\text{g/ml}$  (22.5 nM), 5  $\mu\text{g/ml}$  (45 nM) and 10  $\mu\text{g/ml}$  (45 nM) in solution did not affect the number of O4+ cells as shown in figure 6.33 B. Coated Sema3A together with PDL/PLL did result in a slight decrease in the number of O4+ cells at 2.5  $\mu\text{g/ml}$  (22.5 nM), 5  $\mu\text{g/ml}$  (45 nM) and 10  $\mu\text{g/ml}$  (45 nM) (figure 6.35 B) in our culture. However, the effects on O4+ cells (Kruskal-Wallis test,  $H=6.90$ ,  $n=4,4,4,4$   $p=0.061$ ) was not statistically significant.

Since the area of the bottom of a 384 well plate is 0.0619  $\text{cm}^2$ , our coated concentrations correspond to 4  $\mu\text{g/cm}^2$ , 8  $\mu\text{g/cm}^2$  and 16  $\mu\text{g/cm}^2$  Sema3A which is well within the range used in the previous work [296]. While they see a dose-dependent decrease in O4+ cells peaking at 60% in 10  $\mu\text{g/cm}^2$  Sema3A we see a constant 5% decrease in all tested concentrations. Both studies use rat OPCs and the same recombinant Sema3A and are thus fairly comparable. Overall, the effect was similar but less marked and not significant. What is entirely consistent with the previous report [296] is our observation that OPCs grown on coated Sema3A have a different morphology with less branching (Figure 6.34 B,C and D compared to A) while this was not observed with soluble Sema3A (Figure 6.32).

### **NP1-Sema3A inhibitors**

The anti-NP1(Sema3A) blocking antibody significantly increased the size of MBP+ cells (Figure 6.13 D) indicating that inhibition of NP1 promotes some aspects of maturation. This is exactly what we would expect if Sema3A impairs maturation and therefore blocking its signalling via NP1 would improve it. OPCs secrete Sema3A in culture and the anti-NP1(Sema3A) blocking antibody may prevent the effects of this Sema3A. However, this effect in improving maturation is very small. Since the anti-NP1(Sema3A) blocking antibody may have a small positive effect on maturation, we also expected Xanthofulvin and SICHI to have the same effect. However, neither Xanthofulvin nor SICHI significantly affect maturation indicating that the maturation enhancing effect is specific to the anti-NP1(Sema3A) blocking antibody. Interestingly, combinations of Sema3A and NP1 appeared to change the morphology of the cells and the combination of Sema3A and Xanthofulvin significantly reduced the number of O4+ cells. In addition to this, this combination appeared to decrease MBP+ cell size (not significant effect) (Figure 6.15 C, D) suggesting that xanthofulvin and Sema3A reduce maturation. This could be because this combination is toxic to the cells as they appear to have changed morphology as well.

Inhibition of the VEGF site of NP1 lead to a small but statistically significant reduction in the number of O4+ cells which could be indicate that maturation is improved or decreased depending on the its effect on the proportion of OPCs and mature oligodendrocytes. However, the anti-NP1(VEGF) blocking antibody did not have any significant effects on the these proportions or the size of mature oligodendrocytes so it is hard to speculate whether it has a positive or negative effect on maturation.

### 6.6.5 *In vitro* summary

When investigating the effect of NP1 ligands and inhibitors on OPC behaviour, we found that:

- Sema3A is chemorepellent for OPCs as expected (Section 1.9.2)
- VEGF is a chemoattractant for OPCs as expected (Section 1.9.2)
- All tested NP1-Sema3A inhibitors reduced migration which we hypothesise is because they physically or functionally impair the cell's ability to squeeze through a pore
- None of the tested conditions impaired motility on a flat surface
- Some concentrations of Sema3A and anti-NP1(Sema3A) blocking antibody improve proliferation perhaps because both cause internalisation of NP1
- Sema3A slightly increased survival at low concentrations
- Neither Sema3A in solution nor coated Sema3A significantly reduced maturation unlike previous reports [296]
- anti-NP1(Sema3A) blocking antibody increases maturation of OPCs

For our studies it is clear that coating Sema3A on the surface and adding it in solution is not necessarily identical. Moreover, sometimes the tested NP1-Sema3A inhibitors had the same effect on OPC behaviour as Sema3A instead of having opposite effect. This is highly unexpected as ligand and inhibitors are supposed to have opposite effects. This was true for Sema3A and anti-NP1(Sema3A) blocking antibody/Xanthofulvin in the migration assay and Sema3A and anti-NP1(Sema3A) blocking antibody in the proliferation assay. This is particularly interesting as they act in different ways. The anti-NP1(Sema3A) blocking antibody binds to NP1 while Xanthofulvin binds to Sema3A and yet both impair migration by themselves and fail to rescue the Sema3A-induced decrease in migration. It could be explained by a requirement for low level NP1 activation by Sema3A for cell deformation. Therefore, inhibiting this required low NP1 activation by any of the NP1-Sema3A inhibitors would impair the ability of the cell to migrate. In the proliferation assay, high concentration of Sema3A and certain concentrations of the anti-NP1(Sema3A) blocking antibody increased proliferation. This can be explained by both Sema3A and the blocking antibodies converging on NP1 internalisation which might be beneficial for proliferation.

Although sometimes Sema3A and the inhibitors show identical effects, this was not the case in the maturation assay. In the maturation assay, coated Sema3A has been reported to decrease maturation [296] (similar but smaller and non significant effect in our assay) while the anti-NP1(Sema3A) blocking antibody slightly increased maturation as it made the MBP+ cells bigger (more complex). Therefore, the anti-NP1(Sema3A) blocking antibody had an opposing effect (increases maturation) to the Sema3A effect (decreased maturation). Interestingly, combination of Sema3A and Xanthofulvin significantly reduced maturation and also resulted in

change of morphology indicating that a combination of Sema3A and inhibitor might be toxic to the cells (without affecting survival).

In all of the assays it was clear that concentration of the ligands and inhibitors played a major role in the observed effect. Sometimes increasing or decreasing the ligand/inhibitor concentration even two fold changed its effect on OPC behaviour. It is possible that optimal levels of Sema3A-NP1 signalling are required for certain OPC behaviours and either increasing or decreasing these levels has identical effect.

One of the inhibitors, SICHI, showed no effects in any of the assays. SICHI was believed to be direct inhibitor of Sema3A's binding to NP1 as mentioned in section 1.11.1. However, further studies revealed that SICHI does not bind NP1 or Sema3A directly but instead binds ECM components including heparin and therefore prevents Sema3A's interaction with those ECM components [57]. This means that this function blocking inhibitor is not an inhibitor of NP1 as previously thought but instead impairs the Sema3A-ECM interaction. Since there will be little ECM in our assays, it is not surprising that SICHI did not have any effects.

What is clear is that at certain concentrations Sema3A can induce OPC proliferation and increase survival in addition to its chemorepulsive properties. Therefore, even though Sema3A is extensively well studied, there are unexplored effects on OPCs. However, the concentrations used in this study might not be present *in vivo* thus questioning the *in vivo* relevance of these newly found positive effects of Sema3A on proliferation and survival.

On the other hand, inhibition of the Sema3A site of NP1 by the anti-NP1(Sema3A) blocking antibody slightly improves OPC proliferation, maturation and survival but also impairs their migration in a transwell assay. It is worth noting that all of those beneficial effects on proliferation, maturation and survival are very small while the negative effect on OPC migration is more than two fold. Therefore in the NP1(Sema3A-) mice we could expect to have slightly increased OPC proliferation, maturation and survival but those OPCs might have impaired ability to deform and squeeze their way through. Moreover, in the PDGFR $\alpha$ -Cre x flx-NP1-flx mice, the chemoattraction of VEGF on OPCs will be decreased. Therefore, inhibition of NP1 might be beneficial for certain OPC behaviours but not for others which makes it as unsuitable therapeutic target as all OPC cell behaviours tested above are important for the process of remyelination.

It is important to increase the number of experiments in this study as for some of the conditions we only have 3 independent experiments. In addition to this, a toxicity assay could be performed to ensure that none of the concentrations and particularly combinations are toxic to the cells. While they do not increase cell death, they could put a metabolic strain on the OPCs making them less healthy and impact OPC behaviour that way.

## 6.7 Appendix

This appendix contains *in vitro* data on the effects on OPC behaviour of various conditions which were not presented in the main text of this chapter as they were not statistically significant. Initially representative images are shown and then data is presented with each point being the

average of an individual experiment. All data was analysed by one way ANOVA and a posthoc test if significant difference was found.

### 6.7.1 Motility

Due to the observed migration effects of the NP1 ligands and inhibitors, we then looked at motility. Initially, we coated Sema3A at different concentrations on the bottom of the well together with PDL/PLL. Although the accumulated distance at 45 nM Sema3A appeared to be increased, this change was not significant compared to control (Kruskal-Wallis test,  $H=5.07$ ,  $n=3,3,3,3$ ,  $p=0.172$ )(Figure 6.18 A). Similarly, when we compared velocity, we found that neither concentration of coated Sema3A changed the speed with which the cells moved (Kruskal-Wallis test,  $H=1.17$ ,  $n=3,3,3,3$ ,  $p=0.80$ )(Figure 6.18 B).

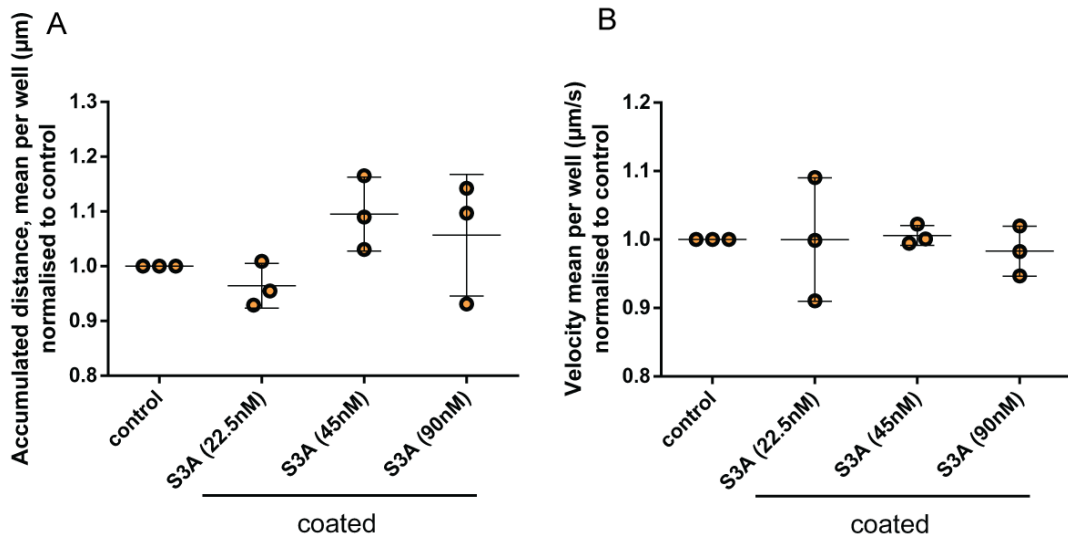


Figure 6.18: Coated Sema3A did not influence motility. Comparison of accumulated distance between control and different concentrations of coated Sema3A showed that there was no significant difference (Kruskal-Wallis test,  $H=5.07$ ,  $n=3,3,3,3$ ,  $p=0.172$ ) (A). Similarly, comparison of velocity between control and different concentrations of coated Sema3A showed that there was no significant difference (Kruskal-Wallis test,  $H=1.17$ ,  $n=3,3,3,3$ ,  $p=0.80$ ) (B)

We also looked at the effect 45 nM Sema3A in solution and 10 µg/ml anti-NP1(Sema3A) blocking antibody have on accumulated distance) and velocity (Figure 6.19). We found that neither Sema3A nor the anti-NP1(Sema3A) blocking antibody affected accumulated distance significantly (Kruskal-Wallis test,  $H=3.36$ ,  $n=6,6,5$ ,  $p=0.193$ ) (Figure 6.19 A). When we looked at velocity, both Sema3A and the anti-NP1(Sema3A) blocking antibody seemed to increase velocity (Figure 6.19 B). However, this increase in velocity was not significant compared to control (Kruskal-Wallis test,  $H=5.51$ ,  $n=6,6,5$ ,  $p=0.057$ ) (Figure 6.19 B).

We did not observe an obvious difference in oligodendrocyte process outgrowth as reported

before [259] and discussed in section 1.8.1.

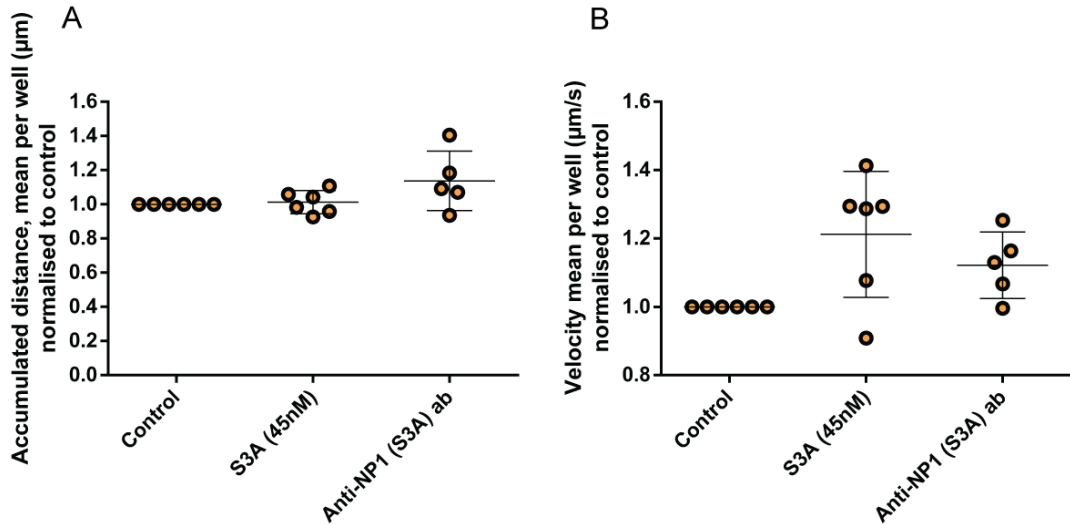


Figure 6.19: Sema3A and anti-NP1(S3A) do not influence motility significantly. Comparison of accumulated distance between control, Sema3a and anti-NP1(Sema3A) blocking antibody showed that there was no significant difference (Kruskal-Wallis test,  $H=3.36$ ,  $n=6,6,5$ ,  $p=0.193$ ) (A). Comparison of accumulated distance revealed that both Sema3A and anti-NP1(Sema3A) blocking antibody induced a little increase in velocity. However, this difference was not significant compared to control (Kruskal-Wallis test,  $H=5.51$ ,  $n=6,6,5$ ,  $p=0.057$ ) (B).

We further looked at the effect of Xanthofulvin and its DMSO control on the motility of cells (Figure 6.20). Comparison of accumulated distance of control, DMSO and Xanthofulvin showed that there was no significant difference of those treatments (Kruskal-Wallis test,  $H=0.819$ ,  $n=6,5,6$ ,  $p=0.681$ ) (Figure 6.20 A). Similarly, comparison of velocity showed that there was no significant difference between the conditions (Kruskal-Wallis test,  $H=0.45$ ,  $n=6,4,6$ ,  $p=0.812$ ) (Figure 6.20 B).

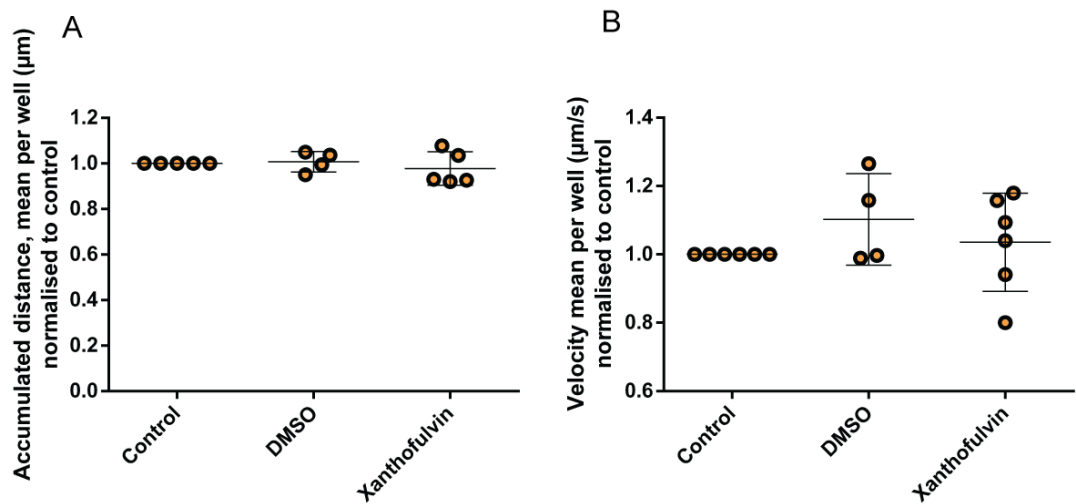


Figure 6.20: Xanthofulvin did not influence motility. Comparison of accumulated distance between control, DMSO and Xanthofulvin showed that there was no significant difference between the conditions (Kruskal-Wallis test,  $H=0.819$ ,  $n=6,5,6$ ,  $p=0.681$ ) (A). Comparison of velocity between control, DMSO and Xanthofulvin showed that there was no significant difference between the conditions (Kruskal-Wallis test,  $H=0.45$ ,  $n=6,4,6$ ,  $p=0.812$ ) (B)

## VEGF

Finally, we looked at VEGF and anti-NP1(VEGF) blocking antibody since VEGF promotes migration and anti-NP1(VEGF) blocking antibody reduces migration. We found that neither VEGF nor anti-NP1(VEGF) blocking antibody affect accumulated distance (Kruskal-Wallis test,  $H=0.359$ ,  $n=4,4,4$ ,  $p=0.872$ ) (Figure 6.21 A) and velocity (Kruskal-Wallis test,  $H=1.12$ ,  $n=4,4,4$ ,  $p=0.601$ ) (Figure 6.21 B).

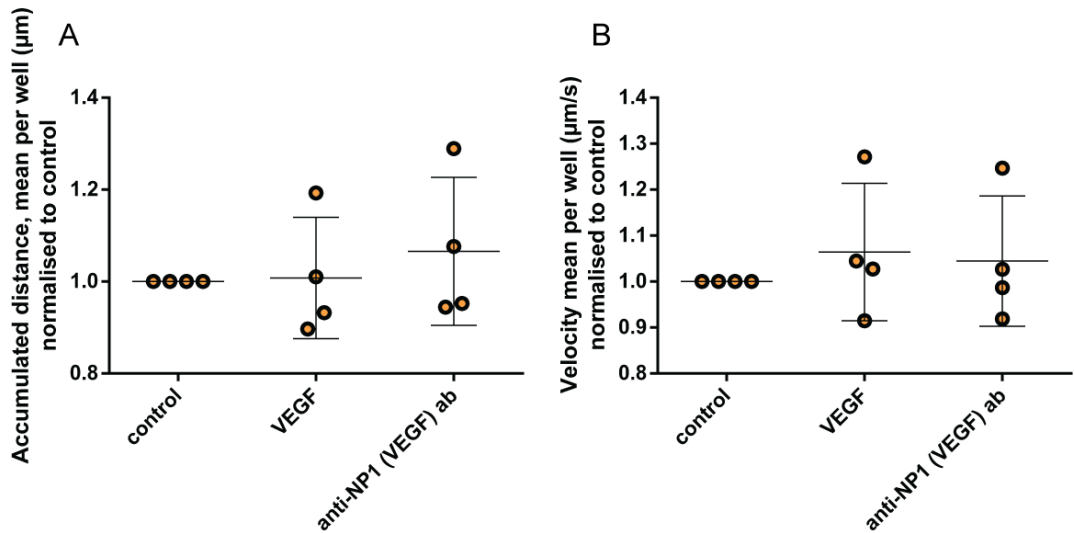


Figure 6.21: VEGF and anti-NP1(VEGF) blocking antibody do not influence motility. Comparison of control, VEGF and anti-NP1(VEGF) blocking antibody showed that those conditions did not affect accumulated distance (Kruskal-Wallis test,  $H=0.359$ ,  $n=4,4,4$ ,  $p=0.872$ ) (A) or velocity (Kruskal-Wallis test,  $H=1.12$ ,  $n=4,4,4$ ,  $p=0.601$ ) (B)

Therefore, none of the tested conditions altered cell motility on a flat surface.

## 6.7.2 Proliferation

### Coated Sema3A

Since Sema3A normally binds to extracellular matrix and is therefore not free floating, we tested the effect of Sema3A coated together with PDL/PLL after we observed the positive effect of soluble Sema3A on proliferation. We found out that the proliferation level in control (Figure 6.22 A) was very similar to the 22.5 nM coated Sema3A (Figure 6.22 B), 45 nM coated Sema3A (Figure 6.22 C) and 90 nM coated Sema3A (Figure 6.22 D). Comparison of those 4 conditions showed that there was no significant difference in the number of proliferating cells (Kruskal-Wallis test,  $H=1.16$ ,  $n=4,4,4,4$ ,  $p=0.789$ ) (Figure 6.22 E).

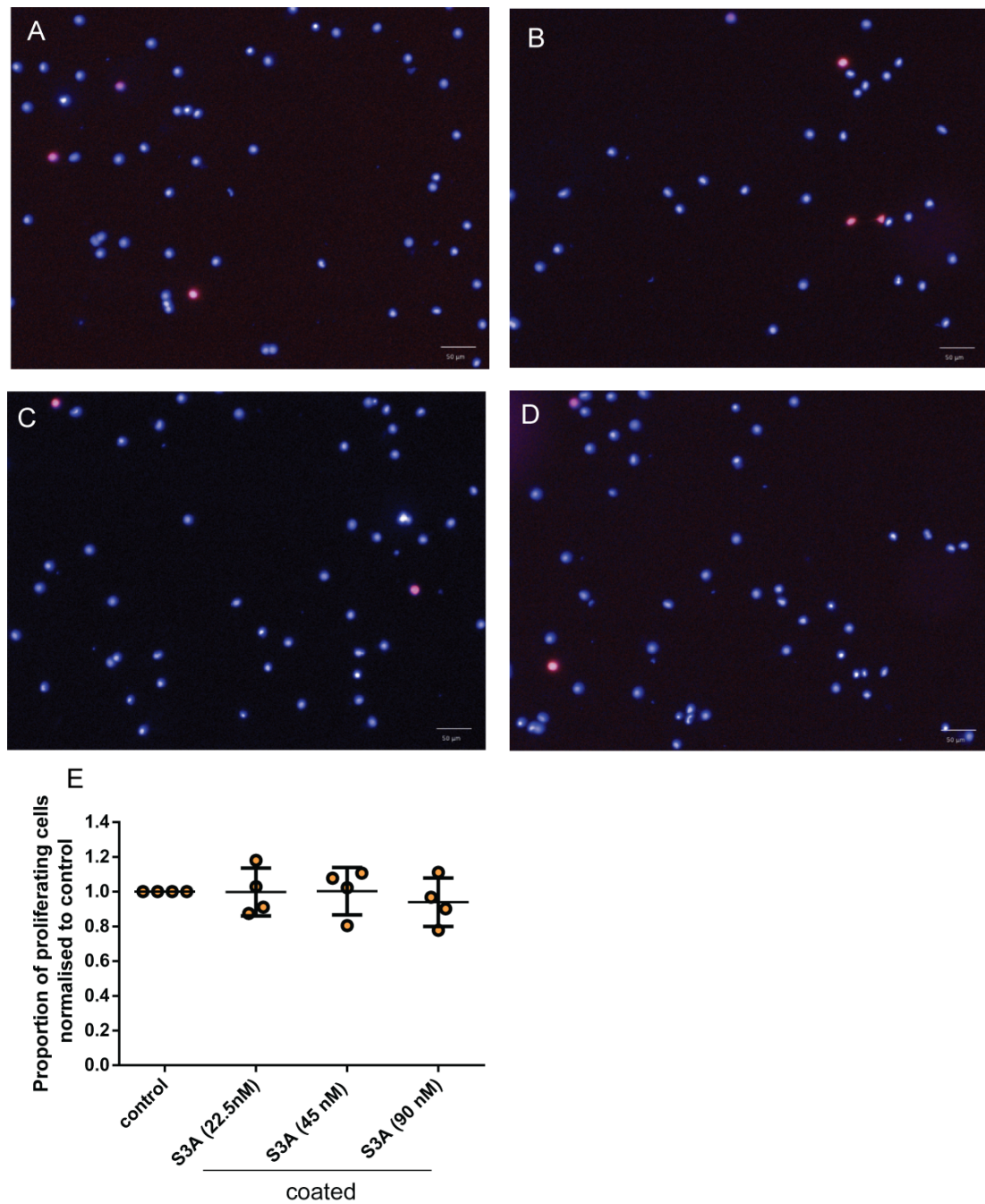


Figure 6.22: Semaphorin3A coated on the surface does not influence proliferation. The proportion of proliferating cells in control (A), 22.5 nM coated Sema3A (B), 45 nM coated Sema3A (C) and 90 nM coated Sema3A (D) was not different (Kruskal-Wallis test,  $H=1.16$ ,  $n=4,4,4,4$ ,  $p=0.789$ ) (E). Blue is Hoechst and red is EDU+ cells.

### **Xanthofulvin**

We then tested Xanthofulvin and found that compared to DMSO (Figure 6.23 A), Xanthofulvin did not change the proportion of proliferating cells at 1  $\mu\text{M}$  (Figure 6.23 B), 2  $\mu\text{M}$  (Figure 6.23 C) or 4  $\mu\text{M}$  (Figure 6.23 D). Comparison of the 3 Xanthofulvin concentrations and DMSO showed that there was no significant difference in the number of proliferating cells (Kruskal-Wallis test,  $H=3.79$ ,  $n=9,3,9,3$ ,  $p=0.285$ ) (Figure 6.23 E)

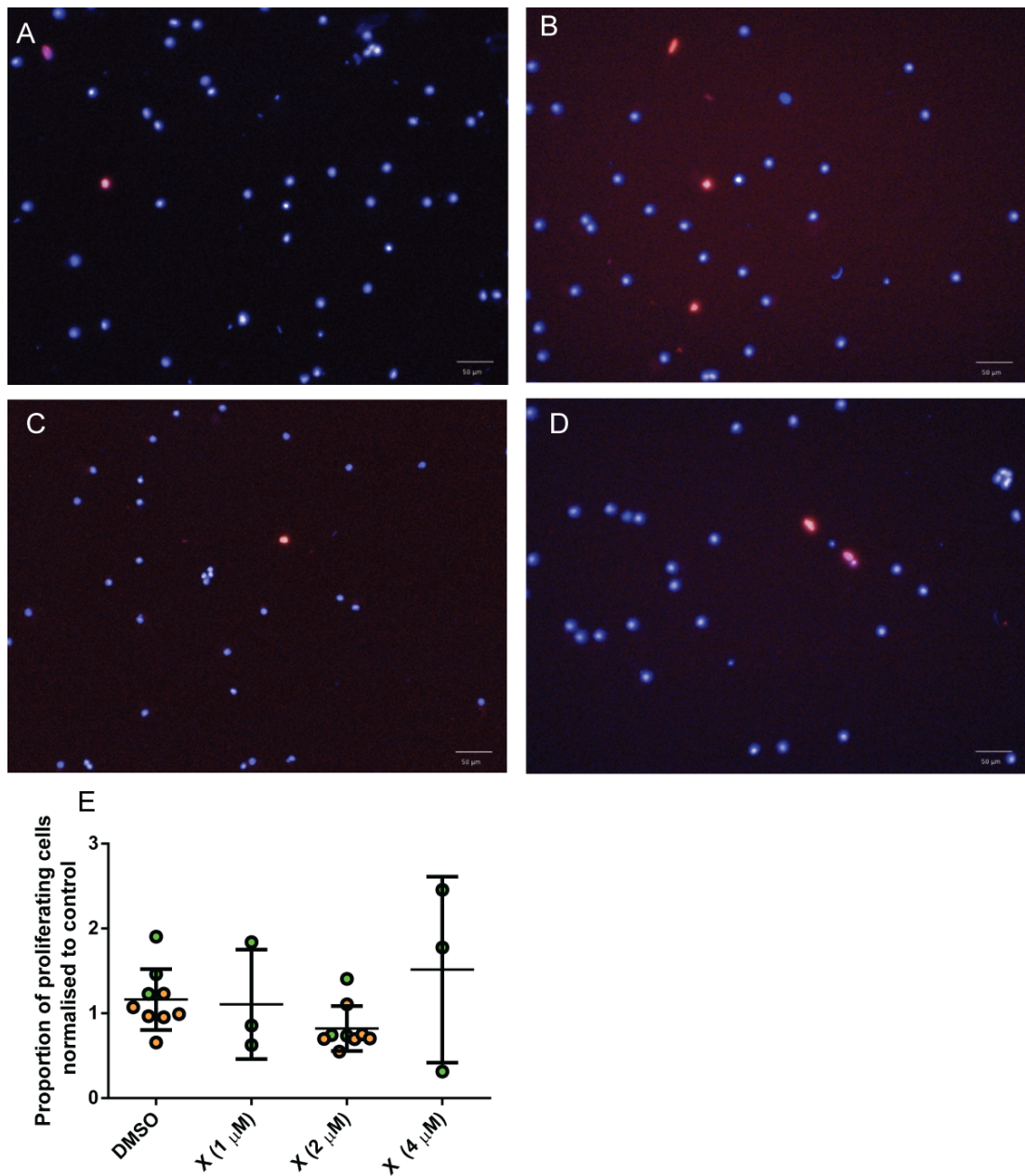


Figure 6.23: Xanthofulvin did not influence proliferation. Compared to DMSO (A), 1  $\mu$ M Xanthofulvin (B), 2  $\mu$ M Xanthofulvin (C) and 4  $\mu$ M Xanthofulvin (D) did not change the proportion of proliferating cells. Comparison of the 3 Xanthofulvin concentrations and DMSO showed that there was no significant difference in the number of proliferating cells (Kruskal-Wallis test,  $H=3.79$ ,  $n=9,3,9,3$ ,  $p=0.285$ ) (E). Blue is Hoechst and red is EDU+ cells.

## SICHI

Similarly, compared to control (Figure 6.24 A), 1 ng/ml SICHI (Figure 6.24 B), 2 ng/ml SICHI (Figure 6.24 C) and 4 ng/ml SICHI (Figure 6.24 D) did not change the proportion of proliferating cells.

erating cells. Comparison of the 3 SICH1 concentrations and control showed that there was no significant difference in the number of proliferating cells (Kruskal-Wallis test,  $H=0.44$ ,  $n=3,3,3,3$ ,  $p=0.957$ ) (Figure 6.24 E).

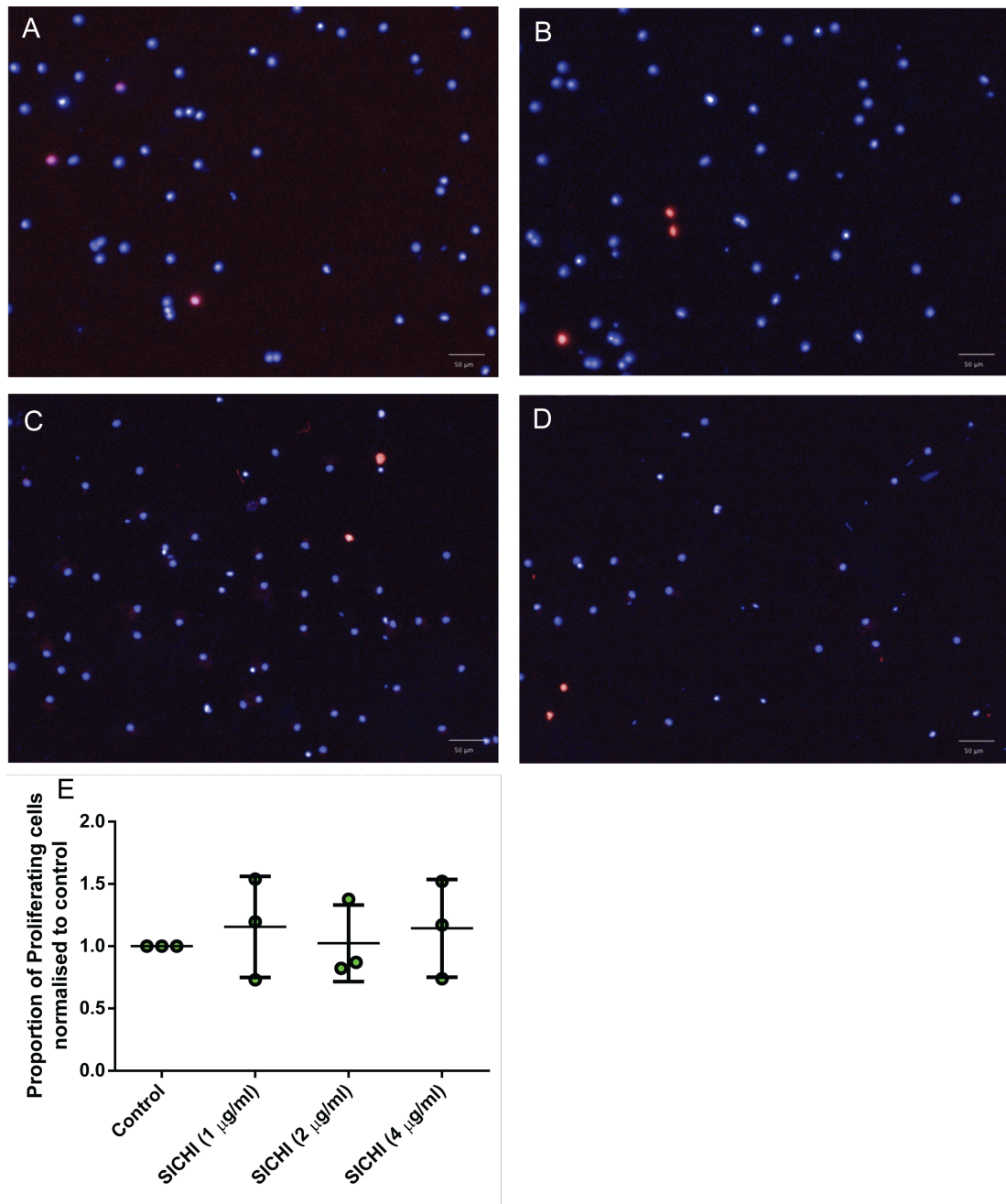


Figure 6.24: SICH1 did not influence proliferation. Compared to control (A), 1 ng/ml SICH1 (B), 2 ng/ml SICH1 (C) and 4 ng/ml SICH1 (D) did not change the proportion of proliferating cells. Comparison of the 3 SICH1 concentrations and control showed that there was no significant difference in the number of proliferating cells (Kruskal-Wallis test,  $H=0.44$ ,  $n=3,3,3,3$ ,  $p=0.957$ ) (E). Blue is Hoechst and red is EDU+ cells.

We found that neither Xanthofulvin, nor SICHI increased the proportion of proliferating cells. This was in sharp contrast to both 90 nM Sema3A and the low and high concentrations of anti-NP1(Sema3A) blocking antibody.

## VEGF

VEGF has been reported to not affect proliferation [124]. Compared to control (Figure 6.25 A), neither VEGF (Figure 6.25 B) nor anti-NP1(VEGF) blocking antibody (Figure 6.25 C) influenced the proportion of proliferating cells. Comparison of VEGF, anti-NP1(VEGF) blocking antibody and control showed that there is no significant difference in the number of proliferating cells (Kruskal-Wallis test,  $H=1.21$ ,  $n=6,6,6$ ,  $p=0.566$ ) (Figure 6.25 D).

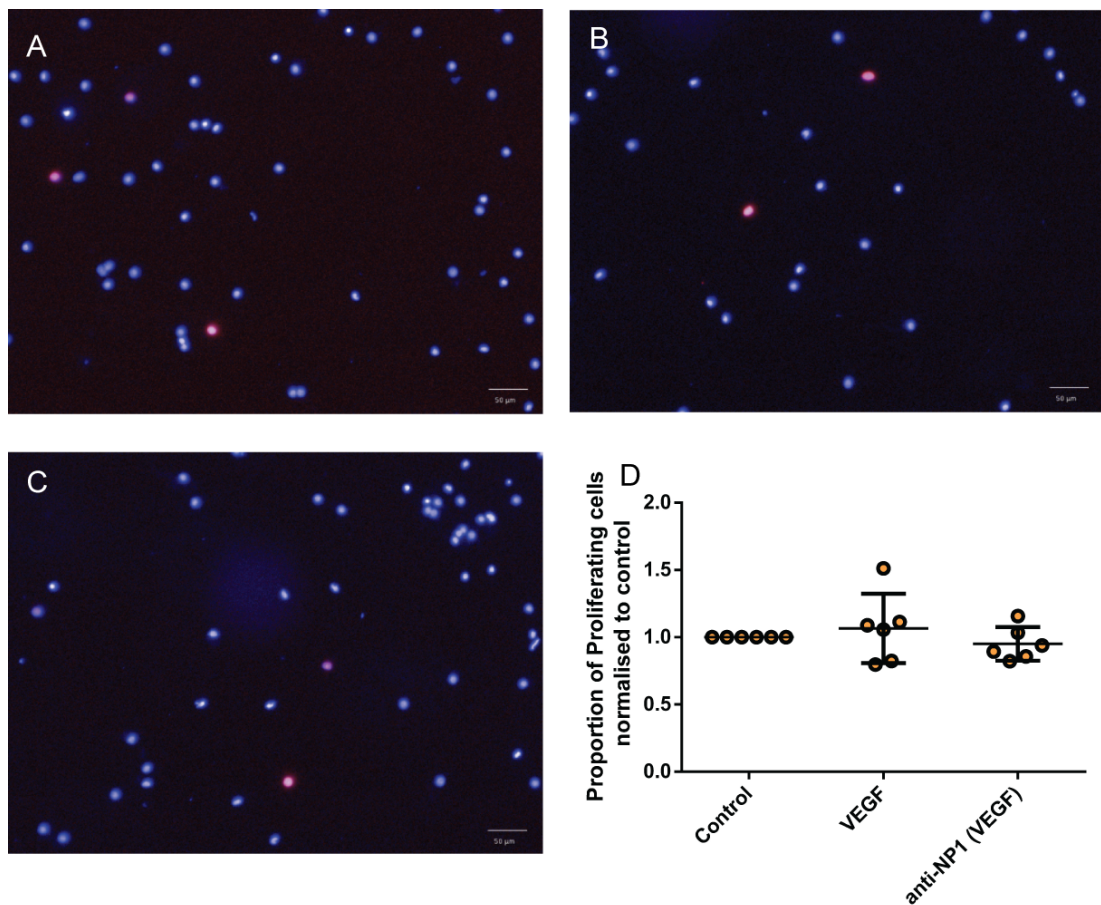


Figure 6.25: VEGF and anti-NP1(VEGF) blocking ab did not influence proliferation. Compared to control (A), VEGF (B) and anti-NP1(VEGF) blocking antibody (C) did not change the number of proliferating cells. Comparison of VEGF, anti-NP1(VEGF) blocking antibody and control showed that there is no significant difference in the number of proliferating cells (Kruskal-Wallis test,  $H=1.21$ ,  $n=6,6,6$ ,  $p=0.566$ ) (D). Blue is Hoechst and red is EDU+ cells.

Therefore VEGF and blocking the VEGF site of NP1 does not affect proliferation.

### 6.7.3 Survival

We then looked at the effect of NP1 ligands and inhibitors on survival.

#### Coated Sema3A

Bearing in mind this concentration dependent effect of soluble Sema3A on survival, we also performed this experiment with coated Sema3A. Compared to control (Figure 6.26 A), 22.5 nM coated Sema3A (Figure 6.26 B), 45 nM coated Sema3A (Figure 6.26 C) and 90 nM Sema3A (Figure 6.26 D) all appeared to increase the proportion of dying cells. However, this effect was not statistically significant (Kruskal-Wallis test,  $H=6.78$ ,  $n=4,4,4,4$ ,  $p=0.066$ )(Figure 6.26 E). There is a change in the morphology of OPCs in figure 6.34 and might indicate that coated Sema3A is toxic to the cells without causing significant change in survival.

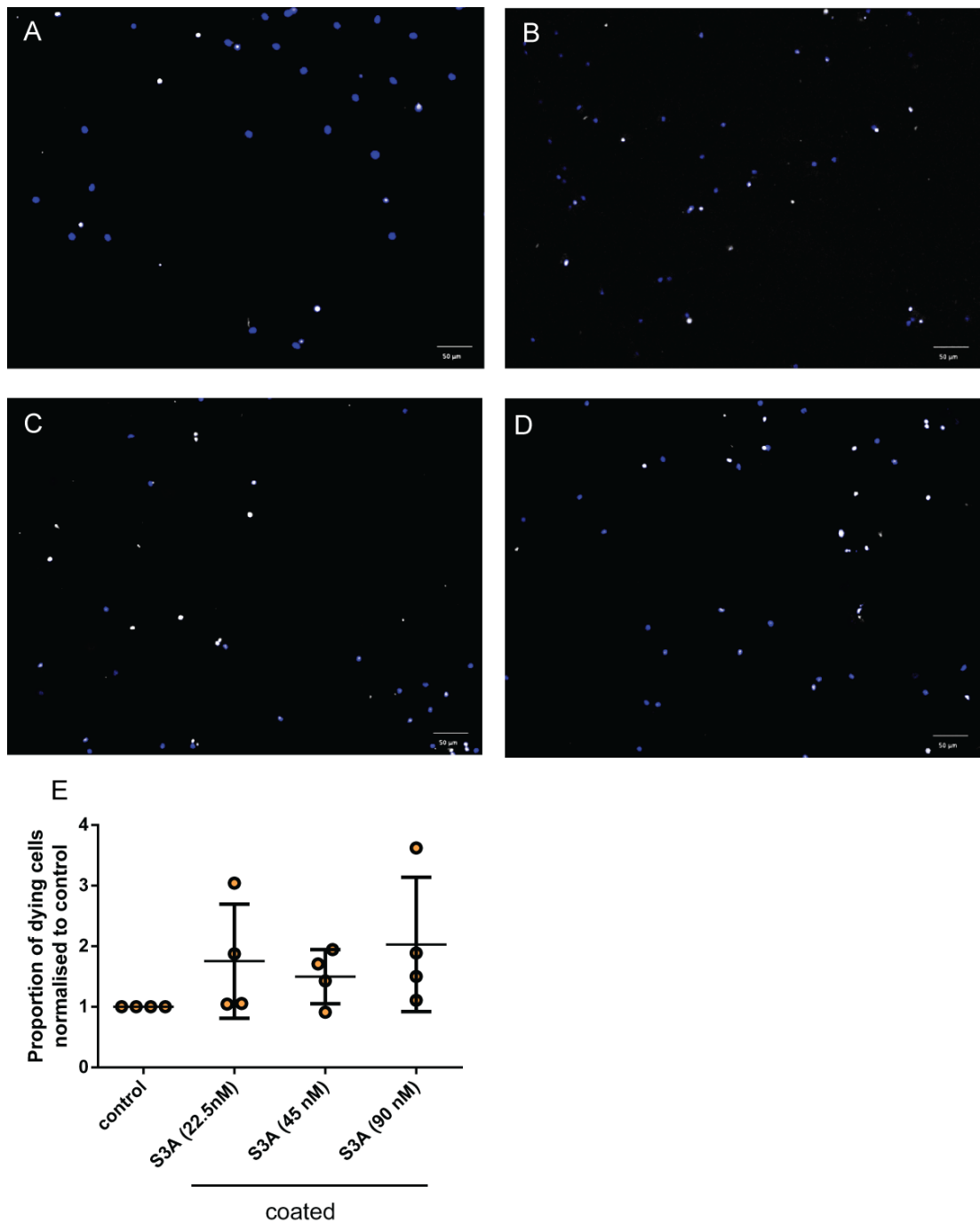


Figure 6.26: Coated Sema3A slightly decreases survival. Compared to control (A), coated 22.5 nM Sema3A (B), coated 45 nM Sema3A (C) and coated 90 nM Sema3A (D) all slightly increased the proportion of dying cells. However, this effect was not statistically significant (Kruskal-Wallis test,  $H=6.78$ ,  $n=4,4,4,4$ ,  $p=0.066$ ) (E). Blue is Hoechst and white is TUNEL+ cells.

**anti-NP1(Sema3A-) blocking antibody**

We then tested the NP1-Sema3A inhibitors. Initially, we tested the anti-NP1(Sema3A) blocking antibody. Compared to control (Figure 6.27 A), 5  $\mu\text{g/ml}$  anti-NP1(Sema3A) blocking antibody (Figure 6.27 B), 10  $\mu\text{g/ml}$  anti-NP1(Sema3A) blocking antibody (Figure 6.27 C) and 20  $\mu\text{g/ml}$  anti-NP1(Sema3A) blocking antibody (Figure 6.27 D) did not affect the proportion of dying cells in any consistent way. Comparison of the 3 concentrations of anti-NP1(Sema3A) blocking antibody and control showed that there was no significant difference (Kruskal-Wallis test,  $H=1.85$ ,  $n=3,7,3$ ,  $p=0.603$ ) (Figure 6.27 E).



## SICHI

We then tested SICHI. Compared to the control (Figure 6.28 A), 1  $\mu\text{g/ml}$  SICHI (Figure 6.28 B), 2  $\mu\text{g/ml}$  SICHI (Figure 6.28 C) and 4  $\mu\text{g/ml}$  SICHI (Figure 6.28 D) did not influence survival. Comparing the 3 SICHI concentrations and control showed that there was no significant difference in the proportion of dying cells (Kruskal-Wallis test,  $H=2.31$ ,  $n=3,3,3,3$ ,  $p=0.56$ ) (Figure 6.28 E).

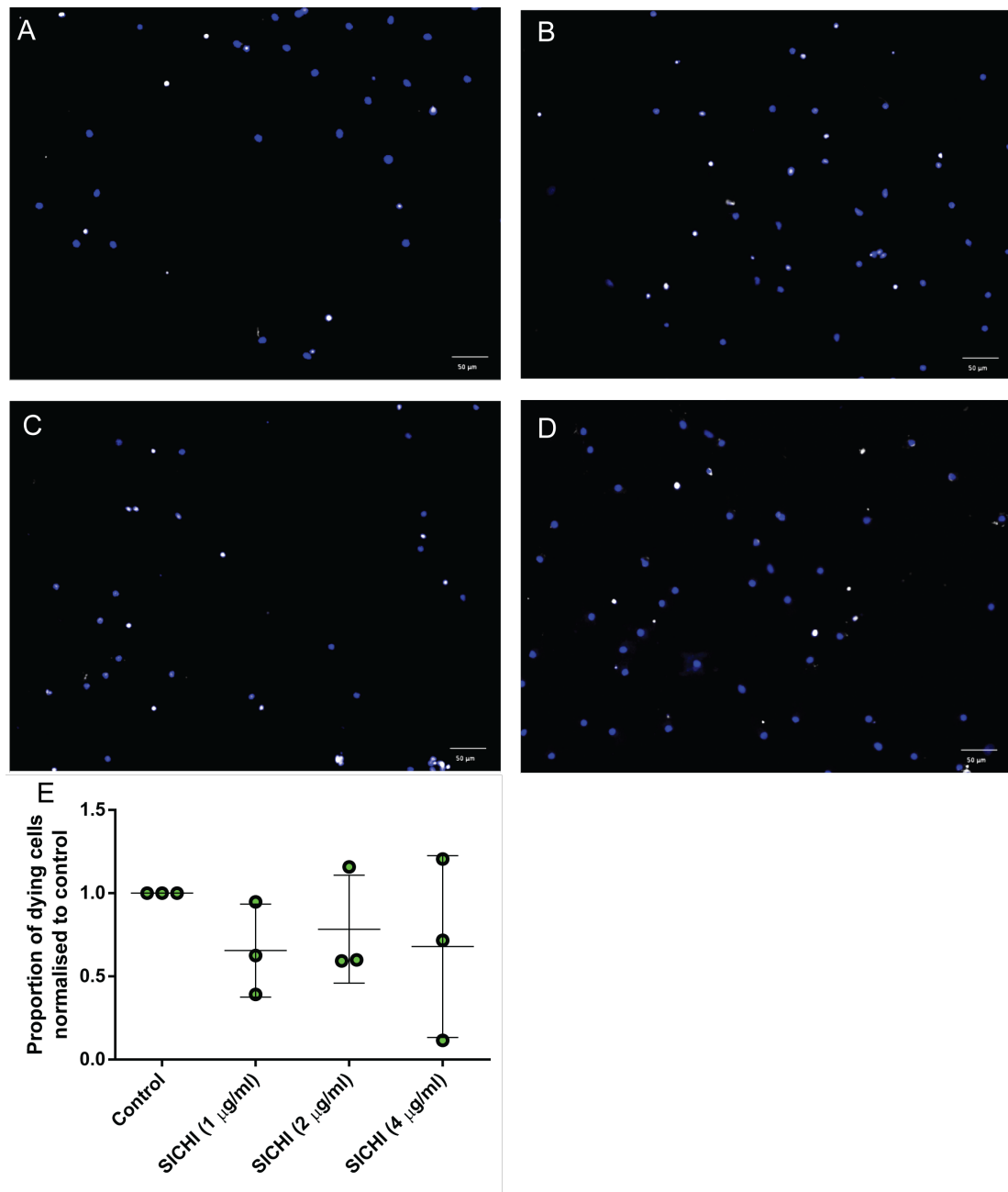


Figure 6.28: SICH1 does not influence survival. Compared to control (A), 1  $\mu\text{g/ml}$  SICH1 (B), 2  $\mu\text{g/ml}$  SICH1 (C) and 4  $\mu\text{g/ml}$  SICH1 (C) did not change the proportion of dying cells. Comparing the 3 SICH1 concentrations and control showed that there was no significant difference in the proportion of dying cells (Kruskal-Wallis test,  $H=2.31$ ,  $n=3,3,3,3$ ,  $p=0.56$ ) (E). Blue is Hoechst and white is TUNEL+ cells.

### Xanthofulvin

We then tested how Xanthofulvin affects survival. Compared to DMSO (Figure 6.29 A), 1  $\mu\text{M}$  Xanthofulvin (Figure 6.29 B), 2  $\mu\text{M}$  Xanthofulvin (Figure 6.29 C) and 4  $\mu\text{M}$  Xanthofulvin (Figure 6.29 D) did not change the proportion of dying cells. Comparison of the 3 concentrations of

Xanthofulvin and control showed that there was no significant difference (Kruskal-Wallis test,  $H=5.08$ ,  $n=6,3,6,3$ ,  $p=0.167$ ) (Figure 6.29 E).

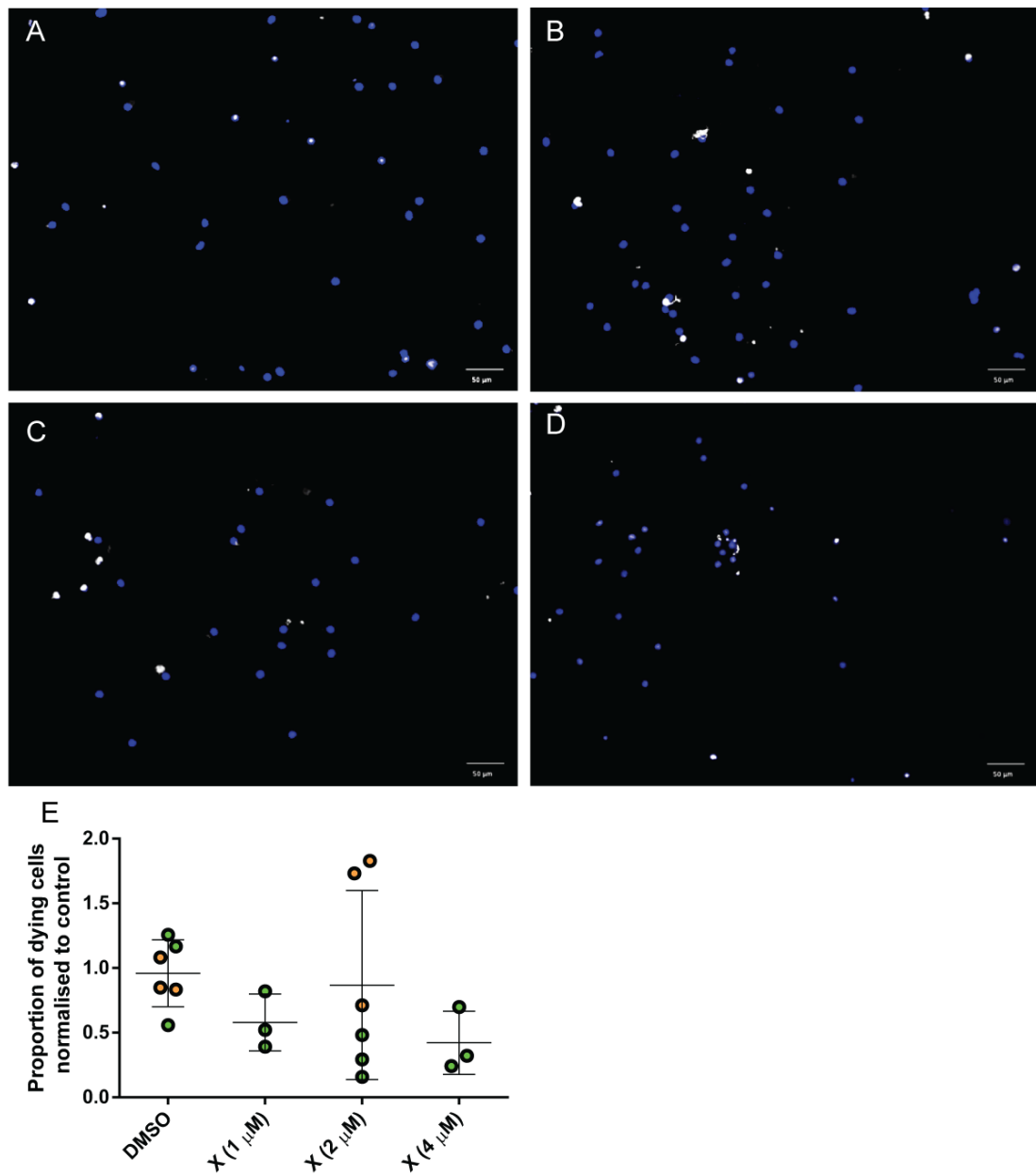


Figure 6.29: Xanthofulvin does not influence survival significantly. Compared to control (A), 1  $\mu$ M Xanthofulvin (B), 2  $\mu$ M Xanthofulvin (C) and 4  $\mu$ M Xanthofulvin (D) did not influence survival. Comparison of the 3 concentrations of Xanthofulvin and control showed that there was no significant difference (Kruskal-Wallis test,  $H=5.08$ ,  $n=6,3,6,3$ ,  $p=0.167$ ) (E). Blue is Hoechst and white is TUNEL+ cells.

### **Sema3A and inhibitors**

Compared to control (Figure 6.30 A), Sema3A (Figure 6.30 B) does not change the proportion of dying cells. However, combinations of Sema3A and anti-NP1(Sema3A) blocking antibody (Figure 6.30 C), Xanthofulvin (Figure 6.30 D) and SICHI (Figure 6.30 E) all appear to increase survival. Comparison of those conditions showed that there was a significant difference in the number of dying cells (Kruskal-Wallis test,  $H=10.03$ ,  $n=7,7,3,3,3$ ,  $p=0.40$ ). However, this difference was very small as Dunn's multiple comparison test did not find any significant comparison. The small effects of individual inhibitors have reached significance when in combination with Sema3A which at 22.5 nM significantly increases survival.

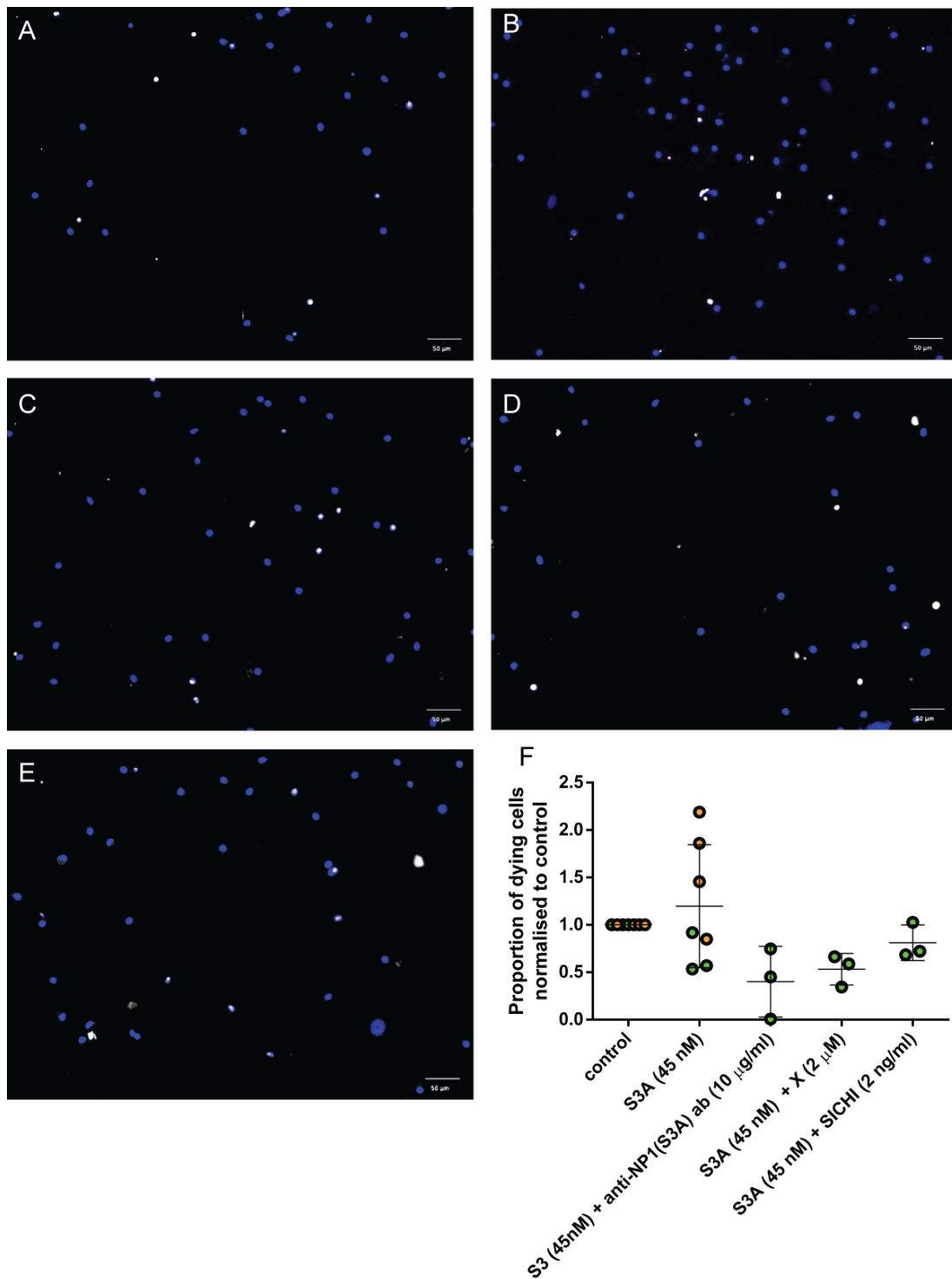


Figure 6.30: Sema3A together with NP1-Sema3A inhibitors do not significantly influence survival. Compared to control (A), Sema3A (B) did not influence the number of dying cells. However, all combinations of Sema3A and anti-NP1(Sema3A) antibody (C), Xanthofulvin (D), SICHI (E) slightly decreased the number of dying cells. Comparison of those conditions showed that there was a significant difference in the number of dying cells (Kruskal-Wallis test,  $H=10.03$ ,  $n=7,7,3,3,3$ ,  $p=0.40$ ). However, this difference was very small as Dunn's multiple comparison test did not find any significant comparison. Blue is Hoechst and white is TUNEL+ cells.

Therefore, low concentrations of Sema3A increases survival. Conversely to expectations, the tested inhibitors of Sema3A and NP1 also slightly but non-significantly increase survival. Addition of Sema3A together with inhibitors then results in further decreased OPC death.

## VEGF

Finally, we tested VEGF and anti-NP1(VEGF) blocking antibody. Compared to control (Figure 6.31 A), VEGF (Figure 6.31 B) and anti-NP1(VEGF) blocking antibody (Figure 6.31 C) did not change the number of dying cells. Comparison of VEGF, anti-NP1(VEGF) blocking antibody and control showed that there were no significant differences in the number of dying cells (Kruskal-Wallis test,  $H=0.0$ ,  $n=4,4,4$   $p>0.99$ ) (Figure 6.31 D).

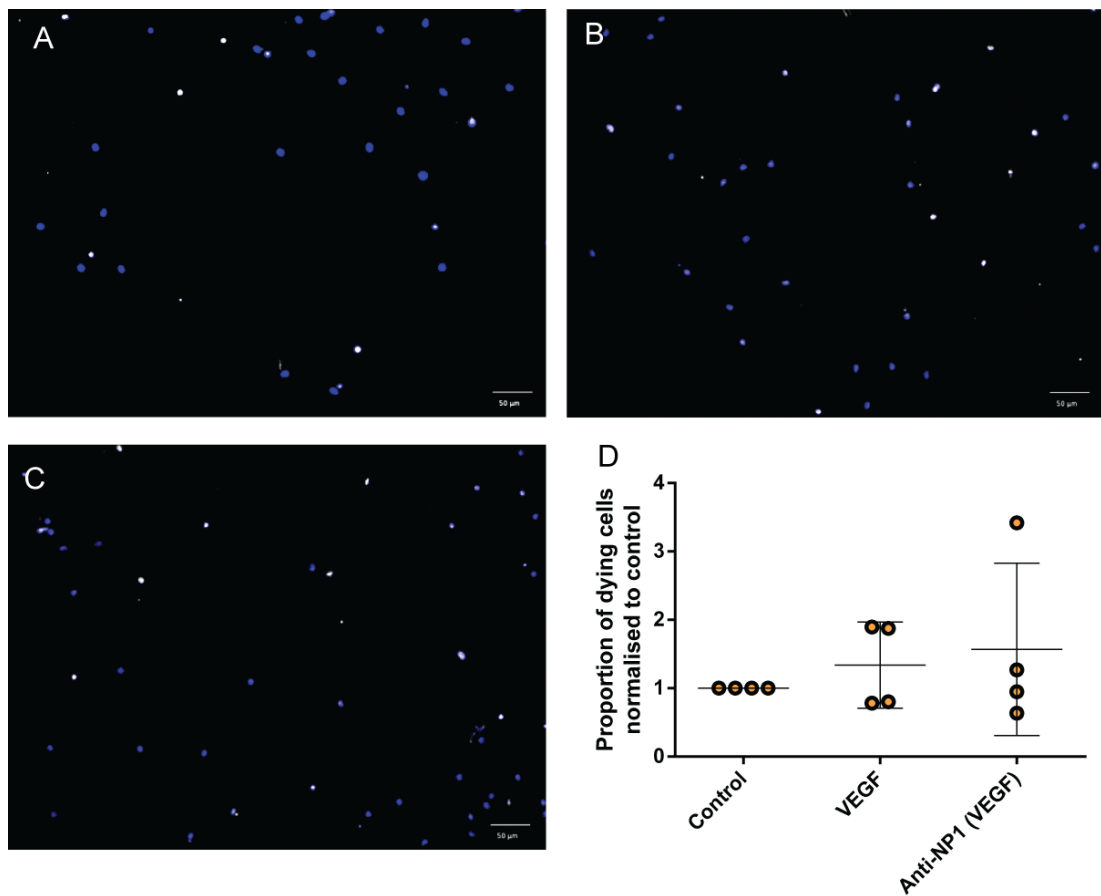


Figure 6.31: VEGF and anti-NP1(VEGF) blocking antibody do not influence survival. Compared to control (A), neither VEGF (B) nor anti-NP1(VEGF) blocking antibody (C) influenced the survival of rat OPCs. Comparison of VEGF, anti-NP1(VEGF) blocking antibody and control showed that there were no significant differences in the number of dying cells (Kruskal-Wallis test,  $H=0.0$ ,  $n=4,4,4$   $p>0.99$ ) (D). Blue is Hoechst and white is TUNEL+ cells.

### 6.7.4 Maturation

#### Sema3A in solution

We initially looked at whether Sema3A in solution influences the maturation of rat OPCs. Compared to control ( 6.32 A), 22.5 nM Sema3A in solution (Figure 6.32 B), 45 nM Sema3A in solution (Figure 6.32 C) and 90 nM Sema3A in solution (Figure 6.32 D) did not change the maturation of rat OPCs.

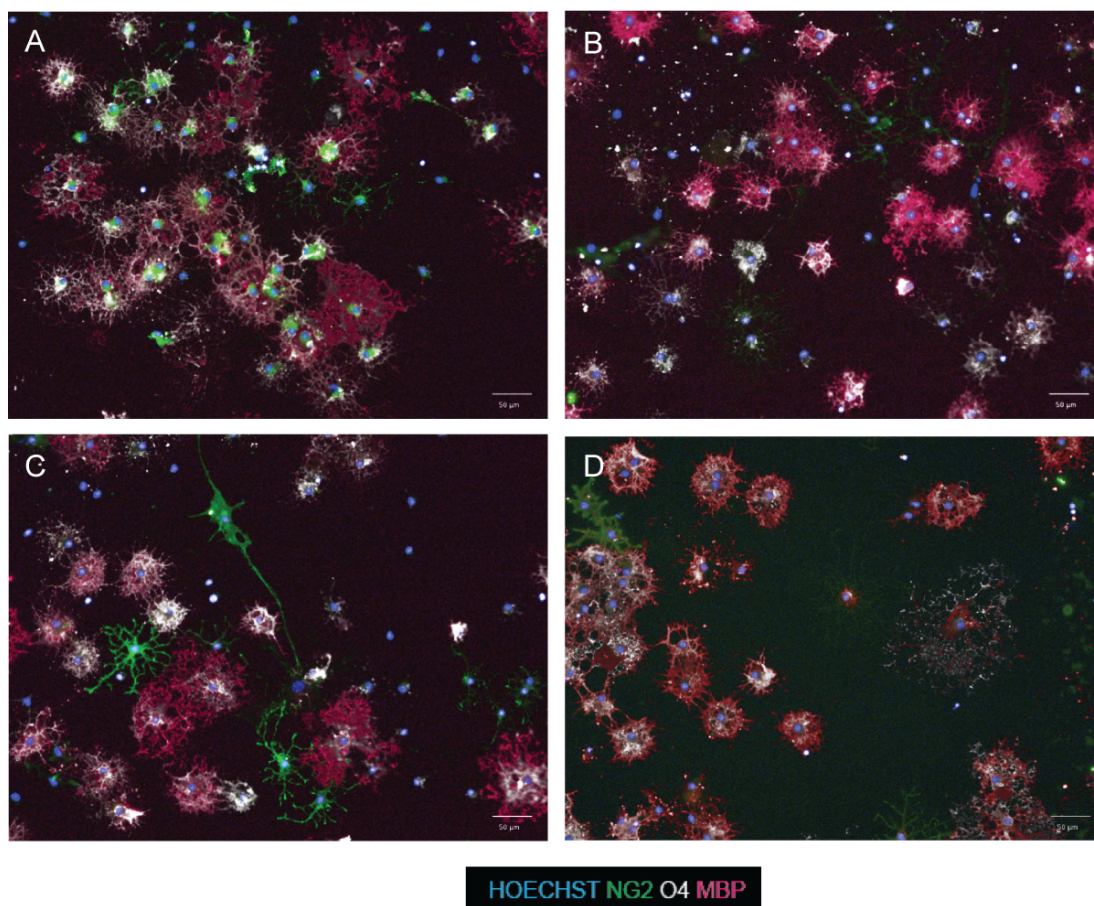


Figure 6.32: Sema3A in solution did not influence maturation of rat OPCs. Compared to control (A), 22.5 nM Sema3A in solution (B), 45 nM Sema3A in solution (C) and 90 nM Sema3A in solution (D) did not change proportion of NG2+, O4+ and MBP+ cells or the size of the MBP+ cells. Scale bar is 50 $\mu$ m. Blue is Hoechst, green is NG2+ cells, white is O4+ cells and red is MBP+ cells.

Comparison between the 3 concentrations of Sema3A in solution and control showed that those did not significantly affect the number of NG2+ cells (Kruskal-Wallis test,  $H=3.26$ ,  $n=3,3,3,3$ ,  $p=0.38$ ) (Figure 6.33 A). When we looked at the number of O4+ cells, we expected to see a reduction in the O4+ cells [296]. However, we found that none of the tested concentrations affected the number of O4+ cells significantly (Kruskal-Wallis test,  $H=4.34$ ,  $n=8,3,8,3$   $p=0.23$ ) (Figure 6.33 B). Similarly, none of the concentrations had a significant effect on the number

of MBP+ cells (Kruskal-Wallis test,  $H=1.54$ ,  $n=8,3,8,3$   $p=0.67$ ) (Figure 6.33 C) or their size (Kruskal-Wallis test,  $H=0.97$ ,  $n=8,3,8,3$   $p=0.808$ ) (Figure 6.33 D).

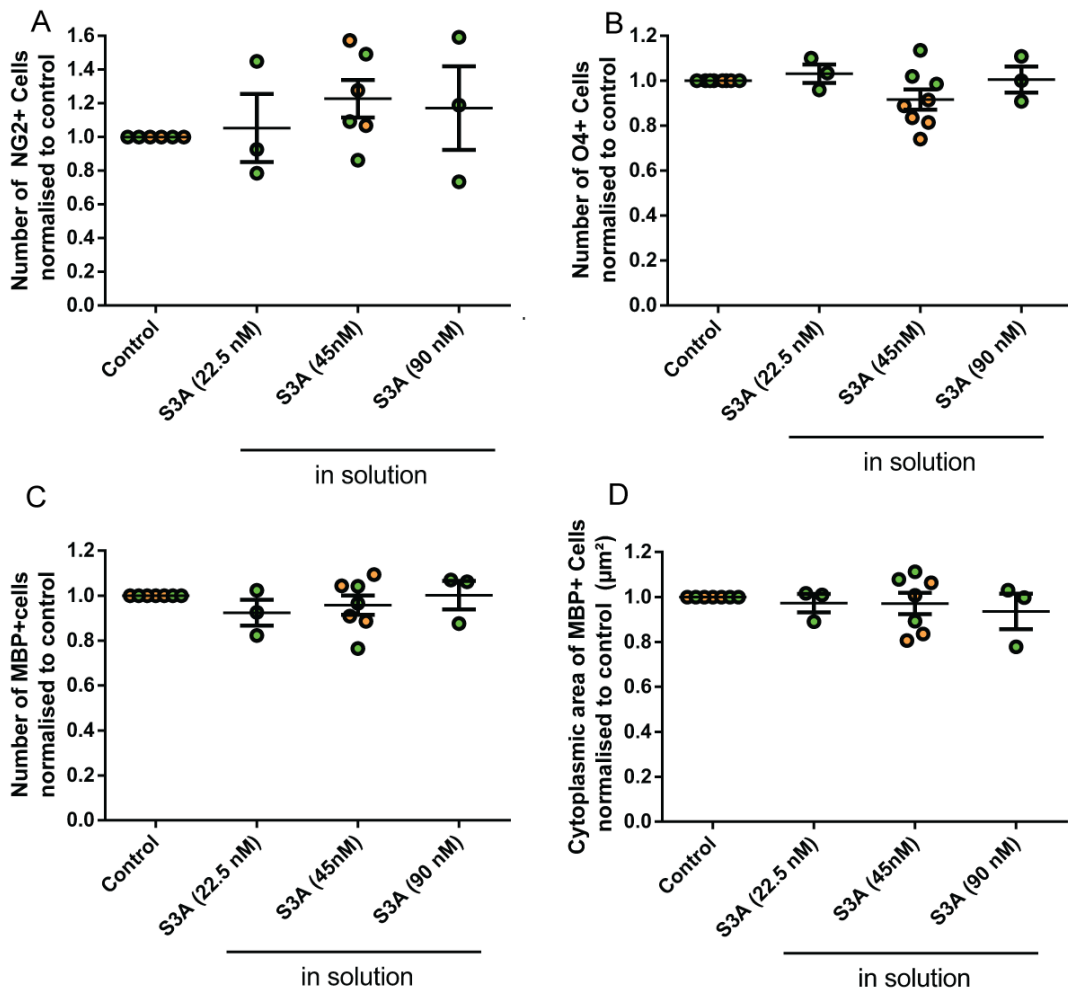


Figure 6.33: Quantification of concentrations of Sema3A in solution and control showed that they did not influence maturation of rat OPCs. We found that neither concentration of Sema3A in solution changed the number of NG2+ cells (Kruskal-Wallis test,  $H=3.26$ ,  $n=3,3,3,3$   $p=0.38$ ) (A), O4+ cells (Kruskal-Wallis test,  $H=4.34$ ,  $n=8,3,8,3$   $p=0.23$ ) (B), MBP+ cells (Kruskal-Wallis test,  $H=1.54$ ,  $n=8,3,8,3$   $p=0.67$ ) (C) and size of MBP+ cells (Kruskal-Wallis test,  $H=0.97$ ,  $n=8,3,8,3$   $p=0.808$ ) (D) compared to control.

We then tested Sema3A coated on the surface of the culture plate. Together with control (Figure 6.34 A), we tested 22.5 nM Sema3A (Figure 6.34 B), 45 nM coated Sema3A (Figure 6.34 C) and 90 nM coated Sema3A coated on the bottom of the culture dish (Figure 6.34 D). 45 nM Sema3A in solution (Figure 6.34 C) seemed to slightly increase the number of NG2+ cells and slightly reduce the number of O4+ cells compared to control (Figure 6.34 A). Moreover, the highest concentration of coated Sema3A, 90 nM, (Figure 6.34 D) appeared to make the MBP+ cells smaller (Figure 6.34 A).

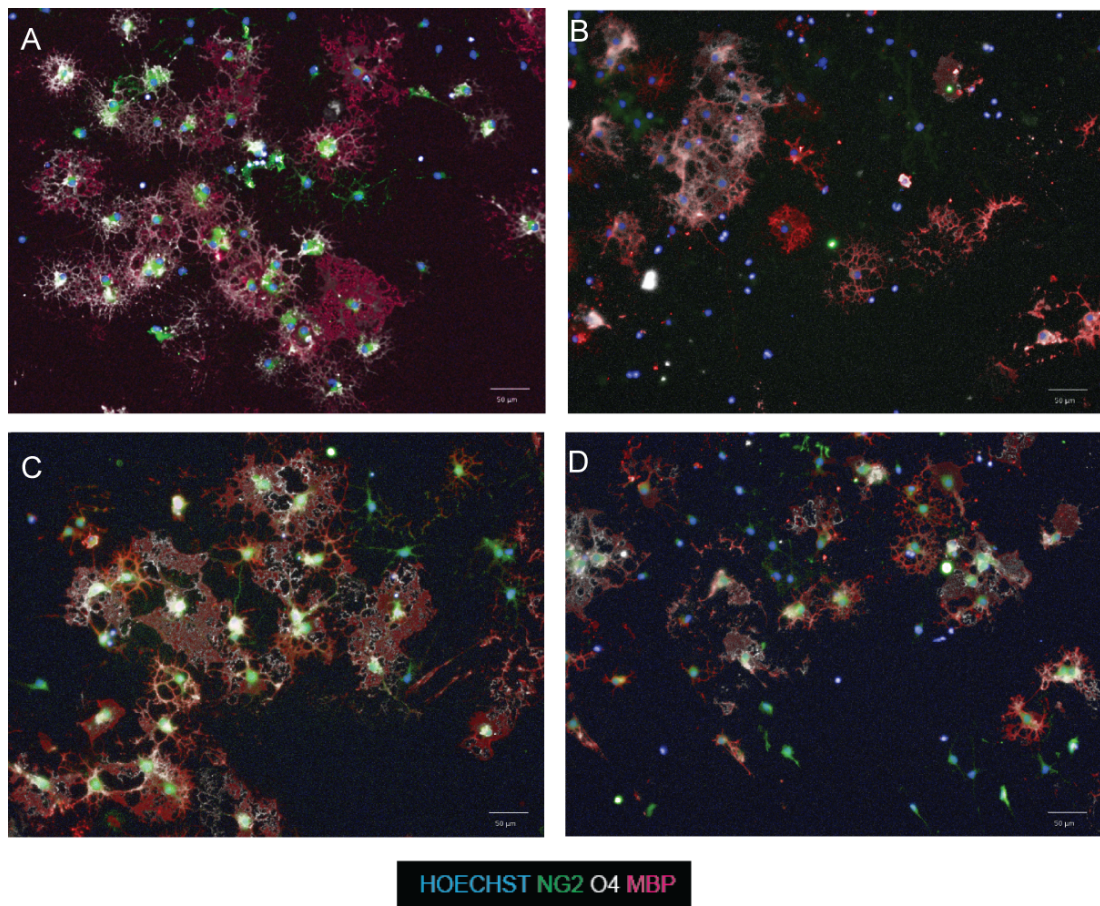


Figure 6.34: Coated Sema3A slightly reduces maturation. Images show control (A), 22.5 nM coated Sema3A (B), 45 nM coated Sema3A (C) and 90 nM coated Sema3A (D). Notably, there seemed to be a small increase in the number of NG2+ cells and a small decrease in number of O4+ cells upon treatment by 45 nM Sema3A (C) compared to control (A). Moreover, 90 nM coated Sema3A (D) also appeared to result in smaller MBP+ cells compared to control (A). Scale bar is 50  $\mu$ m. Blue is Hoechst, green is NG2+ cells, white is O4+ cells and red is MBP+ cells.

However, when we quantified these results, we found that this apparent difference in NG2+ cells was not significant (Kruskal-Wallis test,  $H=3.25$ ,  $n=3,3,3,3$   $p=0.397$ ) (Figure 6.35 A). The apparent compensatory decrease in O4+ cells was also not significant (Kruskal-Wallis test,  $H=6.90$ ,  $n=4,4,4,4$   $p=0.061$ ) (Figure 6.35 B). The concentrations of coated Sema3A did not influence the number of MBP+ cells (Kruskal-Wallis test,  $H=3.56$ ,  $n=4,4,4,4$   $p=0.332$ ) (Figure 6.35 C). The increasing concentration of coated Sema3A resulted in a small decrease in cytoplasmic area of MBP+ cells however this difference was not significant (Kruskal-Wallis test,  $H=6.81$ ,  $n=4,4,4,4$   $p=0.065$ ) (Figure 6.35 D).

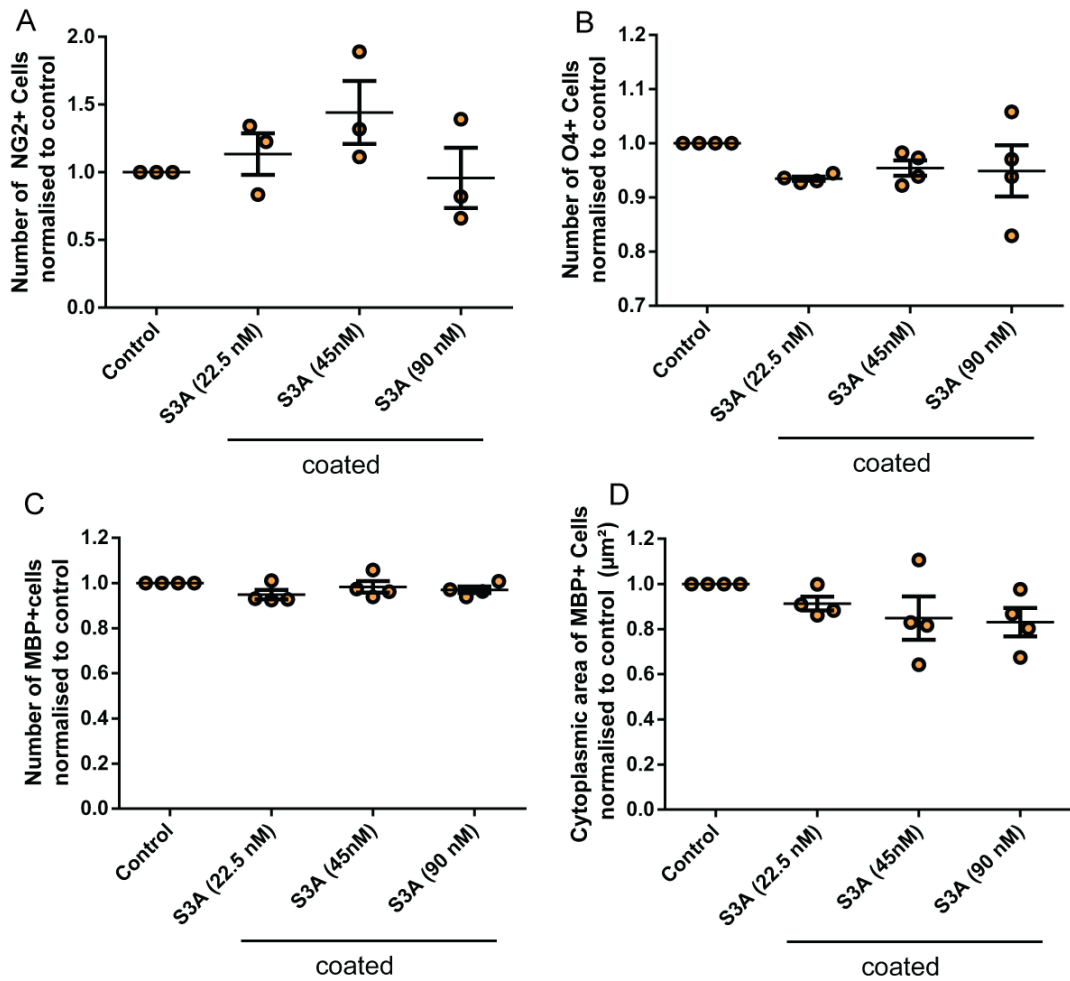


Figure 6.35: Quantification of the effect of coated Sema3A on maturation revealed no statistically significant effect. Graphs represent quantification of NG2+ cells (A), O4+ cells (B), MBP+ cells (C) and size of MBP+ cells (D). Although there is a slight increase in the number of NG2+ cells at 45 nM coated Sema3A compared to control, this difference was not significant (Kruskal-Wallis test,  $H=3.25$ ,  $n=3,3,3,3$   $p=0.397$ ) (A). This slight increase in NG2+ numbers was compensated by slight decrease of O4+ cells (B). However, this decrease was also not significant (Kruskal-Wallis test,  $H=6.90$ ,  $n=4,4,4,4$   $p=0.061$ ). The number of MBP+ cells was unchanged by the different concentrations of Sema3A (Kruskal-Wallis test,  $H=3.56$ ,  $n=4,4,4,4$   $p=0.332$ ) (C). Increasing concentration of coated Sema3A resulted in increasing decrease in the size of MBP+ cells. As before, however, this difference in MBP+ cytoplasmic area was not significant (Kruskal-Wallis test,  $H=6.81$ ,  $n=4,4,4,4$   $p=0.065$ ) (D).

### Xanthofulvin

We then looked at Xanthofulvin expecting it to increase maturation. Compared to control (Figure 6.36 A), 1  $\mu$ M Xanthofulvin (Figure 6.36 B), 2  $\mu$ M Xanthofulvin (Figure 6.36 C) and 4  $\mu$ M Xanthofulvin (Figure 6.36 D) did not have obvious effect on maturation apart from a different cell morphology in the highest concentration of Xanthofulvin.

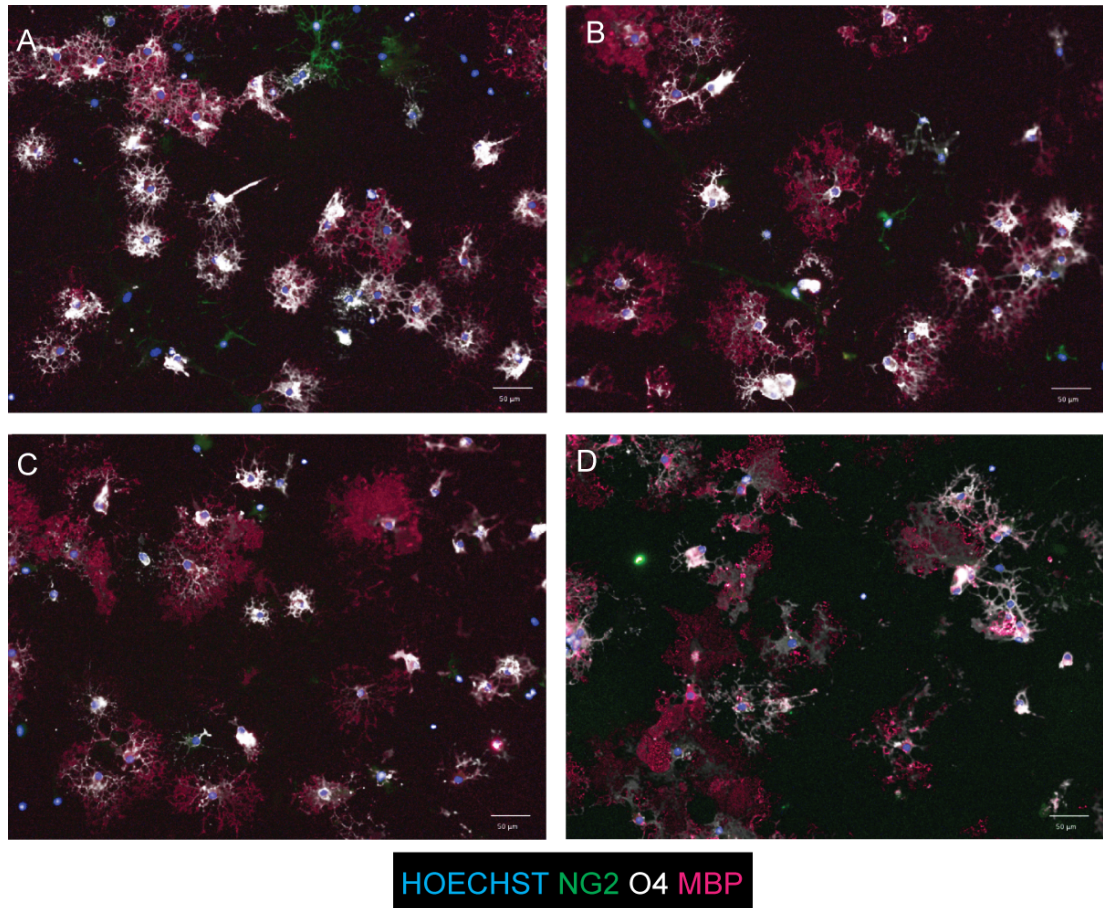


Figure 6.36: Example images of the effect of Xanthofulvin on maturation. Images shown are control (A), 1  $\mu$ M Xanthofulvin (B), 2  $\mu$ M Xanthofulvin (C) and 4  $\mu$ M Xanthofulvin (D). The highest concentration of Xanthofulvin appeared to change the cell morphology. Scale bar is 50  $\mu$ m. Blue is Hoechst, green is NG2+ cells, white is O4+ cells and red is MBP+ cells.

Quantification of those results revealed that Xanthofulvin does not significantly influence the number of NG2+, O4+ and MBP+ cells or their size.

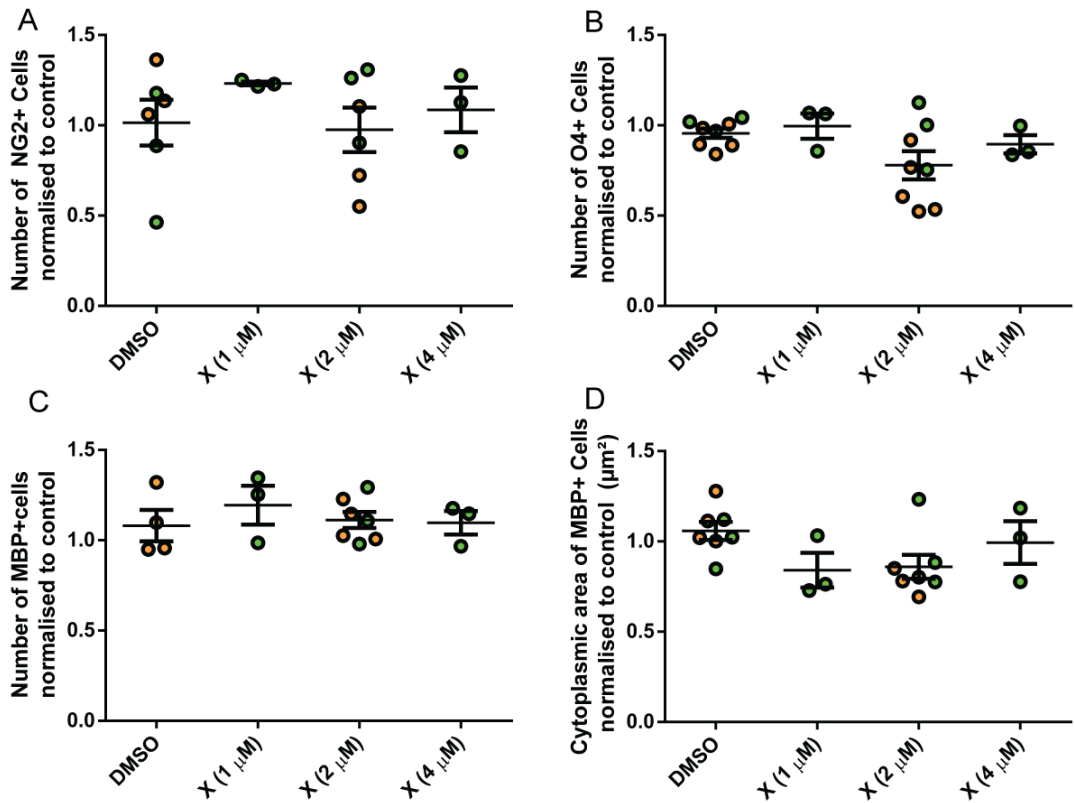


Figure 6.37: Xanthofulvin does not influence maturation. Comparison of the effect of the 3 concentrations of Xanthofulvin and DMSO on NG2+ cells showed that there was no significant difference (Kruskal-Wallis test,  $H=1.65$ ,  $n=6,3,6,3$   $p=0.681$ ) (A). Comparison of the effect of the 3 concentrations of Xanthofulvin and DMSO on proportion of O4+ cells showed that there was no significant difference (Kruskal-Wallis test,  $H=5.16$ ,  $n=8,3,8,3$   $p=0.161$ ) (B). Similarly, comparison of the effect of the 3 concentrations of Xanthofulvin and DMSO on proportion of MBP+ cells showed that there was no significant difference (Kruskal-Wallis test,  $H=1.87$ ,  $n=4,3,7,3$   $p=0.636$ ) (C). Finally, comparison of the effect of the 3 concentrations of Xanthofulvin and DMSO on the cytoplasmic area of MBP+ cells showed that there was no significant difference (Kruskal-Wallis test,  $H=5.28$ ,  $n=7,3,7,3$   $p=0.152$ ) (D).

## SICHI

Finally, we looked at SICHI. It did not appear to influence maturation at 1  $\mu$  g/ml, 2  $\mu$  g/ml SICHI or and 4  $\mu$  (Figure 6.38).

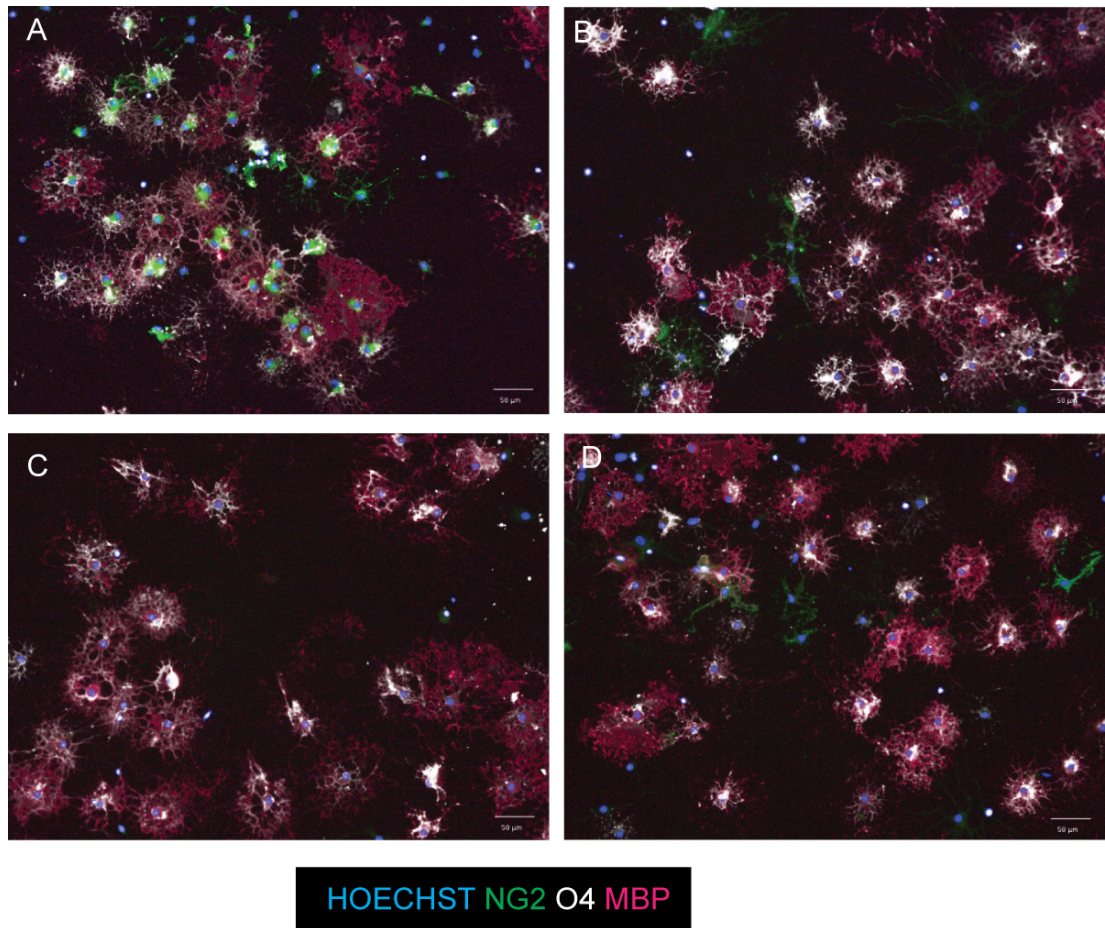


Figure 6.38: Example images of the effect of SICH1 on maturation. Images shown are control (A), 1  $\mu$  g/ml SICH1 (B), 2  $\mu$  g/ml SICH1 (C) and 4  $\mu$  g/ml SICH1 (D). Blue is Hoechst, green is NG2+ cells, white is O4+ cells and red is MBP+ cells.

Quantification of the results showed that SICH1 does not affect the proportion of NG2+ cells, O4+ cells, MBP+ cells or their size (Figure 6.39).

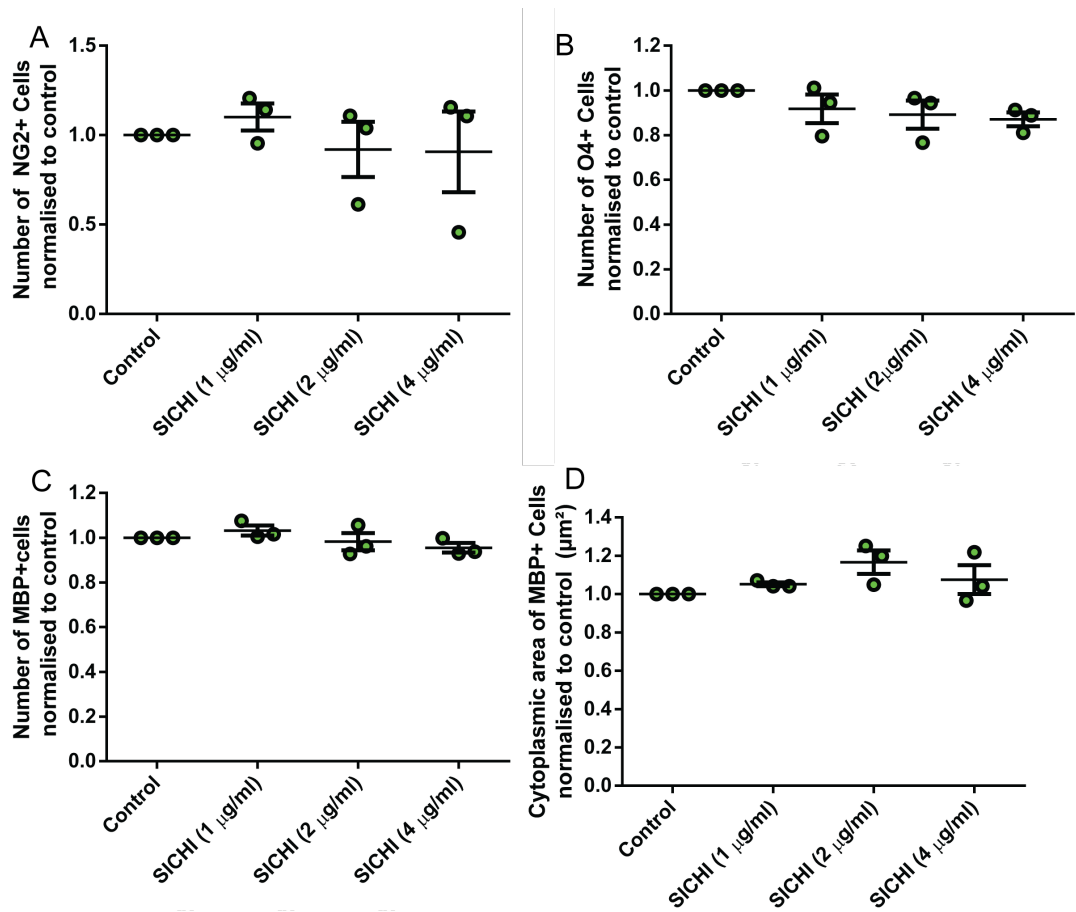


Figure 6.39: SICHI did not influence maturation. Comparison of the effect of the 3 concentrations of SICHI and control on NG2+ cells showed that there was no significant difference (Kruskal-Wallis test,  $H=1.38$ ,  $n=3,3,3,3$   $p=0.759$ ) (A). Comparison of the effect of the 3 concentrations of SICHI and control showed that there is no significant difference in the number of O4+ cells (Kruskal-Wallis test,  $H=4.92$ ,  $n=3,3,3,3$   $p=0.190$ ) (B). Similarly, Comparison of the effect of the 3 concentrations of SICHI and control showed there is no significant difference in the number of MBP+ cells (Kruskal-Wallis test,  $H=6.16$ ,  $n=3,3,3,3$   $p=0.090$ ) (C). Finally, comparison of the effect of the 3 concentrations of SICHI and control showed there is no significant difference in the area of MBP+ cells (Kruskal-Wallis test,  $H=5.85$ ,  $n=3,3,3,3$   $p=0.113$ ) (D).

# 7 Discussion

## 7.1 Remyelination failure

Remyelination is the endogenous repair mechanism of the central nervous system. However, this process is complex and involves multiple steps, cells and molecules. Due to this complexity, there are many reasons for remyelination to fail. Dysregulation of any of the multiple steps, cells and molecules involved in remyelination could lead to its failure [90]. Moreover, in MS remyelination takes place in a hostile environment for the oligodendroglia as it occurs while there is still ongoing inflammation-driven damage. However, repair also happens best when the immune system is active (section 1.4.2.)

The current therapeutic efforts in MS are focused on preventing new lesions, which is reasonably successful, protecting axons from dying and improving remyelination (which as yet are aspirational) [160]. The latter two therapeutic approaches are particularly hard as it is difficult to accurately measure remyelination and understand the remyelination time course in patients as yet [212]. Moreover, in different patients remyelination could fail because of OPC migration or maturation block which would require different therapies (Section 1.6) but differentiating which patients have a failure in each of those and when is currently impossible [212]. Despite these difficulties, the ideal drug would be orally available, long lasting, able to penetrate the BBB and without any side effects [212]. To find therapeutic targets, it is important to not only consider the positive effect their inhibition would have on remyelination, but also that they are not redundant and their loss cannot be compensated for [90].

Moreover, in order to study the suitability of a therapeutic target, we often assess remyelination in genetically modified animal models. However, rodents repair very well after a demyelinating insult while the same is not true for humans. There are other differences which limit the usability of our current animal models. There is a difference in the size of lesions between animal models and human MS. One study estimated that to fully repopulate a 2 cm diameter human lesions adult OPCs would need to migrate for 5 months [48]. As a comparison, LPC-induced mouse lesions are around 1 mm diameter [48] and can be populated by OPCs in less than 10 days [29]. These immense differences between animal models and human are part of the reasons why it is so hard to translate between animal and in vitro and human and why remyelination enhancing clinical trials so far have failed [290].

Bearing in mind the therapeutic goals in the multiple sclerosis field and the difficulties discussed above, we set out to investigate the suitability of two potential therapeutic targets - NDST1/HS and Sema3A/NP1. Since blinding and random allocation to groups have been suggested as important factors to improve the translation of research into clinic [321], we performed

blinded/automatic analysis and random group allocation.

## 7.2 NDST1

NDST1 was shown to be important for OPC migration into lesions and remyelination in animal model by Pascale Durbec's group and we set out to investigate if it is also important in MS. To do this we analysed its expression pattern in *post-mortem* multiple sclerosis tissue and compared it to control tissue. We found that it was overexpressed in MS primarily in oligodendroglia and that the NDST1+ oligodendroglia negatively correlate with the size of the lesion. Moreover, we found marked differences in the number of NDST1+ cells in the lesions between different MS patients. Many pathological features such as oligodendrocyte numbers [179], major type of demyelination [180] and remyelination potential [242] have been observed to be the same within patients but different between patients. Therefore, we asked whether the number of NDST1+ cells is connected to the ability of a patient to repair. We found that the higher the number of NDST1+ cells a patient has in their lesions, the more likely they are to have remyelinated and active lesions instead of chronic lesions (remyelination potential). Therefore, the higher the number of NDST1+ oligodendroglia around the lesion, the more they can deposit heparan sulfate and contribute to repair. This is consistent with the mouse data from Pascale Durbec's group which indicates that loss of NDST1 impairs OPC migration and remyelination. Furthermore, a heparan sulfate proteoglycan called GPC5 has been identified as a MS susceptibility gene [15] further indicating that NDST1 and HS might play role in multiple sclerosis. GPC5 variants have been associated with different patient responses to interferon $\beta$  [33] which might again point to the importance of ECM in sequestering signalling molecules such as immune cytokines and chemorepulsive molecules such as Sema3A. Therefore, in this case, the pathways involved in mouse and human remyelination do seem similar and worth investigating more.

## 7.3 Sema3A and NP1

Sema3A impairs OPC migration [29] [245] [330] and maturation [296] and therefore reduces remyelination [29] [245]. In addition to this, it is involved in numerous immune processes (section 1.9.3). The involvement of Sema3A in both the regeneration and the immune response makes it ideally placed to modulate both those parts in MS [117]. In addition to this, patients with a Sema3A mutation [121] have been identified indicating that inhibition of Sema3A is not lethal in human. Therefore, Sema3A and its receptor NP1 can be explored as a potential therapeutics in MS.

However, Sema3A's effect on the immune system is complex with both anti-inflammatory (section 1.9.3) and pro-inflammatory (section 1.9.3) actions recorded in the literature. To complicate things further, anti-inflammatory effects are not only beneficial in MS as inflammation is important for remyelination (section 1.4.2). For example, transplanted oligodendroglial cell line cells did not migrate far at all in normal brain but migrated up to 6 cm from original in-

jection site in EAE [309] indicating that inflammation increases OPC migration. Therefore, decreasing the inflammatory response might impede migration and hence remyelination [90].

Therefore *Sema3A* may have either beneficial or detrimental effects on the immune system and a detrimental effect in remyelination. Since we can either inhibit or enhance the action of molecules, those different effects in different systems pose a challenge. What would be ideal is to stratify those effects and identify different receptors or coreceptors which mediate those different downstream effects in immunity and CNS. The literature is convincing that NP1 is the only receptor for *Sema3A* [152] [153] [125] [188] [51] (section 1.8.2). However, the majority of those studies have been conducted on neurones and only one on oligodendroglia [259].

Conversely, our *in vivo* data and a few other publications (Section 5.7.1) suggest that NP1 might not be the only receptor mediating *Sema3A* signalling in some cells. NP1 could be the only receptor for *Sema3A* in neurones, as the literature suggests. The same might be true for macrophage/ microglia as loss of NP1 in the NP1(*Sema3A*-) mice resulted in a change of the immune response (Figure 5.16). However, in oligodendrocytes, NP1 might not be the only receptor mediating *Sema3A* effects as the loss of NP1 (in NP1(*Sema3A*-) mouse) did not change their behaviour even though increasing or decreasing *Sema3A* does (Section 1.9.1). Since the *Sema3A* effect in the CNS is unchanged by removal of NP1 but the immune effects of *Sema3A* require NP1, this could allow stratification of those effects and the therapeutic possibility to separately target them. However, targeting NP1 appears to not be a therapeutic possibility as it does not prevent *Sema3A*'s detrimental effect on OPC migration, maturation and therefore remyelination. In addition to this, it appears to alter the immune response to a more pro-inflammatory one with more activated macrophages / microglia and of predominantly the pro-inflammatory subtype which would be harmful to remyelination [205]. It is also worth noting that both NP1-*Sema3A* inhibitors which have been efficient at increasing neuronal regeneration in different models - Xantofulvin [150] and SICHI [208] do not work by inhibiting NP1. Instead, Xantofulvin binds to *Sema3A* while [150] while SICHI binds ECM and prevents *Sema3A* interacting with ECM [57]. This again shows that methods alternative to NP1 inhibition might be more beneficial in therapy. In addition to this, it exemplifies the importance of *Sema3A*'s interaction with ECM and therefore the possible connection between NDST1/HS and *Sema3A*/NP1.

Therefore, we have shown that NP1 is a redundant factor for OPC migration, maturation and therefore remyelination. There are multiple members of the semaphorin, plexin and neuropilin families of proteins so some redundancy and compensation by other molecules in the absence of Neuropilin could be expected [141].

Moreover, we have found that *Sema3A* can also stimulate OPC proliferation and survival at different concentrations at least *in vitro*. In addition to this, we suggest that low concentration *Sema3A* and NP1 activation might be important for the ability of OPCs to deform and squeeze through small gaps *in vivo* or pores in a transwell while higher concentrations are chemorepulsive. This effect could be attributed to the F actin reorganisation after adding class 3 semaphorins which increases cell deformability [62]. This is further supported by the fact that *Sema3A* affects cell migration in a transwell assay (section 6.2.4) but not in flat surface motility or microfluidic chambers migration assay (Roberta Felici unpublished data). The same

effect was observed in with Sema3C which did not affect dendritic cell migration in a microfluidic chamber but increased their speed of migration in a transwell assay and was explained by Sema3C's ability to increase cell deformability [62]. Therefore, a low concentration of Sema3A and NP1 activation might be essential for cell deformability and completely inhibiting the Sema3A site of NP1 might impede this.

## 7.4 Future prospects

Finding therapeutics in MS is particularly challenging as there could be multiple reasons for remyelination failure. The absence of positive modulators and presence of negative modulators of remyelination as well as improper timing of different signals could be responsible [91]. In addition to this, changing only one of the many signalling molecules creating the pro-repair environment might not be enough. Finally, pro-recruitment and pro-maturation therapies might be mutually exclusive as prolonging the recruitment phase of remyelination at the expense of maturation or vice versa might not benefit remyelination [91]. Therefore, we need to find ways to identify which is problematic in each patient and when is the best time to administer treatment.

This section is dedicated to further experiments I would do if I had unlimited resources and time.

For the NDST1 part of the project (Chapter 3), I would like to add further MS patients and controls to the analysis. Even though we used all available tissue for this analysis, the patient number is still low (9 MS patient and 4 controls). In addition, I would like to be able to visualise heparan sulfate proteoglycan in MS tissue which will hopefully be possible with identification of better antibodies against HS. Finally, I would like to test the effect of NDST1 loss using CRISPR/Cas9 or heparinase (loss of HS) on the migration of human embryonic stem cell derived oligodendrocytes [8] or primary isolated human OPCs [195].

In the investigation of the NP1(Sema3A-) mice (Chapter 4) and PDGFR $\alpha$ -Cre x flx-NP1-flx mice (Chapter 5), I would have liked to do complete reconstruction of the lesion sizes in the 4 genotypes. In addition to this, I would have liked to perform IHC with antibodies against O4 to mark the immature oligodendrocytes or Olig2 to mark all oligodendroglia to ensure that in the current analysis we have not missed immature oligodendrocytes. Moreover, to determine the functionality of the double positive microglia/ macrophage cells, IHC with further pro-inflammatory and pro-repair markers should be performed. I would have also liked to investigate and compare the expression of Sema3A in the lesions of TG and WT animals since its level could have changed after loss/mutation of NP1. It would also be interesting to check the levels of the two possible 'mystery' receptors which could also mediate Sema3A signalling in oligodendroglia - PlexinAs and NP2. Finally, addition of more animals to the analysis would further strengthen the confidence in our results.

Those mouse lines were terminated because they were too expensive to maintain, especially as the homozygous NP13A- mice often died very early before they could be used or even sometimes even identified. However, before that we did that, ES cells from both TG an-

imals and their WT animals were derived and frozen down. Those ES cells can be used to differentiate into OPCs which do not have NP1 or have the mutated Sema3A site of NP1. Co-immunoprecipitation with an antibody against Sema3A would help identify its binding partners and comparison of those binding partners between TG and WT cells will identify the 'mystery' receptors which could also mediate Sema3A signalling in oligodendroglia. In addition to this, the ES-cell derived OPCs can be used to study the effects of loss of the Sema3A site on NP1 or loss of NP1 on OPC behaviour (Chapter 6). This is a cleaner way than a blocking antibody which might have side effects or whose binding to a cell can produce a physical effect on the cell. Furthermore, addition of Sema3A to those mutant OPCs will allow us to investigate if NP1 is solely responsible for any of the Sema3A effects on OPC behaviour or they can be compensated. It is possible that NP1 is important for some Sema3A effects but not for others. Dose-response curves of all NP1 ligands and inhibitors could shed further light on the possible concentration dependent effects. Finally, increased number of experiments would ideally be performed with some of the concentrations of NP1 ligands and inhibitors as for some of the conditions we only have 3 independent experiments.

It would be interesting if Sema3A's effects on OPCs can indeed be mediated by receptors other than NP1 and it might open new therapeutic avenues to improve OPC migration, maturation and therefore remyelination in multiple sclerosis.

## Bibliography

- [1] Lisette M Acevedo, Samuel Barillas, Sara M Weis, Joachim R Göthert, and David a Cheresch. Semaphorin 3A suppresses VEGF-mediated angiogenesis yet acts as a vascular permeability factor. *Blood*, 111(5):2674–2680, mar 2008.
- [2] Ralf H. Adams, Marion Lohrum, Andreas Klostermann, Heinrich Betz, and Andreas W. Püschel. The chemorepulsive activity of secreted semaphorins is regulated by furin-dependent proteolytic processing. *EMBO Journal*, 16(20):6077–6086, 1997.
- [3] Neeta Adhikari, David L. Basi, De Wayne Townsend, Melissa Rusch, Ami Mariash, Sureni Mullegama, Adrienne Watson, Jon Larson, Sara Tan, Ben Lerman, Jeffrey D. Esko, Scott B. Selleck, and Jennifer L. Hall. Heparan sulfate Ndst1 regulates vascular smooth muscle cell proliferation, vessel size and vascular remodeling. *Journal of Molecular and Cellular Cardiology*, 49(2):287–293, 2010.
- [4] Neeta Adhikari, Melissa Rusch, Ami Mariash, Qinglu Li, Scott B. Selleck, and Jennifer L. Hall. Alterations in heparan sulfate in the vessel in response to vascular injury in the mouse. *Journal of cardiovascular translational research*, 1(3):236–240, 2008.
- [5] Eitan M. Akirav, Yan Xu, and Nancy H. Ruddle. Resident B Cells Regulate Thymic Expression of Myelin Oligodendrocyte Glycoprotein. *J Neuroimmunol.*, 235(1-2):33–39, 2011.
- [6] Chantal Allamargot, Annick Pouplard-Barthelaix, and Catherine Fressinaud. A single intracerebral microinjection of platelet-derived growth factor (PDGF) accelerates the rate of remyelination in vivo. *Brain Research*, 918(1-2):28–39, 2001.
- [7] Maria Nordheim Alme, Agnes E. Nystad, Lars Bø, Kjell Morten Myhr, Christian A. Vedeler, Stig Wergeland, and Øivind Torkildsen. Fingolimod does not enhance cerebellar remyelination in the cuprizone model. *Journal of Neuroimmunology*, 285:180–186, 2015.
- [8] Walaa F Alsanie, Jonathan C Niclis, and Steven Petratos. Human embryonic stem cell-derived oligodendrocytes: protocols and perspectives. *Stem cells and development*, 22(18):2459–2476, sep 2013.
- [9] Charles ffrench-Constant Anna Setzu, Justin D. Lathia, Chao Zhao, Karen Wells, Mahendra S. Rao and Robin J. M. Franklin. Inflammation Stimulates Myelination by Transplanted Oligodendrocyte Precursor Cells. *Glia*, 54:297–303, 2006.

- [10] Brent a Appleton, Ping Wu, Janice Maloney, JianPing Yin, Wei-Ching Liang, Scott Stawicki, Kyle Mortara, Krista K Bowman, J Michael Elliott, William Desmarais, J Fernando Bazan, Anil Bagri, Marc Tessier-Lavigne, Alexander W Koch, Yan Wu, Ryan J Watts, and Christian Wiesmann. Structural studies of neuropilin/antibody complexes provide insights into semaphorin and VEGF binding. *The EMBO journal*, 26(23):4902–4912, 2007.
- [11] J J Archelos, J Trotter, S Previtali, B Weissbrich, K V Toyka, and H P Hartung. Isolation and characterization of an oligodendrocyte precursor- derived B-cell epitope in multiple sclerosis. *Annals of Neurology*, 43(1):15–24, 1998.
- [12] Heather A. Arnett, Jeff Mason, Mike Marino, Kinuko Suzuki, Glenn K. Matsushima, and Jenny P Y Ting. TNF $\alpha$  promotes proliferation of oligodendrocyte progenitors and remyelination. *Nature Neuroscience*, 4(11):1116–1122, 2001.
- [13] Heather A Arnett, Ying Wang, Glenn K Matsushima, Kinuko Suzuki, and Jenny P-Y Ting. Functional genomic analysis of remyelination reveals importance of inflammation in oligodendrocyte regeneration. *Journal of Neuroscience*, 23(30):9824–32, 2003.
- [14] D Bagnard, C Vaillant, S T Khuth, N Dufay, M Lohrum, a W Puschel, M F Belin, J Bolz, and N Thomasset. Semaphorin 3A-vascular endothelial growth factor-165 balance mediates migration and apoptosis of neural progenitor cells by the recruitment of shared receptor. *The Journal of neuroscience : the official journal of the Society for Neuroscience*, 21(10):3332–3341, 2001.
- [15] Sergio E Baranzini, Joanne Wang, Rachel a Gibson, Nicholas Galwey, Yvonne Naegelin, Frederik Barkhof, Ernst-Wilhelm Radue, Raija L P Lindberg, Bernard M G Uitdehaag, Michael R Johnson, Aspasia Angelakopoulou, Leslie Hall, Jill C Richardson, Rab K Prin-jha, Achim Gass, Jeroen J G Geurts, Jolijn Kragt, Madeleine Sombekke, Hugo Vrenken, Pamela Qualley, Robin R Lincoln, Refujia Gomez, Stacy J Caillier, Michaela F George, Hourieh Mousavi, Rosa Guerrero, Darin T Okuda, Bruce a C Cree, Ari J Green, Em-manuelle Waubant, Douglas S Goodin, Daniel Pelletier, Paul M Matthews, Stephen L Hauser, Ludwig Kappos, Chris H Polman, and Jorge R Oksenberg. Genome-wide as-sociation analysis of susceptibility and clinical phenotype in multiple sclerosis. *Human molecular genetics*, 18(4):767–778, feb 2009.
- [16] Frederik Barkhof, Wolfgang Brück, Corline JA De Groot, Elisabeth Begers, Sandra Hulshof, Jeroen Geurts, and Chris H Polman. Remyelinated Lesions in Multiple Sclerosis. *Archives of neurology*, 60:1073–81, 2003.
- [17] Michael H. Barnett and John W. Prineas. Relapsing and Remitting Multiple Sclerosis: Pathology of the Newly Forming Lesion. *Annals of Neurology*, 55:458–468, 2004.
- [18] M. Baumann, E. Steichen-Gersdorf, B. Krabichler, T. Müller, and A.R. Janecke. A

- recognizable type of syndromic short stature with arthrogryposis caused by bi-allelic *SEMA3A* loss-of-function variants. *Clinical Genetics*, 92(1):86–90, 2017.
- [19] Ahmad Bechara, Homaira Nawabi, Frédéric Moret, Avraham Yaron, Eli Weaver, Muriel Bozon, Karima Abouzid, Jun Lin Guan, Marc Tessier-Lavigne, Vance Lemmon, and Valérie Castellani. FAK-MAPK-dependent adhesion disassembly downstream of L1 contributes to semaphorin3A-induced collapse. *EMBO Journal*, 27(11):1549–1562, 2008.
- [20] O Behar, J a Golden, H Mashimo, F J Schoen, and M C Fishman. Semaphorin III is needed for normal patterning and growth of nerves, bones and heart., oct 1996.
- [21] Dwight E Bergles, J D Roberts, P Somogyi, and Craig E Jahr. Glutamatergic synapses on oligodendrocyte precursor cells in the hippocampus. *Nature*, 405(6783):187–91, 2000.
- [22] Allan J. Bieber, Scott Kerr, and Moses Rodriguez. Efficient central nervous system remyelination requires T cells. *Annals of Neurology*, 53(5):680–684, 2003.
- [23] Andreas Bitsch and Wolfgang Brück. Differentiation of Multiple Sclerosis Subtypes. *CNS Drugs*, 16(6):405–418, 2002.
- [24] C Bjartmar, R P Kinkel, G Kidd, R a Rudick, and B D Trapp. Axonal loss in normal-appearing white matter in a patient with acute MS. *Neurology*, 57(7):1248–1252, 2001.
- [25] C. Bjartmar, J. R. Wujek, and B. D. Trapp. Axonal loss in the pathology of MS: Consequences for understanding the progressive phase of the disease. *Journal of the Neurological Sciences*, 206(2):165–171, 2003.
- [26] W F Blakemore, J M Gilson, and A J Crang. Transplanted Glial Cells Migrate Over a Greater Distance and Remyelinate Demyelinated Lesions More Rapidly Than. *Journal of Neuroscience Research*, 294(March):288–294, 2000.
- [27] Benedetta Bodini, Mattia Veronese, Daniel García-Lorenzo, Marco Battaglini, Emilie Poirion, Audrey Chardain, Léorah Freeman, Céline Louapre, Maya Tchikviladze, Caroline Papeix, Frédéric Dollé, Bernard Zalc, Catherine Lubetzki, Michel Bottlaender, Federico Turkheimer, and Bruno Stankoff. Dynamic Imaging of Individual Remyelination Profiles in Multiple Sclerosis. *Annals of Neurology*, 79(5):726–738, 2016.
- [28] Leonie A. Boven, Marjan Van Meurs, Marloes Van Zwam, Annet Wierenga-Wolf, Rogier Q. Hintzen, Rolf G. Boot, Johannes M. Aerts, Sandra Amor, Edward E. Nieuwenhuis, and Jon D. Laman. Myelin-laden macrophages are anti-inflammatory, consistent with foam cells in multiple sclerosis. *Brain*, 129(2):517–526, 2006.
- [29] Amanda Boyd, Hui Zhang, and Anna Williams. Insufficient OPC migration into demyelinated lesions is a cause of poor remyelination in MS and mouse models. *Acta neuropathologica*, 125(6):841–59, jun 2013.

- [30] Celia Fildes Brosnan, Gerald L Stoner, Barry R Bloom, and Henryk M Wisniewski. Studies on Demyelination by Activated Lymphocytes in the Rabbit Eye : II . Antibody-Dependent Cell-Mediate Demyelination. *J Immunol*, 118:2103–2100, 2018.
- [31] Wolfgang Brück. The pathology of multiple sclerosis is the result of focal inflammatory demyelination with axonal damage. *Journal of neurology*, 252 Suppl:v3–9, nov 2005.
- [32] Mary B Bunge, Richard P. Bunge, and Hans Ris. Ultrastructural study of remyelination in an experimental lesion in adult cat spinal cord. *J Biophys. Biochem. Cytol*, 10:67–94, 1961.
- [33] E Byun, S J Caillier, X Montalban, P Villoslada, O Fernandez, D Brassat, M Comabella, J Wang, L F Barcellos, S E Baranzini, and J R Oksenberg. Genome-wide pharmacogenomic analysis of the response to interferon beta therapy in multiple sclerosis. *Arch.Neurol.*, 65(3):337–344, 2008.
- [34] Costa C., Martinez-Saez E., Gutierrez-Franco A., Ortega-Aznar A., Ramon y Cajal S., and Montalban X. Expression of semaphorin 3A, semaphorin 7A, and their receptors in the central nervous system lesions of multiple sclerosis. *Multiple Sclerosis*, 19(11 SUPPL. 1):129, 2013.
- [35] Graham R. Campbell, Nobuhiko Ohno, Doug M. Turnbull, and Don J. Mahad. Mitochondrial changes within axons in multiple sclerosis: An update. *Current Opinion in Neurology*, 25(3):221–230, 2012.
- [36] Anna Cariboni, Kathryn Davidson, Sonja Rakic, Roberto Maggi, John G. Parnavelas, and Christiana Ruhrberg. Defective gonadotropin-releasing hormone neuron migration in mice lacking SEMA3A signalling through NRP1 and NRP2: Implications for the aetiology of hypogonadotropic hypogonadism. *Human Molecular Genetics*, 20(2):336–344, 2011.
- [37] W. M. Carroll and A. R. Jennings. Early recruitment of oligodendrocyte precursors in CNS demyelination. *Brain*, 117(3):563–578, 1994.
- [38] Andrea Casazza, Damya Laoui, Mathias Wenes, Sabrina Rizzolio, Nicklas Bassani, Marco Mambretti, Sofie Deschoemaeker, Jo a Van Ginderachter, Luca Tamagnone, and Massimiliano Mazzone. Impeding macrophage entry into hypoxic tumor areas by Sema3A/Nrp1 signaling blockade inhibits angiogenesis and restores antitumor immunity. *Cancer cell*, 24(6):695–709, dec 2013.
- [39] Evelyne Cash, Yiping Zhang, and Ortwin Rott. Microglia present myelin antigens to t cells after phagocytosis of oligodendrocytes, 1993.
- [40] V Castellani, a Chédotal, M Schachner, C Faivre-Sarrailh, and G Rougon. Analysis of the L1-deficient mouse phenotype reveals cross-talk between Sema3A and L1 signaling pathways in axonal guidance. *Neuron*, 27(2):237–49, aug 2000.

- [41] V. Castellani, E. De Angelis, S. Kenwrick, and G. Rougon. Cis and trans interactions of L1 with neuropilin-1 control axonal responses to semaphorin 3A. *EMBO Journal*, 21(23):6348–6357, 2002.
- [42] Valérie Castellani, Julien Falk, and Geneviève Rougon. Semaphorin3A-induced receptor endocytosis during axon guidance responses is mediated by L1 CAM. *Molecular and cellular neurosciences*, 26(1):89–100, may 2004.
- [43] Alfonso Catalano. The neuroimmune semaphorin-3A reduces inflammation and progression of experimental autoimmune arthritis. *Journal of immunology (Baltimore, Md. : 1950)*, 185(10):6373–83, 2010.
- [44] Alfonso Catalano, Paola Caprari, Simona Moretti, Monica Faronato, Luca Tamagnone, and Antonio Procopio. Semaphorin-3A is expressed by tumor cells and alters T-cell signal transduction and function. *Blood*, 107(8):3321–3329, 2006.
- [45] M. Cayre, S. Courtes, F. Martineau, M. Giordano, K. Arnaud, A. Zamaron, and P. Durbec. Netrin 1 contributes to vascular remodeling in the subventricular zone and promotes progenitor emigration after demyelination. *Development*, 140(15):3107–3117, 2013.
- [46] a Chang, a Nishiyama, J Peterson, J Prineas, and B D Trapp. NG2-positive oligodendrocyte progenitor cells in adult human brain and multiple sclerosis lesions. *The Journal of neuroscience : the official journal of the Society for Neuroscience*, 20(17):6404–12, sep 2000.
- [47] Ansi Chang, Wallace W Tourtellotte, Richard Rudick, and Bruce D Trapp. Premyelinating oligodendrocytes in chronic lesions of multiple sclerosis. *The New England journal of medicine*, 346(3):165–173, jan 2002.
- [48] D. M. Chari and W. F. Blakemore. New insights into remyelination failure in multiple sclerosis: Implications for glial cell transplantation. *Multiple Sclerosis*, 8(4):271–277, 2002.
- [49] Arnaud Charil, Alex P. Zijdenbos, Jonathan Taylor, Cyrus Boelman, Keith J. Worsley, Alan C. Evans, and Alain Dagher. Statistical mapping analysis of lesion location and neurological disability in multiple sclerosis: Application to 452 patient data sets. *NeuroImage*, 19(3):532–544, 2003.
- [50] Emily M. L. Chastain and Stephen D. Miller. Molecular mimicry as an inducing trigger for CNS autoimmune demyelinating disease. *Immunol Rev.*, 245(1):227–238, 2012.
- [51] H Chen, Z He, a Bagri, and M Tessier-Lavigne. Semaphorin-neuropilin interactions underlying sympathetic axon responses to class III semaphorins. *Neuron*, 21(6):1283–1290, dec 1998.

- [52] Hang Chen, Alain Chédotal, Zhigang He, Corey S. Goodman, and Marc Tessier-Lavigne. Neuropilin-2, a novel member of the neuropilin family, is a high affinity receptor for the semaphorins Sema E and Sema IV but not Sema III. *Neuron*, 19(3):547–559, 1997.
- [53] Hwai Jong Cheng, Anil Bagri, Avraham Yaron, Elke Stein, Samuel J. Pleasure, and Marc Tessier-Lavigne. Plexin-A3 mediates semaphorin signaling and regulates the development of hippocampal axonal projections. *Neuron*, 32(2):249–263, 2001.
- [54] Antonietta Citterio, Loredana La Mantia, Gabriele Ciucci, Livia Candolise, Fabio Brusafferri, Rune Midgard, and Graziella Filippini. Corticosteroids or ACTH for acute exacerbations in multiple sclerosis. *Cochrane Database of Systematic Reviews*, (4), 2000.
- [55] Rick I. Cohen, Daniele M. Rottkamp, Dragan Maric, Jeffery L. Barker, and Lynn D. Hudson. A role for semaphorins and neuropilins in oligodendrocyte guidance. *Journal of Neurochemistry*, 85(5):1262–1278, apr 2003.
- [56] Alastair Compston and Alasdair Coles. Multiple sclerosis. *Lancet*, 359(9313):1221–1231, 2002.
- [57] Miriam Corredor, Roman Bonet, Alejandra Moure, Cecilia Domingo, Jordi Bujons, Ignacio Alfonso, Yolanda Pérez, and Àngel Messeguer. Cationic Peptides and Peptidomimetics Bind Glycosaminoglycans as Potential Sema3A Pathway Inhibitors. *Biophysical Journal*, 110(6):1291–1303, 2016.
- [58] Ronen Cozocov, Katlin Halasz, Tharwat Haj, and Zahava Vadasz. Semaphorin 3A: Is a key player in the pathogenesis of asthma. *Clinical Immunology*, pages 10–12, 2016.
- [59] a H Crawford, C Chambers, and R J M Franklin. Remyelination: the true regeneration of the central nervous system. *Journal of comparative pathology*, 149(2-3):242–254, 2013.
- [60] a H Crawford, J H Stockley, R B Tripathi, W D Richardson, and R J M Franklin. Oligodendrocyte progenitors: Adult stem cells of the central nervous system? *Experimental neurology*, 260:50–55, may 2014.
- [61] Qiao-Ling Cui, Tanja Kuhlmann, Veronique E Miron, Soo Yuen Leong, Jun Fang, Pavel Gris, Timothy E Kennedy, Guillermina Almazan, and Jack Antel. Oligodendrocyte progenitor cell susceptibility to injury in multiple sclerosis. *The American journal of pathology*, 183(2):516–25, aug 2013.
- [62] Sabrina Curreli, Bin Sheng Wong, Olga Latinovic, Konstantinos Konstantopoulos, and Nicholas M Stamatou. Class 3 semaphorins induce F-actin reorganization in human dendritic cells: Role in cell migration. *Journal of leukocyte biology*, 100(6):1323–1334, 2016.
- [63] Xudong Dai, Lauren D Lercher, Patricia M Clinton, Yangzhou Du, Denise L Livingston, Cristina Vieira, Lu Yang, Michael M Shen, and Cheryl F Dreyfus. The trophic role of

- oligodendrocytes in the basal forebrain. *The Journal of Neuroscience*, 23(13):5846–53, 2003.
- [64] C. A. Davie, G. J. Barker, S. Webb, P. S. Tofts, A. J. Thompson, A. E. Harding, W. I. McDonald, and D. H. Miller. Persistent functional deficit in multiple sclerosis and autosomal dominant cerebellar ataxia is associated with axon loss. *Brain*, 118(6):1583–1592, 1995.
- [65] L. M. De Biase, A. Nishiyama, and D. E. Bergles. Excitability and Synaptic Communication within the Oligodendrocyte Lineage. *Journal of Neuroscience*, 30(10):3600–3611, 2010.
- [66] Fernando De Castro and Ana Bribián. The molecular orchestra of the migration of oligodendrocyte precursors during development. *Brain Research Reviews*, 49(2):227–241, 2005.
- [67] N. K. De Rosbo, R. Milo, M. B. Lees, D. Burger, C. C.A. Bernard, and A. Ben-Nun. Reactivity to myelin antigens in multiple sclerosis. Peripheral blood lymphocytes respond predominantly to myelin oligodendrocyte glycoprotein. *Journal of Clinical Investigation*, 92(6):2602–2608, 1993.
- [68] N De Stefano, S Narayanan, G S Francis, R Arnaoutelis, M C Tartaglia, J P Antel, P M Matthews, and D L Arnold. Evidence of axonal damage in the early stages of multiple sclerosis and its relevance to disability. *Archives of neurology*, 58(1):65–70, 2001.
- [69] Nicola De Stefano. Axonal damage correlates with disability in patients with relapsing-remitting multiple sclerosis. Results of a longitudinal magnetic resonance spectroscopy study. *Brain*, 121(8):1469–1477, 1998.
- [70] F. De Winter, M. Oudega, A. J. Lankhorst, F. P. Hamers, B. Blits, M. J. Ruitenbergh, R. J. Pasterkamp, W. H. Gispen, and J. Verhaagen. Injury-induced class 3 semaphorin expression in the rat spinal cord. *Experimental Neurology*, 175(1):61–75, 2002.
- [71] Joris De Wit, Fred De Winter, Jan Klooster, and Joost Verhaagen. Semaphorin 3A displays a punctate distribution on the surface of neuronal cells and interacts with proteoglycans in the extracellular matrix. *Molecular and cellular neurosciences*, 29(1):40–55, may 2005.
- [72] S. Delaire, C. Billard, R. Tordjman, A. Chedotal, A. Elhabazi, A. Bensussan, and L. Bomsell. Biological Activity of Soluble CD100. II. Soluble CD100, Similarly to H-SemaIII, Inhibits Immune Cell Migration. *The Journal of Immunology*, 166(7):4348–4354, 2001.
- [73] Greg M. Delgoffe, Seng-Ryong Woo, Meghan E. Turnis, David M. Gravano, Cliff Guy, Abigail E. Overacre, Matthew L. Bettini, Peter Vogel, David Finkelstein, Jody Bonnevier,

## Bibliography

- Creg J. Workman, and Dario A. A. Vignali. Stability and function of regulatory T cells is maintained by a neuropilin-1-semaphorin-4a axis. *Nature*, 501(7466):252–256, 2013.
- [74] C. Demerens, B. Stankoff, M. Logak, P. Anglade, B. Allinquant, F. Couraud, B. Zalc, and C. Lubetzki. Induction of myelination in the central nervous system by electrical activity. *Proceedings of the National Academy of Sciences*, 93(18):9887–9892, 1996.
- [75] Vishal a Deshmukh, Virginie Tardif, Costas a Lyssiotis, Chelsea C Green, Bilal Kerman, Hyung Joon Kim, Krishnan Padmanabhan, Jonathan G Swoboda, Insha Ahmad, Toru Kondo, Fred H Gage, Argyrios N Theofilopoulos, Brian R Lawson, Peter G Schultz, and Luke L Lairson. A regenerative approach to the treatment of multiple sclerosis. *Nature*, 502(7471):327–332, oct 2013.
- [76] Jill Dixon, Stacie K. Loftus, Amanda J. Gladwin, Peter J. Scambler, John J. Wasmuth, and Michael J. Dixon. Cloning of the human heparan sulfate-N-deacetylase/N-sulfotransferase gene from the treacher Collins syndrome candidate region at 5q32-q33.1. *Genomics*, 26(2):239–244, 1995.
- [77] S. D. D’Souza. Multiple Sclerosis: Fas Signaling in Oligodendrocyte Cell Death. *Journal of Experimental Medicine*, 184(6):2361–2370, 1996.
- [78] I. D. Duncan, A. Brower, Y. Kondoa, Jr. J. F. Curlee, and R. D. Schultz. Extensive remyelination of the CNS leads to functional recovery. *Proceedings of the National Academy of Sciences*, 106(25):6832–6836, 2009.
- [79] George C. Ebers. Environmental factors and multiple sclerosis. *The Lancet Neurology*, 7(3):268–277, 2008.
- [80] Justin P Edwards, Xia Zhang, Kenneth A Frauwirth, and David M Mosser. Biochemical and functional characterization of three activated macrophage populations. *Journal of leukocyte biology*, 80(6):1298–1307, 2009.
- [81] Herena Eixarch, Ana Gutiérrez-Franco, Xavier Montalban, and Carmen Espejo. Semaphorins 3A and 7A: Potential immune and neuroregenerative targets in multiple sclerosis. *Trends in Molecular Medicine*, 19(3):157–164, 2013.
- [82] J D England, F Gamboni, S R Levinson, and T E Finger. Changed distribution of sodium channels along demyelinated axons. *Proceedings of the National Academy of Sciences of the United States of America*, 87(17):6777–6780, 1990.
- [83] J. Fan, S. G. Mansfield, T. Redmond, P. R. Gordon-Weeks, and J. A. Raper. The organization of F-actin and microtubules in growth cones exposed to a brain-derived collapsing factor. *Journal of Cell Biology*, 121(4):867–878, 1993.
- [84] Jinhong Fan and Jonathan A. Raper. Localized collapsing cues can steer growth cones without inducing their full collapse. *Neuron*, 14(2):263–274, 1995.

- [85] Alessandro Fantin, Anastasia Lampropoulou, Gaia Gestri, Claudio Raimondi, Valentina Senatore, Ian Zachary, and Christiana Ruhrberg. NRP1 Regulates CDC42 Activation to Promote Filopodia Formation in Endothelial Tip Cells. *Cell Reports*, 11(10):1577–1590, 2015.
- [86] Alessandro Fantin, Anastasia Lampropoulou, Valentina Senatore, James T Brash, Claudia Prahst, Clemens A Lange, Sidath E Liyanage, Claudio Raimondi, James W Bainbridge, Hellmut G Augustin, and Christiana Ruhrberg. VEGF165-induced vascular permeability requires NRP1 for ABL-mediated SRC family kinase activation. *The Journal of Experimental Medicine*, 214(4):1049–1064, 2017.
- [87] J. Ferent, C. Zimmer, P. Durbec, M. Ruat, and E. Traiffort. Sonic Hedgehog Signaling Is a Positive Oligodendrocyte Regulator during Demyelination. *Journal of Neuroscience*, 33(5):1759–1772, 2013.
- [88] B. Ferguson, M. K. Matyszak, M. M. Esiri, and V. H. Perry. Axonal damage in acute multiple sclerosis lesions. *Brain*, 120(3):393–399, 1997.
- [89] A. K. Foote and W. F. Blakemore. Inflammation stimulates remyelination in areas of chronic demyelination. *Brain*, 128(3):528–539, 2005.
- [90] Robin J M Franklin. Why does remyelination fail in multiple sclerosis? *Nature reviews. Neuroscience*, 3(9):705–14, sep 2002.
- [91] Robin J M Franklin and Charles Ffrench-Constant. Remyelination in the CNS: from biology to therapy. *Nature reviews. Neuroscience*, 9(11):839–855, nov 2008.
- [92] Robin J M Franklin, Charles Ffrench-Constant, Julia M. Edgar, and Kenneth J. Smith. Neuroprotection and repair in multiple sclerosis. *Nature Reviews Neurology*, 8(11):624–634, 2012.
- [93] Robin J M Franklin and Vittorio Gallo. The translational biology of remyelination: past, present, and future. *Glia*, 62(11):1905–15, nov 2014.
- [94] Robin J M Franklin, Jennifer M. Gilson, and William F. Blakemore. Local recruitment of remyelinating cells in the repair of demyelination in the central nervous system. *Journal of Neuroscience Research*, 50(2):337–344, 1997.
- [95] Robin J M Franklin and Mark R Kotter. The biology of CNS remyelination: the key to therapeutic advances. *Journal of neurology*, 255 Suppl:19–25, mar 2008.
- [96] C Fruhbeis, D Frohlich, W P Kuo, J Amphornrat, S Thilemann, A S Saab, F Kirchoff, W Mobius, S Goebbels, K A Nave, A Schneider, M Simons, M Klugmann, J Trotter, and E M Kramer-Albers. Neurotransmitter-triggered transfer of exosomes mediates oligodendrocyte-neuron communication. *PLoS Biol*, 11, 2013.

- [97] H Fujita, B Zhang, K Sato, J Tanaka, and M Sakanaka. Expressions of neuropilin-1, neuropilin-2 and semaphorin 3A mRNA in the rat brain after middle cerebral artery occlusion. *Brain research*, 914(1-2):1–14, 2001.
- [98] K Fukazawa, T; Sasaki, H; Kikuchi, S; Hamanda, T; Tashiro. Genetics of Multiple Sclerosis. *Biomedicine & Pharmacotherapy*, 54(2):103–6, 2000.
- [99] Toru Fukuda, Shu Takeda, Ren Xu, Hiroki Ochi, Satoko Sunamura, Tsuyoshi Sato, Shinsuke Shibata, Yutaka Yoshida, Zirong Gu, Ayako Kimura, Chengshan Ma, Cheng Xu, Waka Bando, Koji Fujita, Kenichi Shinomiya, Takashi Hirai, Yoshinori Asou, Mitsuhiro Enomoto, Hideyuki Okano, Atsushi Okawa, and Hiroshi Itoh. *Sema3A regulates bone-mass accrual through sensory innervations. Nature*, 497(7450):490–3, 2013.
- [100] Ursula Fünfschilling, Lotti M Supplie, Don Mahad, Susann Boretius, Aiman S Saab, Julia Edgar, Bastian G Brinkmann, Celia M Kassmann, Iva D Tzvetanova, Wiebke Möbius, Francisca Diaz, Dies Meijer, Ueli Suter, Bernd Hamprecht, Michael W Sereda, Carlos T Moraes, Jens Frahm, Sandra Goebbels, and Klaus-Armin Nave. Glycolytic oligodendrocytes maintain myelin and long-term axonal integrity. *Nature*, 485(7399):517–21, may 2012.
- [101] Valeria Gagliardini and Christoph Fankhauser. Semaphorin III Can Induce Death in Sensory Neurons. *Molecular and Cellular Neuroscience*, 14(4):301–316, 1999.
- [102] J.T. Gallagher and J.E. Turnbull. Heparan sulphate in the binding and activation of basic fibroblast growth factor. *Glycobiology*, 2(6):523–528, 1992.
- [103] James Y Garbern, Donald A Yool, Gregory J Moore, Ian B Wilds, Michael W Faulk, Matthias Klugmann, Klaus-amin Nave, Erik A Sistermans, Marjo S van der Knaap, Thomas D Bird, Michael E Shy, John A Kamholz, and Ian R Griffiths. Patients lacking the major CNS myelin protein, proteolipid protein 1, develop length-dependent axonal degeneration in the absence of demyelination and inflammation. *Brain : a journal of neurology*, 125(Pt 3):551–61, 2002.
- [104] JAM Gensert and JE Goldman. Endogenous progenitors remyelinate demyelinated axons in the adult CNS. *Neuron*, 19:197–203, 1997.
- [105] Paolo Giacobini, Jyoti Parkash, Céline Campagne, Andrea Messina, Filippo Casoni, Charlotte Vanacker, Fanny Langlet, Barbara Hobo, Gabriella Cagnoni, Sarah Gallet, Naresh Kumar Hanchate, Danièle Mazur, Masahiko Taniguchi, Massimiliano Mazzone, Joost Verhaagen, Philippe Ciofi, Sébastien G. Bouret, Luca Tamagnone, and Vincent Prevot. Brain Endothelial Cells Control Fertility through Ovarian-Steroid-Dependent Release of Semaphorin 3A. *PLoS Biology*, 12(3):e1001808, mar 2014.
- [106] A J Gladwin, J Dixon, S K Loftus, J J Wasmuth, and M J Dixon. Genomic organization of the human heparan sulfate-N-deacetylase/N-sulfotransferase gene: exclusion from a

- causative role in the pathogenesis of Treacher Collins syndrome. *Genomics*, 32(3):471–473, 1996.
- [107] R.F. Gledhill, B.M. Harrison, and W.I. McDonald. Pattern of Remyelination in the CNS. *Nature*, 249:577–578, 1974.
- [108] Isaias Glezer. Innate immunity triggers oligodendrocyte progenitor reactivity and confines damages to brain injuries. *The FASEB Journal*, 20(4):750–752, 2006.
- [109] T Goldschmidt, J Antel, F B König, W Brück, and T Kuhlmann. Remyelination capacity of the MS brain decreases with disease chronicity. *Neurology*, 72(22):1914–1921, jun 2009.
- [110] Bertrand Gonthier, Eric Koncina, Saulius Satkauskas, Martine Perraut, Guy Roussel, Dominique Aunis, Josef P. Kapfhammer, and Dominique Bagnard. A PKC-dependent recruitment of MMP-2 controls semaphorin-3A growth-promoting effect in cortical dendrites. *PLoS ONE*, 4(4), 2009.
- [111] Evelin Grage-Griebenow, Stefan Löseke, Marion Kauth, Kirsten Gehlhar, Rainer Zatzky, and Albrecht Bufe. Anti-BDCA-4 (neuropilin-1) antibody can suppress virus-induced IFN-alpha production of plasmacytoid dendritic cells. *Immunology and Cell Biology*, 85(5):383–390, 2007.
- [112] Ari J. Green, Jeffrey M. Gelfand, Bruce A. Cree, Carolyn Bevan, W. John Boscardin, Feng Mei, Justin Inman, Sam Arnow, Michael Devereux, Aya Abounasr, Hiroko Nobuta, Alyssa Zhu, Matt Friessen, Roy Gerona, Hans Christian von Büdingen, Roland G. Henry, Stephen L. Hauser, and Jonah R. Chan. Clemastine fumarate as a remyelinating therapy for multiple sclerosis (ReBUILD): a randomised, controlled, double-blind, crossover trial. *The Lancet*, 390(10111):2481–2489, 2017.
- [113] Andrew D. Greenhalgh, Rosmarini Passos dos Santos, Juan Guillermo Zarruk, Christopher K. Salmon, Antje Kroner, and Samuel David. Arginase-1 is expressed exclusively by infiltrating myeloid cells in CNS injury and disease. *Brain, Behavior, and Immunity*, 56:61–67, 2016.
- [114] Ian Griffiths, Matthias Klugmann, Thomas Anderson, Donald Yool, Christine Thomson, Markus H. Schwab, Armin Schneider, Frank Zimmermann, Mailise McCulloch, Nancy Nadon, and Klaus Armin Nave. Axonal swellings and degeneration in mice lacking the major proteolipid of myelin. *Science*, 280(5369):1610–1613, 1998.
- [115] Chenghua Gu, Brian J Limberg, G Brian Whitaker, Ben Perman, Daniel J Leahy, Jan S Rosenbaum, David D Ginty, and Alex L Kolodkin. Characterization of neuropilin-1 structural features that confer binding to semaphorin 3A and vascular endothelial growth factor 165. *The Journal of biological chemistry*, 277(20):18069–76, may 2002.

- [116] Chenghua Gu, E Rene Rodriguez, Dorothy V Reimert, Tianzhi Shu, Bernd Fritzsich, Linda J Richards, Alex L Kolodkin, and David D Ginty. Neuropilin-1 conveys semaphorin and VEGF signaling during neural and cardiovascular development. *Developmental cell*, 5(1):45–57, jul 2003.
- [117] Ana Gutiérrez-Franco, Carme Costa, Herena Eixarch, Mireia Castillo, Eva M. Medina-Rodríguez, Ana Bribián, Fernando de Castro, Xavier Montalban, and Carmen Espejo. Differential expression of sema3A and sema7A in a murine model of multiple sclerosis: Implications for a therapeutic design. *Clinical Immunology*, 163:22–33, 2016.
- [118] Noga Guttmann-Raviv, Niva Shraga-Heled, Asya Varshavsky, Cinthya Guimaraes-Sternberg, Ofra Kessler, and Gera Neufeld. Semaphorin-3A and semaphorin-3F work together to repel endothelial cells and to inhibit their survival by induction of apoptosis. *The Journal of biological chemistry*, 282(36):26294–26305, sep 2007.
- [119] Lukas Haider, Marie T. Fischer, Josa M. Frischer, Jan Bauer, Romana Höftberger, Gergö Botond, Harald Esterbauer, Christoph J. Binder, Joseph L. Witztum, and Hans Lassmann. Oxidative damage in multiple sclerosis lesions. *Brain*, 134:1914–1924, 2011.
- [120] S M Hall. The effect of injections of lysophosphatidyl choline into white matter of the adult mouse spinal cord. *Journal of cell science*, 10:535–546, 1972.
- [121] Naresh Kumar Hanchate, Paolo Giacobini, Pierre Lhuillier, Jyoti Parkash, Cécile Espy, Corinne Fouveaut, Chrystel Leroy, Stéphanie Baron, Céline Campagne, Charlotte Vanacker, Francis Collier, Corinne Cruaud, Vincent Meyer, Alfons García-Piñero, Didier Dewailly, Christine Cortet-Rudelli, Ksenija Gersak, Chantal Metz, Gérard Chabrier, Michel Pugeat, Jacques Young, Jean Pierre Hardelin, Vincent Prevot, and Catherine Dodé. SEMA3A, a Gene Involved in Axonal Pathfinding, Is Mutated in Patients with Kallmann Syndrome. *PLoS Genetics*, 8(8):1–9, 2012.
- [122] Meredith D Hartley, Ghadah Altowajri, and Dennis Bourdette. Remyelination and multiple sclerosis: therapeutic approaches and challenges. *Current neurology and neuroscience reports*, 14(10):485, oct 2014.
- [123] Masayuki Hashimoto, Hidetoshi Ino, Masao Koda, Masazumi Murakami, Katsunori Yoshinaga, Masashi Yamazaki, and Hideshige Moriya. Regulation of semaphorin 3A expression in neurons of the rat spinal cord and cerebral cortex after transection injury. *Acta Neuropathologica*, 107(3):250–256, 2004.
- [124] Kazuhide Hayakawa, Loc-Duyen D Pham, Angel T Som, Brian J Lee, Shuzhen Guo, Eng H Lo, and Ken Arai. Vascular endothelial growth factor regulates the migration of oligodendrocyte precursor cells. *The Journal of neuroscience : the official journal of the Society for Neuroscience*, 31(29):10666–10670, jul 2011.
- [125] Zhigang He and Marc Tessier-Lavigne. Neuropilin is a receptor for the axonal chemorepellent Semaphorin III. *Cell*, 90(4):739–751, 1997.

- [126] A. L. Hodgkin and A. F. Huxley. A quantitative description of membrane current and its application to conduction and excitation in nerve. *Bulletin of Mathematical Biology*, 52(1-2):25–71, 1990.
- [127] K a Houck, D W Leung, a M Rowland, J Winer, and N Ferrara. Dual regulation of vascular endothelial growth factor bioavailability by genetic and proteolytic mechanisms. *The Journal of biological chemistry*, 267(36):26031–26037, 1992.
- [128] Yinghui Hu, Xinhua Lee, Benxiu Ji, Kevin Guckian, Daniel Apicco, R. Blake Pepinsky, Robert H. Miller, and Sha Mi. Sphingosine 1-phosphate receptor modulator fingolimod (FTY720) does not promote remyelination in vivo. *Molecular and Cellular Neuroscience*, 48(1):72–81, 2011.
- [129] Jeffrey K Huang and Robin J M Franklin. Regenerative medicine in multiple sclerosis: identifying pharmacological targets of adult neural stem cell differentiation. *Neurochemistry international*, 59(3):329–332, sep 2011.
- [130] Donald E Humphries, Brandon M Sullivan, M Deize Aleixo, and Jennifer L Stow. Localization of human heparan glucosaminyl N-deacetylase/N-sulphotransferase to the trans-Golgi network. *Biochem J.*, 325:351–357, 1997.
- [131] Masaru Inatani, Fumitoshi Irie, Andrew S. Plump, Marc Tessier-Lavigne, and Yu Yamaguchi. Mammalian Brain Morphogenesis and Midline Axon Guidance Require Heparan Sulfate. *Science*, 302(5647):1044–1046, 2003.
- [132] K. A. Irvine and W. F. Blakemore. Age increases axon loss associated with primary demyelination in cuprizone-induced demyelination in C57BL/6 mice. *Journal of Neuroimmunology*, 175(1-2):69–76, 2006.
- [133] K. A. Irvine and W. F. Blakemore. Remyelination protects axons from demyelination-associated axon degeneration. *Brain*, 131(6):1464–1477, 2008.
- [134] Yasuto Itoyama, Henry De F. Webster, Edward P. Richardson, and Bruce D. Trapp. Schwann cell remyelination of demyelinated axons in spinal cord multiple sclerosis lesions. *Annals of Neurology*, 14(3):339–346, 1983.
- [135] Sindhu Jacob, Asmaa Al-Kandari, Raed Alroughani, and Rabeah Al-Temaimi. Assessment of plasma biomarkers for their association with Multiple Sclerosis progression. *Journal of Neuroimmunology*, 305:5–8, 2017.
- [136] Bert J C Janssen, Tomas Malinauskas, Greg a Weir, M Zameel Cader, Christian Siebold, and E Yvonne Jones. Neuropilins lock secreted semaphorins onto plexins in a ternary signaling complex. *Nature Structural & Molecular Biology*, 19(12):1293–1299, 2012.
- [137] AA A Jarjour, CM M Manitt, SW W Moore, KM M Thompson, SJ J Yuh, and Timothy E Kennedy. Netrin-1 is a chemorepellent for oligodendrocyte precursor cells in the

- embryonic spinal cord. *The Journal of neuroscience : the official journal of the Society for Neuroscience*, 23(9):3735–3744, 2003.
- [138] N. D. Jeffery and W. F. Blakemore. Locomotor deficits induced by experimental spinal cord demyelination are abolished by spontaneous remyelination. *Brain*, 120(1):27–37, 1997.
- [139] Jong-Dae Ji, Kyung-Hyun Park-Min, and Lionel B. Ivashkiv. Expression and function of semaphorin 3A and its receptors in human monocyte-derived macrophages. *Human Immunology*, 70(4):211–217, 2009.
- [140] E. Stidworthy Johnson and S. K. Ludwin. The demonstration of recurrent demyelination and remyelination of axons in the central nervous system. *Acta Neuropathologica*, 53(2):93–98, 1981.
- [141] B. C. Jongbloets and R. J. Pasterkamp. Semaphorin signalling during development. *Development*, 141(17):3292–3297, 2014.
- [142] Y Kakuta, T Sueyoshi, M Negishi, and L C Pedersen. Crystal structure of the sulfotransferase domain of human heparan sulfate N-deacetylase/ N-sulfotransferase 1. *The Journal of biological chemistry*, 274(16):10673–10676, 1999.
- [143] Hiroyuki Kamiguchi, Mary Louise Hlavin, and Vance Lemmon. Role of L1 in neural development: What the knockouts tell us. *Molecular and Cellular Neurosciences*, 12(1-2):48–55, 1998.
- [144] Shinjiro Kaneko, Akio Iwanami, Masaya Nakamura, Akiyoshi Kishino, Kaoru Kikuchi, Shinsuke Shibata, Hirotaka J Hideyuki Okano, Takeshi Ikegami, Ayako Moriya, Osamu Konishi, Chikao Nakayama, Kazuo Kumagai, Toru Kimura, Yasufumi Sato, Yoshio Goshima, Masahiko Taniguchi, Mamoru Ito, Zhigang He, and Yoshiaki Toyama. A selective Sema3A inhibitor enhances regenerative responses and functional recovery of the injured spinal cord. *Nature medicine*, 12(12):1380–1389, dec 2006.
- [145] Ragnhildur K arad ttir, Nicola B Hamilton, Yamina Bakiri, and David Attwell. Spiking and nonspiking classes of oligodendrocyte precursor glia in CNS white matter. *Nature neuroscience*, 11(4):450–456, 2008.
- [146] Kosuke Kawaguchi, Eiji Suzuki, Mariko Nishie, Isao Kii, Tatsuki R. Kataoka, Masahiro Hirata, Masashi Inoue, Fengling Pu, Keiko Iwaisako, Moe Tsuda, Ayane Yamaguchi, Hironori Haga, Masatoshi Hagiwara, and Masakazu Toi. Downregulation of neuropilin-1 on macrophages modulates antibody-mediated tumoricidal activity. *Cancer Immunology, Immunotherapy*, pages 1–12, 2017.
- [147] T Kawasaki, T Kitsukawa, Y Bekku, Y Matsuda, M Sanbo, T Yagi, and H Fujisawa. A requirement for neuropilin-1 in embryonic vessel formation. *Development*, 126(21):4895–4902, 1999.

- [148] Hans S. Keirstead, Joel M. Levine, and William F. Blakemore. Response of the oligodendrocyte progenitor cell population (Defined by NG2 labelling) to demyelination of the adult spinal cord. *Glia*, 22(2):161–170, 1998.
- [149] Aharon Kessel, Chen Lin, Zahava Vadasz, Regina Peri, Nasren Eiza, and Drora Berkowitz. The association between semaphorin 3A levels and gluten-free diet in patients with celiac disease. *Clinical Immunology*, 2017.
- [150] Kaoru Kikuchi, Akiyoshi Kishino, Osamu Konishi, Kazuo Kumagai, Nobuo Hosotani, Ikutaro Saji, Chikao Nakayama, and Toru Kimura. In Vitro and in Vivo Characterization of a Novel Semaphorin 3A Inhibitor, SM-216289 or Xanthofulvin. *Journal of Biological Chemistry*, 278(44):42985–42991, 2003.
- [151] S. Kiryu-Seo, N. Ohno, G. J. Kidd, H. Komuro, and B. D. Trapp. Demyelination Increases Axonal Stationary Mitochondrial Size and the Speed of Axonal Mitochondrial Transport. *Journal of Neuroscience*, 30(19):6658–6666, 2010.
- [152] T Kitsukawa, M Shimizu, M Sanbo, T Hirata, M Taniguchi, Y Bekku, T Yagi, and H Fujisawa. Neuropilin-semaphorin III/D-mediated chemorepulsive signals play a crucial role in peripheral nerve projection in mice. *Neuron*, 19(5):995–1005, nov 1997.
- [153] Alex L. Kolodkin, Dorothy V. Levengood, Erica G. Rowe, Yu Tzu Tai, Roman J. Giger, and David D. Ginty. Neuropilin is a semaphorin III receptor. *Cell*, 90(4):753–762, 1997.
- [154] Adam M. Koppel and Jonathan A. Raper. Collapsin-1 covalently dimerizes, and dimerization is necessary for collapsing activity. *Journal of Biological Chemistry*, 273(25):15708–15713, 1998.
- [155] Barbara Kornek, Maria K. Storch, Robert Weissert, Erik Wallstroem, Andreas Stefferl, Tomas Olsson, Christopher Lington, Manfred Schmidbauer, and Hans Lassmann. Multiple sclerosis and chronic autoimmune encephalomyelitis: A comparative quantitative study of axonal injury in active, inactive, and remyelinated lesions. *American Journal of Pathology*, 157(1):267–276, 2000.
- [156] Sonja Körner, Sebastian Bösel, Klaudia Wichmann, Nadine Thau-Habermann, Antonia Zapf, Sarah Knippenberg, Reinhard Dengler, and Susanne Petri. The Axon Guidance Protein Semaphorin 3A Is Increased in the Motor Cortex of Patients With Amyotrophic Lateral Sclerosis. *Journal of neuropathology and experimental neurology*, 75(4):nlw003, 2016.
- [157] Mark R Kotter, Wen-Wu Li, Chao Zhao, and Robin J M Franklin. Myelin impairs CNS remyelination by inhibiting oligodendrocyte precursor cell differentiation. *The Journal of neuroscience : the official journal of the Society for Neuroscience*, 26(1):328–332, jan 2006.

- [158] Mark R. Kotter, Anna Setzu, Fraser J. Sim, Nico Van Rooijen, and Robin J M Franklin. Macrophage depletion impairs oligodendrocyte remyelination following lysolecithin-induced demyelination. *Glia*, 35(3):204–212, 2001.
- [159] Mark R. Kotter, Chao Zhao, Nico Van Rooijen, and Robin J.M. Franklin. Macrophage-depletion induced impairment of experimental CNS remyelination is associated with a reduced oligodendrocyte progenitor cell response and altered growth factor expression. *Neurobiology of Disease*, 18(1):166–175, 2005.
- [160] D. Kremer, P. Kury, and R. Dutta. Promoting remyelination in multiple sclerosis: Current drugs and future prospects. *Multiple Sclerosis Journal*, 2015.
- [161] Robert P Kruger, Jennifer Aurandt, and Kun-Liang Guan. Semaphorins command cells to move. *Nature reviews. Molecular cell biology*, 6:789–800, 2005.
- [162] T. Kuhlmann, V. Miron, Q. Cuo, C. Wegner, J. Antel, and W. Brück. Differentiation block of oligodendroglial progenitor cells as a cause for remyelination failure in chronic multiple sclerosis. *Brain*, 131(7):1749–1758, 2008.
- [163] Tanja Kuhlmann, Gueanelle Lingfeld, Andreas Bitsch, Jana Schuchardt, and Wolfgang Brück. Acute axonal damage in multiple sclerosis is most extensive in early disease stages and decreases over time. *Brain : a journal of neurology*, 125(Pt 10):2202–2212, 2002.
- [164] Tanja Kuhlmann, Samuel Ludwin, Alexandre Prat, Jack Antel, Wolfgang Brück, and Hans Lassmann. An updated histological classification system for multiple sclerosis lesions. *Acta Neuropathologica*, 133(1):13–24, 2017.
- [165] Saji Kumagai, Kazuo Hosotani, Nobuo Kikuchi, Kaoru Kimuta, Toru Ikitaro. Xanthofulvin, a Novel Semaphorin Inhibitor Produced by a Strain of Penicillium. 56(7), 2003.
- [166] Atsushi Kumanogoh and Hitoshi Kikutani. Immunological functions of the neuropilins and plexins as receptors for semaphorins. *Nature Immunology*, 13(November):802–814, 2013.
- [167] Corinna Lappe-Siefke, Sandra Goebbels, Michel Gravel, Eva Nicksch, John Lee, Peter E. Braun, Ian R. Griffiths, and Klaus Armin Navel. Disruption of Cnp1 uncouples oligodendroglial functions in axonal support and myelination. *Nature Genetics*, 33(3):366–374, 2003.
- [168] Catherine Larochelle, Jorge Ivan Alvarez, and Alexandre Prat. How do immune cells overcome the blood-brain barrier in multiple sclerosis? *FEBS Letters*, 585(23):3770–3780, 2011.
- [169] Hans Lassmann. Hypoxia-like tissue injury as a component of multiple sclerosis lesions. *Journal of the Neurological Sciences*, 206(2):187–191, feb 2003.

## Bibliography

- [170] Youngjin Lee, Brett M Morrison, Yun Li, Sylvain Lengacher, Mohamed H Farah, Paul N Hoffman, Yiting Liu, Akivaga Tsingalia, Lin Jin, Ping-Wu Zhang, Luc Pellerin, Pierre J Magistretti, and Jeffrey D Rothstein. Oligodendroglia metabolically support axons and contribute to neurodegeneration. *Nature*, 487(7408):443–8, jul 2012.
- [171] The Lenercept, Multiple Sclerosis, and Study Group. TNF neutralization in MS Results of a randomized , placebo-controlled multicenter study. *Lenercept, T., Sclerosis, M., & Group, S. (1999). TNF neutralization in MS Results of a randomized , placebo-controlled multicenter study.*, 1999.
- [172] J M Levine, R Reynolds, and J W Fawcett. The oligodendrocyte precursor cell in health and disease. *Trends in neurosciences*, 24(1):39–47, jan 2001.
- [173] J M Levine, F Stincone, and Y S Lee. Development and differentiation of glial precursor cells in the rat cerebellum. *Glia*, 7(4):307–21, 1993.
- [174] Wen Wu Li, Jacques Penderis, Chao Zhao, Michael Schumacher, and Robin J.M. Franklin. Females remyelinate more efficiently than males following demyelination in the aged but not young adult CNS. *Experimental Neurology*, 202(1):250–254, 2006.
- [175] Wen Wu Li, Anna Setzu, Chao Zhao, and Robin J.M. Franklin. Minocycline-mediated inhibition of microglia activation impairs oligodendrocyte progenitor cell responses and remyelination in a non-immune model of demyelination. *Journal of Neuroimmunology*, 158(1-2):58–66, 2005.
- [176] Wei-Ching Liang, Mark S Dennis, Scott Stawicki, Yvan Chanthery, Qi Pan, Yongmei Chen, Charles Eigenbrot, JianPing Yin, Alexander W Koch, Xiumin Wu, Napoleone Ferrara, Anil Bagri, Marc Tessier-Lavigne, Ryan J Watts, and Yan Wu. Function blocking antibodies to neuropilin-1 generated from a designed human synthetic antibody phage library. *Journal of molecular biology*, 366(3):815–829, feb 2007.
- [177] David Liebetanz and Doron Merkler. Effects of commissural de- and remyelination on motor skill behaviour in the cuprizone mouse model of multiple sclerosis. *Experimental Neurology*, 202(1):217–224, 2006.
- [178] Ulf Lindahl, Marion Kusche, Kerstin Lidholt, and Lars-Goran Oscarsson. Biosynthesis of heparin and heparan sulfate. *Ann. N. Y. Acad. Sci*, 556:36–50, 1989.
- [179] C Lucchinetti, W Brück, J Parisi, B Scheithauer, M Rodriguez, and H Lassmann. A quantitative analysis of oligodendrocytes in multiple sclerosis lesions. A study of 113 cases. *Brain : a journal of neurology*, 122 ( Pt 1:2279–2295, dec 1999.
- [180] C Lucchinetti, W Brück, J Parisi, B Scheithauer, M Rodriguez, and H Lassmann. Heterogeneity of multiple sclerosis lesions: implications for the pathogenesis of demyelination. *Annals of neurology*, 47(6):707–717, jun 2000.

- [181] Samuel K. Ludwin and Marion Maitland. Long-term remyelination fails to reconstitute normal thickness of central myelin sheaths. *Journal of the Neurological Sciences*, 64(2):193–198, 1984.
- [182] Y Luo, D Raible, and J a Raper. Collapsin: a protein in brain that induces the collapse and paralysis of neuronal growth cones. *Cell*, 75(2):217–27, oct 1993.
- [183] Takehiko Maeda, Daisuke Yamada, and Kohichi Kawahara. Cancer pain relief achieved by disrupting tumor-driven semaphorin 3A signaling in mice. *Neuroscience Letters*, 632:147–151, 2016.
- [184] S. Mah, M. R. Nelson, L. E. DeLisi, R. H. Reneland, N. Markward, M. R. James, D. R. Nyholt, N. Hayward, H. Handoko, B. Mowry, S. Kammerer, and A. Braun. Identification of the semaphorin receptor PLXNA2 as a candidate for susceptibility to schizophrenia. *Molecular Psychiatry*, 11(5):471–478, 2006.
- [185] H. H. Majed. A Novel Role for Sema3A in Neuroprotection from Injury Mediated by Activated Microglia. *Journal of Neuroscience*, 26(6):1730–1738, 2006.
- [186] J. Malemud, Charles. Matrix metalloproteinases (MMPs) in health and disease: an overview. *Frontiers in Bioscience*, 11(1):1696, 2006.
- [187] Jean Marie Mangin, Peijun Li, Joseph Scafidi, and Vittorio Gallo. Experience-dependent regulation of NG2 progenitors in the developing barrel cortex. *Nature Neuroscience*, 15(9):1192–1194, 2012.
- [188] Richard P C Manns, Geoffrey M W Cook, Christine E Holt, and Roger J Keynes. Differing semaphorin 3A concentrations trigger distinct signaling mechanisms in growth cone collapse. *The Journal of neuroscience : the official journal of the Society for Neuroscience*, 32(25):8554–8559, jun 2012.
- [189] Natalia Manrique-Hoyos, Tanja Jürgens, Mads Grønberg, Mario Kreutzfeldt, Mariann Schedensack, Tanja Kuhlmann, Christina Schrick, Wolfgang Brück, Henning Urlaub, Mikael Simons, and Doron Merkler. Late motor decline after accomplished remyelination: impact for progressive multiple sclerosis. *Annals of neurology*, 71(2):227–244, feb 2012.
- [190] J L Mason, K Suzuki, D D Chaplin, and G K Matsushima. Interleukin-1beta promotes repair of the CNS. *Journal of Neuroscience*, 21(18):7046–7052, 2001.
- [191] Jeffrey L. Mason, Arrel Toews, Janell D. Hostettler, Pierre Morell, Kinuko Suzuki, James E. Goldman, and Glenn K. Matsushima. Oligodendrocytes and Progenitors Become Progressively Depleted within Chronically Demyelinated Lesions. *American Journal of Pathology*, 164(5):1673–1682, 2004.

## Bibliography

- [192] Ken D. McCarthy and Jean De Vellis Vellis. Preparation of separate astroglial and oligodendroglial cell cultures from rat cerebral tissue. *The Journal of cell biology*, 85(June):890–902, 1980.
- [193] W. I. McDonald and T. A. Sears. Effect of demyelination on conduction in the central nervous system. *Brain*, 93:583–598, 1970.
- [194] Isabelle Medana, Marianne A. Martinic, Hartmut Wekerle, and Harald Neumann. Transection of major histocompatibility complex class I-induced neurites by cytotoxic T lymphocytes. *American Journal of Pathology*, 159(3):809–815, 2001.
- [195] Eva María Medina-Rodríguez, Francisco Javier Arenzana, Ana Bribián, and Fernando de Castro. Protocol to isolate a large amount of functional oligodendrocyte precursor cells from the cerebral cortex of adult mice and humans. *PloS one*, 8(11):e81620, jan 2013.
- [196] Feng Mei, Stephen P J Fancy, Yun An A Shen, Jianqin Niu, Chao Zhao, Bryan Presley, Edna Miao, Seonok Lee, Sonia R. Mayoral, Stephanie A. Redmond, Ainhua Etxeberria, Lan Xiao, Robin J M Franklin, Ari Green, Stephen L. Hauser, and Jonah R. Chan. Micropillar arrays as a high-throughput screening platform for therapeutics in multiple sclerosis. *Nature Medicine*, 20(8):954–960, 2014.
- [197] B. Menn, J. M. Garcia-Verdugo, C. Yaschine, O. Gonzalez-Perez, D. Rowitch, and A. Alvarez-Buylla. Origin of Oligodendrocytes in the Subventricular Zone of the Adult Brain. *Journal of Neuroscience*, 26(30):7907–7918, 2006.
- [198] D J Messersmith, J C Murtie, T Q Le, E E Frost, and R C Armstrong. Fibroblast growth factor 2 (FGF2) and FGF receptor expression in an experimental demyelinating disease with extensive remyelination. *J.Neurosci.Res.*, 62(2):241–256, 2000.
- [199] Elizabeth K. Messersmith, E. David Leonardo, Carla J. Shatz, Marc Tessier-Lavigne, Corey S. Goodman, and Alex L. Kolodkin. Semaforin III can function as a selective chemorepellent to pattern sensory projections in the spinal cord. *Neuron*, 14(5):949–959, 1995.
- [200] Sha Mi, R. Blake Pepinsky, and Diego Cadavid. Blocking LINGO-1 as a therapy to promote CNS repair: From concept to the clinic. *CNS Drugs*, 27(7):493–503, 2013.
- [201] Hua Quan Miao, Shay Soker, Leonard Feiner, José Luis Alonso, Jonathan A. Raper, and Michael Klagsbrun. Neuropilin-1 mediates collapsin-1/semaphorin III inhibition of endothelial cell motility: Functional competition of collapsin-1 and vascular endothelial growth factor-165. *Journal of Cell Biology*, 146(1):233–241, 1999.
- [202] Joanna Mikita, Nadège Dubourdieu-Cassagno, Mathilde Sa Deloire, Antoine Vekris, Marc Biran, Gérard Raffard, Bruno Brochet, Marie Hélène Canron, Jean Michel Franconi, Claudine Boiziau, and Klaus G. Petry. Altered M1/M2 activation patterns of mono-

- cytes in severe relapsing experimental rat model of multiple sclerosis. Amelioration of clinical status by M2 activated monocyte administration. *Multiple Sclerosis Journal*, 17(1):2–15, 2011.
- [203] D H Miller, R I Grossman, S C Reingold, and H F McFarland. The Role of Magnetic Resonance Techniques in Understanding and Managing Multiple Sclerosis. *Brain : a journal of neurology*, 121 ( Pt 1:3–24, 1998.
- [204] Erik Mire, Nicole Thomasset, Lyn B. Jakeman, and Geneviève Rougon. Modulating Sema3A signal with a L1 mimetic peptide is not sufficient to promote motor recovery and axon regeneration after spinal cord injury. *Molecular and Cellular Neuroscience*, 37(2):222–235, 2008.
- [205] Veronique E Miron, Amanda Boyd, Jing-Wei Zhao, Tracy J Yuen, Julia M Ruckh, Jennifer L Shadrach, Peter van Wijngaarden, Amy J Wagers, Anna Williams, Robin J M Franklin, and Charles Ffrench-Constant. M2 microglia and macrophages drive oligodendrocyte differentiation during CNS remyelination. *Nature neuroscience*, 16(9):1211–1218, sep 2013.
- [206] Veronique E Miron, Cha Gyun Jung, Hye Jung Kim, Timothy E Kennedy, Betty Soliven, and Jack P Antel. FTY720 modulates human oligodendrocyte progenitor process extension and survival. *Annals of neurology*, 63(1):61–71, jan 2008.
- [207] Veronique E. Miron, Samuel K. Ludwin, Peter J. Darlington, Andrew A. Jarjour, Betty Soliven, Timothy E. Kennedy, and Jack P. Antel. Fingolimod (FTY720) enhances remyelination following demyelination of organotypic cerebellar slices. *American Journal of Pathology*, 176(6):2682–2694, 2010.
- [208] Marisol Montolio, Joaquim Messeguer, Isabel Masip, Patricia Guijarro, Rosalina Gavin, José Antonio del Río, Angel Messeguer, and Eduardo Soriano. A Semaphorin 3A Inhibitor Blocks Axonal Chemorepulsion and Enhances Axon Regeneration. *Chemistry & Biology*, 16(7):691–701, 2009.
- [209] Simona Moretti, Antonio Procopio, Raffaella Lazzarini, Maria Rita Rippon, Roberto Testa, Maurizio Marra, Luca Tamagnone, and Alfonso Catalano. Semaphorin3A signaling controls Fas (CD95)-mediated apoptosis by promoting Fas translocation into lipid rafts. *Blood*, 111(4):2290–2299, 2008.
- [210] S. Moyon, a. L. Dubessy, M. S. Aigrot, M. Trotter, J. K. Huang, L. Dauphinot, M. C. Potier, C. Kerninon, S. Melik Parsadaniantz, R. J. M. Franklin, and C. Lubetzki. Demyelination Causes Adult CNS Progenitors to Revert to an Immature State and Express Immune Cues That Support Their Migration. *Journal of Neuroscience*, 35(1):4–20, 2015.
- [211] Lars Muhl, Erika Bergsten Folestad, Hanna Gladh, Yixin Wang, Christine Moessinger, Lars Jakobsson, and Ulf Eriksson. Neuropilin 1 binds platelet-derived growth factor

- (PDGF)-D and is a co-receptor in PDGF-D/PDGF receptor  $\beta$  signaling. *Journal of Cell Science*, page jcs.200493, 2017.
- [212] E Jolanda Münzel, E Jolanda Münzel, and Anna Williams. Promoting remyelination in multiple sclerosis-recent advances. *Drugs*, 73(18):2017–29, dec 2013.
- [213] Matilde Murga, Oscar Fernandez-capetillo, and Giovanna Tosato. Neuropilin-1 regulates attachment in human endothelial cells independently of vascular endothelial growth factor receptor-2. *Cell*, 105(5):1992–1999, 2005.
- [214] P.D. Murray, D.B. McGavern, S. Sathornsumrtte, and M. Rodrigez. Spontaneous remyelination following extensive demyelination is associated with improved neurological function in a viral model of multiple sclerosis. *Brain*, 124(7):1403–1416, 2001.
- [215] Brahim Nait-Oumesmar, Laurence Decker, François Lachapelle, Virginia Avellana-Adalid, Corinne Bachelin, and Anne Baron-Van Evercooren. Progenitor cells of the adult mouse subventricular zone proliferate, migrate and differentiate into oligodendrocytes after demyelination. *European Journal of Neuroscience*, 11(12):4357–4366, 1999.
- [216] Brahim Nait-Oumesmar, Nathalie Picard-Riera, Christophe Kerninon, Laurence Decker, Danielle Seilhean, Günter U Höglinger, Etienne C Hirsch, Richard Reynolds, and Anne Baron-Van Evercooren. Activation of the subventricular zone in multiple sclerosis: evidence for early glial progenitors. *Proceedings of the National Academy of Sciences*, 104(11):4694–4699, 2007.
- [217] Fadi J Najm, Anita Zaremba, Andrew V Caprariello, Shreya Nayak, Eric C Freundt, Peter C Scacheri, Robert H Miller, and Paul J Tesar. Rapid and robust generation of functional oligodendrocyte progenitor cells from epiblast stem cells. *Nature Methods*, 8(11):957–962, 2011.
- [218] Fumio Nakamura, Masaki Tanaka, Takuya Takahashi, Robert G Kalb, and Stephen M Strittmatter. Neuropilin-1 extracellular domains mediate semaphorinD/III-induced growth cone collapse. *Neuron*, 21(5):1093–1100, 1998.
- [219] Masashi Narazaki, Marta Segarra, and Giovanna Tosato. Sulfated polysaccharides identified as inducers of neuropilin-1 internalization and functional inhibition of VEGF 165 and semaphorin3A. *Blood*, 111(8):4126–4136, 2008.
- [220] Masashi Narazaki and Giovanna Tosato. Ligand-induced internalization selects use of common receptor neuropilin-1 by VEGF165 and semaphorin3A. *Blood*, 107(10):3892–3901, 2006.
- [221] Klaus Armin Nave. Myelination and the trophic support of long axons. *Nature Reviews Neuroscience*, 11(4):275–283, 2010.

- [222] Harald Neumann, Isabelle M. Medana, Jan Bauer, and Hans Lassmann. Cytotoxic T lymphocytes in autoimmune and degenerative CNS diseases. *Trends in Neurosciences*, 25(6):313–319, 2002.
- [223] Simone P. Niclou, Elske H.P. Franssen, Erich M.E. Ehlert, Masahiko Taniguchi, and Joost Verhaagen. Meningeal cell-derived semaphorin 3A inhibits neurite outgrowth. *Molecular and Cellular Neuroscience*, 24(4):902–912, 2003.
- [224] Antje Niehaus, Jian Shi, Martina Grzenkowski, Marianne Diers-Fenger, Juan Archelos, Hans Peter Hartung, Klaus Toyka, Wolfgang Brück, and Jacqueline Trotter. Patients with active relapsing-remitting multiple sclerosis synthesize antibodies recognizing oligodendrocyte progenitor cell surface protein: Implications for remyelination. *Annals of Neurology*, 48(3):362–371, 2000.
- [225] S N Nona, a M Thomlinson, C a Bartlett, and J Scholes. Schwann cells in the regenerating fish optic nerve: evidence that CNS axons, not the glia, determine when myelin formation begins. *J.Neurocytol.*, 29(4):285–300, 2000.
- [226] John H. Noseworthy, Claudia Lucchinetti, Moses Rodriguez, and Brain G. Weinshenker. Multiple sclerosis. *The New England Journal of Medicine*, 343:938–952, 2000.
- [227] Atsumasa Okada, Mitsutoshi Tominaga, Makoto Horiuchi, and Yasuhiro Tomooka. Plexin-A4 is expressed in oligodendrocyte precursor cells and acts as a mediator of semaphorin signals. *Biochemical and Biophysical Research Communications*, 352(1):158–163, 2007.
- [228] Masashi Okubo, Tokuhiko Kimura, Yoshinari Fujita, Satsuki Mochizuki, Yasuo Niki, Hiroyuki Enomoto, Yasunori Suda, Yoshiaki Toyama, and Yasunori Okada. Semaphorin 3A is expressed in human osteoarthritic cartilage and antagonizes vascular endothelial growth factor 165-promoted chondrocyte migration: An implication for chondrocyte cloning. *Arthritis and Rheumatism*, 63(10):3000–3009, 2011.
- [229] Tatsusada Okuno, Yuji Nakatsuji, and Atsushi Kumanogoh. The role of immune semaphorins in multiple sclerosis. *FEBS Letters*, 585(23):3829–3835, 2011.
- [230] John a. Olsen and Eitan M. Akirav. Remyelination in multiple sclerosis: Cellular mechanisms and novel therapeutic approaches. *Journal of Neuroscience Research*, 696(October 2014):n/a–n/a, 2014.
- [231] Tomas Olsson, Lisa F. Barcellos, and Lars Alfredsson. Interactions between genetic, lifestyle and environmental risk factors for multiple sclerosis. *Nature Reviews Neurology*, 13(1):26–36, 2016.
- [232] L.-J. Oluich, J. A. S. Stratton, Y. Lulu Xing, S. W. Ng, H. S. Cate, P. Sah, F. Windels, T. J. Kilpatrick, and T. D. Merson. Targeted Ablation of Oligodendrocytes Induces Axonal

- Pathology Independent of Overt Demyelination. *Journal of Neuroscience*, 32(24):8317–8330, 2012.
- [233] Masahiro Omoto, Satoru Yoshida, Hideyuki Miyashita, Tetsuya Kawakita, Kenji Yoshida, Akiyoshi Kishino, Toru Kimura, Shinsuke Shibata, Kazuo Tsubota, Hideyuki Okano, and Shigeto Shimmura. The semaphorin 3A inhibitor SM-345431 accelerates peripheral nerve regeneration and sensitivity in a murine corneal transplantation model. *PloS one*, 7(11):e47716, jan 2012.
- [234] S S Ousman and S David. Lysophosphatidylcholine induces rapid recruitment and activation of macrophages in the adult mouse spinal cord. *Glia*, 30(1):92–104, 2000.
- [235] Baohan Pan, Susan E. Fromholt, Ellen J. Hess, Thomas O. Crawford, John W. Griffin, Kazim A. Sheikh, and Ronald L. Schnaar. Myelin-associated glycoprotein and complementary axonal ligands, gangliosides, mediate axon stability in the CNS and PNS: Neuropathology and behavioral deficits in single- and double-null mice. *Experimental Neurology*, 195(1):208–217, 2005.
- [236] Qi Pan, Yvan Chanthery, WC Wei-Ching C Wei-Ching Liang, Scott Stawicki, Judy Mak, Nisha Rathore, Raymond K Tong, Joe Kowalski, Sharon Fong Yee, Glenn Pacheco, Sarajane Ross, Zhiyong Cheng, Jennifer Le Couter, Greg Plowman, Franklin Peale, Alexander W Koch, Yan Wu, Anil Bagri, Marc Tessier-Lavigne, and Ryan J Watts. Blocking neuropilin-1 function has an additive effect with anti-VEGF to inhibit tumor growth. *Cancer cell*, 11(1):53–67, jan 2007.
- [237] R J Pasterkamp, F De Winter, a J Holtmaat, and J Verhaagen. Evidence for a role of the chemorepellent semaphorin III and its receptor neuropilin-1 in the regeneration of primary olfactory axons. *The Journal of neuroscience : the official journal of the Society for Neuroscience*, 18(23):9962–76, 1998.
- [238] R. J. Pasterkamp, R. J. Giger, M. J. Ruitenber, A. J.G.D. Holtmaat, J. De Wit, F. De Winter, and J. Verhaagen. Expression of the gene encoding the chemorepellent semaphorin III is induced in the fibroblast component of neural scar tissue formed following injuries of adult but not neonatal CNS. *Molecular and Cellular Neurosciences*, 13(2):143–166, 1999.
- [239] R Jeroen Pasterkamp and Alex L Kolodkin. Semaphorin junction: making tracks toward neural connectivity. *Current Opinion in Neurobiology*, 13(1):79–89, feb 2003.
- [240] R. Patani, M. Balaratnam, A. Vora, and R. Reynolds. Remyelination can be extensive in multiple sclerosis despite a long disease course. *Neuropathology and Applied Neurobiology*, 33(3):277–287, 2007.
- [241] Amita Patnaik, Patricia M Lorusso, Wells A Messersmith, Kyriakos P Papadopoulos, Lia Gore, Muralidhar Beeram, Vanitha Ramakrishnan, Amy H Kim, Joseph C Beyer,

- L Mason Shih, Walter C Darbonne, Yan Xin, Ron Yu, Hong Xiang, Rainer K Brachmann, and Colin D Weekes. A Phase Ib study evaluating MNRP1685A , a fully human anti NRP1 monoclonal antibody , in combination with bevacizumab and paclitaxel in patients with advanced solid tumors. *Cancer Chemother Pharmacol*, 73:951–960, 2014.
- [242] Peter Patrikios, Christine Stadelmann, Alexandra Kutzelnigg, Helmut Rauschka, Manfred Schmidbauer, Henning Laursen, Per Soelberg Sorensen, Wolfgang Brück, Claudia Lucchinetti, and Hans Lassmann. Remyelination is extensive in a subset of multiple sclerosis patients. *Brain*, 129(12):3165–3172, 2006.
- [243] Laura A N Peferoen, Daphne Y S Vogel, Kimberley Ummenthum, and Marjolein Breur. Activation Status of Human Microglia Is Dependent on Lesion Formation Stage and Remyelination in Multiple Sclerosis Activation Status of Human Microglia Is Dependent on Lesion Formation Stage and Remyelination in Multiple Sclerosis. *Journal of Neuropathology and Experimental Neurology*, 74(December), 2014.
- [244] A Perier, O and Gregoire. Electron microscopic features of multiple sclerosis lesions. *Brain*, 88(5):937–952, 1965.
- [245] Gabrièle Piaton, Marie-Stéphane Aigrot, Anna Williams, Sarah Moyon, Vanja Tepavcevic, Imane Moutkine, Julien Gras, Katherine S Matho, Alain Schmitt, Heidi Soellner, Andrea B Huber, Philippe Ravassard, and Catherine Lubetzki. Class 3 semaphorins influence oligodendrocyte precursor recruitment and remyelination in adult central nervous system. *Brain : a journal of neurology*, 134(Pt 4):1156–1167, apr 2011.
- [246] H. B. F. Pohl, C. Porcheri, T. Mueggler, L. C. Bachmann, G. Martino, D. Riethmacher, R. J. M. Franklin, M. Rudin, and U. Suter. Genetically Induced Adult Oligodendrocyte Cell Death Is Associated with Poor Myelin Clearance, Reduced Remyelination, and Axonal Damage. *Journal of Neuroscience*, 31(3):1069–1080, 2011.
- [247] Franck Polleux, Theresa Morrow, and Anirvan Ghosh. Semaphorin 3A is a chemoattractant for cortical apical dendrites. *Nature*, 404(6778):567–573, 2000.
- [248] C M Poser, D W Paty, L Scheinberg, W I McDonald, F A Davis, G C Ebers, K P Johnson, W A Sibley, D H Silberberg, and W W Tourtellotte. New diagnostic criteria for multiple sclerosis: guidelines for research protocols. *Ann Neurol*, 13(3):227–231, 1983.
- [249] J. W. Prineas, R. O. Barnard, E. E. Kwon, L. R. Sharer, and E. S Cho. Multiple sclerosis: Remyelination of nascent lesions: Remyelination of nascent lesions. *Annals of Neurology*, 33(2):137–151, 1993.
- [250] J. W. Prineas, E. E. Kwon, EunSook S Cho, and L. R. Shaper. Continual Breakdown and Regeneration of Myelin in Progressive Multiple Sclerosis Plaques. *Annals of the New York Academy of Sciences*, 436(1):11–32, 1984.

- [251] F. Prineas, John W. ; Connell. Remyelination In Multiple Sclerosis. *Ann Neurol*, 5:22–31, 1979.
- [252] G J Prud'homme, Y Glinka, Z Lichner, and G M Yousef. Neuropilin-1 is a receptor for extracellular miRNA and AGO2/miRNA complexes and mediates the internalization of miRNAs that modulate cell function. *Oncotarget.*, 7(42):10, 2016.
- [253] Gérald J Prud'homme and Yelena Glinka. Neuropilins are multifunctional coreceptors involved in tumor initiation, growth, metastasis and immunity. *Oncotarget*, 3(9):921–39, 2012.
- [254] Maura Pugliatti, Stefano Sotgiu, and Giulio Rosati. The worldwide prevalence of multiple sclerosis. *Clinical Neurology and Neurosurgery*, 104(3):182–191, 2002.
- [255] MC C Raff, RH H Miller, and M Noble. A glial progenitor cell that develops in vitro into an astrocyte or an oligodendrocyte depending on culture medium. *Nature*, 303(2):390–396, 1983.
- [256] E. J. Redford, R. Kapoor, and K. J. Smith. Nitric oxide donors reversibly block axonal conduction: Demyelinated axons are especially susceptible. *Brain*, 120(12):2149–2157, 1997.
- [257] Jeffrey M. Redwine and Regina C. Armstrong. In vivo proliferation of oligodendrocyte progenitors expressing PDGF $\beta$  during early remyelination. *Journal of Neurobiology*, 37(3):413–428, 1998.
- [258] Mahsa Rezaeepoor, Shima Shapoori, Mazdak Ganjalikhani-hakemi, Masoud Etemadifar, Fereshteh Alsahebhosoul, Nahid Eskandari, and Marjan Mansourian. Decreased expression of Sema3A, an immune modulator, in blood sample of multiple sclerosis patients. *Gene*, 610:59–63, 2017.
- [259] D Ricard, V Rogemond, E Charrier, M Aguera, D Bagnard, M F Belin, N Thomasset, and J Honnorat. Isolation and expression pattern of human Unc-33-like phosphoprotein 6/collapsin response mediator protein 5 (Ulip6/CRMP5): coexistence with Ulip2/CRMP2 in Sema3a- sensitive oligodendrocytes. *The Journal of neuroscience : the official journal of the Society for Neuroscience*, 21(18):7203–7214, 2001.
- [260] D. Ricard, B. Stankoff, D. Bagnard, M. Aguera, V. Rogemond, J. C. Antoine, N. Spassky, B. Zalc, C. Lubetzki, M. F. Belin, and J. Honnorat. Differential expression of collapsin response mediator proteins (CRMP/Ulip) in subsets of oligodendrocytes in the postnatal rodent brain. *Molecular and Cellular Neurosciences*, 16(4):324–337, 2000.
- [261] Maria Ringvall, Johan Ledin, Katarina Holmborn, Toin Van Kuppevelt, Fredrik Ellin, Inger Eriksson, Anne Mari Olofsson, Lena Kjellén, and Erik Forsberg. Defective heparan sulfate biosynthesis and neonatal lethality in mice lacking N-deacetylase/N-sulfotransferase-1. *Journal of Biological Chemistry*, 275(34):25926–25930, 2000.

- [262] Shenandoah Robinson and Robert H. Miller. Contact with central nervous system myelin inhibits oligodendrocyte progenitor maturation. *Developmental Biology*, 216(1):359–368, 1999.
- [263] Enrique Garea Rodriguez, Wegner, and Enrique Garea Rodriguez · Christiane Wegner · Mario Kreutzfeldt · Katharina Neid · Dietmar R. Thal · Tanja Jürgens · Wolfgang Brück · Christine Stadelmann · Doron Merkler. Oligodendroglia in cortical multiple sclerosis lesions decrease with disease progression , but regenerate after repeated experimental demyelination. *Acta Neuropathologica*, 128:231–246, 2014.
- [264] M Rossignol, M L Gagnon, and M Klagsbrun. Genomic organization of human neuropilin-1 and neuropilin-2 genes: identification and distribution of splice variants and soluble isoforms. *Genomics*, 70(2):211–222, dec 2000.
- [265] Lise Roth, Claudia Prahst, Tina Ruckdeschel, Soniya Savant, Simone Weström, Alessandro Fantin, Maria Riedel, Mélanie Héroult, Christiana Ruhrberg, and Hellmut G Augustin. Neuropilin-1 mediates vascular permeability independently of vascular endothelial growth factor receptor-2 activation. *Science Signaling*, 9(425):1–11, 2016.
- [266] P M Rothwell and D Charlton. High incidence and prevalence of multiple sclerosis in south east Scotland: evidence of a genetic predisposition. *Journal of neurology, neurosurgery, and psychiatry*, 64(6):730–735, jun 1998.
- [267] Francesca Ruffini, Nathalie Arbour, Manon Blain, André Olivier, and Jack P. Antel. Distinctive properties of human adult brain-derived myelin progenitor cells. *American Journal of Pathology*, 165(6):2167–2175, 2004.
- [268] S. Saad, A. A S S K Dharmapatni, T. N. Crotti, M. D. Cantley, K. Algate, D. M. Findlay, G. J. Atkins, and D. R. Haynes. Semaphorin-3a, neuropilin-1 and plexin-A1 in prosthetic-particle induced bone loss. *Acta Biomaterialia*, 30:311–318, 2016.
- [269] A. Sahay. Secreted Semaphorins Modulate Synaptic Transmission in the Adult Hippocampus. *Journal of Neuroscience*, 25(14):3613–3620, 2005.
- [270] Milka Sarris, Kristian G. Andersen, Felix Randow, Luzia Mayr, and Alexander G. Betz. Neuropilin-1 Expression on Regulatory T Cells Enhances Their Interactions with Dendritic Cells during Antigen Recognition. *Immunity*, 28(3):402–413, 2008.
- [271] J I Satoh, H Tabunoki, and T Yamamura. Molecular network of the comprehensive multiple sclerosis brain-lesion proteome. *Multiple sclerosis (Houndmills, Basingstoke, England)*, 15(5):531–541, may 2009.
- [272] K W Selmaj and C S Raine. Tumor necrosis factor mediates myelin and oligodendrocyte damage in vitro. *Annals of neurology*, 23(4):339–346, 1988.

- [273] Guido Serini, Donatella Valdembrì, Sara Zanivan, Giulia Morterra, Constanze Burkhardt, Francesca Caccavari, Luca Zammataro, Luca Primo, Luca Tamagnone, Malcolm Logan, Marc Tessier-Lavigne, Masahiko Taniguchi, Andreas W. Püschel, and Federico Bussolino. Class 3 semaphorins control vascular morphogenesis by inhibiting integrin function. *Nature*, 424(6947):391–397, 2003.
- [274] Simon A. Shields, Jennifer M. Gilson, William F. Blakemore, and Robin J M Franklin. Remyelination occurs as extensively but more slowly in old rats compared to young rats following gliotoxin-induced CNS demyelination. *Glia*, 28(1):77–83, 1999.
- [275] Anat Shirvan, Michal Kimron, Vered Holdengreber, Ilan Ziv, Yehuda Ben-Shaul, Shlomo Melamed, Eldad Melamed, Ari Barzilai, and Arieh S. Solomon. Anti-semaphorin 3A antibodies rescue retinal ganglion cells from cell death following optic nerve axotomy. *Journal of Biological Chemistry*, 277(51):49799–49807, 2002.
- [276] Anat Shirvan, Ilan Ziv, Gideon Fleminger, Ronit Shina, Zhigang He, Irene Brudo, Eldad Melamed, and Ari Barzilai. Semaphorins as mediators of neuronal apoptosis. *Journal of Neurochemistry*, 73(3):961–971, 1999.
- [277] Fraser J Sim, Chao Zhao, Jacques Penderis, and Robin J M Franklin. The age-related decrease in CNS remyelination efficiency is attributable to an impairment of both oligodendrocyte progenitor recruitment and differentiation. *The Journal of neuroscience : the official journal of the Society for Neuroscience*, 22(7):2451–9, 2002.
- [278] David Anak Simon Davis and Christopher R. Parish. Heparan sulfate: A ubiquitous glycosaminoglycan with multiple roles in immunity. *Frontiers in Immunology*, 4(DEC):1–7, 2013.
- [279] I. Smets, L. Van Deun, C. Bohyn, V. van Pesch, L. Vanopdenbosch, D. Dive, V. Bissay, and B. Dubois. Corticosteroids in the management of acute multiple sclerosis exacerbations. *Acta Neurologica Belgica*, 117(3):623–633, 2017.
- [280] K. J. Smith, W F Blakemore, and W. I. McDonald. Central remyelination restores secure conduction. *Nature*, 280:395–396, 1979.
- [281] Kenneth J. Smith. Axonal protection in multiple sclerosis - A particular need during remyelination? *Brain*, 129(12):3147–3149, 2006.
- [282] Kenneth J. Smith, Raju Kapoor, Susan M. Hall, and Meirion Davies. Electrically active axons degenerate when exposed to nitric oxide. *Annals of Neurology*, 49(4):470–476, 2001.
- [283] P Sobocki, M Pugliatti, K Lauer, and G Kobelt. Estimation of the cost of MS in Europe: extrapolations from a multinational cost study. *Multiple sclerosis (Houndmills, Basingstoke, England)*, 13(8):1054–1064, oct 2007.

- [284] S Soker, S Takashima, H Q Miao, G Neufeld, and M Klagsbrun. Neuropilin-1 is expressed by endothelial and tumor cells as an isoform-specific receptor for vascular endothelial growth factor. *Cell*, 92(6):735–745, mar 1998.
- [285] Benjamin D. Solomon, Cynthia Mueller, Wook-Jin Chae, Leah M. Alabanza, and Margaret S. Bynoe. Neuropilin-1 attenuates autoreactivity in experimental autoimmune encephalomyelitis. *Proceedings of the National Academy of Sciences*, 108(5):2040–2045, 2011.
- [286] I. Sommer and M. Schachner. Monoclonal antibodies (O1 to O4) to oligodendrocyte cell surfaces: An immunocytological study in the central nervous system. *Developmental Biology*, 83(2):311–327, 1981.
- [287] Nathalie Spassky, Fernando de Castro, Barbara Le Bras, Katharina Heydon, Françoise Quéraud-LeSaux, Evelyne Bloch-Gallego, Alain Chédotal, Bernard Zalc, and Jean-Léon Thomas. Directional guidance of oligodendroglial migration by class 3 semaphorins and netrin-1. *The Journal of neuroscience : the official journal of the Society for Neuroscience*, 22(14):5992–6004, 2002.
- [288] Peter S. Spencer and P. K. Thomas. Ultrastructural studies of the dying-back process II. The sequestration and removal by Schwann cells and oligodendrocytes of organelles from normal and diseased axons. *Journal of Neurocytology*, 3(6):763–783, 1974.
- [289] William B. Stallcup. The NG2 antigen, a putative lineage marker: Immunofluorescent localization in primary cultures of rat brain. *Developmental Biology*, 83(1):154–165, 1981.
- [290] Martin Stangel and Hans-Peter Hartung. Remyelinating strategies for the treatment of multiple sclerosis. *Progress in neurobiology*, 68(5):361–76, dec 2002.
- [291] P K Stys, S G Waxman, and B R Ransom. Ionic mechanisms of anoxic injury in mammalian CNS white matter: role of Na<sup>+</sup> channels and Na<sup>(+)</sup>-Ca<sup>2+</sup> exchanger. *The Journal of neuroscience : the official journal of the Society for Neuroscience*, 12(2):430–9, 1992.
- [292] Kimmy G Su, Gary Banker, Dennis Bourdette, and Michael Forte. Axonal degeneration in multiple sclerosis- The mitochondrial hypothesis. *Current neurology and neuroscience reports*, 9:411–417, 2009.
- [293] Yoshihiko Sugimoto, Masahiko Taniguchi, Takeshi Yagi, Yoshio Akagi, Yoshiaki Nojyo, and Nobuaki Tamamaki. Guidance of glial precursor cell migration by selected cues in the developing optic nerve. *Development*, 128:3321–3330, 2001.
- [294] Fumikazu Suto, Yasunori Murakami, Fumio Nakamura, Yoshio Goshima, and Hajime Fujisawa. Identification and characterization of a novel mouse plexin, plexin-A4. *Mechanisms of Development*, 120(3):385–396, 2003.

- [295] R J Swingle and D Compston. The distribution of multiple sclerosis in the United Kingdom. *Journal of neurology, neurosurgery, and psychiatry*, 49(10):1115–24, 1986.
- [296] Yasir a Syed, Elisabeth Hand, Wiebke Möbius, Chao Zhao, Matthias Hofer, Klaus a Nave, and Mark R Kotter. Inhibition of CNS remyelination by the presence of semaphorin 3A. *The Journal of neuroscience : the official journal of the Society for Neuroscience*, 31(10):3719–3728, mar 2011.
- [297] S Takagawa, F Nakamura, K Kumagai, Y Nagashima, Y Goshima, and T Saito. Decreased semaphorin3A expression correlates with disease activity and histological features of rheumatoid arthritis. *BMC.Musculoskelet.Disord.*, 14:40. doi:14–40, 2013.
- [298] S Takagi, T Hirata, K Agata, M Mochii, G Eguchi, and H Fujisawa. The A5 antigen, a candidate for the neuronal recognition molecule, has homologies to complement components and coagulation factors. *Neuron*, 7(2):295–307, aug 1991.
- [299] S Takagi, Y Kasuya, M Shimizu, T Matsuura, M Tsuboi, A Kawakami, and H Fujisawa. Expression of a cell adhesion molecule, neuropilin, in the developing chick nervous system., 1995.
- [300] T Takahashi, a Fournier, F Nakamura, L H Wang, Y Murakami, R G Kalb, H Fujisawa, and S M Strittmatter. Plexin-neuropilin-1 complexes form functional semaphorin-3A receptors. *Cell*, 99(1):59–69, oct 1999.
- [301] T Takahashi, F Nakamura, Z Jin, R G Kalb, and S M Strittmatter. Semaphorins A and E act as antagonists of neuropilin-1 and agonists of neuropilin-2 receptors. *Nature neuroscience*, 1(6):487–493, 1998.
- [302] Takuya Takahashi and Stephen M Strittmatter. PlexinA1 autoinhibition by the Plexin sema domain. *Neuron*, 29(2):429–439, feb 2001.
- [303] Hyota Takamatsu, Noriko Takegahara, Yukinobu Nakagawa, Michio Tomura, Masahiko Taniguchi, Roland H Friedel, Helen Rayburn, Marc Tessier-Lavigne, Yutaka Yoshida, Tatsusada Okuno, Masayuki Mizui, Sujin Kang, Satoshi Nojima, Tohru Tsujimura, Yuji Nakatsuji, Ichiro Katayama, Toshihiko Toyofuku, Hitoshi Kikutani, and Atsushi Kumanogoh. Semaphorins guide the entry of dendritic cells into the lymphatics by activating myosin II. *Nature immunology*, 11(7):594–600, 2010.
- [304] Emma C. Tallantyre, Lars Bø, Omar Al-Rawashdeh, Trudy Owens, Chris H. Polman, James S. Lowe, and Nikos Evangelou. Clinico-pathological evidence that axonal loss underlies disability in progressive multiple sclerosis. *Multiple Sclerosis*, 16(4):406–411, 2010.
- [305] Luca Tamagnone, Stefania Artigiani, Hang Chen, Zhigang He, Guo Li Ming, Hong Jun Song, Alain Chedotal, Margaret L. Winberg, Corey S. Goodman, Mu Ming Poo, Marc Tessier-Lavigne, and Paolo M. Comoglio. Plexins are a large family of receptors for

- transmembrane, secreted, and GPI-anchored semaphorins in vertebrates. *Cell*, 99(1):71–80, 1999.
- [306] M Taniguchi, S Yuasa, H Fujisawa, I Naruse, S Saga, M Mishina, and T Yagi. Disruption of semaphorin III/D gene causes severe abnormality in peripheral nerve projection. *Neuron*, 19(3):519–530, sep 1997.
- [307] Giulio Srubek Tomassy and Valentina Fossati. How big is the myelinating orchestra? Cellular diversity within the oligodendrocyte lineage: facts and hypotheses. *Frontiers in cellular neuroscience*, 8(July):201, jan 2014.
- [308] Rafaèle Tordjman, Yves Lepelletier, Valerie Lemarchandel, Marie Cambot, Philippe Gaulard, Olivier Hermine, and Paul Henri Roméo. A neuronal receptor, neuropilin-1, is essential for the initiation of the primary immune response. *Nature Immunology*, 3(5):477–482, 2002.
- [309] a Tourbah, C Linnington, C Bachelin, V Avellana-Adalid, H Wekerle, and a Baron-Van Evercooren. Inflammation promotes survival and migration of the CG4 oligodendrocyte progenitors transplanted in the spinal cord of both inflammatory and demyelinated EAE rats. *Journal of neuroscience research*, 50(5):853–61, dec 1997.
- [310] Bruce D Trapp and Klaus-Armin Nave. Multiple sclerosis: an immune or neurodegenerative disorder? *Annual review of neuroscience*, 31:247–69, jan 2008.
- [311] Bruce D. Trapp, John Peterson, Richard M. Ransohoff, Richard Rudick, Sverre Mörk, and Lars Bö. Axonal Transection in the Lesions of Multiple Sclerosis. *New England Journal of Medicine*, 338(5):278–285, 1998.
- [312] Bruce D Trapp and Peter K Stys. Virtual hypoxia and chronic necrosis of demyelinated axons in multiple sclerosis. *The Lancet. Neurology*, 8(3):280–91, mar 2009.
- [313] U. Traugott, E. L. Reinherz, and C. S. Raine. Multiple sclerosis. Distribution of T cells, T cell subsets and Ia-positive macrophages in lesions of different ages. *Journal of Neuroimmunology*, 4(3):201–221, 1983.
- [314] R. Tyler Hillman, Brian Y. Feng, Jun Ni, Wei Meng Woo, Ljiljana Milenkovic, Melanie G. Hayden Gephart, Mary N. Teruel, Anthony E. Oro, James K. Chen, and Matthew P. Scott. Neuropilins are positive regulators of Hedgehog signal transduction. *Genes and Development*, 25(22):2333–2346, 2011.
- [315] Zahava Vadasz, Tharwat Haj, Katalin Halasz, Itzhak Rosner, Gleb Slobodin, Dina Attias, Aharon Kessel, Ofra Kessler, Gera Neufeld, and Elias Toubi. Semaphorin 3A is a marker for disease activity and a potential immunoregulator in systemic lupus erythematosus. *Arthritis research & therapy*, 14(3):R146, jan 2012.
- [316] Anna Vallstedt, Joanna M. Klos, and Johan Ericson. Multiple dorsoventral origins of oligodendrocyte generation in the spinal cord and hindbrain. *Neuron*, 45(1):55–67, 2005.

- [317] Jack van Horssen, Lars Bö, Christien D. Dijkstra, and Helga E. de Vries. Extensive extracellular matrix depositions in active multiple sclerosis lesions. *Neurobiology of Disease*, 24(3):484–491, 2006.
- [318] Jack Van Horssen, Christine D. Dijkstra, and Helga E. De Vries. The extracellular matrix in multiple sclerosis pathology. *Journal of Neurochemistry*, 103(4):1293–1301, 2007.
- [319] Adam C Vana, Nicole C Flint, Norah E Harwood, Tuan Q Le, Marcus Fruttiger, and Regina C Armstrong. Platelet-derived growth factor promotes repair of chronically demyelinated white matter. *J Neuropathol Exp Neurol*, 66(11):975–988, 2007.
- [320] James E. Vaughan and Alan Peters. A third neuroglial cell types. An electron microscopic study. *The Journal of Comparative Neurology*, 133(2):269–287, 1968.
- [321] Hanna M Vesterinen, Emily S Sena, Charles Ffrench-Constant, Anna Williams, Sidharthan Chandran, and Malcolm R Macleod. Improving the translational hit of experimental treatments in multiple sclerosis. *Multiple sclerosis (Houndmills, Basingstoke, England)*, 16(9):1044–1055, sep 2010.
- [322] Majken Wallerius, Tatjana Wallmann, Margarita Bartish, Jeanette Östling, Artur Mezheyeuski, Nicholas P. Tobin, Emma Nygren, Pradeepa Pangigadde, Paola Pellegrini, Mario Leonardo Squadrito, Fredrik Ponten, Johan Hartman, Jonas Bergh, Angelo De Milito, Michele De Palma, Arne Östman, John Andersson, and Charlotte Rolny. Guidance molecule SEMA3A restricts tumor growth by differentially regulating the proliferation of tumor-associated macrophages. *Cancer Research*, 76(11):3166–3178, 2016.
- [323] Y Wang, Y Cao, A K Mangalam, Y Guo, R G LaFrance-Corey, J D Gamez, P A Atanga, B D Clarkson, Y Zhang, E Wang, R S Angom, K Dutta, B Ji, I Pirko, C F Lucchinetti, C L Howe, and D Mukhopadhyay. Neuropilin-1 modulates interferon-gamma-stimulated signaling in brain microvascular endothelial cells. *J. Cell Sci.*, page jcs, 2016.
- [324] Masahiko Watanabe, Yoshiaki Toyama, and Akiko Nishiyama. Differentiation of proliferated NG2-positive glial progenitor cells in a remyelinating lesion. *Journal of Neuroscience Research*, 69(6):826–836, 2002.
- [325] Stephen G. Waxman. Axonal conduction and injury in multiple sclerosis: The role of sodium channels. *Nature Reviews Neuroscience*, 7(12):932–941, 2006.
- [326] Amanda B Wehner, Houari Abdesslem, Travis L Dickendesher, Fumiyasu Imai, Yutaka Yoshida, Roman J Giger, and Brian A Pierchala. Semaphorin 3A is a retrograde cell death signal in developing sympathetic neurons. *Development (Cambridge, England)*, 143(9):1560–70, 2016.
- [327] Z Wei, S J Swiedler, M Ishihara, A Orellana, and C B Hirschberg. A single protein catalyzes both N-deacetylation and N-sulfation during the biosynthesis of heparan sul-

- fate. *Proceedings of the National Academy of Sciences of the United States of America*, 90(9):3885–8, 1993.
- [328] Elise Whitley and Jonathan Ball. Statistics review 4: sample size calculations. *Critical care (London, England)*, 6:335–41, 2002.
- [329] C. J. Willer, D. A. Dymont, N. J. Risch, A. D. Sadovnick, and G. C. Ebers. Twin concordance and sibling recurrence rates in multiple sclerosis. *Proceedings of the National Academy of Sciences*, 100(22):12877–12882, 2003.
- [330] Anna Williams, Gabrièle Piaton, Marie-Stéphane Aigrot, Aisha Belhadi, Marie Théaudin, Franziska Petermann, Jean-Léon Thomas, Bernard Zalc, and Catherine Lubetzki. Semaphorin 3A and 3F: key players in myelin repair in multiple sclerosis? *Brain : a journal of neurology*, 130(Pt 10):2554–2565, oct 2007.
- [331] Gareth Williams, Britta J Eickholt, Patrick Maison, Rabinder Prinjha, Frank S Walsh, and Patrick Doherty. A complementary peptide approach applied to the design of novel semaphorin/neuropilin antagonists. *Journal of neurochemistry*, 92(5):1180–90, mar 2005.
- [332] Margaret L. Winberg, Jasprina N. Noordermeer, Luca Tamagnone, Paolo M. Comoglio, Melanie K. Spriggs, Marc Tessier-Lavigne, and Corey S. Goodman. Plexin A is a neuronal semaphorin receptor that controls axon guidance. *Cell*, 95(7):903–916, 1998.
- [333] Martha S. Windrem, Marta C. Nunes, William K. Rashbaum, Theodore H. Schwartz, Robert A. Goodman, Guy McKhann, Neeta S. Roy, and Steven A. Goldman. Fetal and adult human oligodendrocyte progenitor cell isolates myelinate the congenitally demyelinated brain. *Nature Medicine*, 10(1):93–97, 2004.
- [334] H Wolburg. Myelination and remyelination in the regenerating visual system of the goldfish. *Exp Brain Res*, 43(2):199–206, 1981.
- [335] G Wolswijk. Chronic stage multiple sclerosis lesions contain a relatively quiescent population of oligodendrocyte precursor cells. *The Journal of neuroscience : the official journal of the Society for Neuroscience*, 18(2):601–9, 1998.
- [336] Guus Wolswijk. Oligodendrocyte precursor cells in the demyelinated multiple sclerosis spinal cord. *Brain*, 125:338–349, 2002.
- [337] Rachel H Woodruff, Marcus Fruttiger, William D Richardson, and Robin J M Franklin. Platelet-derived growth factor regulates oligodendrocyte progenitor numbers in adult CNS and their response following CNS demyelination. *Molecular and cellular neurosciences*, 25(2):252–262, feb 2004.
- [338] Thomas Worzfeld and Stefan Offermanns. Semaphorins and plexins as therapeutic targets. *Nature reviews. Drug discovery*, 13(8):603–21, aug 2014.

- [339] Xin Xiang, Xuan Zhang, and Qi Lin Huang. Plexin A3 is involved in semaphorin 3F-mediated oligodendrocyte precursor cell migration. *Neuroscience Letters*, 530(2):127–132, 2012.
- [340] Y. L. Xing, P. T. Roth, J. a. S. Stratton, B. H. a. Chuang, J. Danne, S. L. Ellis, S. W. Ng, T. J. Kilpatrick, and T. D. Merson. Adult Neural Precursor Cells from the Subventricular Zone Contribute Significantly to Oligodendrocyte Regeneration and Remyelination. *Journal of Neuroscience*, 34(42):14128–14146, oct 2014.
- [341] Midori Yamamoto, Kazuhiro Suzuki, Tatsusada Okuno, Takehiro Ogata, Noriko Takegahara, Hyota Takamatsu, Masayuki Mizui, Masahiko Taniguchi, Alain Chédotal, Fumikazu Suto, Hajime Fujisawa, Atsushi Kumanogoh, and Hitoshi Kikutani. Plexin-A4 negatively regulates T lymphocyte responses. *International Immunology*, 20(3):413–420, 2008.
- [342] M Yamasaki, P Thompson, and V Lemmon. CRASH syndrome: mutations in L1CAM correlate with severity of the disease. *Neuropediatrics*, 28(3):175–8, 1997.
- [343] Wan-jen Yang, Junhao Hu, Akiyoshi Uemura, Fabian Tetzlaff, Hellmut G Augustin, and Andreas Fischer. Semaphorin- 3 C signals through Neuropilin- 1 and PlexinD 1 receptors to inhibit pathological angiogenesis. *EMBO Molecular medicine*, pages 1–18, 2015.
- [344] Sarah Younan, Shereen Elhoseiny, Amira Hammam, Rania Gawdat, Mohamed El-wakil, and Mohamed Fawzy. Role of Neuropilin-1 and its expression in Egyptian Acute Myeloid and Acute Lymphoid Leukemia patients. *Leukemia Research*, 36(2):169–173, 2012.
- [345] Ian C Zachary, Paul Frankel, Ian M Evans, and Caroline Pellet-Many. The role of neuropilins in cell signalling. *Biochemical Society transactions*, 37(Pt 6):1171–1178, 2009.
- [346] Ian S. Zagon and Patricia J. McLaughlin. *Multiple Sclerosis: Perspective in Treatment and Pathogenesis*. 2017.
- [347] Jessica L. Zambonin, Chao Zhao, Nobuhiko Ohno, Graham R. Campbell, Sarah Engham, Iryna Ziabreva, Nadine Schwarz, Sok Ee Lee, Josa M. Frischer, Doug M. Turnbull, Bruce D. Trapp, Hans Lassmann, Robin J.M. Franklin, and Don J. Mahad. Increased mitochondrial content in remyelinated axons: Implications for multiple sclerosis. *Brain*, 134(7):1901–1913, 2011.
- [348] Stephanie Elizabeth Johanna Zandee, Richard Anthony O’Connor, Iris Mair, Melanie Dawn Leech, Anna Williams, and Stephen Mark Anderton. IL-10-producing, ST2-expressing Foxp3 + T cells in multiple sclerosis brain lesions. *Immunology and Cell Biology*, 95(5):484–490, 2017.
- [349] Robert J. Zatorre, R. Douglas Fields, and Heidi Johansen-Berg. Plasticity in gray and white: Neuroimaging changes in brain structure during learning. *Nature Neuroscience*, 15(4):528–536, 2012.

## Bibliography

- [350] Malgorzata Zawadzka, Leanne E. Rivers, Stephen P.J. Fancy, Chao Zhao, Richa Tripathi, Franoise Jamen, Kaylene Young, Alexander Goncharevich, Hartmut Pohl, Matteo Rizzi, David H. Rowitch, Nicoletta Kessaris, Ueli Suter, William D. Richardson, and Robin J.M. Franklin. CNS-Resident Glial Progenitor/Stem Cells Produce Schwann Cells as well as Oligodendrocytes during Repair of CNS Demyelination. *Cell Stem Cell*, 6(6):578–590, 2010.
- [351] Thomas Zeis, LukasENZ, and Nicole Schaeren-Wiemers. The immunomodulatory oligodendrocyte. *Brain Research*, 1641:139–148, 2016.
- [352] S C Zhang, B Ge, and I D Duncan. Adult brain retains the potential to generate oligodendroglial progenitors with extensive myelination capacity. *Proceedings of the National Academy of Sciences of the United States of America*, 96(7):4089–94, mar 1999.